



The
University
Of
Sheffield.

Investigating the potential of metformin as an anti-cancer therapeutic in a model of breast disease

Aesha Makhtar
MBBS, MSc

A thesis submitted in partial fulfilment of the requirements for the degree of
Doctor of Philosophy
February 2018

The University Of Sheffield
Faculty Of Medicine
Academic Unit Of Surgical Oncology

Dedication

This thesis is dedicated to my backbone “My Mother”

Acknowledgment

First and Foremost praise is to **ALLAH**, the Almighty, the greatest of all, for giving me strength, determination and opportunity to undertake this research study.

I am deeply indebted to my supervisor, Dr. Carolyn Staton for her valuable guidance and constructive suggestions at every stage of my work. I am extremely grateful for her invaluable encouragement; kindness and patience that enabled me in carrying out this project, and without her assistance, this thesis would not obviously be completed.

Abstract

Metformin has been one of the most widely prescribed oral medications for type II diabetes for over six decades. It has recently received considerable attention because there is now evidence to show that metformin has a potential role in reducing the risk of cancer development and progression. However, the mechanisms behind the growth-inhibitory effect of metformin on breast cancer cells are not fully understood with little consensus on which tumour subtypes and/or patient populations will benefit from metformin treatment. Furthermore, it should be noted that much of the *in vitro* work published to date has used drug concentrations greatly exceeding the recommended clinical dose and most preclinical studies have given little attention to the cellular pharmacology of metformin uptake including the expression of metformin transporter molecules and intratumoral accumulation. As a result these studies may not translate directly into clinical practice. This project therefore tests the hypothesis that the anti-tumour effect of clinically relevant doses (0.03-0.3 mM) of metformin depends on breast cancer subtype and the presence of metformin transporters on breast cancer cells. Using immunohistochemistry on patient-derived tissues and various *in vitro* cell-based assays in a panel of increasingly transformed breast cell lines representing an *in vitro* model of breast disease progression, the expression of metformin transporters and the potential anti-proliferative effects of the clinical (0.03-0.3 mM) and potential tissue accumulation (1-5 mM) doses of metformin were evaluated. In parallel, global proteomic profiling was performed on three metastatic breast cancer cell lines to identify new potential molecular targets for metformin treatment. The data in this thesis show that metformin transporters are present on breast epithelial cells, pre-neoplastic, pre-invasive, invasive and metastatic breast cancer cells and that metformin has a cytostatic effect on the proliferation of these cells, causing cell cycle arrest, but not apoptosis at clinically relevant doses. The proteomic data suggest that metformin inhibits the expression of proteins within key cellular pathways in both triple negative breast cancer and the bone and lung-homed variants, with the lung-homed cells showing a greater response to metformin treatment. Taken together these data provide important novel insight into the useful role of metformin in breast cancer treatment, but further research is certainly required to identify biomarkers of response and mechanisms of action in breast cancer before metformin can be recommended in clinical practice.

Table of Contents

| | |
|---|-------------|
| Dedication..... | I |
| Acknowledgment..... | II |
| Abstract..... | III |
| List of Figures..... | VIII |
| List of Tables | X |
| List of Abbreviations | XII |
| Chapter 1: Introduction..... | 1 |
| 1.1 The Breast | 1 |
| 1.1.1 Breast anatomy and development | 1 |
| 1.1.2 Benign breast disease and subsequent risk of breast cancer | 2 |
| 1.1.3 Pre-malignant breast diseases | 3 |
| 1.1.3.1 Atypical hyperplasias (Ductal and lobular)..... | 3 |
| 1.1.3.2 <i>In situ</i> carcinomas (Ductal and Lobular)..... | 4 |
| 1.1.4 Invasive breast carcinomas | 7 |
| 1.1.4.1 Epidemiology of invasive breast cancer..... | 7 |
| 1.1.4.2 Aetiology of invasive breast cancer | 8 |
| 1.1.4.3 Classification of invasive breast cancer | 10 |
| 1.1.4.4 Current treatment strategies of invasive breast cancer..... | 12 |
| 1.1.5 Metastatic breast cancer | 14 |
| 1.2 The emerging hallmark of cancer: deregulating cellular energetics..... | 19 |
| 1.3 Metformin as a potential chemopreventive and chemotherapeutic agent in breast cancer | 20 |
| 1.3.1 Metformin's botanical background..... | 20 |
| 1.3.2 Clinical pharmacokinetics of metformin | 21 |
| 1.3.3 Pharmacodynamics of metformin and insulin-mediated action | 25 |
| 1.3.4 Metformin and breast cancer; early clues | 25 |
| 1.3.4.1 Breast cancer chemoprevention: clinical aspects and population benefits | 26 |
| 1.3.5. Pre-clinical studies with metformin in breast cancer..... | 28 |
| 1.3.5.1 Direct anti-neoplastic effects of metformin | 30 |
| 1.3.6 Clinical trials with metformin in breast cancer | 36 |
| 1.3.7 Limitations of preclinical models, and translational challenges | 39 |
| 1.3.7.1 Therapeutic concentrations and clinically relevant doses of metformin | 39 |
| 1.3.7.2 Metformin uptake, accumulation and export by cancer cell | 41 |
| 1.3.7.3 Outstanding questions in preclinical and clinical settings | 42 |
| 1.4 Project's hypothesis and aims | 44 |
| Chapter 2: Materials and methods..... | 45 |
| 2.1 Materials | 45 |
| 2.1.1 Commercial kits | 46 |
| 2.1.2 Equipment | 46 |
| 2.1.3 Cell culture media | 47 |
| 2.1.4 Quantitative polymerase chain reaction (qPCR) Primers | 49 |
| 2.1.5 Commercial human tissue slides..... | 50 |
| 2.1.6 Antibodies | 50 |
| 2.2 Methods | 51 |
| 2.2.1 Cell culture | 51 |
| 2.2.1.1 Cell lines..... | 51 |
| 2.2.1.2 Mycoplasma testing of cell lines | 53 |
| 2.2.1.3 Routine cell culture | 53 |
| 2.2.1.4 Cell subculture..... | 54 |

| | |
|---|-----------|
| 2.2.1.5 Cryopreservation of cell culture stocks | 54 |
| 2.2.1.6 Retrieval of stored cells | 55 |
| 2.2.1.7 Cell counting | 55 |
| 2.2.2 Preparation of metformin | 55 |
| 2.2.3 Quantitative real time polymerase chain reaction (qRT-PCR) | 56 |
| 2.2.3.1 RNA extraction | 56 |
| 2.2.3.2 Assessment of RNA yield and quality | 57 |
| 2.2.3.3 Reverse transcription polymerase chain reaction (RT-PCR) | 57 |
| 2.2.3.4 Primers validation | 58 |
| 2.2.3.5 Quantitative polymerase chain reaction (qPCR) | 59 |
| 2.2.3.6 Data analysis | 59 |
| 2.2.4 SDS-PAGE and Western blot | 60 |
| 2.2.4.1 Preparation of cell lysis buffer | 61 |
| 2.2.4.2 Preparation of cell extract | 61 |
| 2.2.4.3 Protein quantification with bicinchoninic acid protein assay..... | 61 |
| 2.2.4.4 Sample preparation and loading | 63 |
| 2.2.4.5 Protein electrophoresis (SDS-PAGE) | 64 |
| 2.2.4.6 Western blot | 64 |
| 2.2.4.7 Chemiluminescence development | 65 |
| 2.2.4.8 Stripping and re-probing of membranes..... | 65 |
| 2.2.4.9 Analysis of Western blot | 66 |
| 2.2.5 Immunohistochemical staining for metformin-transporters expression in a breast tissue microarray | 66 |
| 2.2.5.1 Principles of immunohistochemistry | 66 |
| 2.2.5.2 Protocol for immunohistochemistry | 67 |
| 2.2.5.3 Analysis of immunohistochemical staining | 69 |
| 2.2.6 Assessment of breast cell proliferation and survival | 71 |
| 2.2.6.1 MTS cell proliferation assay | 71 |
| 2.2.6.1.1 Principles of the MTS assay | 71 |
| 2.2.6.1.2 Protocol of the MTS assay | 71 |
| 2.2.6.1.3 Optimization of the MTS assay | 72 |
| 2.2.6.2 Proliferation/viability assay using trypan blue cell counting | 73 |
| 2.2.6.3 BrdU (bromodeoxyuridine) proliferation assay | 74 |
| 2.2.6.3.1 Principles of the BrdU assay | 74 |
| 2.2.6.3.2 BrdU assay protocol | 75 |
| 2.2.7 Cell survival assay | 76 |
| 2.2.7.1 Principles of the clonogenic assay | 76 |
| 2.2.7.2 Clonogenic assay on adherent cells (traditional method)..... | 77 |
| 2.2.7.3 Optimization of the plating densities for the clonogenic assay | 77 |
| 2.2.8 DNA cell cycle analysis..... | 79 |
| 2.2.8.1 Principles of cell cycle analysis | 79 |
| 2.2.8.2 Sample preparation..... | 80 |
| 2.2.8.3 Flow cytometry analysis..... | 80 |
| 2.2.9 Scratch wound-healing assay | 81 |
| 2.2.9.1 Optimization of the scratch wound healing assay | 81 |
| 2.2.9.2 Optimization of the starvation period..... | 82 |
| 2.2.9.3 Optimization of the migration time period..... | 82 |
| 2.2.9.4 Control proliferation experiment | 84 |
| 2.2.9.5 Wound healing assay protocol | 85 |
| 2.2.10 Mass spectrometry-proteomic analysis..... | 86 |
| 2.2.11 Statistical analysis | 87 |
| Chapter 3: Analysis of metformin-transporters expression, <i>in vitro</i>..... | 88 |
| 3.1 Introduction | 88 |
| 3.2 Methods | 93 |
| 3.3 Results | 94 |
| 3.3.1 Evaluation of metformin-transporter genes expression in the tumour and non-tumour breast cell lines | 94 |

| | |
|---|------------|
| 3.3.2 Evaluation of metformin-transporter proteins in the tumour and non-tumour breast cell lines..... | 96 |
| 3.3.3 Analysis of metformin-transporter expression in human breast tissues | 99 |
| 4.4 Discussion..... | 106 |
| Chapter 4: Evidence of anti-Cancer effects of clinically relevant doses of metformin, <i>in vitro</i> | 112 |
| 4.1 Introduction | 113 |
| 4.2 Methods | 114 |
| 4.3 Results | 115 |
| 4.3.1 Comparison of growth rate between tumour and non-tumour breast cell lines | 115 |
| 4.3.2 Assessment of the anti-proliferative effect of metformin using MTS assays... | 117 |
| 4.3.3 The effects of metformin on breast cells number and viability as assessed by trypan blue exclusion assay | 120 |
| 4.3.4 The effects of metformin on DNA replication activity of the breast cells as measured by the BrdU assay..... | 125 |
| 4.3.5 Assessment of the anti-survival effect of metformin using clonogenic assays | 128 |
| 4.3.6 The effects of metformin on cell cycle progression in breast cells | 130 |
| 4.3.7 Assessment of the anti-migration effect of metformin as measured by in vitro scratch wound healing assay | 133 |
| 4. Discussion..... | 135 |
| Chapter 5: Comparative proteomic analysis of differentially-expressed proteins in response to metformin in metastatic breast cancer cell lines | 145 |
| 5.1 Introduction | 145 |
| 5.2 Methods | 147 |
| 5.2.1 Label-free quantification (LFQ) proteomics..... | 147 |
| 5.2.2 SILAC-based quantitative proteomics | 150 |
| 5.2.3 Data analysis and statistical methods..... | 153 |
| 5.2.4 Determination of the labelling efficiency with heavy-SILAC-labelled MDA-MB-231 | 154 |
| 5.3 Results | 155 |
| 5.3.1 Metformin action- label free quantification; proteomics pilot-experiment | 155 |
| 5.3.1.1 Label free quantification's data correlation and quality check | 155 |
| 5.3.1.2 Proteins identified and candidate selection | 158 |
| 5.3.1.3 Global pathway regulation in response to metformin treatment | 163 |
| 5.3.1.4 Verification of protein expression for selected targets using Western blotting | 167 |
| 5.3.2 Spike-In SILAC (SIS)-labelled proteomics quantification: first run | 171 |
| 5.3.3 SILAC-based proteomics analysis of the repeat dataset..... | 172 |
| 5.3.3.1 Method | 172 |
| 5.3.3.2 Quality-check and sample correlation | 172 |
| 5.3.3.3 Inter-group comparison and candidate selection; proteins detected exclusively in either parental, bone or lung homed cells | 174 |
| 5.3.3.4 Inter-group comparison of metformin-untreated mammary cancer cells..... | 181 |
| 5.3.3.5 Global pathway regulation in response to metformin treatment within the Spike-In SILAC (SIS) proteomics experiment | 185 |
| 5.3.3.6 Re-testing for candidate proteins identified in the pilot study | 188 |
| 5.4 Discussion..... | 190 |
| 5.4.1 Quantitative proteomic analysis of metformin-action within breast cancer: current knowledge and literature gaps | 190 |
| 5.4.2 Comparison of cell lines by global proteomics | 191 |
| 5.4.3 Issues in performing proteomics studies using cell lines..... | 195 |
| 5.4.3.1 Candidate selection | 195 |
| 5.4.3.2 Technical issues and methodological constraints..... | 196 |
| 5.4.4 Candidate proteins | 197 |

| | |
|--|------------|
| 5.4.4.1 Tumour necrosis factor alpha-induced protein 8 (TNFAIP8, 21kDa) | 197 |
| 5.4.4.2 Growth factor receptor-bound protein 2 (25 kDa) | 198 |
| 5.4.4.3 Signal transducer and activator of transcription-3 (85 kDa) | 200 |
| 5.4.4.4 Translocator protein (TSPO, 18kDa) | 203 |
| 5.4.4.5 Calmodulin (17 kDa)..... | 204 |
| Chapter 6: General discussion..... | 204 |
| 6.1 General limitations of the this thesis | 215 |
| 6.2 Final conclusion | 217 |
| References | 217 |
| Supplementary materials..... | CD |
| Supplementary material S1: Raw data (Ct values) of metformin transporter mRNAs expression..... | CD |
| Supplementary material S2: Uncropped blots of metformin transporter proteins expression..... | CD |
| Supplementary material S3: Un-cropped blots of the 5 candidates identified in the label-free quantification experiment..... | CD |
| Supplementary material S4: Representative scatter plots of all aligned charge group intensities from paired samples; SILAC-based experiment..... | CD |
| Supplementary material S5: Excel spread sheet of the SILAC-based experiment raw data..... | CD |

List of Figures

| | |
|---|-----|
| Figure 1.1: Schematic representation of the basic anatomical structure of the breast. | 2 |
| Figure 1.2: Schematic drawing of the model of multi-step breast cancer evolution and some of the factors involved in each step. | 9 |
| Figure 1.3: The steps involved in breast cancer-cell metastasis from a primary site to distant organs. | 18 |
| Figure 1.4: Metformin structure and synthesis. | 21 |
| Figure 1.5: Putative determinants of metformin's kinetics in main organs. | 22 |
| Figure 1.6: The proposed direct (non-insulin mediated) and indirect (insulin mediated) effects of metformin in oncology. | 32 |
| Figure 1.7: Doses of metformin used in preclinical and clinical studies. | 40 |
| Figure 1.8: Requirements of the direct effect of metformin on tumour cells, compared to the indirect effect. | 42 |
| Figure 2.1: Microscopic appearance of the cell lines utilized. | 53 |
| Figure 2.2: Serial dilutions of 1 molar metformin stock solution. | 56 |
| Figure 2.3: The scheme of Western blot. | 60 |
| Figure 2.4: BCA standard curve example. | 63 |
| Figure 2.5: Principles of immunohistochemistry. | 67 |
| Figure 2.6: Immunohistochemical analysis of transporter proteins staining on normal breast tissues. | 70 |
| Figure 2.7: Generalized scheme of the MTS cytotoxicity assay. | 72 |
| Figure 2.8: Optimisation of the MTS assay (n=3). | 73 |
| Figure 2.9: BrdU cell proliferation assay principles. | 75 |
| Figure 2.10: Traditional clonogenic assay setting up. | 77 |
| Figure 2.11: Plating densities for the clonogenic assay. | 78 |
| Figure 2.12: A schematic representation of the cell cycle, including the flow cytometric components of each phase. | 79 |
| Figure 2.13: A representative cell cycle analysis of untreated MDA-MB-231 cells using FACSDiva 8.0.1 software. | 81 |
| Figure 2.14: Optimisation of the migration time period. Images were taken at different time points post scratch of untreated cells. | 83 |
| Figure 2.15: A representative picture of the effect caused by different doses of mitomycin C on MDA-MB-231 monolayers. | 84 |
| Figure 2.16: Control proliferation experiment. | 85 |
| Figure 2.17: Calculation of the percentage of wound closure. | 86 |
| Figure 3.1: Baseline expression of metformin-transporter genes and proteins in normal organs and tissues. | 89 |
| Figure 3.2: An <i>in vitro</i> model of breast cancer and disease progression. | 91 |
| Figure 3.3: Expression profiling of the cation-selective transporters OCT1-3, PMAT, MATE1 and MATE2 mRNAs in various human breast cell lines. | 95 |
| Figure 3.4: Representative cropped Western blots of transporter expression in normal, pre-malignant, pre-invasive, invasive, bone-homed breast cell lines and hepatoma cell control (HepG2). | 97 |
| Figure 3.5: Representative Western blot analysis of metformin-transporter proteins expression (OCT1-3, PMAT and MATE1-2) by all breast cell lines. | 98 |
| Figure 3.6: Expression of metformin transporters OCT1-3, PMAT and MATE1-2 in a spectrum of breast tissue lesions. | 102 |

| | |
|---|-----|
| Figure 3.7: Examples of metformin uptake transporters staining (OCT1 and OCT2) in human breast tissues | 103 |
| Figure 3.8: Examples of metformin uptake transporters staining (OCT3 and PMAT) in human breast tissues..... | 104 |
| Figure 3.9: Examples of metformin extrusion transporters staining (MATE1 and MATE2) in human breast tissues..... | 105 |
| Figure 4.1: The growth curves of normal, premalignant, pre-invasive, invasive and the fully bone-homed human breast cells | 116 |
| Figure 4.2: Clinically relevant concentrations of metformin reduced the viability of the non-tumorigenic (MCF10A), premalignant (MCF10AT) and pre-invasive (DCIS) cells | 118 |
| Figure 4.3: Clinically relevant doses of metformin reduce the growth and viability of the premalignant cells and suppress the proliferation of invasive cells without affecting their viability. | 122 |
| Figure 4.4: Experimentally relevant doses of metformin significantly reduced the proliferation in all cell cultures after 72 hours of treatment. | 125 |
| Figure 4.5: Metformin is able to significantly suppress colony formation at the lowest concentration of 0.03mM in all cell lines tested..... | 128 |
| Figure 4.6: Metformin induced cell cycle arrest in the premalignant and pre-invasive breast cells. | 130 |
| Figure 4.7: Metformin induced cell cycle arrest in the invasive and fully bone-homed breast cancer cells. | 131 |
| Figure 4.8: The migration of invasive breast cancer cells is reduced by metformin treatment. | 133 |
| Figure 5.1 : Schematic workflow of the mass spectrometry method..... | 148 |
| Figure 5.2: Schematic depiction of the experimental setup and subsequent workflow used for proteomic analysis of cell lines of interest. | 154 |
| Figure 5.3: Reproducibility assessment of the label-free quantification data..... | 157 |
| Figure 5.4: Networks identified by STITCH analysis and the patterns of interaction between the proteins up and down-regulated by metformin, with non-connected nodes removed. | 165 |
| Figure 5.5: Metformin modulates key biological processes and pathways in metastatic breast cancer cells. | 166 |
| Figure 5.6: Representative cropped Western blots of target protein expression (TNFAIP8, GRB2, STAT3, TSPO and calmodulin). | 169 |
| Figure 5.7: Representative Western blot analysis of target protein expression (TNFAIP8, GRB2, STAT3, TSPO and Calmodulin). | 170 |
| Figure 5.8: Example of an LC-MSMSMS-spectrum showing the separation pattern of polyethylene glycol (PEG)-like detergent. | 172 |
| Figure 5.9: Reproducibility assessment of the SILAC-based quantification data. | 173 |
| Figure 5.10: Key biological processes and pathways modified by metformin treatment in the parental, bone and lung metastatic breast cancer cells..... | 184 |
| Figure 5.11: Networks identified by STITCH analysis showing the pattern of interactions between the proteins up-regulated by metformin treatment in the three cell lines, with non-connected nodes removed. | 185 |
| Figure 5.12: GRB2 mediates signalling between various receptor tyrosine kinases (RTKs) and the Raf/MEK/AMPK and PI3K/ERK pathways..... | 198 |
| Figure 5.13: Activation and regulation of the STAT3 signalling pathway. | 200 |
| Figure 6.1: Mechanisms by which metformin is therapeutically beneficial in LKB1-positive and LKB1-negative cancer cells. | 211 |

List of Tables

| | |
|--|-----------|
| Table 1.1: Classification of benign breast diseases and relative risk of invasive breast cancer..... | 3 |
| Table 1.2: Intrinsic subtypes of breast cancer..... | 11 |
| Table 1.3: Metformin-transporter proteins; their localization, site of expression and potential functions..... | 24 |
| Table 1.4: Observational studies of metformin in breast cancer..... | 28 |
| Table 1.5: Proposed mechanisms of anti-neoplastic effect of metformin (direct and indirect) | 34 |
| Table 1.6: Metformin trials in non-diabetic breast cancer patients..... | 38 |
| Table 2.1: General materials listed with suppliers | 45 |
| Table 2.2: Commercial kits and suppliers | 46 |
| Table 2.3: Items listed with suppliers | 46 |
| Table 2.4: MCF10A growth medium..... | 47 |
| Table 2.5: MCF10AT and DCIS.com cell culture and assay medium | 48 |
| Table 2.6: MCF7, T47D, MDA-MB-231, MDA-MB-231(BM) and HepG ₂ cell culture and assay medium..... | 48 |
| Table 2.7: MDA-MB-231(LM) cell culture and assay medium..... | 49 |
| Table 2.8: Metformin-transporters validated All-in-One™ qPCR Primers ID and sequences (GeneCopoeia) | 49 |
| Table 2.9: Tissue microarray slides used in this project | 50 |
| Table 2.10: Primary antibodies | 50 |
| Table 2.11: Secondary antibodies | 51 |
| Table 2.12: Classification and characteristics of the invasive breast cancer cell lines used | 52 |
| Table 2.13: Components of the reverse transcription master mix | 58 |
| Table 2.14: Preparation of different concentrations of protein standards of BSA and dH ₂ O..... | 62 |
| Table 2.15: Total number of breast tissue cases from TMA slides used in this project | 68 |
| Table 3.1: Metformin transporters | 90 |
| Table 3.2: Analysis of metformin transporter gene expression relative to GAPDH..... | 94 |
| Table 4.1: Summary of the cell lines used in this chapter and their population doubling times (PDTs) | 116 |
| Table 4.2: Analysis of the inhibition in cellular metabolic activity following 72 hours of metformin treatment | 119 |
| Table 4.3: Analysis of the reduction in viable cells number following 72 hours of metformin treatment..... | 123 |
| Table 4.4: Analysis of the inhibition in BrdU incorporation in breast cells following 72 hours of metformin treatment | 126 |
| Table 5.1: An illustration of the sample mixing. | 151 |
| Table 5.2: Proteins identified as significantly differentially expressed within the parental MDA-MB-231 PCC cell-line and its bone homed (BM) variant from pilot the Label-free quantification (LFQ) study..... | 160 |
| Table 5.3: Proteins identified as significantly differentially expressed within the parental MDA-MB-231 (PCC) and its bone (BM) and lung (LM) homed variant cell lines. | 175 |

| | |
|---|-----|
| Table 5.4: Proteins identified as significantly differentially expressed within the untreated bone and lung homing cells compared to the parental MDA-MB-231 cell-line. | 180 |
| Table 5.5: Proteins identified as potential targets and reasons why not further validated by Western blot | 182 |
| Table 5.6: Re-test of candidate proteins within the Spike-In SILAC (SIS)-analysis data identified as potential targets for metformin. | 187 |

List of Abbreviations

| | |
|-----------------------|---|
| ABC | Avidin-Biotin Complex |
| ACE | Acetyl-CoA Carboxylase |
| ACN | Acetonitrile |
| ADH | Atypical Ductal Hyperplasia |
| Akt | Protein Kinase B |
| AMP | Adenosine Monophosphate |
| AMPK | Adenosine Monophosphate-Activated Protein Kinase |
| ANOVA | Analysis of Variance |
| ATCC | American Tissue Culture Collection |
| ATP | Adenosine Triphosphate |
| BC | Breast Cancer |
| BRCA1, BRCA2 | Breast Cancer Antigen 1 and 2 |
| BrdU | 5-Bromo-2-Deoxyuridine |
| BSA | Bovine Serum Albumin |
| °C | Degree Celsius |
| CCL | Columnar Cell Lesions |
| CD44/CD24 | Cluster of Differentiation 44/24 |
| cDNA | Complementary DNA |
| Cmax | Maximum (or Peak) Serum Concentration |
| CRP | C-reactive Protein |
| CSCs | Cancer Stem Cells |
| CO₂ | Carbon Dioxide |
| Ct | Cycle Threshold |
| DAB | 3,3'-Diaminobenzidine |
| DCIS | Ductal Carcinoma <i>in situ</i> |
| DDT | Dithiothreitol |
| DMEM | Dulbecco's Modified Eagle Medium |
| DMEM/F12 | Dulbecco's Modified Eagle Medium: Nutrient Mixture F-12 |
| DMSO | Dimethyl Sulfoxide |
| DNA | DeoxyriboNucleic Acid |
| dNTP | Deoxyribonucleotide Triphosphate |
| ECM | Extracellular Matrix |
| EDTA | Ethylenediaminetetraacetic Acid |
| EGF | Epidermal Growth Factor |
| EGFR | Epidermal Growth Factor Receptor |
| EMT | Epithelial–Mesenchymal Transition |
| ER | Oestrogen Receptor |
| FACS | Fluorescence-Activated Cell Sorting |
| FCD | Fibrocystic Disease |
| FCS | Foetal Calf Serum |
| FSC | Forward Scatter |

| | |
|-----------------|--|
| g | Gram |
| g/l | Gram/litre |
| GAPDH | Glyceraldehyde 3-Phosphate Dehydrogenase |
| GPCR | G-protein Coupled Receptor |
| GRB2 | Growth Factor Receptor-Bound Protein 2 |
| HER2 | Human Epidermal Growth Factor Receptor 2 |
| HELU | Hyperplastic Enlarged Lobular Unit |
| HIER | Heat Induced Epitope Retrieval |
| HRP | Horseradish Peroxidase |
| Hrs | Hours |
| IBC | Invasive Breast Cancer |
| IDC | Invasive Ductal Carcinoma |
| IGF1 | Insulin-Like Growth Factor-1 |
| IGFBP | Insulin-Like Growth Factor -Binding Protein |
| IHC | Immunohistochemistry |
| IL6 | Interleukin-6 |
| ILC | Invasive Lobular Carcinoma |
| IRS | Insulin Receptor Substrate |
| JAK | Janus Kinase |
| KEGG | Kyoto Encyclopedia of Genes and Genomes |
| L | Litre |
| LC | Liquid Chromatography |
| LC-MS/MS | Liquid Chromatography Tandem Mass Spectrometry |
| LFQ | Label-Free Quantification |
| LKB1 | Liver Kinase B1 or STK11: Serine-Threonine kinase 11 |
| LTQ | Linear Trap Quadrupole |
| MATE | Multidrug and Toxin Extrusion Protein |
| MAPK | Mitogen-Activated Protein Kinase |
| MCF7 | Michigan Cancer Foundation-7 |
| MEGM | Mammary Epithelial Cell Growth Medium |
| µg | Microgram |
| µl | Microliter |
| ml | Millilitre |
| mM | Millimolar |
| MMC | Mitomycin C |
| MMP | Matrix Metalloproteinase |
| mol/l | Moles per Litre |
| ms | Milliseconds |
| MS | Mass Spectrometry |
| mTOR | Mammalian Target Of Rapamycin |
| mTORC1 | Mammalian Target Of Rapamycin Complex 1 |
| MW | Molecular Weight |
| NF-κB | Nuclear Factor-κB |

| | |
|----------------------|--|
| O₂ | Oxygen |
| OCT | Organic Cation Transporter |
| OD | Optic Density |
| PBR | Translocator Protein (TSPO) |
| PBS | Phosphate Buffered Saline |
| PBST | Phosphate Buffered Saline Tween |
| PCA | Principle Component Analysis |
| PCR | Polymerase Chain Reaction |
| PEG | Polyethylene Glycol |
| PI | Propidium Iodide |
| PI3K | Phosphatidylinositol-3-Kinase |
| PMAT | Plasma Membrane Monoamine Transporter |
| PR | Progesterone Receptor |
| qRT-PCR | Quantitative Real Time Polymerase Chain Reaction |
| RCC | Respiratory Chain Complex |
| RNA | Ribonucleic Acid |
| rpm | Revolutions per minute |
| RPMI-1640 | Roswell Park Memorial Institute 1640 |
| RT | Reverse Transcription |
| RTK | Receptor Tyrosin Kinase |
| SDS-PAGE | Sodium Dodecyl Sulfate Polyacrylamide Gel Electrophoresis |
| SEM | Standard Error of Mean |
| SILAC | Stable Isotope Labelling By Amino Acids |
| SIS | Spike-In SILAC |
| SREs | Skeletal-related Events |
| SSC | Side Scatter |
| STAT3 | Signal Transducer And Activator Of Transcription 3 |
| T2DM | Type 2 Diabetes Mellitus |
| TDLU | Terminal Ductal Lobular Unit |
| TGF-β | Tumour Growth Factor β |
| TLR-4 | Toll-Like Receptor 4 |
| TMA | Tissue Microarray |
| TMB | 3,3',5,5'-Tetramethylbenzidine |
| TN | Triple Negative |
| TNBC | Triple Negative Breast Cancer |
| TNFAIP8 | Tumour Necrosis Factor Alpha-Induced Protein 8 |
| TSC2 | Tuberous Sclerosis Complex 2 |
| TUNEL | Terminal Deoxynucleotidyl Transferase dUTP Nick End Labeling |
| v/v | Volume/Volume |
| VEGF | Vascular Endothelial Growth Factor |
| VEGFR | Vascular Endothelial Growth Factor Receptor |

1. Chapter 1: Introduction

1.1 The Breast

1.1.1 Breast anatomy and development

Adolescent female breast development commences at puberty in response to cyclical oestrogen and progesterone secretion. The main function of the breast is milk production. The acinus or terminal ductal-lobular unit (TDLU) represents the fundamental functional glandular unit of the breast and the biological most actively proliferating part and hence the more susceptible to mutative changes. The TDLU comprises the lobules and its paired terminal ducts, which are lined by columnar epithelium, supported by myoepithelial cells, a basement membrane and embedded in specialized hormonally responsive fibro-fatty stroma. The acini are interconnected by a series of branches of ducts, which increase in calibre until they terminate and exit the breast at the nipple via several major lactiferous ducts (Figure 1.1).

Throughout the lifetime, there are three main periods that constitute the breast life cycle; these are the early reproductive life (lobular development), mature reproductive life (cyclical hormonal modifications) and involution. These changes occur in response to the alteration in hormonal levels of oestrogen and progesterone. The aberration of normal development and involution of the breast (ANDI) includes a variety of benign breast lesions such as fibroadenoma, cystic diseases and sclerosis¹.

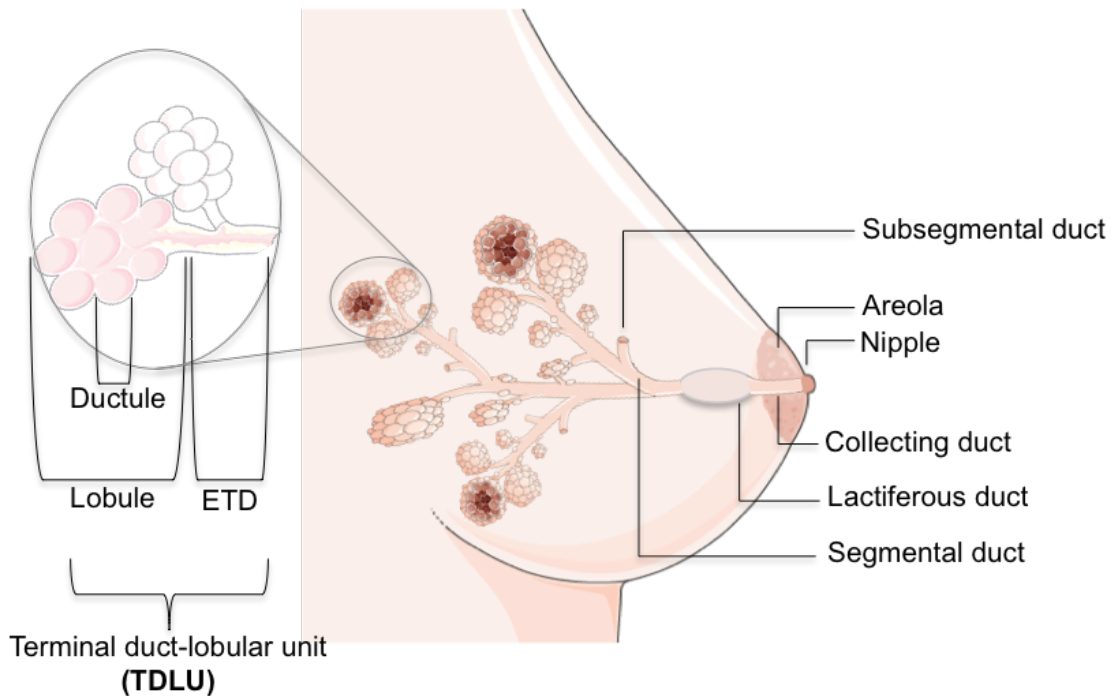


Figure 1.1: Schematic representation of the basic anatomical structure of the breast.

The normal female breast contains tens of thousands of lobules; each of these lobules composed of small grape-like clusters of glandular tissues that lined by the functional epithelial cells, which specialized to produce milk. The lobules are interconnected by milk ducts, which join to form larger ducts that eventually open into the nipple. ETD: Extralobular terminal duct (This figure was produced using Servier Medical Art: <http://www.servier.com/Powerpoint-image-bank>).

1.1.2 Benign breast disease and subsequent risk of breast cancer

Based on the degree of proliferation and atypia, benign lesions of the breast are histologically classified into three categories: non-proliferative, proliferative without atypia and atypical hyperplasia² (Table 1.1). It is noteworthy that the fibrocystic changes (FCCs) constitute the most common benign diseases of the breast, which comprises both cystic and solid lesions. However, it is currently evaluated under the three category classification system depending on the presence or absence of cellular atypia^{2,3}.

Table 1.1: Classification of benign breast diseases and relative risk of invasive breast cancer

| Class | Types | Relative risk for invasive breast cancer |
|--|---|---|
| Non-proliferative breast lesions | Breast cysts Papillary apocrine change Mild hyperplasia of usual type (UTH) Apocrine metaplasia Non-sclerosing adenosis Mammary duct ectasia | No increased risk ⁴ |
| Proliferative breast lesions without atypia | Moderate or florid UTH Sclerosing adenosis Radial scar Intra-ductal papilloma | Slightly increased risk (1.5-2 times) ⁴ compared with women who have not had a breast biopsy |
| Proliferative breast lesions with atypia | Atypical ductal hyperplasia (ADH) Atypical lobular hyperplasia (ALH) | Moderately increased risk (4-5 times, in 10 years) ⁵ , if associated with family history of breast cancer, the absolute risk rises to 20-25% |

1.1.3 Pre-malignant breast diseases

1.1.3.1 Atypical hyperplasia (Ductal and lobular)

For several decades atypical hyperplasia was known to be one of the few benign conditions that has a significant increased risk for developing breast cancer⁶⁻⁹. Epithelial hyperplasia is an increase in the number of cells lining the TDLU that can be histologically graded into mild, moderate and severe. Atypical hyperplasia (AH) is diagnosed if the hyperplastic cells show evidence of cellular atypia. Atypical hyperplasia can consist of cells with lobular or ductal morphology. Lesions exhibiting an intra-ductal monomorphic cellular proliferation that display all histological characteristics of ductal carcinoma *in situ* but measure less than 2mm are diagnosed as atypical ductal hyperplasia (ADH). However, atypical lobular hyperplasia (ALH) is now classified with lobular carcinoma *in situ* as a well-established histopathological entity called lobular intraepithelial neoplasia (IEN)¹⁰.

ADH is recognised as a mid-point in the histological spectrum of invasive breast cancer (IBC) evolution. Until recently, it was accepted that usual type hyperplasia (UTH) constitutes a non-obligate precursor of ADH and ductal carcinoma

in situ (DCIS)⁶. Perhaps the most persuasive histological evidence to suggest that UTH and ADH are progressive stages of an evolutionary continuum is based on the association between UTH lesions that showed relative over-expression of oestrogen receptors by their heterogeneous hyperplastic cell population and the pivotal role of oestrogen in promoting the growth and proliferation of cancer cells⁸. However, in the majority of UTH lesions no evidence of neoplasia is observed with only rare if any random chromosomal changes.

Recently, columnar cell lesions (CCLs) have been identified as the more likely precursor to ADH and DCIS (well-differentiated type) and these represent the link between normal breast and ADH¹⁰. CCL is characterized by the presence of columnar epithelial cells, which are tightly packed. Other features include ovoid nuclei, intraluminal secretions and prominent apical cytoplasmic snouts¹⁰.

Despite the plethora of available information, it remains a central issue to determine whether to consider the atypical hyperplastic lesions as precursor lesions or risk markers for IBC, particularly as IBCs do not necessarily develop in the same anatomical area of atypia but might subsequently occur in the contralateral breast. Nonetheless, it is well accepted that ADH is the non-obligate precursor of the well-differentiated DCIS. Moreover, the differentiation between ADH and DCIS is in fact arbitrary and subjective, as the similarities between them are not restricted to the morphological features only, but also their genetic and immunohistochemical features; which for example includes loss of heterozygosity at loci of 16q and 17p chromosomes¹¹⁻¹⁴.

1.1.3.2 *In situ* carcinomas (Ductal and Lobular)

In the UK, due to its increasing incidence, *in situ* breast carcinoma has become a formidable clinical challenge. Since the early 1990s, the incidence rates of *in situ* breast cancers increased by more than 172% with the peak incidence rates being in females in their 50-60s¹⁵. *In situ* carcinomas refer to the epithelial cells that still reside in their normal place within the breast ducts but have become cancerous. The malignant cells can accumulate within the ducts and lobules causing them to be greatly expanded, but do not break through the basement membrane. It can be further

subdivided into ductal carcinoma *in situ* (DCIS) and lobular carcinoma *in situ* (LCIS)¹⁶.

Ductal carcinoma *in situ* (DCIS) is the earliest stage of breast cancer (stage 0) and the most common type of *in situ* breast carcinoma, representing 80-90%. The widespread introduction of mammographic screening has dramatically increased the frequency of DCIS detection, where the majority of lesions are detected as mammographic micro-calcifications and confirmed by biopsy¹⁷. Around 4,800 cases of DCIS are diagnosed each year in the UK accounting for 25-30% of all newly diagnosed breast cancer (BC) cases (approximately 1 in 4 BC cases)¹⁸.

Although DCIS is a non-invasive malignancy, if left untreated, up to 30-50% of the cases could progress to invasive BC, particularly the high grade DCIS which tend to progress more rapidly than the low and moderate grade lesions¹⁹. For this reason, currently, all DCIS cases are treated as potentially invasive as neither the significant drivers of the invasive transition nor a robust marker to identify cases that have the potential to progress to IBC from those that are unlikely to, have been identified.

ADH is thought to be a precursor lesion of low-grade ductal carcinoma *in situ* whereas the high-grade ductal carcinoma *in situ* has no obvious precursor lesion and tends to develop into high-grade invasive disease^{16, 20}. Generally, DCIS lesions have a relative risk of 8 to 11-fold for the development of subsequent IBC^{20, 21}.

It is commonly accepted that DCIS is the immediate non-obligate precursor of the majority of IBCs cases, due to the fact that there is an evolutionary continuum between them where they affect the same anatomical site. This occurs as follows. In DCIS, the lumen of the ductal tree becomes filled with proliferating pre-cancerous and cancerous cells but is separated from the surrounding stromal compartments by the intact myoepithelial–basement membrane interface¹⁷. At some point during progression, cancer cells breach the myoepithelial cell layer to the interstitial matrix and become an established IBC with metastatic potential. Recent work by Allen and colleagues discovered changes occur in the myoepithelial cells that switch their behaviour from being tumour-suppressor to cancer promoting and that up-regulation of the $\alpha\beta 6$ on the myoepithelial cells might be used as a potential tumour marker to predict disease progression and recurrence²².

Based on the expression patterns of oestrogen, progesterone and human epidermal growth factor 2 receptors, DCIS can be classified into similar molecular subtypes as IBC^{17, 23-25}. This is because, histologically, the only major difference between DCIS and IBC is often that IBC does not retain an intact basement membrane.

Historically, the classification of DCIS was based on the most predominant microscopic growth pattern where it was broadly classified into five recognised subtypes which include comedo (a central area of necrosis surrounded by a layer of malignant cells), cribriform (glandular lumina formed by radially oriented malignant cells), solid (ducts are filled with malignant cells), micropapillary (finger-like papillary projections extend into the ductal spaces) and papillary (large papillae with fibrovascular stalks)²⁶. However, some overlap in the architectural features usually exist. Other prognostic features such as the presence or absence of necrosis, polarization (architectural differentiation) and nuclear grade (low, intermediate or high) were not traditionally taken into account. A relatively recent method of classification is based on the degree of differentiation of the tumour cells (the degree of tumour cell resemblance to normal cells) as well as the rate of cell proliferation. There are also several histological grading systems that assign scores based on certain cellular features such as size and shape of the nucleus, mitotic figures, amount of necrosis and the degree of gland or papillae formation. The most commonly recognized grades are well, moderately, and poorly differentiated DCIS corresponding to grade 1, 2 and 3 respectively¹⁶.

If detected, current management strategies for DCIS is actually quite effective, namely, breast-conserving surgery followed by radiotherapy and/or selective oestrogen modulator (e.g., Tamoxifen), is the treatment option in the vast majority of the patients. However, there is growing concern that the majority may never develop aggressive IBC and therefore these patients are unnecessarily over-treated.

1.1.4 Invasive breast carcinomas

Invasive breast cancer (IBC) emerges through a multistep process or a non-obligatory series of increasingly abnormal stages that can be broadly attributed to the transformation of normal epithelial cells. The multistep model of breast carcinogenesis suggested the existence of a continuum in the transition from normal to IBC via atypical hyperplasia and *in situ* carcinoma, over long periods of time, plausibly few decades in most cases²⁷. However, this process is non-obligatory in nature and only a small proportion of atypical ductal carcinoma lesions progress to invasive carcinomas.

Although the morphological classification of pre-invasive breast lesions remains controversial, there is a consensus that the risk of IBC development correlates with the degree of cellular proliferation and atypia. Initiation, invasion and metastasis of BC are highly complex series of events, involving the interaction between multiple cell types and the microenvironment²⁷. Figure 1.2 shows the current consensus of the evolution of invasive breast cancer based on the modified Wellings Jensen model of breast cancer evolution and some of the factors that influence this multigenic, multi-step process. This model of breast cancer evolution based almost entirely on the evidence of histologic continuity between the hyperplastic breast epithelial cells; which gradually enlarge to form hyperplastic epithelial lobular units (HELUs), which may progress to more complex lesions including ADH and DCIS. As the cells continue to proliferate and distend the acini the DCIS may eventually progress to invasive breast cancer^{6, 28}. In the context of this multistep cascade, it is crucial to distinguish between tumour formation, tumour progression and metastasis. Tumorigenesis refers to the ability of a cell to proliferate constantly in the absence of stimulation by the initiating carcinogenic agents, while tumour progression refers to the evolution of the already transformed tumorigenic populations towards increasing malignancy. Also the terms migration and invasion are not equivalent to metastasis; both of them are necessary, but insufficient to develop metastasis²⁹.

1.1.4.1 Epidemiology of invasive breast cancer

According to the Cancer Registration Statistics, England 2015 (published in May-2017), Breast cancer (BC) was the most common cancer diagnosed in 2015, affecting 46,083 individuals, accounting for 31.2% or 1 in 3 of female cancer

registrations in the UK³⁰. The age-standardised incidence rate of BC has dramatically increased from 163.6 to 170.2 cases per 100,000 females between 2005 and 2015 respectively.

Worldwide, breast cancer (BC) is the most commonly diagnosed cancer in women. According to GLOBOCAN 2012³¹, it represents 11.9% of all cancers. Since 2008, both the incidence and mortality rates of BC have sharply risen by more than 20% and 14% respectively^{31, 32}. In 2012, it accounted for 1.67 million of all newly diagnosed cancers and 552,000 deaths worldwide, corresponding to 25% of all cancer deaths³². Indeed, it is the most frequently diagnosed and the leading cause of death among women globally. This is because it is the foremost cause of cancer mortality in developing countries, whereas in developed countries, it is the second biggest contributor to cancer mortality³³ despite its higher incidence rates³⁴. The death figures are comparatively high in less developed countries because of the less developed facilities for early detection, a lack of education and less advanced management plans³³. It should be pointed out that although breast cancer is 100 times more common in females than males, it also accounts for 2360 newly diagnosed cancers and 430 deaths among men each year in the USA alone³⁵.

1.1.4.2 Aetiology of invasive breast cancer

Some BCs are attributed to the inheritance of a mutation in *BRCA1* and *BRCA2* genes³⁶, accounting for half of those BC patients with strong family history. However, the majority of BCs are sporadic and multifactorial. The two major risk factor categories in this sporadic group are (1) reproductive factors, such as early menarche, late menopause, low parity, hormonal replacement therapies, late first full-term pregnancy and shorter duration of breastfeeding³⁷, most of which are related to prolonged exposure of breast tissues to the growth-promoting effects of oestrogen and the genotoxicity of estradiol metabolites which increase the risk of DNA mutations³⁸; and (2) environmental and lifestyle factors, such as obesity, diet rich in unsaturated fatty acids, physical inactivity, alcohol ingestion, smoking, vitamin D deficiency and environmental contaminants e.g. radiation exposure^{39, 40}, all of which increase the risk of DNA mutations and have been extensively reviewed elsewhere.⁴¹

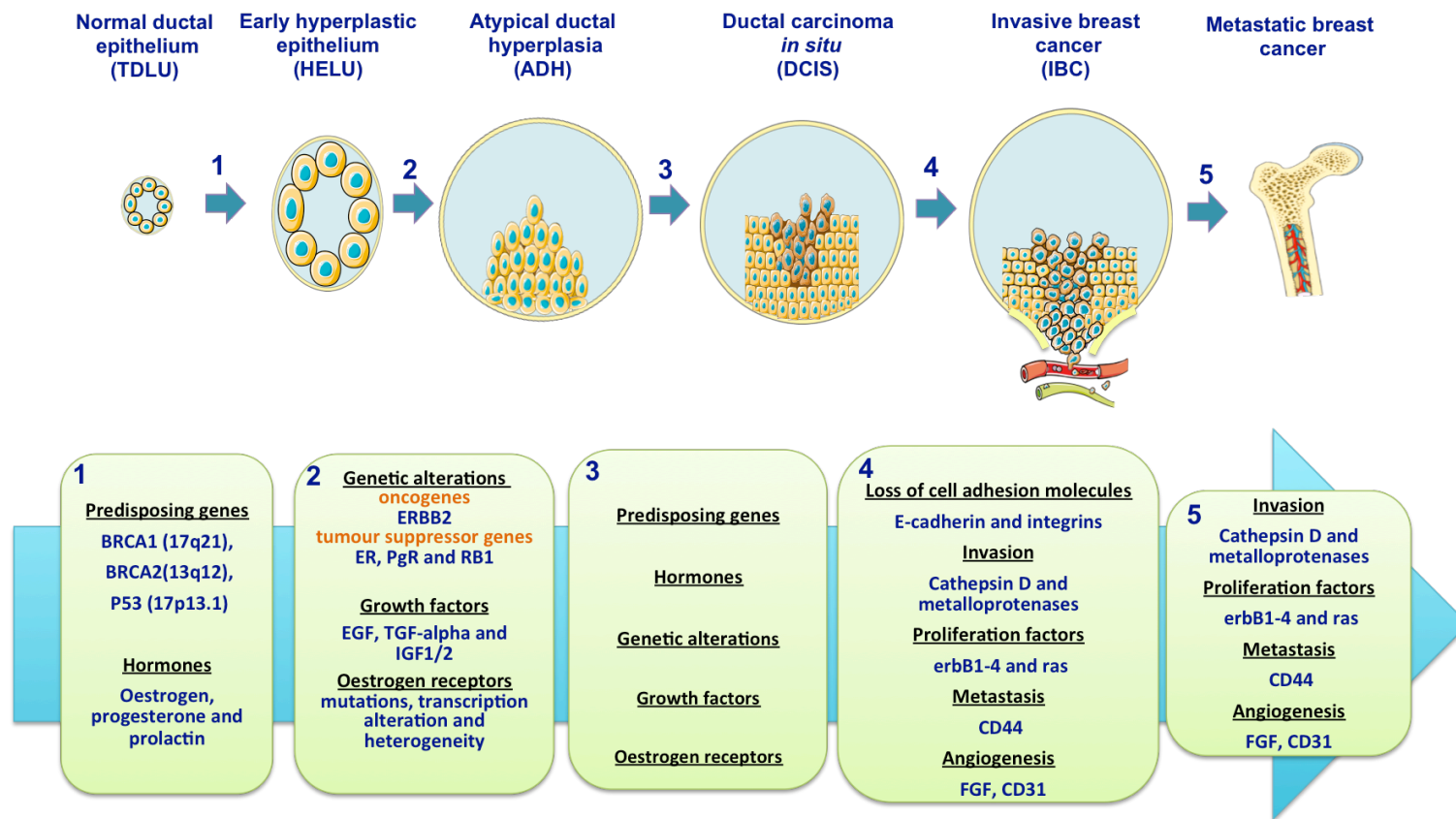


Figure 1.2: Schematic drawing of the model of multi-step breast cancer evolution and some of the factors involved in each step.

The model shows enlargement of TDLU to hyperplastic epithelial lobular units (HELU). The HELU differentiate to more complex lesions such as ADH. ADH may then progress to DCIS and onward to IBC and finally metastasize to distant organs such as bone and lungs. Some factors involved in each step are summarised in the boxes, however, the transformation from ADH to DCIS requires all the factors mentioned in boxes 1 and 2 (adopted from references^{27, 42}, this model was originally proposed by Wellings Jensen²⁸) (Some elements of this figure were produced using Servier Medical Art: <http://www.servier.com/Powerpoint-image-bank>).

1.1.4.3 Classification of invasive breast cancer

Clinically, morphologically and genetically, IBC is a complex and heterogeneous disease. The growth and survival of BC cells is tightly regulated and driven by diverse molecular alterations, which might explain the differences in their therapeutic response and prognosis⁴³. Since its discovery, pathologists have endeavoured to identify a standard morphological classification of BC. It was difficult to adopt the concept that the differences in biological behaviour among different histological subtypes were the only reason behind this heterogeneity⁴⁴. This remained the case until recently when advances in gene expression profiling techniques enabled Perou and colleagues to reveal that the natural biological diversity of different types of BC was due to the diversity of genetic expression of specific genes⁴⁵. This has undeniably changed the biological understanding of the similarity and differences in growth rate, cellular composition, and signalling pathways, not only within, but also among different breast tumours, and as a result has enabled greater tailoring of treatment to the specific type of BC.

Morphologically, the majority of breast carcinomas are invasive ductal carcinomas⁴⁶. However, at the molecular level, recent advances in molecular profiling have demonstrated that there are several distinct molecular subtypes of BC^{6, 24, 47-49}. The main subtype classification is based on their expression of oestrogen, progesterone and human epidermal growth factor-2 receptors (HER-2)⁵⁰.

These subtypes are: luminal A, luminal B, HER2-positive, basal-like, claudin-low and normal breast⁵¹ (Table 1.2). Although triple-negative (TN) and basal-like is an interchangeably used term in clinical practice, 30% discordance has been described between the two groups, and therefore they are non-identical⁵². Both basal-like and claudin-low can be considered as subtypes of TN breast cancer⁴⁶. Moreover, Luminal A and B subtypes can be differentiated further by their expression of Ki67-antigen; low in luminal A / high in luminal B^{53, 54}. High expression of Ki67 has been reported to be associated with increased risk of BC recurrence and mortality⁵⁵ (Reviewed by Eroles *et al.*, 2012⁵⁰). This molecular classification and heterogeneity is extremely important not only for further understanding of pathogenesis and speculating the drivers of BC development, but also for (1) choosing the most appropriate treatment strategies; (2) providing promising targets for most of the currently licensed drugs and

the development of novel agents; (3) enhancing patient response to adjuvant therapy⁵⁶,
⁵⁷; (4) explaining the development of drug resistance; (5) use as biomarkers in predicting the disease outcomes and correlating with clinical prognosis; and (6) opening the horizon for personalized medicine in the near future⁴⁶.

Table 1.2: Intrinsic subtypes of breast cancer

| Receptor type | Receptor status | | | Prevalence |
|----------------------------------|---------------------------------------|----------|----------|--|
| | ER | PR | HER-2 | |
| Luminal A | ER ⁺ and PR ^{+/-} | | Negative | 50-60%, Commonest Low histological grade, low proliferative index, Ki67 low, endocrine and chemotherapy responsive with good prognosis ⁵⁸ |
| Luminal B | ER ⁺ and PR ^{+/-} | | Positive | 10-20% High histological grade, High proliferative index, Ki67 high, usually endocrine responsive, variable response to chemotherapy with poor prognosis ⁵⁹ |
| HER-2 positive | Negative | Negative | Positive | 15-20% Ki67 high, trastuzumab responsive, chemotherapy responsive ⁶⁰ |
| Basal-like or Triple negative | Negative | Negative | Negative | 8-37% Positive for EGFR and/or cytokeratins (5/6), Ki67 high, chemotherapy responsive and endocrine nonresponsive ⁵⁸ |
| Normal breast | Negative | Negative | Negative | 5-10% Express gene characteristics of adipose tissue, do not respond to neoadjuvant chemotherapy ⁵⁸ |
| Claudin-low | Negative | Negative | Negative | 7-14% Claudin (3,4,7) and E-cadherin low (Intercellular adhesion molecules), enriched in epithelial-to-mesenchymal transition (EMT) features, intermediate response to chemotherapy ^{61, 62} |

1.1.4.4 Current treatment strategies of invasive breast cancer

Despite this relatively new knowledge about the molecular subtypes of BC, complete surgical excision of the primary tumour along with selective axillary surgery remains the main stay of treatment. Loco-regional radiotherapy and systemic treatment, including chemotherapy, hormone-therapy and treatment with biological inhibitors targeting the main receptors, such as Trastuzumab targeting HER2, are used mainly as adjuvant therapies⁶³. The ultimate goal of treatment is to reduce the risk of recurrence and improve disease-related morbidity and mortality⁶⁴⁻⁶⁶. There is no doubt that the current management strategies have been greatly influenced by the rapid advances in the field of molecular biology and the ability to identify new molecules to be targeted by novel drugs.

The majority of breast cancer cells express oestrogen receptor (~ 75%), especially in postmenopausal women⁶⁷. The crucial role of oestrogen, the main female sex hormone, in BC growth and development has received considerable attention. It was more than a century ago when Beatson reported a regression of the tumour size and cellular proliferation of advanced inoperable BC after oophorectomy⁶⁸. In light of this finding, it has been postulated that growth of BC can be either regressed or prevented by the use of oestrogen-depriving agents. This concept has rationalized the use of hormonal therapy as an adjunct to surgery and radiotherapy in BC treatment over the past 20 years⁶⁹.

It is noteworthy that oestrogen-depriving agents can reversibly inhibit oestrogen production or block its action with fewer side effects when compared with the cytotoxic effect of chemotherapeutic drugs. However, treatment using anti-hormonal therapy needs to take into consideration that the site of oestrogen biosynthesis varies according to the menopausal status. Oestrogen is produced exclusively by ovaries in premenopausal and synthesised extra-gonadally by fatty, muscular and breast tumour tissues in postmenopausal women^{70, 71}, and therefore the treatment may vary depending on the patient's menopausal status.

For nearly 3 decades, Tamoxifen - a selective oestrogen receptor modulator, has both selective agonistic and antagonistic actions, the former action directed against the deleterious effect of oestrogen on breast and endometrium while the latter potentiates oestrogen-beneficial activity on bone and brain tissues. It had been the

cornerstone of endocrine therapy for patients with ER-positive BC, irrespective of menopausal status. Tamoxifen was approved by US food and drug administration for a full range of breast diseases ranging from chemoprevention to advanced metastatic disease⁷².

However, in postmenopausal women the production of oestrogen relies completely on the peripheral conversion of androgen into estradiol E1 and estron E2 by the aromatase enzyme. Aromatase; a cytochrome P-450 enzyme complex; is a key player that control local biosynthesis of oestrogen within the mammary glands³⁸. Suppression of aromatase activity has been a subject of intensive research since 1970s, when the first aromatase inhibitor; aminoglutethimide, was accidentally discovered during a preliminary trial testing its efficacy as an anticonvulsant drug and reported an inhibition of adrenal glands androgen synthesis as a major side effect⁷³. This resulted in the development of aromatase inhibitors as an alternative effective hormonal strategy to antagonise/block the growth-promoting effects of oestrogen in postmenopausal hormone-sensitive breast cancer by lowering circulating-oestrogen⁷³⁻⁷⁵. However, it is important to note that AIs have no benefits in premenopausal women with functioning ovaries and in postmenopausal with ER-/PR- or HER2+ve subtypes of BC. Generally, the positivity of HER2; the major driver of human BC cells proliferation, is considered as a marker of resistance to anti-oestrogen therapy⁷⁶.

AIs have been developed over the past 40 years to increase their potency and specificity with three different generations of inhibitors recognised. Aromatase inhibitors are classified into three different generations with the 3rd generation being the most potent and specific inhibitors. Furthermore, they are subdivided according to the reversibility of their inhibitory action into: steroidal and non-steroidal molecules. Steroidal aromatase inhibitors attached irreversibly to the substrate-binding site of the aromatase enzyme. In contrast, non-steroidal inhibitors interact reversibly with the heme group of the cytochrome P450 component of the enzyme⁷⁷.

Although both steroidal and non-steroidal aromatase inhibitors are believed to be equally effective, the 3rd generation aromatase inhibitors are specifically highly recommended as a first line endocrine therapy⁶⁶. Currently, three of the third generation aromatase inhibitors, letrozole, anastrozole and exemestane are licenced for postmenopausal ER+ve early BC as primary and extended adjuvant, primary adjuvant, and unplanned switching therapies, respectively⁷⁸. Results from several

randomized clinical studies comparing the efficacy and disease free survival outcome between tamoxifen and AIs have proven the superiority of these agents in terms of lowering the recurrence rate, improving the disease free survival, increasing tolerability, reducing serious side effects such as thromboembolic events and endometrial cancer when compared to tamoxifen^{65, 79}. However, the risk of arthralgia, bone loss and fractures increases dramatically among users of AIs⁸⁰ and needs to be carefully monitored.

1.1.5 Metastatic breast cancer

Tumour metastasis is a term that comprises specific molecular and biological characteristics that together enable the spread of aggressive malignant cells from the primary site to the surrounding tissues and distant organs. It is suggested that the acquisition of metastatic capacity occurs as a late event in tumour progression. Most patients with breast cancer die not because of the primary breast tumour, but rather because of its spread to other distant sites. Metastasis can be viewed as an evolutionary process and is defined as the progressive growth of cancer cells at a site that is distant and discrete from the primary lesion. Tumour cells can disperse into blood vessels, lymphatic vessels, or within body cavities (Figure 1.3).

Currently, it is not possible to precisely predict the risk of breast cancer metastasis development or to determine which organ system will be invaded, although approximately 40% of the patients may suffer relapse and 90% of these patients die of metastatic spread of breast cancer. In an attempt to prevent this almost 80% of patients receive adjuvant cytotoxic chemotherapy, some of them unnecessarily and therefore needlessly suffer the acute and long-term toxic side effects of the chemotherapy^{81, 82}. Despite this, there are some well-established clinical features of the primary breast tumour that are indicative of the risk of metastatic recurrence which include tumour size, histological grade, axillary lymph node status, angioinvasion in patients with negative lymph nodes (the presence of tumour emboli in >3 blood vessels), HER2 gene amplification and steroid receptor expression; the last two in particular, are also used for adjuvant therapy decision⁸³⁻⁸⁷.

Nonetheless, based on the recent advances of genome-wide technologies, primary breast tumours can further be classified into those that have a poor-prognosis signature or a good-prognosis signature, which means they are more

likely or less likely to metastasize, respectively. These signatures can more accurately predict patients who are destined to relapse and should therefore receive adjuvant therapy. This classification is based on the presence/up-regulation or absence/down-regulation of specific genes; for example, the poor-prognosis signature included the up-regulation of genes involved in signal transduction, cell cycle, angiogenesis, invasion and metastasis. Interestingly, up-regulation of genes that are exclusively highly expressed by the tumour stromal cells is also involved in the poor-prognosis signature for breast cancer metastasis; an example is the matrix metalloproteinases genes (MMP1 and MMP9) which are essential for the degradation of extracellular matrix (ECM) and tumour invasion⁸⁸.

Under the influence of several factors, different primary tumours metastasize to distinct secondary organs. These factors include, the origin of cancer cells, the aggressiveness of the primary tumour type, the direction of circulation, and the ability of cells to homogenize with the supporting components of the new microenvironment. The genetic determinants underlying each of these factors are largely distinct from those that mediate the malignant transformation of breast cells. One of the most interesting biological aspects of metastasis is the remarkably variable pattern of organ dissemination. The dissemination of cancer cells frequently involves invasion through the lymphatic system to local lymph nodes, however, some aggressive cells typically invade the bloodstream and reach distant tissues⁸⁹.

Breast cancer primarily metastasizes to bone and lung and less frequently to liver and brain⁹⁰. While oestrogen receptor positive tumours preferentially spread to bone⁹¹; oestrogen receptor negative tumours have a predilection for metastasis to visceral organs whereas invasive lobular carcinomas (ILC) relapse more frequently in the gastrointestinal tract and ovaries^{92, 93}. This can be attributed to the cell of origin: hormone receptor positive tumours emerge from the luminal progenitor cells, whereas hormone receptor negative tumours originate from the basal cell layer. The striking preference of various breast cancer cells to metastasize to these organs forms the basic concept of the “seed and soil” hypothesis by Paget in 1889, in which he proposed that the malignant cells (seeds) arrest, survive and proliferate only in those tissues that provide a hospitable environment or a congenial ground for their growth (soil)⁹⁴. Therefore, failure of cells to metastasize can be due to either

genetic deficiencies within the malignant cells or impaired responses to the new host environment (epigenetics).

In order to metastasize, cancer cells must fulfil some prerequisites and gain certain tumorigenic functions in order to complete the multistep metastatic cascade. These include an indefinite proliferative capacity, capacity to evade both cellular and environmental constraints, ability to attract a blood supply, and to eventually detach from their primary site. If a cell fails any of the many steps in the metastatic cascade, then it will not metastasize. The “metastatic cascade” can be divided into six distinct steps each of which represents a potential target for development of novel therapeutics to reverse or prevent metastatic breast disease (and have been extensively reviewed in references^{29, 95}).

Step 1: Local invasion and intravasation. Tumour dissemination starts when the aggressive malignant cells begin to invade the bloodstream through the new vasculature they have previously formed through angiogenesis. Tumour cells utilize a variety of extracellular proteases to break down extracellular matrix (ECM) and invade from primary tumour to the adjacent parenchyma such as urokinase type plasminogen activator (uPA) and matrix metalloproteases (MMPs); a family of at least 20 zinc-dependant endopeptidases capable of degrading most known extracellular matrix components⁹⁶, of which MMP1 and MMP9 were found to be up-regulated in breast cancer⁹⁷. Entry of malignant cells into the circulation is facilitated by the pathologically leaky vasculature formed by tumour angiogenesis. Departure from the primary site and intravasation can be also enhanced by the embryonic plasticity and added motility endowed by the development of epithelial-to-mesenchymal transition phenotype^{98,99}. Furthermore, the invasion of cancer cells can be promoted by the presence of tumour-associated macrophages and fibroblasts; both are required for the production of pro-migratory factors and deposition of collagen, respectively¹⁰⁰⁻¹⁰³.

Step 2: Dissemination in the circulation. To enhance their survival during dissemination, malignant cells may circulate as solitary cells or associate with non-neoplastic cells and/or platelets to form multi-cellular clusters to protect them from immune cell detection and shear stress destruction until they arrest in the narrow capillary beds of a discontinuous organ and extravasate⁸³.

Step 3 and 4: Arrest at the distant site and extravasation. Once within the parenchyma of the target organ, metastatic cells can breach the microvasculature in which they are lodged either by disruption of their walls by the expanding tumour emboli or, more frequently, by penetration of the fenestrated capillary walls and extravasation into the parenchyma. Following extravasation, the efficient metastatic seeding, survival and subsequent tumour growth is directly enhanced by the recruitment of the metastasis-associated macrophages; a distinct population of an *in situ* differentiated monocyte¹⁰⁴. It is of note that metastasis from breast cancers tend to tend to migrate to lung, liver and bone marrow and the homing/establishment of metastasis of breast cancer cells to these sites would appear to be mediated by interactions of certain receptors on cancer cells and the expression of the appropriate ligand in the “preferred” tissue such as CXCR4 and CXCR8 expression on breast cancer cells and the paracrine secretion of CXCL12 in the target organs⁹⁶. CXCR4 and CXCR8 are members of the chemokine receptor family while CXCL12 is a stromal-cell derived factor (SDF1). The chemokines are by far the most studied tumour-derived chemo-attractants.

Step 5 and 6: Survival as micrometastasis and colonization of target organs. Once they abandon their original host organ, the tumour cells will encounter different stresses caused by the loss of their supportive original microenvironment as well as the unfavourable surroundings at the distant sites which do not support the growth of individual cells which wander in from elsewhere, and subsequently, most cells will die. However, because of their inherent genetic instability, breast cancers have a limited chance of generating cells which are able to overcome stringent biological barriers, survive the stresses of bloodstream and withstand otherwise incompatible microenvironments with their phenotypic attributes. Once extravasated, active colonization of secondary organs can be promoted by certain co-opted organ-specific cells present in the new microenvironment, such as the bone-resorbing osteoclasts in the bone microenvironment. From these disseminated tumour cell populations only a few cancer cells may establish full colonization where they are triggered to proliferate and form metastatic colonies immediately upon their extravasation, others may enter a prolonged period of micrometastatic dormancy. The survival of dormant lesions, and their prospected activation requires additional factors, which might be tumour-intrinsic or tumour-extrinsic. Distinct sets of functions are

thought to be required for the cells to preferentially colonize different organs as each tissue presents a highly specialized microenvironment⁸⁹.

Colonization of distant organs represents the most dangerous aspect of cancer. Cancers that remain confined to the breast is associated with excellent cure rates, exceeding 90%. As the cells spread, the long-term survival decreases depending on the site as well as the extent of colonization. Brain and visceral organs metastasis are the most life threatening, with less than 20% of patients surviving for 5-years¹⁰⁵.

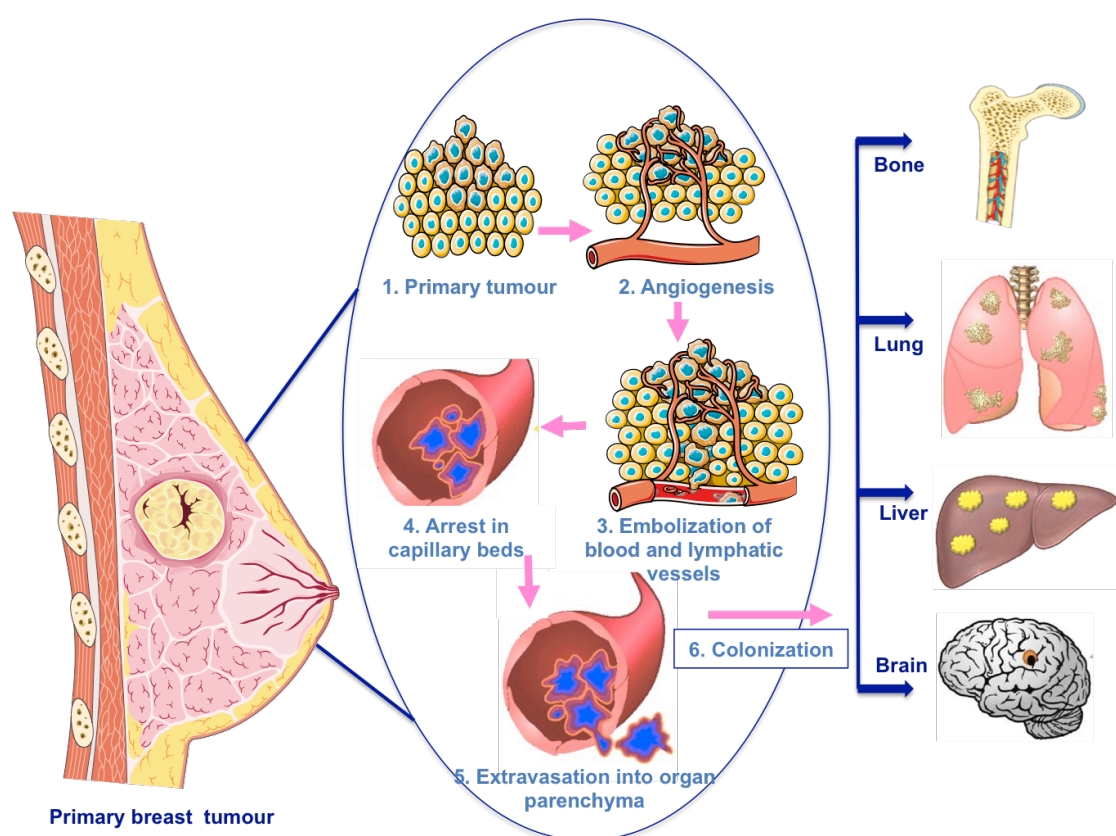


Figure 1.3: The steps involved in breast cancer-cell metastasis from a primary site to distant organs.

The proclivity of cells to disseminate can be acquired when the primary malignant neoplasm becomes locally aggressive and promotes new blood-vessel formation. The cells invade these new blood vessels, and the vasculature carries the cancer cells to capillary beds in distant organs as aggregates with other blood cells, which eventually form embolisms that arrest in distant capillaries. These cancer cells can then adhere to the endothelial cells and escape into the surrounding parenchyma where they become exposed to the microenvironment that can support the growth of metastases (This figure was produced using Servier Medical Art:

<http://www.servier.com/Powerpoint-image-bank>).

1.2 The emerging hallmark of cancer: deregulating cellular energetics

The hallmarks of cancer were initially characterized as six biologically distinctive capabilities attained during the multistep development of human cancers and directly contribute to tumour complexity, tumour growth and metastatic dissemination (reviewed in detail in reference¹⁰⁶). These hallmarks include sustained proliferative signalling, evading growth suppressors, mechanisms to resist cell death, replicative immortality, induction of angiogenesis, and activation of invasion and metastasis¹⁰⁷. Recently, two more characteristics have been added to this list including reprogramming of energy metabolism and evasion of immune destruction¹⁰⁶.

Owing to its key role in human malignancies, cancer cell metabolism is now the focus of intense research. This concept was identified by Warburg¹⁰⁸ in the 1920s and is termed the “Warburg effect”^{109, 110} and in recent years has received a great deal of interest and traction. Based on the evident relationship between metabolic dysregulation and cancer, attention has focused on the possibility of tackling the metabolic alterations as a potential for treating cancer patients, following the recent development in methods to study its regulation.

An example of this concept is the many lines of evidence that suggest a connection between the metabolic syndrome, obesity-related insulin resistance and/or diabetes mellitus with increased risk of diverse cancer types. Over the past few years, multiple meta-analyses and large cohort studies have examined this association and strengthened the proposed synergistic relationship between type 2 diabetes mellitus and an increased risk and incidence of several site-specific malignancies^{111, 112} including breast^{113, 114}, liver¹¹⁵, pancreas¹¹⁶, kidney¹¹⁷, colon¹¹⁸ and endometrial/ovarian¹¹⁹ cancers. It is now becoming clear that sustained hyperglycaemia and hyperinsulinemia are critical regulators of not only the development of malignancy but also of treatment outcome¹²⁰.

This growing awareness has resulted in a desire to extensively investigate the potential of anti-diabetic therapy for cancer prevention and treatment. Over the past decade research has emphasized an emerging role of metformin in reducing both cancer incidence and cancer-related mortality in diabetics. Therefore, metformin might have a profound impact on public health worldwide and it is now becoming an attractive subject of intense basic and clinical research on both chemoprevention and

chemotherapy. This strongly suggests a critical role for metabolic alteration as an early change in cancer development and highlights the importance of metabolic reprogramming as a potential prevention strategy. However, the potential anti-cancer properties of metformin need to be thoroughly investigated to explain how it affects cancer cell metabolism and deregulates cellular energetics, and whether it can have the same effect in non-diabetic patients.

1.3 Metformin as a potential chemopreventive and chemotherapeutic agent in breast cancer

Most malignant cells rely primarily on non-efficient, non-oxidative breakdown of glucose in the cytosol by a process called “aerobic glycolysis” to generate the required energy for their survival, independently of the mitochondrial oxidative phosphorylation, a common efficient mechanism of ATP generation by proliferating normal cells in presence of oxygen; the “Warburg effect”. Metformin has been reported to concomitantly reduce the anti-senescence effects of the ATP-generating glycolytic metabolic type thereby down-regulating the self-renewal and proliferation of breast cancer stem cells¹²¹.

1.3.1 Metformin’s botanical background

Metformin (N',N'-dimethylbiguanide hydrochloride) is a safe, non-toxic, low cost and widely prescribed biguanide-derivative for the treatment of high blood glucose associated with type 2 diabetes mellitus (T2DM) worldwide¹²². Its use can be backdated to ancient Egypt and medieval Europe where it was derived from the *Galega Officinalis* herb (i.e. French Lilac or Goat’s Rue) and it was used to relieve polyuria and sweet odour breath, both of which are common symptoms of hyperglycemia¹²³. The isoamylene guanidine was identified as the active ingredient, however, when purified, guanidines were discovered to be fairly toxic. Chemists made the compounds more tolerable by bonding two guanidines together forming a biguanide and agents such as phenformin, buformin and metformin were developed for therapeutic uses (Figure 1.4). Phenformin was the first to be commercialized, but was withdrawn rapidly and replaced with metformin due to the high incidence of lactic acidosis among diabetics using phenformin¹²³. In 1958, metformin was licensed for use in Britain for the prevention and treatment of hyperglycaemia associated with T2DM, along with dietary restriction and physical activity^{124, 125}. In

addition to its anti-hyperglycaemic effect, metformin has both plasma-lipid and weight lowering effects; a mimicry effect of calorie-restriction¹²⁶.

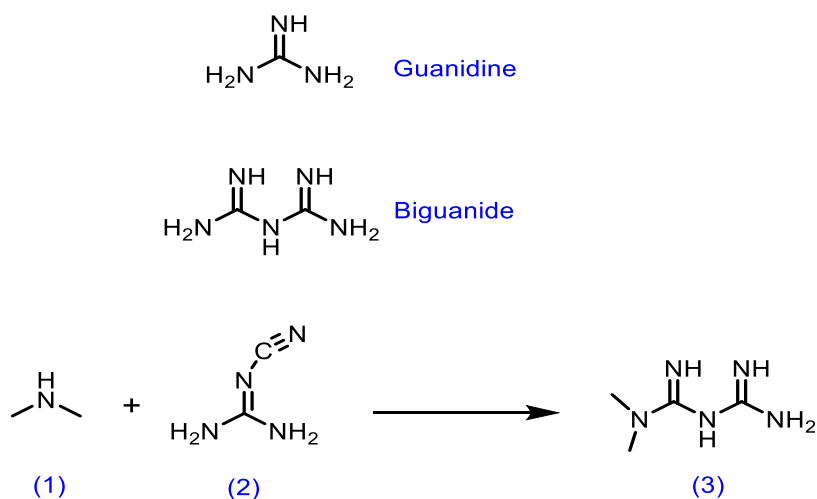


Figure 1.4: Metformin structure and synthesis.

Metformin (3) is synthesized by equimolar fusion of hydrochloride dimethylamine (1) and dicyandiamide (2) at 130-1500 C for 0.5-2 hours¹²⁷ (Figure created by ChemDraw Prime 16.0).

1.3.2 Clinical pharmacokinetics of metformin

Chemically, metformin is a small hydrophilic base (molecular weight: 129 g/mol), which exists as an organic cation at physiological pH. Following oral consumption, it is absorbed predominantly from the upper small intestine and has a relatively low bioavailability of about 50-60%. The peak plasma concentration of metformin is reached within 3 hours while its average elimination half-life in plasma is about 6.2 hours¹²⁸⁻¹²⁹. Therefore, effective treatment with metformin can be achieved by repeated administration of high doses (e.g. 850 mg twice a day or 500 mg three times a day, orally). Metformin tends to accumulate in the kidneys, salivary glands and the small intestine. Interestingly, metformin is also distributed to red blood cells, and accumulates in these with a much longer elimination half-life of about 17.6 hours. It is not metabolized in cells and 80 % of it is renally eliminated and excreted unchanged in urine¹²⁴.

Metformin binding to plasma proteins is negligible and its cellular uptake via passive diffusion across cell membranes is very limited¹²⁹. Therefore, metformin requires a set of influx and efflux transporters to facilitate its transport into and out of the cell and mediate its oral absorption, hepatic uptake and renal excretion

(Summarized in table 1.3). Several transporters have been identified as putative determinants of metformin's pharmacokinetics in the main organs such as liver, kidney and small intestine (Figure 1.5).

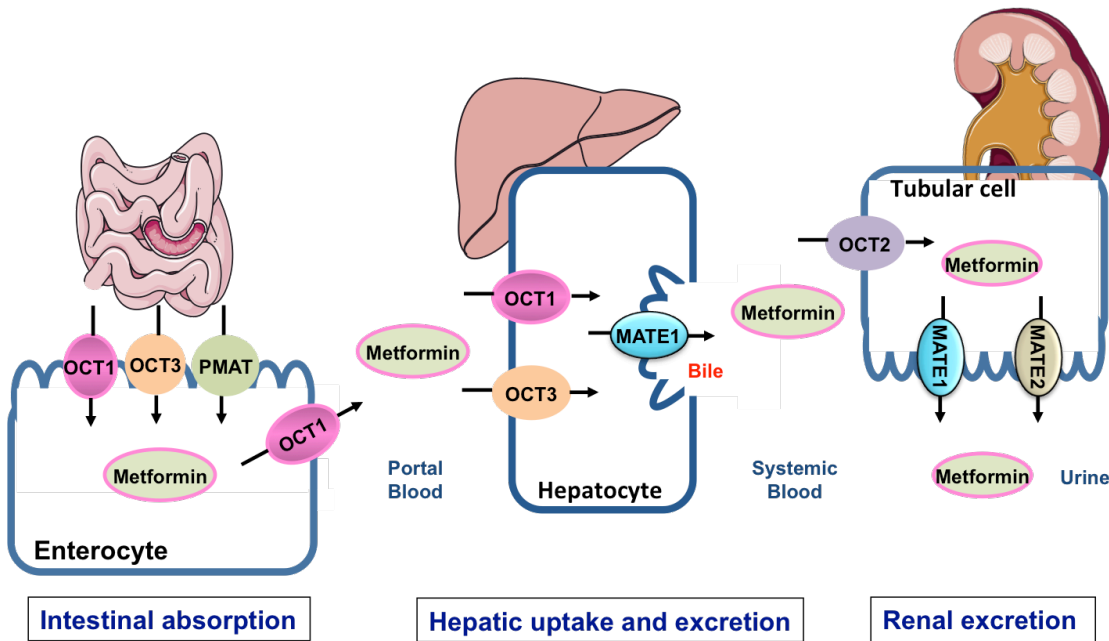


Figure 1.5: Putative determinants of metformin's kinetics in main organs.

After oral administration, metformin is widely distributed into the body tissues including the small intestine, liver and kidneys. The absorbed dose is mostly excreted unchanged in urine. In the liver and kidneys, organic-cation transporters (OCTs) are localized on basolateral membranes, whereas multidrug and toxin extrusion (MATEs) proteins are localized on apical membranes. Although metformin is not an exclusive substrate of these transporters, the mechanisms underlying its transport kinetics in the clearance organs has been quite well investigated. It is noteworthy that OCT1 can act as an importer as well as an exporter in the enterocyte (This figure was produced using Servier Medical Art: <http://www.servier.com/Powerpoint-image-bank>).

Influx transporters such as organic cation transporters OCT1, OCT2 and OCT3, which are members of the solute carrier family 22 encoded *SLC22A1*, *SLC22A2* and *SLC22A3* genes respectively, are involved in metformin translocation into cells¹³⁰. Recently, metformin has been shown to be a substrate for a novel proton-activated organic cation transporter known as PMAT (plasma membrane monoamine transporter), a member of solute carrier family 29 encoded by *SLC29A4 gene*, which has been shown to be important for intestinal uptake of metformin¹³¹.

Efflux transporters such as MATE1 and MATE2; the multidrug and toxin extrusion family, which are members of solute carrier family 47 encoded by *SLC47A1*, *SLC47A2* genes, facilitate the H⁺ coupled export of metformin from the intracellular to the extracellular space (H⁺/organic cation antiporters; drive the secretion of metformin from low to high pH gradient through H⁺ or proton activated pump)¹³². In terms of transport capacity and substrate affinity, metformin is known to be a superior substrate for renal OCT2 more than the hepatic OCT1¹³³, but not for OCT3¹³⁴. Recently, OCT4 (*SLC22A4*), also known as carnitine/organic cation transporter OCTN1, has also been identified to be involved in metformin absorption in the small intestine¹³⁵. The complex interplay between the influx and efflux transporters governs metformin disposition, efficacy and cellular response. Therefore, elucidating the difference in transporters expression is central to determine the intracellular concentration, and optimum dosing, as well as the most relevant *in vitro* cell model for exploring the anticancer efficacy of metformin.

Furthermore, the potential importance of glucose transporter-1 expression (GLUT1) has been recently demonstrated as a biomarker for response to metformin; where AMPK activation has been shown to up-regulate glucose transporter expression, in addition to the importance of glucose concentrations in determining the sensitivity to biguanides drugs in general¹³⁶. Additionally, mitochondrial DNA mutations in particular in complex I genes (i.e ubiquinone oxidoreductase) may also be considered as a key marker of resistance to metformin¹³⁶.

Another interesting marker is the glutamine reductive carboxylation pathway which allows cancer cells treated with metformin to utilize glutamine as a carbon source at a time of mitochondrial toxicity and changes in expression of its regulators such as isocitrate dehydrogenase is also of interest¹³⁷.

Table 1.3: Metformin-transporter proteins; their localization, site of expression and potential functions

| Transporter | Membrane localization and tissue distribution | Functions and relevant studies |
|----------------------------|---|--|
| OCT1 (SLC22A1) | <p>The main transporter across cell membrane which mediates hepatic and intestinal uptake of metformin¹²⁸</p> <p>Mainly on the basolateral membrane of hepatocytes and enterocytes</p> <p>Predominantly expressed in liver followed by small intestine</p> | <p>OCT1 gene deletion in mice reduces hepatocytes metformin uptake dramatically¹³⁸</p> <p>Human individuals carrying <i>SLC22A1</i> polymorphisms suffer an impaired response to metformin in reducing blood glucose levels¹³⁸</p> |
| OCT2 (SLC22A2) | <p>Mainly on the basolateral membrane of renal tubular cells</p> <p>Expressed in kidney, testis and prostate</p> | Responsible for 80% of total metformin clearance, it mediates the entry of metformin into tubular cells and together with MATE1-2 mediates its secretion into urine ¹³² |
| OCT3 (SLC22A3) | <p>Apical membrane of human enterocytes</p> <p>Expressed by multiple tissues and their corresponding tumours</p> | The contribution of OCT3 to metformin absorption is still unknown ¹³⁰ |
| PMAT (SLC29A4) | <p>Apical membrane of epithelial cells</p> <p>Expressed by intestinal tract, skeletal muscle, liver, kidney and brain</p> | May play a role in intestinal absorption of metformin ¹³¹ |
| MATE1 (SLC47A1) | <p>Bile canaliculi of the liver and brush border membrane of the renal tubular cells</p> <p>Primarily expressed by Kidneys, adrenal glands, testis, liver and skeletal muscles</p> | Responsible for renal clearance of metformin with OCT2 ¹³² |
| MATE2 (SLC47A2) | <p>Widely expressed in humans</p> <p>Predominantly expressed by kidneys</p> | Renal clearance of metformin ¹³² |

1.3.3 Pharmacodynamics of metformin and insulin-mediated action

Generally, the biguanides act by reducing hyperglycaemia without leading to coincidental hypoglycaemia. Hence, the term “anti-glycaemic” drug was coined for metformin. As an anti-hyperglycaemic agent, metformin exerts its effect by reducing hepatic gluconeogenesis, the process by which glucose is generated from non-carbohydrate substrates, and increasing glucose uptake by muscles^{139, 140}. These effects are mediated by adenosine monophosphate-activated protein kinase (AMPK) transcriptional regulation of genes that encode glucose transporters in liver and muscles. Reduction in blood glucose level will subsequently lead to reduction in circulatory insulin, and possible improvement in tissue sensitivity to circulating insulin. For this reason, metformin has been classified as an “insulin sensitizer”^{141, 142}. Most of the adverse effects of metformin are mild, temporary, reversible and mainly gastrointestinal in origin. These include nausea, gastric upsets and diarrhoea. This may occur in up to 30% of cases and can be overcome by introducing the drug slowly and gradually increasing the dose¹⁴³. Lactic acidosis, a rare complication, affects 3 in 10000 of diabetics on metformin, most commonly in elderly patients with impaired cardiac, hepatic and renal functions¹⁴⁴. When used as a monotherapy, the anti-hyperglycaemic action of metformin doesn’t affect the pancreatic insulin secretion nor cause overt clinical hypoglycaemia in both normal and diabetic subjects¹⁴³. Additionally, at the cellular level, metformin is believed to have pleiotropic effects which include disruption of mitochondrial function by partially inhibiting NADH dehydrogenase¹⁴⁵ or by inhibiting glycerol phosphate dehydrogenase in liver cells which results in alterations to the electron transport chain (ETC). Moreover, metformin has been documented to affect several processes that are central to numerous aspects of cell physiology such as AMPK signalling, protein kinase A signalling, folate and anabolic metabolism^{136, 137, 145}. Most of these mechanisms point toward the mitochondrial biology as a main mechanistic target for metformin¹⁴⁶.

1.3.4 Metformin and breast cancer; early clues

In addition to the potent anti-diabetic properties of metformin, it has recently received considerable attention because of its potential anti-neoplastic and chemopreventive activities. The term chemoprevention means either stabilization, arrest or reversal of the malignant growth during its pre-neoplastic phase, either

physiologically or pharmacologically¹⁴⁷. The potential use of metformin in cancer was first identified by numerous retrospective observational studies evaluating the potential diabetes-cancer association. Epidemiologic observations reported lower incidence and reduced cancer-related mortality among metformin-treated diabetics (receiving adult therapeutic dose: 1.5-2.5 gm/day), compared to those on other hypoglycaemic agents^{120, 148-155}. This led to speculations about the integral and potential role of metformin in reducing the risk of cancer development, progression, and metastasis, and improving the overall survival outcomes. Following on from the epidemiologic studies, a significant number of preclinical studies have also suggested a possible anti-cancer effect of metformin, and attempted to identify the potential mechanisms of action, as detailed in section 1.3.5.1. Indeed, as a result of these pre-clinical observations more than 100 clinical trials at different phases are currently underway to explore the impact of metformin treatment on: prevention, treatment and survival outcomes of cancer patients, including prostate, lung, thyroid, ovarian, endometrial cancers, with 36 of them evaluating breast cancers (can be viewed at www.Clinicaltrials.gov - last accessed 30th-December-2017).

1.3.4.1 Breast cancer chemoprevention: clinical aspects and population benefits

A landmark epidemiologic study in the field of oncology by Evans *et al.* in 2005¹⁴⁸, reported a reduced overall cancer incidence in diabetics receiving metformin in comparison to those on other oral hypoglycaemic agents and this protective effect was closely linked to the duration of metformin exposure. Shortly thereafter, the research field expanded rapidly with about 17 more epidemiological studies evaluating the potential link between metformin administration and reduced cancer burden (reviewed by Dowling *et al.*¹⁵⁶).

Various epidemiologic and population-based studies have demonstrated an association between T2DM and a higher risk of cancer development, morbidity and mortality^{114, 157, 158}. The presence of insulin receptors and insulin-related growth factor-1 (IGF-1) on many cancer cells provides a biological rationale for a potential role of insulin on breast cancer growth, progression and poor survival outcomes¹¹². Since insulin and its related growth factors are widely believed to be mitogenic, metformin has been proposed as an anticancer agent based on its ability to systemically reduce serum insulin levels. Initially this was thought to be the main

mechanism of action of metformin against cancer, at least in diabetics. Further research has suggested a number of additional underlying potential mechanisms of action as summarised in Table 1.5.

In contrast to the large reduction in the risk of liver¹⁵⁹ and pancreatic¹⁶⁰ cancers development (60%–80%) reported by several meta-analyses, findings regarding breast cancer risk have been mixed. Of interest, metformin-treated diabetic patients have been shown to have a lower risk of breast cancer^{153, 161} compared to their counterparts with diabetes who are non-metformin users, as well as better clinical outcomes than the diabetic breast cancer patients treated with other anti-diabetic drugs¹⁶¹. On the other hand, some observational studies reported a non-significant reduction in the risk of breast cancer in type 2 diabetic patients^{162, 163} (Table 1.4). However, the observational nature and different comparison groups limit the interpretation of these studies¹⁶⁴.

The results of numerous epidemiological studies, although inconclusive, suggest that metformin use is associated a reduction in most cancer incidents in both pre-diabetics and diabetics and better outcomes in cancer patients. However, the variations in the response to metformin among breast cancer patients can possibly be attributed to the duration of treatment and the cumulative dose. As the definite data on the efficacy of metformin in different subpopulations of breast cancer patients is currently largely lacking, it seems important to determine target populations. These observations also justify the need for clinical trials to evaluate the potential role of metformin in the prevention and treatment of breast cancer.

Table 1.4: Observational studies of metformin in breast cancer.

| Author/ Reference | Sample size | Study design (Endpoint) | Relative risk (95%CI) | Treatment comparison |
|--|------------------------------|---|--------------------------|---|
| Currie <i>et al.</i> ¹⁶⁵ | n=373 at risk=7897 | Retrospective cohort (Incidence) | 1.02 (0.71– 1.45); | Metformin vs. sulfonylureas |
| Libby <i>et al.</i> ¹⁵⁰ | n=771 at risk=8170 | Retrospective cohort (Incidence and mortality) | 0.60 (0.32– 1.10); | Metformin users vs. nonusers |
| Bodmer <i>et al.</i> ¹⁵³ | n=17 control= 120 | Retrospective nested case-control (Incidence) | 0.44 (0.24– 0.82) | Metformin users of more than 40 prescriptions for > 5 years) vs. nonusers |
| Bosco <i>et al.</i> ¹⁶⁶ | n=393 control=3930 | Retrospective nested case-control (Incidence) | 0.81 (0.63– 0.96) | Metformin for at least 1 year vs. control |
| Ferrara <i>et al.</i> ¹⁶⁷ | n=9082 at risk =252467 | Prospective cohort (Incidence) | 0.90 (0.80– 1.00); | Ever use of metformin and pioglitazone vs. never use of metformin |
| Morden <i>et al.</i> ¹⁶⁸ | n=5466 at risk =81681 | Retrospective cohort (Incidence) | 1.28 (1.05– 1.57); | Metformin vs. not in insulin treated patients |
| Chlebowski <i>et al.</i> ^{80, 169} | n=233 at risk =68019 | Prospective Cohort (Incidence) | 0.65 (0.46– 0.91) | Metformin vs. other anti-diabetic drugs |
| Ruiter <i>et al.</i> ¹⁷⁰ | n=3552 at risk =85289 | Prospective cohort (Incidence) | 0.95 (0.91– 0.98); | Metformin vs. sulphonylurea |
| Van Staa <i>et al.</i> ¹⁷¹ | n=109708 | Retrospective cohort (Incidence) | 0.96 (0.83, 1.12) | Metformin vs. sulfonylureas, thiazolidinediones , and insulin |

1.3.5. Pre-clinical studies with metformin in breast cancer

A plethora of *in vitro* and *in vivo* studies evaluating the role and the mechanisms of metformin action in several cancers has emerged and several mechanisms have been proposed to explain its anti-neoplastic activity, although the exact mechanism remains to be elucidated (Summarized in table 1.5). Metformin activity *in vitro* has been shown to involve most of the molecular subtypes of BC

regardless of their hormone-receptor or *p53* statuses¹⁷², although not all BC cell lines respond, and the reasons why still need to be elucidated¹⁷³.

In ER-expressing BC cell lines (around 75% of cases), metformin has been shown to inhibit cellular proliferation and suppress the expression of the aromatase gene *in vitro*, when it is present¹⁷⁴. Metformin is also efficacious in reducing the proliferation of ER-positive BC cells when combined with tamoxifen¹⁷⁵, which may be of specific benefit to premenopausal women. The mechanisms involved in the suppression of ER-expressing cell lines *in vitro*, are thought to be activation of the AMPK-pathway¹⁷⁶, inhibition of the mTOR-pathway¹⁷⁷, down-regulation of D1-cyclin^{172, 173}, caspase and polymerase-dependent cell death¹⁷⁸, arrest of cell cycle at G1 phase¹⁷⁹, induction of apoptosis and necrosis via oxidative stress and activation of FOXO3a, a conserved subfamily of proteins involved in tumour suppression via cell cycle arrest¹⁸⁰.

In HER-2 expressing BCs (15-20% of patients), both cell lines and mice models were sensitive to the growth repressive activity of metformin^{181, 182}. An *in vivo* study has suggested a link between long term treatment of transgenic HER-2/neu mice with metformin and a significant reduction in the initiation and progression of mammary tumours as well as a reduction in the size of those that do form¹⁸¹. These data suggest that metformin could potentially be used as an adjuvant to the standard HER-2 targeting therapy such as Herceptin. Furthermore, this may provide one possible explanation for the differential response and resistance of different breast tumour sub-populations to metformin treatment, i.e. that metformin response is based on their HER-2 receptor status, a hypothesis that requires further investigation.

In triple-negative BCs, which accounts for 30% of all BCs and represent a major challenge due to their lack of response to most current therapeutic agents, metformin has been shown to induce a response both *in vitro* and *in vivo* via AMPK-dependent suppression of EGF-receptors, MAP-kinase signalling proteins, Cyclin D1¹⁵² and the metastasis-inducing CD24-protein¹⁸³ or by dose-dependent activation of MAPK-p38 pathway, a significant regulator of the proliferation and invasiveness of BC cells in normoglycaemic but not in hyperglycaemic media¹⁸⁴.

Findings arising from mechanistic preclinical settings are mostly in favour of a potent broad-spectrum effect of metformin in most breast cancer subtypes and this effect is to a greater or lesser extent dependent upon the dose and the cell lines used. However, these studies are not without limitations and these limitations are discussed in section 1.3.7.

The anticancer action of metformin is exerted through both direct (insulin-independent) and indirect (insulin-dependent) actions of the drug (Figure 1.6). The insulin dependent (indirect) effect of metformin is reviewed in table 1.5.

1.3.5.1 Direct anti-neoplastic effects of metformin

The mechanisms involved in the direct anti-neoplastic effects of metformin are most likely very diverse. Data from preclinical studies with BC cell lines have established that anti-proliferative activity of metformin is mediated by up-regulation of AMP-activated protein kinase (AMPK) activity and downstream suppression of signaling through the mammalian target of rapamycin (mTOR)^{182, 185-190}. Other proposed mechanisms include influences on cancer cell metabolism, cell cycle, apoptosis, estrogen biosynthesis and estrogenic signal transduction, all of which are reviewed in detail in table 1.5.

AMPK is an important energy sensor which is triggered by intracellular metabolic stresses such as cellular hypoxia¹⁹¹, ischaemia¹⁹², glucose deprivation¹⁹³ and skeletal muscle contraction^{194, 195}. Metformin enters the cell via a cellular transporter and interrupts complex-I of the mitochondrial respiratory chain (the main target of metformin treatment), reducing ATP synthesis leading to increased cellular AMP:ATP ratio, thereby activating the AMPK pathway¹⁴⁵. Consequently, AMPK down-regulates energy-consuming processes, such as protein synthesis and cell cycle progression¹⁹⁶. Importantly, in cancer settings, metformin-induced AMPK-dependent suppression of breast¹⁵², pancreatic¹⁹⁷ and colon cancer growth¹⁹⁸ was demonstrated by recent *in vivo* studies.

Upon activation of AMPK, the tuberous sclerosis complex 2 (TSC2), which is a protein located upstream of mTOR, is phosphorylated and stabilized thus inhibiting the tumorigenic effect of mTOR, a pathway thought to increase the risk of metastasis, poor outcomes and resistance to targeted therapies^{187, 189} (Figure 1.6). Recent

evidence from *in vitro* BC studies suggest that the inhibition of mTOR signalling pathway is AMPK-dependent^{177, 199}, however, metformin may also work directly on malignant cells by suppressing the mammalian target of rapamycin (mTOR) pathway independently of AMPK activation^{187, 189}.

Metformin can also activate the AMPK-pathway via a set of alternative upstream kinases including Liver kinase-B1 (LKB1)²⁰⁰ and Calcium/Calmodulin-dependent kinase²⁰¹. The activation of AMPK seems to be mostly dependent on the major upstream LKB1; also known as serine-threonine kinase (STK11), which was previously identified as a tumour suppressor gene²⁰². The activation of LKB1-AMPK pathway results in inhibition and down-regulation of all the cellular energy consuming processes, which are vital for the growth and survival of all cells, such as protein synthesis, lipogenesis and hepatic gluconeogenesis. Therefore, the LKB1-AMPK pathway activation is responsible for inhibition of anabolism and activation of catabolism^{195, 203} as well as changing gene and protein expression^{204, 205}.

Indeed, as already stated, in the liver, metformin has been shown to reduce hepatic gluconeogenesis, improve insulin sensitivity and decrease insulin level via the phosphorylation of AMPK and downstream inactivation of the mTOR transcription factor in an LKB1-dependent manner²⁰⁶, whereas in cancer cells the activation of LKB1-AMPK causes cell cycle arrest²⁰⁷. As a tumour suppressor gene, absent or mutated LKB1 leads to the development of Peutz-Jeghers syndrome which predisposes to the development of several malignancies including breast and colon cancers²⁰². The reduced or absent expression of LKB1 was also associated with advanced histological grade and poor survival of BC patients²⁰⁸. A pioneer study by Zakikhani and colleagues reported a metformin-induced inhibitory effect on a panel of malignant epithelial cells including ovarian, cervical, breast and prostate but not the LKB1-deficient cervical cancer cells and this inhibition was linked to the phosphorylation of mTOR in an AMPK dependent manner¹⁷⁶. These data therefore suggest that metformin may work in an LKB1-dependent manner because it was ineffective against the LKB1- deficient cells.

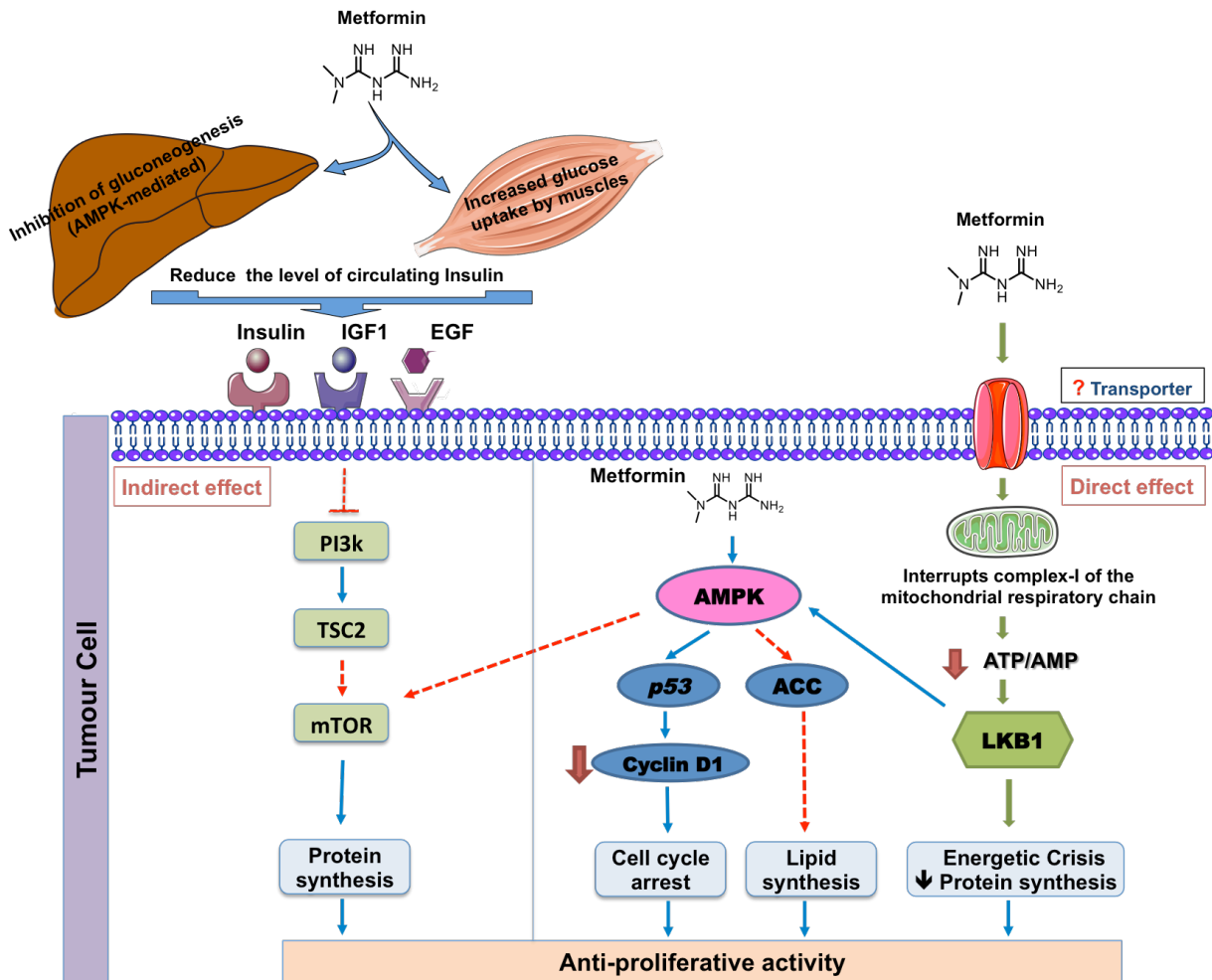


Figure 1.6: The proposed direct (non-insulin mediated) and indirect (insulin mediated) effects of metformin in oncology.

Systemically/Indirectly, metformin reduces hepatic gluconeogenesis, increases glucose uptake by muscles, sensitizes tissues to insulin, and indirectly diminishes receptor tyrosine kinase activation and PI3K signalling. Within cancer cells/directly, metformin (1) Interrupts complex-I of the mitochondrial respiratory chain, leading to ↓ ATP synthesis, ↑ cellular AMP:ATP ratio and stimulates LKB1/AMPK pathway. (2) Directly activates AMPK leading to stabilization of TSC2 and inhibition of mTOR signalling and protein synthesis. (3) Activated AMPK also inhibits p53 and down-regulates cyclin D1, thus arrests cell cycle progression. (4) Activated AMPK phosphorylates and inhibits acetyl-CoA carboxylase (ACC), thus decreases fatty acid synthesis and intracellular lipid contents. (5) Targets mTOR independently of AMPK. Solid Lines represent the activation reactions and dashed lines represent inhibitory reactions. ACC, Acetyl-CoA carboxylase; AMP, Adenosine monophosphate; AMPK, AMP-activated protein kinase; ATP, Adenosine triphosphate; EGF, Epidermal growth factor; IGF1, Insulin-like growth factor-1; LKB1, Liver kinase B1; mTOR, Mammalian target of rapamycin; PI3K, Phosphatidylinositol-3-kinase; TSC2, Tuberous sclerosis complex 2.

Metformin was also reported as being able to suppress prostate cancer cell growth via suspending the progression of cell cycle at the resting phase and down-regulating Cyclin D1 protein independently of AMPK-activation²⁰⁹. Similar results have been reported on other cancer cell lines including glioma²¹⁰, melanoma²¹¹, endometrial²¹² and ovarian carcinoma²¹³. Conversely, cell cycle arrest in BC was reported to be AMPK-dependent¹⁷³. These data suggest that depending upon the cancer type and its molecular pathology, metformin can inhibit the growth of cancer cells both dependent on AMPK activation and independently of AMPK activation. Moreover, the genetic constitution and particularly the metabolic characteristic of the different cancers should be considered to be important variables that might also contribute to the mechanism of metformin action, and to the treatment efficacy.

Table 1.5: Proposed mechanisms of anti-neoplastic effect of metformin (direct and indirect)

| Proposed mechanism of metformin action | Studies/references |
|---|--|
| 1. Metformin alters circulatory insulin levels (Indirect or insulin-mediated action) | Metformin is known to inhibit hepatic gluconeogenesis, thereby improving tissue sensitivity to insulin, thus reducing the level of circulating insulin and overcoming insulin resistance ²¹⁴ . It is possible that this mechanism of action may also be indirectly anti-tumorigenic as a growing body of evidence has demonstrated a link between increased expression of insulin/insulin-like growth factors receptors by most cancer cells and the accelerated proliferation of these transformed cells in response to the stimulatory effect of insulin ^{157, 215} . Thus, reducing circulatory insulin is expected to suppress the insulin-mediated mitogenesis and inhibit the proliferation of cancer cells. Hyperinsulinemia can also reduce the hepatic production of the circulating sex hormone-binding globulins and increased androgen synthesis by ovaries and adrenal glands ²¹⁶ . Therefore, increased circulating insulin can indirectly increase the bioavailability of oestrogen, which in turn, participates in the development of hormone-dependent malignancies such as breast and endometrial cancers ¹¹⁰ . Thus the reduction in insulin levels caused by metformin may specifically be important in preventing the development of these cancer types. |
| 2. Metformin affects cancer cell metabolism | Although data are sparse, at least one epidemiological study has reported hyperglycaemia as a risk factor for cancer development ¹¹¹ , and although the link is not clear, it could be due to allowing the rapidly dividing cancer cells to consume glucose at an accelerated rate. Therefore, the anti-hyperglycaemic effect of metformin cannot be excluded as a possible anti-neoplastic mechanism. In addition to the anti-glycaemic effect, emerging data from recent studies suggest a role of metformin as a negative modulator of lipid metabolism within the cancer cells in an AMPK-independent manner ^{217, 218} . This effect might be considered as a new prospective strategy in preventing cancer development and progression ¹¹⁰ . |
| 3. Metformin effect on cancer stem cells | Interestingly, in addition to its effects on the general cancer cell population, some data has suggested that metformin has a specific effect on cancer stem cells (CSCs). Cancer stem cells are a genetically distinct subpopulation of cancer cells responsible for treatment resistance and recurrence after definitive therapy, thus inhibiting them is a distinct therapeutic advantage ^{219, 220} . The treatment of a BC xenograft mouse model with metformin specifically eliminated the CD44+/CD24-/low CSCs and sensitized the tumour cells to doxorubicin, resulting in reduced tumour burden and delayed tumour recurrence ²²¹ . In the same context, metformin has been shown to work effectively with other chemotherapeutics such as paclitaxel and carboplatin to reduce tumour growth and prevent recurrence and to lower the required dose of the standard chemotherapeutics and improve their efficacy ²²² . Moreover, in HER2-overexpressing tumours, metformin was able to target the Herceptin-resistant CSCs ²²³ . A possible proposed mechanism of metformin mediated inhibition of tumour-initiating stem cells is the reduction of transcriptional factors such as TGF-β cytokines as these factors are the key drivers of epithelial to mesenchymal transition (EMT) ²²⁴ . |

Table 1.5: Continued (Legend on previous page)

| | |
|---|---|
| 4. Metformin effects on cell cycle and apoptosis | The downstream result of activating the AMPK pathway may lead to cytotoxic, apoptotic or cytostatic effects dependent upon the dose of metformin and the cancer cell type. One recent <i>in vitro</i> study ¹⁷³ suggested that metformin may have alternate effects on different BC cells, and reported that some BC cell lines underwent apoptosis in response to metformin treatment (T47D and MCF7) while others remain viable and resistant to metformin for up to 14 days of treatment (MDA-MB-453, BT474 and MDA-MB-231). In metformin-responsive cells, treatment causes significant, concentration-dependant suppression of cell proliferation with G1 cell cycle arrest, and this has been seen in both ER-positive and ER-negative cell lines, although the authors didn't establish why some cells responded and others didn't ¹⁷⁹ . An <i>in vivo</i> study ²²⁵ then went on to combine metformin with a chemotherapeutic drug, Paclitaxel, demonstrating that when they are in combination, they synergistically inhibit the cell cycle at the DNA-damage checkpoint (G2-M), induce apoptosis and reduce tumour burden in severe combined immunodeficient (SCID) mice inoculated with either human MCF-7 BC cells or A549 lung cancer cells. In both studies these effects were mediated by the activation of AMPK and inhibition of mTOR signalling pathway. |
| 5. Metformin effect on p53 gene | Several studies suggested that <i>p53</i> status might be important to metformin activity. <i>p53</i> , is a tumour suppressor gene which tends to be mutated or absent in many cancers which is an extremely important determinant of cellular fates, as it is involved in regulation of cell cycle and DNA-repair ²²⁶ . Upon activation, <i>p53</i> pathway can induce AMPK-mediated reversible cell cycle arrest at the glucose-dependent checkpoint of the cell cycle, which can be reversed upon restoration of normal metabolic conditions, unless AMPK-stimulation persists in which case it leads to apoptotic cell death ^{226, 227} . However, data from mechanistic studies of metformin and <i>p53</i> are contradictory. Although both breast and prostate cancer cells (MCF7 and LNCaP) with functional- <i>p53</i> were sensitive to the anti -proliferative effect of metformin <i>in vitro</i> ^{173, 176, 209} ; the <i>p53</i> -functional cells were as sensitive as the <i>p53</i> -null cells in the same studies. Conversely, metformin treatment resulted in selective toxicity and apoptosis-induced activity in colorectal <i>p53</i> -deficient cells; both <i>in vitro</i> and <i>in vivo</i> ¹⁹⁸ . |
| 6. Metformin effect on sex hormones and aromatase | Metformin has been shown to reduce the bioavailability of circulating oestrogen and androgens in BC patients. This action was achieved by counteracting the inhibitory effect of insulin on the hepatic synthesis of sex-hormones binding globulins and reducing insulin-mediated activation of cytochrome P450 enzyme; responsible for androgen synthesis ²²⁸ . In addition, two studies have reported an AMPK-dependent inhibition of aromatase gene in the adipose stromal cells of the human breast in response to metformin ^{174, 229} . This inhibition was influenced by metformin and occurs selectively in breast adipose tissue without suppressing the adrenal glucocorticoids synthesis. |
| 7. Metformin alters intracellular pathway regulators | Metformin impairs signalling molecules for cancer survival such as the AMPK which signals to numerous proteins involved in cell survival and cell death (Reviewed in section 1.3.5.1) |

1.3.6 Clinical trials with metformin in breast cancer

It is not really surprising that enthusiasm for repurposing metformin for use in breast cancer clinical trials is continuously growing, based on the evidence presented from epidemiological and preclinical studies, the safety, tolerability, favourable toxicity profile, and manageable side effects in addition to its current worldwide use by huge number of diabetic patients (120 million worldwide)¹²⁴. The most recent data suggest metformin has a wide spectrum of clinical usefulness for breast cancer ranging from disease prevention, neoadjuvant, adjuvant and extended adjuvant (beyond 5 years), as well as use in advanced disease settings²³⁰. Moreover, advanced breast cancer clinical trials combining metformin with established anticancer agents are under way or proposed.

In neoadjuvant chemotherapy settings, a remarkable complete pathologic response effect among diabetic metformin users has been reported²³¹. Data from prospective trials using the standard diabetic dose of metformin in non-diabetic cancer patients have also emerged and are promising. For example, a novel pre-operative trial randomized the participants for 2 weeks of metformin treatment pre-operatively in primary operable non-diabetic BC patients. It was the first study to evaluate both *in vivo* and systematic effect of metformin in BC cases, and reported a significant reduction in Ki-67, a marker of tumour proliferation²³², suggesting longer treatment may result in tumour shrinkage, alongside reduced serum insulin levels²³³. Similarly, other neoadjuvant monotherapy trials have reported proliferation-inhibitory and apoptosis-stimulatory effects in non-diabetic patients newly diagnosed with early BC²³⁴. These studies relieved part of the major concerns that the protective and therapeutic effects of metformin might be seen only in presence of metabolic derangement.

Unsurprisingly, as metformin is known to affect insulin, fasting insulin level has also reported to be reduced by 22.4% ($P=0.024$) when metformin is administrated to non-diabetic patients with non-metastatic disease, an effect which is believed to improve the outcome and lower the risk of disease recurrence by modifying the growth-stimulatory effect of insulin on tumour cells¹⁴².

Similarly, in non-diabetic patients with BC, metformin was able to reduce the circulating levels of oestrogen, androstenedion and testosterone, hormone parameters known to be associated with recurrence of BC^{228, 235}. Table 1.6 summarizes metformin trials in non-diabetic BC patients published to date. Overall, these pre-operative window studies in breast cancer demonstrate that metformin is safe for women with primary BC and confirm the attraction of metformin as a therapeutic agent.

However, all of the clinical trials to date have assessed the serum metabolic markers as well as markers of intratumoral proliferation (Ki67) and/or apoptosis (TUNEL), using immunohistochemistry. Of note, there is now only one ongoing study that uses functional imaging to assess the intratumoral pre- and post metformin pharmacodynamics in addition to evaluating the metabolic serum markers²³⁶. The preliminary results of this study suggesting that metformin can directly target cancer cells metabolism by inhibiting fatty acids oxidation and altering mitochondrial gene expression, therefore, providing an important novel insight to the direct effect that metformin might have on breast cancer cells in clinical settings²³⁷.

Table 1.6: Metformin trials in non-diabetic breast cancer patients

| Author/Reference | Enrolment and study population | Setting | Metformin dosing | Effects of metformin on metabolic and immunohistochemical markers |
|--|--|--------------------|--|--|
| Goodwin <i>et al.</i> ^{142, 238} | (1) 22 early BC patients: insulin>45mmol/L (2) 3649 treated early BC patients | Adjuvant | 500 mg three times for 6 months 850 twice for 5 years (results recorded after 6 months) | Metformin treatment significantly reduced the weight and blood variables including, insulin, glucose, leptin, and CRP at six months. Effects did not vary by baseline BMI or fasting insulin. |
| Hadad <i>et al.</i> ^{233, 239} | (1) 8 operable IBC (2) 47 operable IBC | Neoadjuvant window | 500 mg once a day for a week, then 1000 mg twice for another week | No significant change in serum insulin. 5.1% reduction in the proliferation marker Ki67, decrease in phosphorylated Akt and increase in phosphorylated AMPK. |
| Bonanni <i>et al.</i> ²⁴⁰ Cazzaniga <i>et al.</i> ²⁴¹ | 200 operable BC | Neoadjuvant window | 850 twice for 4 weeks | Metformin treatment significantly reduced glucose, total cholesterol and CRP with trend toward decreased insulin if BMI>27. 10.5% reduction in the proliferation marker Ki67, reduced IGFBP-3. No effect on TUNEL. |
| Kalinsky <i>et al.</i> ²⁴² | 35 obese/overweight invasive BC or DCIS versus matched untreated control | Neoadjuvant window | 500 mg am 1000 mg pm for 2-4 weeks | Metformin treatment significantly reduced the weight and blood variables including, total cholesterol, leptin, and trend toward decrease insulin and adiponectin with no significant change in glucose or IGFBP-3. |
| Niraula <i>et al.</i> ²³⁴ Dowling <i>et al.</i> ¹⁵⁶ | 39 operable BC | Neoadjuvant window | 500 mg three times a day for 13-40 days | Metformin treatment significantly reduced the weight and blood glucose level. No significant change in insulin, leptin and CRP. 3% reduction in the proliferation marker Ki67 and 0.5% increase in TUNEL. Reduction of phosphorylated Akt, AMPK and ACC. |

ACC, Acetyl-CoA reductase;; AMPK, AMP-activated protein kinase; IBC, Invasive breast cancer; BMI, Body mass index; CRP, C-reactive protein, DCIS, Ductal carcinoma *in situ*; IGFBP-3, Insulin –like growth factor-binding protein 3, TUNEL, Terminal deoxynucleotidyl transferase dUTP nick end labelling.

1.3.7 Limitations of preclinical models, and translational challenges

As previously mentioned, not all BC cell lines responded to metformin treatment either *in vitro* or *in vivo* studies, and as yet it is not clear why some respond while others don't. Despite that concern, it is clear that metformin does have a great impact on BC growth both directly and indirectly. However, much of the *in vitro* work published to date suffers a number of methodological limitations as follows.

1.3.7.1 Therapeutic concentrations and clinically relevant doses of metformin

It is of crucial importance when seeking to characterize the pre-clinical effects of metformin to distinguish between its therapeutic and supra-therapeutic concentrations. Although metformin has now been available for over 50 years, there is still no clear definition of its “therapeutic concentrations”; which has resulted in huge variation between the concentrations used in different studies. This is due to lack of studies that would measure and relate dose efficacy to corresponding plasma metformin concentrations in long-term treated patients. The dose efficacy here is considered to be in terms of blood glucose control.

A recent systematic analysis of therapeutic metformin doses used in pre-clinical studies identified 120 publications that cited 65 different concentrations and ranges of therapeutic plasma level of metformin. Surprisingly, the vast majority of these studies (116 publications) have not directly established the therapeutic concentrations of the drug and therefore cited previous publications that have not cited a supporting reference when referring to the therapeutic concentrations they used²⁴³. It is noteworthy that except four studies, none of the 116 studies performed so far were designed to identify the therapeutic concentration for metformin.

Pharmacokinetic parameters are the most reliable criteria to define the therapeutic concentrations of metformin i.e. the plasma steady state level achieved by the prescribed long-term multiple-dosage regimen. Therefore, the use of a parameter such as the maximum plasma concentration (C_{max}), which is the peak value obtained after administration of a single metformin dose, is conceptually flawed and non-reliable²⁴³.

Given the aforementioned pitfalls, questions have been raised about the safety and relevance of metformin concentrations utilised in the pre-clinical studies and whether they are of use in clinical practice. A recent review has already drawn attention to the fact that much of the *in vitro* and *in vivo* preclinical work published to date involved the use of a wide range of extremely high, supra-pharmacological and non-physiological concentrations of metformin (5-50 mM) which are greatly exceeding the feasible recommended clinical dose (2.5 g/day) and far in excess of those doses featured in the epidemiological studies and therefore may not translate directly into clinical practice¹⁵⁶ (Figure 1.7).

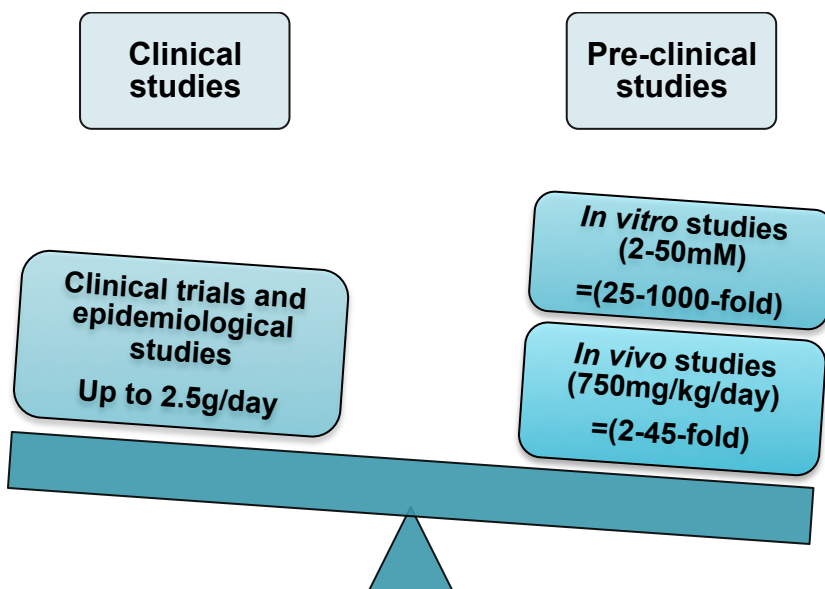


Figure 1.7: Doses of metformin used in preclinical and clinical studies.

Most of the population-based studies and clinical trials have featured standard pharmacological doses of metformin (up to 2.5 g/day). The vast majority of the preclinical studies have utilised extremely high concentrations exceeding 45-1000 fold (*in vivo* and *in vitro*, respectively) of the recommended therapeutic levels in humans.

To date, only four original research studies have assayed the plasma concentrations of metformin in diabetic subjects and determined a therapeutic concentration in long term well-tolerated metformin treatment^{244, 245} as well as in patients with chronic kidney disease²⁴⁶ and in steady state without lactic acidosis¹²⁹. Despite the fact that metformin concentration within tumour tissues has never been determined, the clinically relevant doses of metformin were calculated based on a consensus in the normal therapeutic and toxic plasma concentrations reported in diabetic subjects by these 4 different references^{244, 247-249}. These concentrations were in the range of **4 mg/L** up to **40 mg/L** respectively. By dividing these concentrations by the molecular weight of metformin (**129.2 g/mol**), a range of **0.03-0.3 mM** was obtained (normal-to- associated with serious toxicity) that can be considered as pharmacologically relevant doses. However, it has been reported that metformin tissue concentrations are 10-20 folds higher than plasma concentrations due to its tendency to accumulate in peripheral tissue such as salivary gland, small intestine, stomach, colon, liver and kidney and liver; in an *in vivo* study using diabetic mouse²⁵⁰. Therefore, some *in vitro* studies have gone further and considered 2-8 mM as relevant human therapeutic concentrations^{173, 251, 252}. In this thesis, the range of 1-5 mM was considered as potential tissue accumulated dose of metformin.

1.3.7.2 Metformin uptake, accumulation and export by cancer cell

Another important factor for a proper understanding of the cellular uptake, intracellular accumulation, excretion and the optimum dosing required to achieve a strong inhibitory effect on BC cells, is to explore metformin transport into different subtypes of BC cells. This can be achieved by investigating the expression of different candidate transporters by BC cell lines (OCT1-3, PMAT and MATE1-2). The potential presence and role of these carrier proteins in BC settings should be explored further, as this may also provide a further insight into the differential responses of BC cell lines to metformin treatment and help to identify a useful *in vitro* model to assess the anticancer effect of metformin in breast cancer (Figure 1.8).

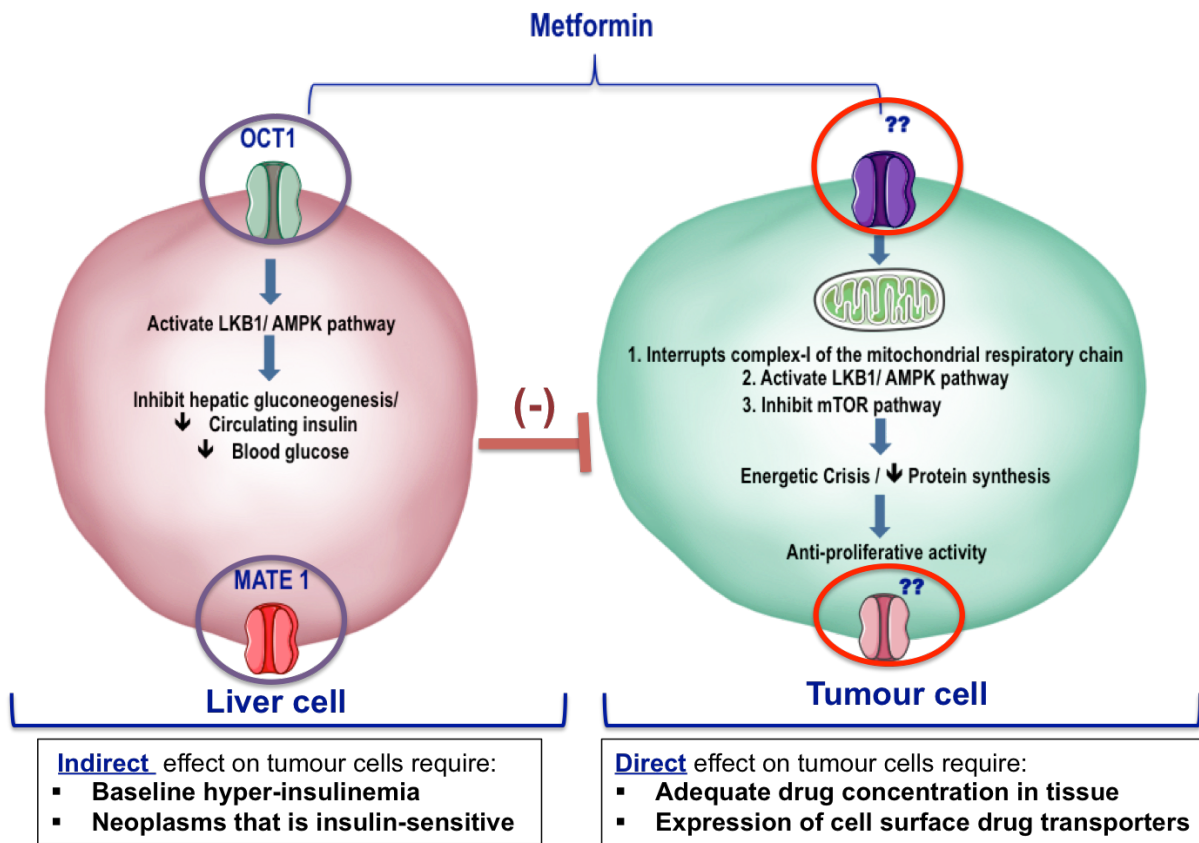


Figure 1.8: Requirements of the direct effect of metformin on tumour cells, compared to the indirect effect.

This is a schematic representation of the suggested hypothesis of metformin uptake and excretion by cancer cells. It also highlights the importance of using an adequate drug concentration that can accumulate in the tumour cell and achieve the anti-cancer effect.

1.3.7.3 Outstanding questions in preclinical and clinical settings

Despite extensive work on the preclinical effects of metformin on breast cancer cell lines, certain questions still remain which include:

- How does metformin enter and leave breast cancer cells?
- Is there an altered expression of metformin transporters during the progression from normal breast tissue into various disease states?
- Will the suggested clinically relevant doses of metformin inhibit breast cancer proliferation and/or cause cell cycle arrest?
- Are there any specific subtypes of breast cancer that respond more than others?
- Can metformin help prevent or treat metastatic dissemination of breast cancer, for example, to the bone and lung?

Clinical trials with metformin as a treatment for BC are still in early phases, and a number of unanswered questions still persist. For example, which cancer subtype is the most promising target, which population should be targeted, and what should metformin be combined with? Equally it is important to look for possible synergy with other clinically useful chemotherapeutics to evaluate whether metformin can work as a radio- or chemo-sensitizer.

In the preventative BC clinical trial settings, it is still not clear which tumour subtype is likely to benefit more from metformin prevention strategy, which population subsets should be targeted in the chemoprevention strategy (diabetics, non-diabetics, pre- or postmenopausal women), what is the best time to start the chemoprevention strategy, what is the best dose and for how long should the treatment last.

With regard to the mechanisms of metformin's action, some unanswered questions are: (A) Is the anticancer effect attributed to its indirect (anti-diabetic), direct or both effects; (B) Are hyperinsulinemia and metabolic disturbances required for the effectiveness of metformin; (C) Which of the direct effects reported *in vitro* with the supra-pharmacological concentrations is most relevant clinically; (D) Is AMPK activation required in both tumour and hepatic tissues to elicit the anti-proliferative effect of metformin; and (E) What pharmacokinetics and pharmacodynamics factors might contribute to the tissue distribution and the anticancer activity of metformin.

Despite these continuing questions, there is no doubt that metformin has some advantages over the current chemotherapeutic regimes as it is non-toxic and has extensive anti-proliferative activity against most of the molecular subtypes of BC.

1.4 Project's hypothesis and aims

Based on the emerging reports on the potent antitumor activity of metformin in various experimental models of hormone-sensitive breast cancers, this PhD project aims to test the hypothesis that:

“The anti-tumour effect of clinically relevant doses of metformin (0.03-0.3mM) depends on breast cancer subtype and the presence of metformin transporters on breast cancer cells”

To date, data on the effect of the pharmacologically relevant doses of metformin on breast cancer is extremely limited and therefore our aims are:

- **Firstly:** To explore the expression of several metformin transporters in a panel of increasingly transformed breast cell lines and diverse molecular subtypes including, non-transformed, hyperplastic ductal epithelial, *in situ* ductal carcinoma, luminal A (ER⁺, HER-2⁻), triple-negative (ER⁻, PR⁻, HER-2⁻) and metastatic bone-seeking cell lines.
- **Secondly:** To assess the direct anticancer effect of metformin at clinically relevant concentrations against our 2D *in vitro* model of breast cancer progression represented by the panel of increasingly transformed breast cell lines and relate this to the expression of metformin transporters.
- **Thirdly:** To investigate the potential anti-metastasis effect of metformin in breast cancer by identifying protein changes in response to metformin using global proteomic analysis, and determining whether these changes differ between the wild-type triple negative, bone- and lung-homed breast cancer cells.

By combining proteomic and molecular biology approaches, this project will provide an exciting opportunity to advance our knowledge and understanding by offering an important translational insight to the potency and effectiveness of clinically relevant doses of metformin, the key players of its transport in breast cancer as well as effects of metformin on specific phenotypic changes in breast cancer metastasis.

2. Chapter 2: Materials and methods

2.1 Materials

All reagents and equipment are listed in alphabetical order

Table 2.1: General materials listed with suppliers

| Material | Supplier |
|--|--|
| Ammonium Per Sulphate (APS) | Bio-Rad Laboratories Ltd., UK |
| Ammonium Bicarbonate | Sigma-Aldrich, Poole, Dorset, UK |
| Antigen Retrieval Solution (citrate buffer) | Dako, Barcelona, Spain |
| Bovine Insulin | Sigma-Aldrich, Poole, Dorset, UK |
| Cholera Toxin | Sigma-Aldrich, Poole, Dorset, UK |
| Deionised Water | Millipore-Q™ Water Purification system |
| Developing Solution | AGFA, Mortsel, Belgium |
| Dimethyl Sulphoxide (DMSO) | Sigma-Aldrich, Poole, Dorset, UK |
| 1,4-Dithiothreitol (DTT) | Sigma-Aldrich, Poole, Dorset, UK |
| Dulbecco's Modified Eagle's Medium (DMEM) | Lonza, Slough, UK |
| Dulbecco's Modified Eagle Medium; Nutrient Mixture F-12 (DMEM/F12) | Lonza, Slough, UK |
| Epidermal Growth Factor (EGF) | PeproTech EC Ltd., London, UK |
| Ethanol | Fisher Scientific, Loughborough, UK |
| Ethidium Bromide | Sigma-Aldrich, Poole, Dorset, UK |
| Fetal Bovin Serum (FBS) | Biosera, Ringmer, UK |
| Films | Amersham Hyperfilm™ ECL, UK |
| Filter Paper, Gel Blot Paper | GE Healthcare, UK |
| Fixing Solution | AGFA, Mortsel, Belgium |
| Formic Acid | Sigma-Aldrich, Poole, Dorset, UK |
| Haematoxylin | Fisher Scientific, Loughborough, UK |
| Horse Serum | Sigma-Aldrich, Poole, Dorset, UK |
| Hydrocortisone | Sigma-Aldrich, Poole, Dorset, UK |
| Industrial Methylated Spirit (IMS) | Fisher Scientific, Loughborough, UK |
| Iodoactamide (IAA) | Sigma-Aldrich, Poole, Dorset, UK |
| L-glutamine | Sigma-Aldrich, Poole, Dorset, UK |
| Laemmli Sample Buffer | Sigma-Aldrich, Poole, Dorset, UK |
| MEGM™ Mammary Epithelial Cell Growth Medium | Lonza, Slough, UK |
| MEGM™ Cell Growth Medium Supplement Mix | Lonza, Slough, UK |
| Methanol | Fisher Scientific, Loughborough, UK |
| Methylene Blue | Sigma-Aldrich, Poole, Dorset, UK |
| Nuclease-Free Water | Qiagen, Hilden, Germany |
| Penicillin/Streptomycin | Invitrogen, Paisley, UK |
| Phosphate Buffer Saline (PBS) | Lonza, Slough, UK |
| Precision Plus Protein™ Standard | Bio-Rad Laboratories Ltd., UK |
| Propidium Iodide staining solution (PI) | Sigma-Aldrich, Poole, Dorset, UK |
| Protease Phosphatase Inhibitor Cocktail | Sigma-Aldrich, Poole, Dorset, UK |

| | |
|---|-------------------------------------|
| Pure Water | Sigma-Aldrich, Poole, Dorset, UK |
| Ribonuclease A From Bovine Pancreas | Sigma-Aldrich, Poole, Dorset, UK |
| RIPA Buffer, Cell Lysis Buffer | Fisher Scientific, Loughborough, UK |
| Roswell Park Memorial Institute 1640 (RPMI 1640) Medium | Lonza, Slough, UK |
| Sequencing Grade Modified Trypsin | Promega, Southampton, UK |
| SDS-PAGE Running Buffer | Sigma-Aldrich, Poole, Dorset, UK |
| Stripping Buffer | Sigma-Aldrich, Poole, Dorset, UK |
| Trypan Blue | Life Technologies, Paisley, UK |
| Trypsin (0.05%)/EDTA (0.02%) | Sigma-Aldrich, Poole, Dorset, UK |
| TBS-Tween 20x | Fisher Scientific, Loughborough, UK |

2.1.1 Commercial kits

Table 2.2: Commercial kits and suppliers

| Commercial Kits | Supplier |
|--------------------------------------|---|
| Brdu Cell Proliferation ELISA Kit | Abcam, Cambridge, UK |
| 3,3-Diaminobenzidine (DAB) Substrate | Vector Labs, Peterborough, UK |
| Ez-PCR Mycoplasma Test Kit | Geneflow Ltd, Litchfield, UK |
| High Capacity RNA-To-cDNA Kit | Applied Biosystems, Life Technologies, Paisly, UK |
| MEMG™ Bulletkit | Lonza, Slough, UK |
| Pierce™ BCA Protein Assay Kit | Fisher Scientific, Loughborough, UK |
| Rnase-Free Dnase Set | Qiagen, Hilden, Germany |
| Rneasy Mini Kit | Qiagen, Hilden, Germany |
| Vectorstain Elite ABC Kit | Vector Labs, Peterborough, UK |

2.1.2 Equipment

Table 2.3: Items listed with suppliers

| Equipment | Supplier |
|--|--|
| 0.2µm Sterile Filters | Merck Millipore, Nottingham, UK |
| 1.8ml Cryo.S™ Cryogenic Tubes | Greiner Bio-One Ltd., Stonehouse, UK |
| 20µl Microloader Tips | Eppendorf UK Limited, Stevenage, UK |
| 15 And 50ml Universal Tubes | Sarstedt, Leicester, UK |
| 6, 12 and 24 Well Tissue Culture Plates | Nunc Ltd., London, UK |
| 25, 75 And 175 Cm ² Tissue Culture Flasks | Greiner Bio-One Ltd., Stonehouse, UK |
| 96 Well Plate | Cole-Parmer, Hanwell, UK |
| 348 PCR Plate | Sigma-Aldrich, Poole, Dorset, UK |
| ABI Prism 7900HT Sequence Detection System | Applied Biosystems, Life Technologies, Paisley, UK |
| Antigen Retriever (Pressure Cooker) | Aptum, Southampton, UK |
| Biopette™ Variable Volume Pipettes | Gilson Inc., Middleton, USA |
| Cellquestpro™ Software | Becton Dickinson, San Jose, USA |
| Centrifuges | Sanyo and Harrier 18/80 |
| Concentrator Plus | Eppendorf UK Limited, Stevenage, UK |
| DNA Engine DYAD™ Thermal Cycler | Bio-Rad Laboratories Ltd., UK |

| | |
|---|--|
| Electrophoresis System | Bio-Rad Laboratories Ltd., UK |
| Flustar Galaxy Microplate Reader | BMG LABTECH, London, UK |
| Freezer | -20 from REV'ECO, -80 from SANYO |
| Grant JB Series Water Bath | Wolflabs, UK |
| Heat Block | Hybride Thermal Reactor, UK |
| Ice Machine | Ziegra Eis machine, Stockport, UK |
| Immedge™ Hydrophobic Barrier Pen | Vector Labs, Peterborough, UK |
| Microamp Optical Adhesive Film | Life Technologies, Paisley, UK |
| LSRII Cell Sorting Instrument | BD Bioscience, London, UK |
| Laminar Flow Hood (Class II) | Walker Safety Cabinet Ltd., UK |
| Minifuge And Microfuge Tubes | Sarstedt, Leicester, UK |
| 'Mr.Frosty' Freezing Container | Nalgene, New York, USA |
| Nanodrop© Lite Spectrophotometer | Nanodrop Technologies, Wilmington, USA |
| Nikon Eclipse TS 100 Inverted Microscope | Nikon Uk Ltd., Surrey, UK |
| Pierce C-18 Spin Columns | Sigma-Aldrich, Poole, Dorset, UK |
| Pipettes Tips (P2-P1000) | Sarstedt, Leicester, UK |
| Powerpac™ HC Power Supply | Bio-Rad Laboratories Ltd., UK |
| Q Exactive™ HF hybrid quadrupole-Orbitrap mass spectrometer | Thermo Scientific, Bremen, Germany |
| Shaker | Stuart, Staffordshire, UK |
| Stirrer | Stuart, Staffordshire, UK |
| Vortex | VWR , Lutterworth, UK |

2.1.3 Cell culture media

The components of all media used for cell culture are summarised in the following tables. Once prepared, all media were stored at 4°C.

Table 2.4: MCF10A, MCF10AT and DCIS.com cells growth medium

| Component | Growth Medium | Resuspension medium |
|--|--|---------------------|
| Dulbecco's Modified Eagle Medium/Nutrient Mixture F-12 (DMEM/F12) (1x) | 469 ml (93.8%) | 400 ml |
| Horse Serum | 25 ml (5% final) | 100 ml (20% final) |
| Epidermal Growth Factor (EGF) (100 µg/ml stock) | 100 µl (20 ng/ml final) | -- |
| Hydrocortisone (1 mg/ml stock) | 250 µl (0.5 µg/ml final) | -- |
| Cholera Toxin (1 mg/ml stock) | 50 µl (100 ng/ml final) | -- |
| Insulin (10 mg/ml stock) | 500 µl (10 µg/ml final) | -- |
| Penicillin/Streptomycin (100x solution) | 5 ml (100 IU/ml penicillin and 100 µg/ml streptomycin) | 5 ml |

Notes:

1. All additives were re-suspended in sterile dH₂O; aliquoted and stored at -20°C, except the hydrocortisone, which was re-suspended in absolute ethanol.
2. All the appropriate additives were premixed and sterile filtered through a 0.2 µm filter before adding to the DMEM/F12 medium.
3. This medium contains 17.4 mmol/l of glucose, 2 mM L-glutamine and 0.049 uM L-asparagine monohydrate.
4. In order to reduce the variability within the experiments, the Mammary Epithelial Cell Growth Medium (MEGM)TM Bulletkit containing necessary supplements (Table 2.5) was used as the assay medium for MCF10A, MCF10AT and DCIS.com cells.

Table 2.5: MCF10A, MCF10AT and DCIS.com cells assay medium

| Component | Growth Medium | Resuspension Medium |
|---|--------------------------|----------------------------|
| Mammary Epithelial Basal Medium (MEBM) | 500 ml | 400 ml |
| Bovine pituitary extract (BPE) | 2 ml (5% final) | 100 ml (20% final) |
| Human Epidermal Growth Factor (hEGF) | 500 µl (20 ng/ml final) | -- |
| Hydrocortisone | 500 µl (0.5 mg/ml final) | -- |
| Human Insulin | 500 µl (10 µg/ml final) | -- |
| Gentamicin sulphate (30 mg/ml) Amphotericin-B (15 mg/ml) | 5 ml | 5 ml |
| 50 µl of 100 ng/ml Cholera toxin was added separately to the medium; not provided by the kit. | | |

Note: This is the “Mammary Epithelial Cell Growth Medium (MEGM)TM Bulletkit”, which contains 15.49 mmol/l of glucose, 2 mM L-glutamine and 0.049 mM L-asparagine monohydrate.

Table 2.6: MCF7, T47D, MDA-MB-231, MDA-MB-231(BM) and HepG₂ cell culture and assay medium

| Component | Growth Medium |
|---|--|
| Roswell Park Memorial Institute 1640 (RPMI 1640) medium without L-Glutamine (1x)* | 440 ml (88% final) |
| Foetal Bovine Serum | 50 ml (10% final) |
| L- Glutamine (200 mM) | 5 ml (2 mM final) |
| Penicillin/Streptomycin (100x solution) | 5 ml (100 IU/ml penicillin and 100 µg/ml streptomycin) |

*RPMI1640 without L-glutamin formulation contains 15.49 mmol/l of glucose.

Note: For the MTS assay, RPMI-1640 medium without phenol red was used which contains 15.49 mmol/l of glucose and 0.37 mM L-asparagine monohydrate.

Table 2.7: MDA-MB-231(LM) cell culture and assay medium

| Component | Growth Medium |
|--|--|
| Dulbecco's Modified Eagle Medium (DMEM) with L-Glutamine (1x)* | 445 ml (89% final) |
| Foetal Bovine Serum | 50 ml (10% final) |
| Penicillin/Streptomycin (100x solution) | 5 ml (100 IU/ml penicillin and 100 µg/ml streptomycin) |

*DMEM formulation contains 15.49 mmol/l of D-glucose, 2 mM of L-glutamine and no L-asparagine monohydrate.

2.1.4 Quantitative polymerase chain reaction (qPCR) primers

Table 2.8: Metformin-transporters validated All-in-One™ qPCR Primers ID and sequences (GeneCopoeia)

| Gene Name | Primer ID | Primers Sequence |
|------------------|--|---|
| <i>SLC22A1</i> | NM_003057.2 Catalog number: HQP017490 | Forward: TCCCTGTGTGACATAGGTGGG Reverse: CAACACCGCAAACAAAATGAGG |
| <i>SLC22A2</i> | NM_003058.2 Catalog number: HQP017493 | Forward: GACATTGGTGGCATCATCAC Reverse: CTCGATGGTCTCAGGCAAAG |
| <i>SLC22A3</i> | NM_021977.2 Catalog number: HQP017492 | Forward: AACCATGGCCTTGAAATTG Reverse: GCCGAAAGAGCAGAAATGG |
| <i>SLC29A4</i> | NM_001300847.1 Catalog number: HQP071320 | Forward: CCATGCCGTGACCTACTTC Reverse: GGATCTGCCACGAAGTCT |
| <i>SLC47A1</i> | NM_018242.2 Catalog number: HQP014217 | Forward: TAAACAACGTGCCTCGGAGT Reverse: GGCAAAGGTTCTTCTGGCG |
| <i>SLC47A2</i> | NM_001099646.1 Catalog number: HQP058785 | Forward: TGAGATCGGGAGCTTCCTCA Reverse: GAGCCCCAAGGGAATCATGT |
| * <i>GAPDH</i> | NM_002046.3 Catalog number: HQP006940 | Forward: GTGGACCTGACCTGCCGTCT Reverse: GGAGGAGTGGGTGTCGCTGT |

*GAPDH was used as an endogenous control

2.1.5 Commercial human tissue slides

Table 2.9: Tissue microarray slides used in this project

| Slide used | Details | Supplier |
|--|--|------------------|
| Beast cancer tissue array with progressive changes | A breast disease tissue array containing 48 cases from normal, premalignant and cancer tissues with progressive grades and stages. | Abcam (ab178111) |
| Breast common disease array of 102 cases | A breast disease tissue array containing 102 cases of normal breast, fibrocystic changes, proliferative breast diseases (atypical) and various types and stages of breast cancers. | Abcam (ab178113) |
| Kidney (human) normal tissue slides | Normal human kidney tissue sections used as a positive control for some transporters. | Abcam (ab4347) |

2.1.6 Antibodies

Table 2.10: Primary antibodies

| Antibody | Details | Dilutions used | Product code and Supplier |
|----------------------|-----------------------------|------------------------------------|-----------------------------------|
| Anti-SLC22A1 (OCT1) | Polyclonal raised in rabbit | Western Blot: 1:1000 IHC: 1:200 | Sigma-Aldrich (AV41516) |
| Anti-SLC22A2 (OCT2) | Polyclonal raised in rabbit | Western Blot: 1:500 IHC: 1:200 | Abcam (Ab198800) |
| Anti-SLC22A3 (OCT3) | Polyclonal raised in rabbit | Western Blot: 1:50 IHC: 1:100 | Abcam (Ab183071) |
| Anti-SLC29A4 (PMAT) | Polyclonal raised in mouse | Western Blot: 1:200 IHC: 1:100 | Abcam (Ab56554) |
| Anti-SLC47A1 (MATE1) | Polyclonal raised in rabbit | Western Blot: 1:200 IHC: 1:100 | Abcam (Ab104016) |
| Anti-SLC47A2 (MATE2) | Polyclonal raised in rabbit | Western Blot: 1:50 IHC: 1:100 | Abcam (ab106117) |
| Anti-STAT3 | Rabbit monoclonal | Western Blot: 1:250 | Abcam (ab68153) (EPR787Y) |
| Anti-PBR | Rabbit monoclonal | Western Blot: 1:10,000 | Abcam (ab109497) (EPR5384) |
| Anti-TNFAIP8 | Rabbit monoclonal | Western Blot: 1:1000 | Abcam (ab195810) (EPR10058(3)) |
| Anti-GRB2 | Rabbit monoclonal | Western Blot: 1:5000 | Abcam (ab32037) (Y237) |
| Anti-Calmodulin | Rabbit monoclonal | Western Blot: 1:250 | Abcam (ab45689) (EP799Y) |
| Anti Beta-actin | Mouse monoclonal | Western Blot: 1:10000 | Sigma-Aldrich (A2228) (AC-74) |

IHC: immunohistochemistry

Table 2.11: Secondary antibodies

| Antibody | Details | Supplier | Dilutions used |
|--|---------------------------|-----------------------|------------------------------|
| Anti-mouse IgG-horseradish Peroxidase (HRP) | Polyclonal raised in goat | Vector Labs, PI-2000 | Western Blot: 1:1000 |
| Anti-mouse biotinylated IgM | Polyclonal raised in goat | GE healthcare, NA931V | IHC: 1:200 |
| Anti-rabbit IgG-horseradish Peroxidase (HRP) | Polyclonal raised in goat | Dako, P0448 | Western Blot: 1:2000-1-20000 |
| Anti-rabbit biotinylated IgM | Polyclonal raised in goat | Vector Labs, BA-1000 | IHC: 1:200 |

IHC: immunohistochemistry

2.2 Methods

2.2.1 Cell culture

2.2.1.1 Cell lines

MCF-10A cell line; is most commonly used *in vitro* model for studying normal breast cell function and transformation. These cells are non-tumorigenic, do not express oestrogen receptor, derived from benign proliferative breast tissue (from a patient with fibrocystic disease) and spontaneously immortalized after extended cultivation in low calcium concentrations²⁵³. Purchased from the American Type Culture Collection (ATCC® CRL-10317™).

MCF-10AT cell line; is a model for the evolution of cancer from proliferative breast disease, obtained from Dan Arbour institute, USA. Implantation of MCF10AT cells in mice gives rise to lesions resembling usual ductal hyperplasia (UH) and atypical ductal hyperplasia (ADH) over 12-16 week periods. Therefore, the MCF-10AT cell line is considered to represent the pre-malignant stage of breast cancer²⁵⁴.

DCIS.com cell line; a model of malignant precursor cells; is a clonal breast cancer cell line originating from premalignant MCF10AT cells that were injected into severe immune deficient mice leading to lesions predominantly resembling ductal carcinoma *in situ*, with further progression to invasive carcinoma (IC) after 9 weeks²⁵⁵. DCIS.com cells were obtained from Karmanos institute, USA.

Three breast cancer cell lines were chosen to represent different breast cancer subtypes and aggressiveness, namely **MCF7** (ATCC® HTB-22™), **T47D** (ATCC® HTB-133™) and **MDA-MB-231** (ATCC® HTB-26™) cell lines, which were purchased from the ATCC. Both MCF7 and T47D are classified as luminal A, while MDA-MB-

231 is classified as triple negative, highly metastatic cells (Table 2.12).

The **MDA-MB-231(BM)** and **MDA-MB-231(LM)** cells are the metastatic variants of the human breast cancer cell line MDA-MB-231 which either home to the bone (BM) or lungs (LM) when administered intravenously to nude mice, whereas the ‘parental’ MDA-MB-231 cells do not. They were generated by injecting the MDA-MB-231 cells into the tail vein of nude mice then collecting either the bone or lung metastatic cells which were then expanded in culture and re-injected into the tail vein, and the process repeated. Once the cells have been passaged through the mice 7 times, the cells are fully bone and lung seeking and will establish bone and lung metastases, respectively, when injected into the tail vein^{256, 257}. These cells were a kind gift from Professor Janet Brown.

Table 2.12: Classification and characteristics of the invasive breast cancer cell lines used

| Cell line | Immuno-profile | p53-status | Classification | Tumour type and origin |
|-------------------|---|------------|------------------------------|---|
| MCF7 | ER ⁺ , PR ⁺ , HER2 ⁻ | Wild type | Luminal A | Well differentiated, invasive ductal carcinoma, derived from pleural effusion from patient with adenocarcinoma |
| T47D | ER ⁺ , PR ⁻ , HER2 ⁻ | Mutant | Luminal A | Differentiated, infiltrating ductal carcinoma, derived from pleural effusion from patient with ductal carcinoma |
| MDA-MB-231 | ER ⁻ , PR ⁻ , HER2 ⁻ | Mutant | Claudin-low, Triple negative | Least differentiated, adenocarcinoma, derived from pleural effusions from patient with adenocarcinoma |

HepG2; human-derived hepatocellular carcinoma cell line was used as a positive control for OCTs and MATEs receptors expression in the qRT-PCR and Western blot experiments. These cells were a kind gift from Dr Karen Sisley.

MCF-10A, MCF-10AT and MCF10DCIS.com cell lines were cultured in advanced DMEM/F12 medium with additional supplements as stated in (Table 2.4). MCF7, T47D, MDA-MB-231 and MDA-MB-231(BM) cell lines were cultured in supplemented RPMI-1640. MDA-MB-231(LM) cell line was cultured in supplemented DMEM medium. The morphology of the premalignant, pre-invasive, invasive and metastatic cells is shown in figure 2.1.

2.2.1.2 Mycoplasma testing of cell lines

Routine mycoplasma testing of the cell lines was carried out shortly after their arrival into the laboratory and at six-month intervals thereafter. It is noteworthy that no short tandem repeat (STR) analysis was performed in this study as most of the human breast cell lines used were purchased from ATCC (MCF10A, MCF7, T47D and MDA-MB-231).

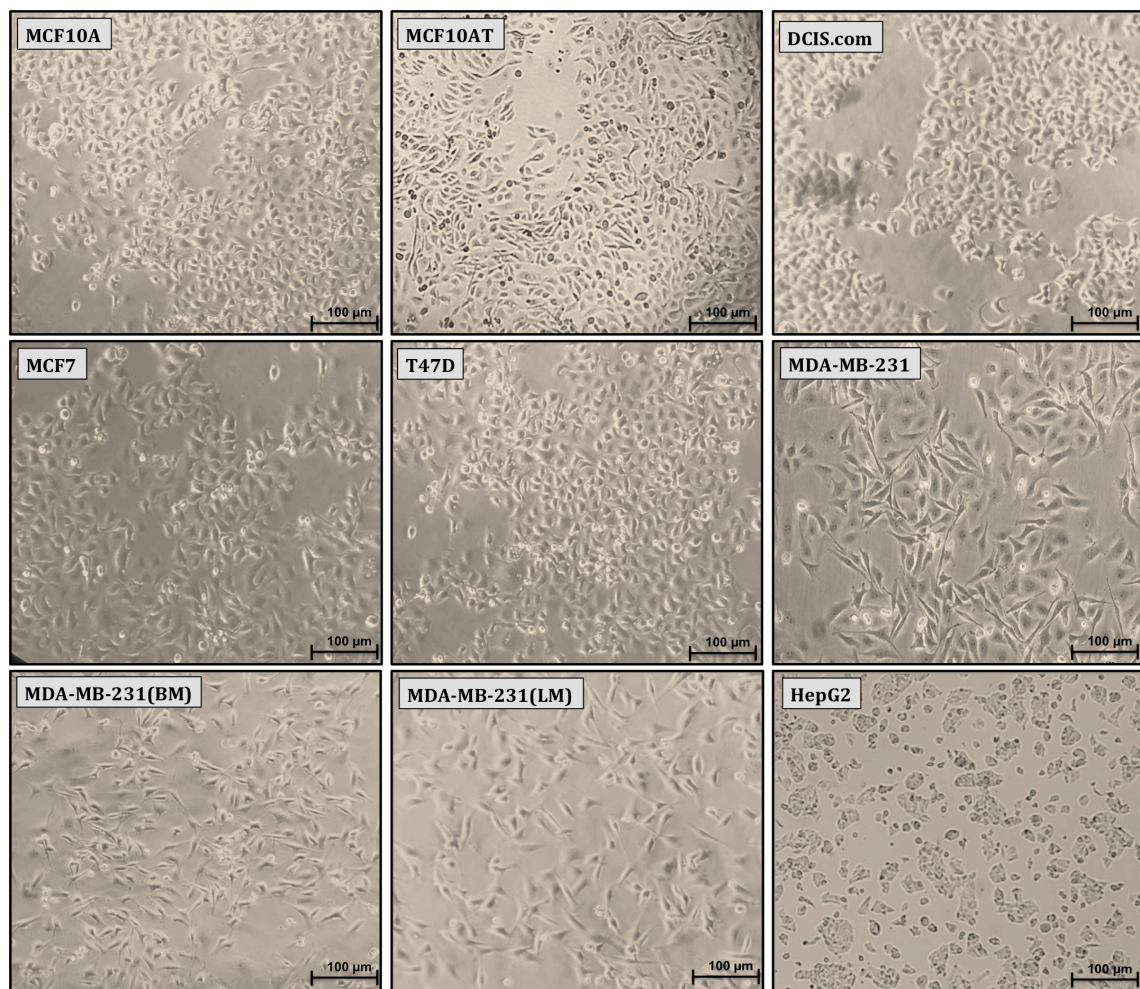


Figure 2.1: Microscopic appearance of the cell lines utilized.

All are 60-70% confluent, at 10x magnification. Scale bar represents 100 μm .

2.2.1.3 Routine cell culture

All the equipment and solutions were sterile and all the cell culture work was performed in a class II laminar flow hood using aseptic techniques. The cabinets were switched on and off at least 15 minutes before and after the completion of any work, to allow the air to circulate. The cabinets were also cleaned thoroughly with industrial methylated spirit (IMS) prior to and following each usage. All cell lines were grown as a monolayer in T75 cm^2 flasks and incubated in a humidified atmosphere at 37°C and

5% CO₂ in a LEEC incubator. The cultures were monitored on a day-to-day basis to make sure that the cells kept growing and were free of contamination. The cells were fed with the appropriate full growth media every 48 hours. Upon achievement of 70-80% confluence, cells were sub-cultured as described below.

2.2.1.4 Cell subculture

The cells were routinely passaged upon reaching 70-80% confluence. The spent media in the flasks was discarded and the cell monolayers were washed twice with 10 ml of phosphate buffered saline (PBS) without calcium and magnesium, to remove any residual serum that would block the trypsin action. The PBS was aspirated and discarded and then 1-3 ml of pre-warmed 0.05% trypsin in 0.02% EDTA solution was added followed by 2-5 minutes incubation at 37°C and 5% CO₂ to detach the cells from the surface of the culture flask. A longer period of incubation of up to 20 minutes was necessary to detach the extremely adherent MCF-10A, MCF-10AT and DCIS.com cells from the surface of the flask. To ensure that all cells had detached, the flasks were observed under a light microscope and if not, the side of the flask was tapped sharply to disrupt the large clumps and release the cells. Once detached, 5-7 ml of fresh media was added to neutralize the trypsin activity with extensive pipetting up and down to disaggregate all cell clumps in the flask. The mixture was then pelleted by centrifugation at 150 x g for 5 minutes. The supernatant was discarded and the cell pellet re-suspended in 5 ml of complete media. 0.5-1 ml of the cell suspension was added to 10ml of fresh media in T75 flask to generate a split ratio of 1:5-1:10 depending on the growth rate of the different cell lines, and maintained as previously described. When it was important to generate cells at 70% confluent by a particular date, cell counting was performed as described in section 2.2.1.7 and cells seeded at a specific number per flask instead of simply using a split ratio.

2.2.1.5 Cryopreservation of cell culture stocks

Frozen stocks were prepared using cells at less than 80% confluence, in the Log phase of the growth curve. Cells were washed twice with PBS and trypsin added. The recovered cells were pelleted in 10ml of relevant media by centrifugation at 800 x g for 5 minutes. The cell pellet was re-suspended at a concentration of 5x10⁵ cell/ml in a solution of the relevant media and dimethyl sulphoxide (DMSO). A mixture of DMEM/F12 with 20% FBS and 10% DMSO was used for the normal, pre-malignant

and pre-invasive cells. For the invasive and metastatic cells, a solution of 20% DMSO in FBS was utilised. 1ml aliquots of cell suspension were added to the cryovials and placed in a styrofoam rack (Mr. Frosty) at -80⁰C for 24 hours before being transferred for long-term storage in liquid nitrogen.

2.2.1.6 Retrieval of stored cells

The previously stored cryovials were thawed rapidly from liquid nitrogen in a 37⁰C water bath. Cells were spun down at 5000 x g for 5 minutes to remove DMSO from the media and then gently re-suspended in 5 ml pre-warmed appropriate full growth media and transferred into T25 flasks and kept at 37⁰C. The medium was changed to fresh medium the following day. When 70-80% confluent, cells were transferred to a T75 flask and cultured by passage as normal.

2.2.1.7 Cell counting

Following trypsinization and centrifugation at 1000 x g for 5 minutes (as described in section 2.2.1.3), cells were re-suspended in 0.5-5 ml of media. 10 µl was taken from each suspension tube and thoroughly mixed with 10 µl of 0.4% trypan blue solution (1:1). 10 µl of this mixture was pipetted into one side of the dual-chamber counting slide of the TC20TM Automated Cell Counter. Dead cells take up trypan blue; therefore this machine detects the % viability, total number of cells and the number of viable cells. TC20TM Automated Cell Counter automates the widely used trypan blue cell exclusion assay and has replaced the historical cell viability determinations that were manually performed using a light microscope and haemocytometer. This technique enables accurate, reliable and rapid cell counting.

2.2.2 Preparation of metformin

A stock solution of 1 molar of metformin (MW: 165.6) was freshly prepared and diluted in purified water prior to each experiment following this formula:

$$\text{Mass (g)} = \text{Concentration (mol/L)} \times \text{Volume (L)} \times \text{Formula Weight (g/mol)}$$

The stock solution was then serially diluted to a final volume of 10 ml of full growth medium per each concentration, as detailed in Figure 2.2.

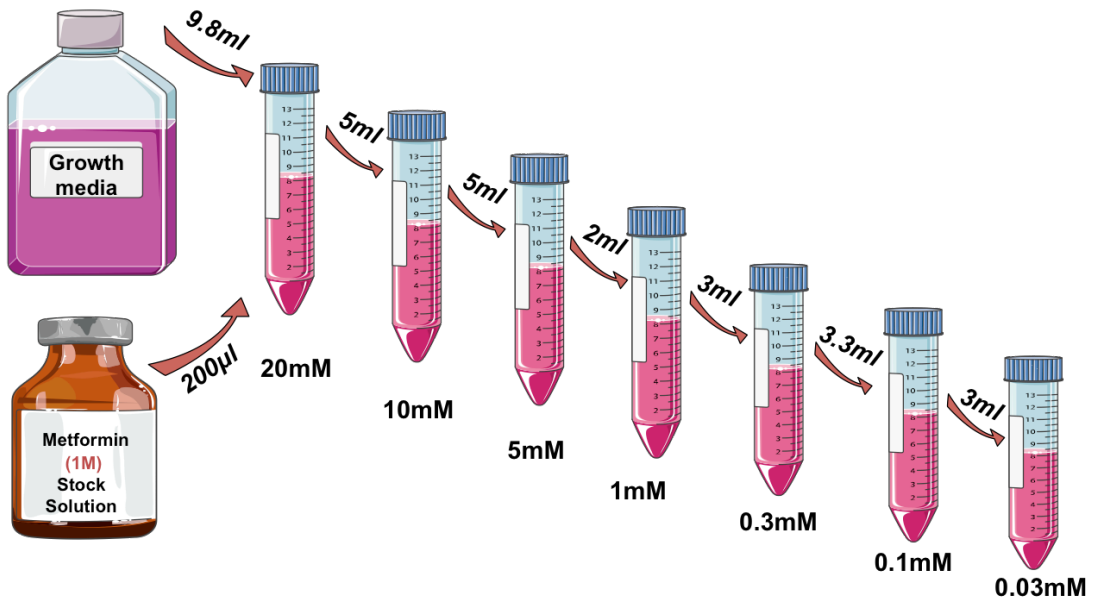


Figure 2.2: Serial dilutions of 1 molar metformin stock solution.

2.2.3 Quantitative real time polymerase chain reaction (qRT-PCR)

The expression of transporters potentially involved in metformin-uptake by breast cells was studied at the mRNA level using quantitative real time PCR (qRT-PCR). HepG2 cells were used as a positive control for the transporter proteins investigated. The protocol of qRT-PCR was carried out for genes of interest in duplicate at least three times on ABI Prism 7900HT sequence detection system. The qRT-PCR assay is based on measuring the fluorescence using SYBR Green as a fluorescent reporter molecule. The first cycle at which the amplification fluorescence generated is called the “C_t” or threshold cycle. The fluorescence intensity increases proportionally with each amplification cycle in response to the increased target concentration, and the numerical value of the C_t is inversely related to the amount of target in the reaction (i.e. the lower the C_t, the greater the amount of target)²⁵⁸.

2.2.3.1 RNA extraction

Total RNA from the cultured breast cells was extracted using an RNeasy™ Mini Kit and RNase-free pipette tips according to manufacturer's instructions. The RNeasy™ protocol relies on the properties of RNA binding to silica at different salt and buffer conditions and is a column (silica) based extraction technique where the guanidine isothiocyanate (GITC) is used to lyse cells and denature proteins, RNases and DNases.

The cells are first collected by gentle trypsinization using 0.25% trypsin EDTA, counted, centrifuged and collected as a cell pellet. Approximately 1×10^6 cells were then lysed in 350 μl of RLT buffer (guanidine isothiocyanate containing lysis buffer), which immediately deactivated the RNases, and the sample was homogenized using a 21-gauge needle and 1ml syringe. 350 μl of 70% ethanol was then added to the homogenized sample, to provide optimal RNA-binding conditions, and mixed thoroughly by inversion. The lysate was then transferred to a silica-based total RNA capture spin column, which was centrifuged at 8000 x g for 15 seconds. The RNAeasy silica membrane selectively excludes short RNA molecules of <200 nucleotides and thus provides enrichment for mRNA.

To remove contaminants, 700 μl of the guanidine salt containing washing buffer (RW1) was applied to the spin column and centrifuged at 8000 x g for 15 seconds, followed by two applications of 500 μl of the RPE buffer to remove any excess traces of salt using the same process. The RNA was then eluted into a fresh 1.5 ml reaction tube by adding 50 μl nuclease free water and centrifuged at 8000 x g for 1 minute and collected. The extracted RNA was then either used immediately or stored at -80°C until required.

2.2.3.2 Assessment of RNA yield and quality

The quantity and quality of extracted RNA was determined using a Nanodrop Lite spectrophotometer. A ratio of ~1.9-2.1 of sample absorbance at 260/280 nm was considered pure for RNA samples. 1 μl of sample volume was used to analyse the concentration and the purity of the extracted RNA and then a concentration of 50 ng/ μl was used for the reverse transcription reaction for all cell lines.

2.2.3.3 Reverse transcription polymerase chain reaction (RT-PCR)

In order to ensure that any potential genomic DNA contamination was removed from the samples prior to complementary DNA synthesis (cDNA), RNase-free DNase set was used. 50 μl of RNA sample was incubated with 1 μl DNase I and 5 μl of the RNase-free DNase 10x reaction buffer for 30 minutes at 37°C. The DNase reaction was terminated by the addition of 5 μl of the stop solution (inactivation enzyme) and left for 10 minutes at room temperature.

Complementary DNA (cDNA) synthesis was then performed using the High-Capacity cDNA Reverse Transcription Kit, following the supplier's instructions. The RT-PCR reaction was started by the addition of the RNA template (50 ng in 10 µl) to a 20 µl reaction mixture of random hexamer primers, reverse transcriptase buffer, dNTP mix, RNase inhibitor and MultiScribe reverse transcriptase (Table 2.13). To ensure that subsequent PCR amplification was derived from RNA and not genomic DNA or other contaminants, a no-RT control (no reverse transcription) was included in every reverse transcription experiment²⁵⁹. All components were added into thin-walled 0.5 ml reaction tubes on ice. The tubes were then placed in a thermal cycler and the RT-PCR programme initiated using the following conditions: 25°C for 10 minutes, 37°C for 120 minutes, 85°C for 5 minutes and finally kept at 4°C until collected. The yield and quality of cDNA synthesized was determined using a Nanodrop Lite spectrophotometer. A ratio of ~1.8 of sample absorbance at 260/280nm was considered pure for cDNA samples.

Table 2.13: Components of the reverse transcription master mix

| Reagents | Final volume (per 20-µL reaction) | Description |
|---|-----------------------------------|---|
| Nuclease-free H ₂ O | 4.2 µl | For dilutions |
| MultiScribe™ Reverse Transcriptase, 50 U/µl | 1 µl | RNA-dependent DNA polymerase which uses single-stranded RNA as a template to generate a cDNA strand |
| 10x RT Buffer, 1.0 ml | 2 µl | Obtains higher yield of cDNA |
| 10x RT Random Primers, 1.0 ml | 2 µl (0.5 µg/µl) | Produces short cDNA fragments that would convert mRNA to cDNA |
| 25x dNTP Mix (100 mM) | 0.8 µl (0.5 µg/µl) | Contains premixed aqueous solutions of dATP, dCTP, dGTP and dTTP, |
| Extracted RNA | 50 ng | - |
| Total | 20 µl | |

2.2.3.4 Primers validation

The manufacturer has experimentally validated each of our All-in-One™ qPCR primers to yield a single dissociation curve peak and to generate a single amplification of the correct size for the targeted gene. Therefore, the primers were not further validated.

2.2.3.5 Quantitative polymerase chain reaction (qPCR)

Cycling was performed using ABI 7900HT Thermal Cycler under the following conditions: 1x hotstart (enzyme activation) at 95°C for 10 minutes followed by 40 cycles of amplification: 95°C for 10 seconds (denaturing, causes the intertwined DNA strands to separate), 60°C for 20 seconds (annealing, allows the primers to anneal to the template of interest), and finally 72°C for 15 seconds (extending, optimal temperature for Taq polymerase function). At the end of the last cycle, the temperature was increased from 72 to 95°C to produce a melting curve. After completion of the amplification cycles, the DNA synthesized can be analysed or used as required. The following is a typical reaction mix for qPCR:

| Reagents | Final volume (per 10µL reaction) |
|-------------------|----------------------------------|
| Nuclease-free H2O | 3 µl |
| SYBR green | 5 µl |
| Primers | 1 µl (0.2 µM) |
| cDNA sample | 1 µl |
| Total | 10 µl |

The 10 µl reaction mix was transferred into a standard 384-well reaction plate, which was then sealed with an optical adhesive film, briefly centrifuged at 2000rpm for 2 minutes using Sovrall Legend X1 centrifuge and then loaded into the Real-Time PCR system.

2.2.3.6 Data analysis

The threshold cycle (Ct) values were automatically determined by the ABI 7900HT PCR system. Relative quantification was used to evaluate the transcript expression levels for each respective gene by normalising to GAPDH (ΔCt sample). The ΔCt values were calculated using the following equation and these values were compared between samples being analysed:

$$\Delta Ct \text{ sample} = Ct \text{ gene of interest} - Ct \text{ GAPDH gene}$$

2.2.4 SDS-PAGE and Western Blot

To explore the differences in the expression of potential metformin-transporters between all cell lines, in an attempt to investigate why they respond differently to metformin treatment, cell lysates were collected for Western blot analysis. HepG2 cells were used as a positive control for the transporter proteins investigated.

Western blotting is a widely used analytical technique to detect the presence of specific cytoplasmic or cell surface proteins in cell extracts. It involves several steps including sample preparation, sample loading, electrophoresis, protein transfer, antibody incubation, and signal detection (Figure 2.3).

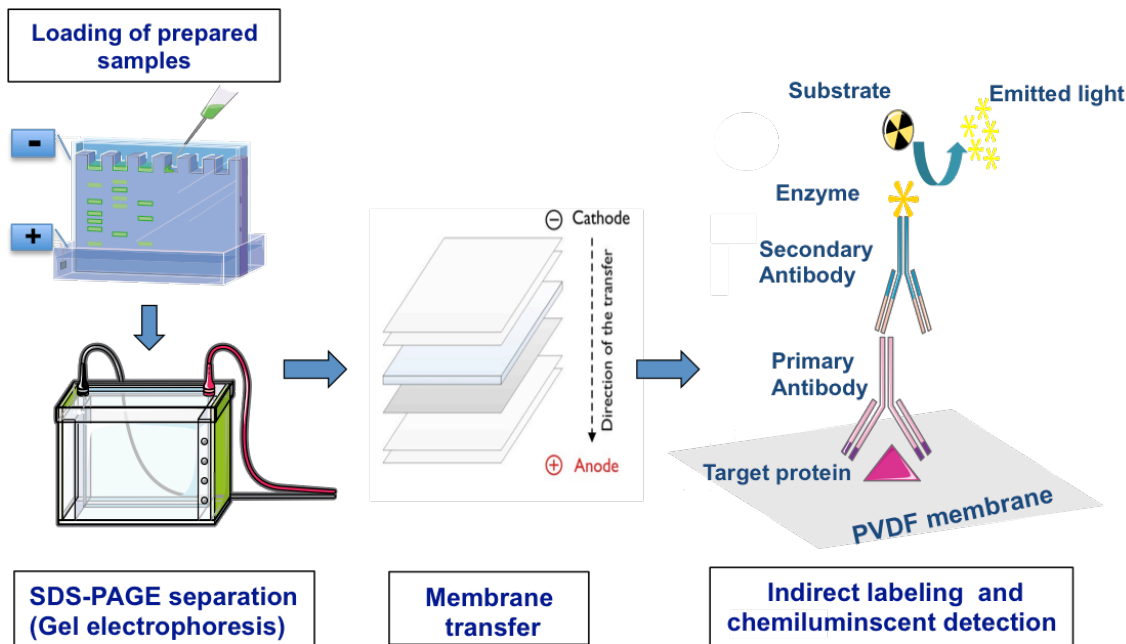


Figure 2.3:The scheme of Western blot.

After preparation, the samples are loaded onto the gel and proteins are separated by SDS-PAGE according to their molecular weights, and then transferred to a membrane. The target protein can be specifically detected using a highly selective primary antibody. A secondary antibody can then recognise the primary antibody. In the presence of a soluble enzyme substrate, the reaction can be detected by the emitted chemiluminescent light (This figure produced using Servier Medical Art: <http://www.servier.com/Powerpoint-image-bank>).

2.2.4.1 Preparation of cell lysis buffer

Prior to the preparation of fresh lysis buffer, all stock solutions were kept on ice. 1 ml of ice-cold radioimmunoprecipitation buffer (RIPA) was mixed with 10 µl of the halt protease phosphatase inhibitor cocktail to make up a 1 ml solution (1:100 dilution) and kept on ice. The RIPA buffer contains: 5 M NaCl, 0.5 M EDTA (pH 8.0), 1 M Tris (pH 8.0), Nonidet P-40 (NP-40), 10% sodium deoxycholate and 10% SDS. 1 ml of freshly prepared buffer was used to lyse and extract protein from 10^6 - 10^7 cells.

2.2.4.2 Preparation of cell extract

Cell lysis was performed to recover cellular proteins whilst removing cell debris. Cells were initially cultured to 70-80% confluence and then cells were incubated in serum free media for 24 hours to avoid any cross reactivity between the FBS and the antibodies of interest. Cell extracts were generated by discarding the serum free media from the flask, washing the cells twice with 10 ml of cold PBS followed by removal of the residual PBS to prevent dilution of the final protein extraction and then addition of 1 ml lysis buffer to each flask. The flasks were placed on ice for 10 minutes with continuous movement to allow the lysis buffer to detach the cells from the flask surface. A cell scraper was used to scrape any remaining cells off the flask surface thus ensuring all the cells were in suspension. The collected cells were then pipetted into pre-labelled eppendorf tubes. 25-gauge needles and 1ml syringes were used to suck the suspension up and down 10 times to break up the cells, disrupt the cell membranes and release the proteins into the solution. Cells were then incubated on ice for 30 minutes in order for full lysis to occur and then centrifuged for 10 minutes at 4°C at 17,900 x g to pellet the cell debris. The supernatant containing proteins was transferred into a fresh tube and stored at - 80°C ready for quantification and usage.

2.2.4.3 Protein quantification with bicinchoninic acid protein assay

The bicinchoninic acid protein assay is a colorimetric assay, which enables quantification of the protein concentrations in cell lysates. Under alkaline conditions, Cu⁺² will be reduced into Cu⁺¹ by the proteins. This reduction can be detected by bicinchoninic acid, which is highly sensitive and selective for Cu⁺¹. The reaction produces an intense purple colour with an absorbance at 562 nm. The relationship between the absorbance and the protein concentration in each sample is almost linear allowing determination of unknown protein concentrations from a standard curve. The

standard BSA (2 mg/ml) stock solutions were prepared with bovine serum albumin (BSA) and diluted to make a final concentration of 0.2 mg/ml (100 µl stock to 900 µl of the sample diluent, RIPA buffer). This solution was used to generate different standards at known concentrations as shown in Table 2.14.

Table 2.14: Preparation of different concentrations of protein standards of BSA and dH₂O.

The BSA protein standards range from (0-20 µg/ml). From the BSA stock solution (2 mg/ml) initially a 1:10 dilution with dH₂O was performed to obtain a 200 µg /ml stock for use in the dilutions shown in the table.

| Standard (µg/ml) | BSA (µl of 0.2mg/ml working stock) | dH ₂ O (µl) |
|------------------|------------------------------------|------------------------|
| 0 | 0 | 1000 |
| 2.5 | 12.5 | 987.5 |
| 5 | 25 | 975 |
| 7.5 | 37.5 | 962.5 |
| 10 | 50 | 950 |
| 15 | 75 | 925 |
| 20 | 100 | 900 |

Cell extracts were assayed for protein concentration prior to SDS-PAGE and Western blot, to ensure equal loading of protein/cell line to each well. Protein samples from all cell lines were prepared by diluting them into 1ml of dH₂O using three different dilutions for each cell line to ensure that the absorbance was in the range of the BSA standard curve. The BCA working reagent was prepared by mixing 25 parts of reagent A (Alkaline tartrate-carbonate buffer), 24 parts of reagent B (Bicinchoninic acid solution) and 1 part solution C (Copper sulphate solution) (2.5 ml, 2.4 ml and 0.1 ml respectively). The BCA working reagent was mixed thoroughly until it was light green in colour.

150 µl of the BSA standard and unknown protein sample at different dilutions were added in to flat-bottomed 96-well plate in triplicates. 150 µl of BCA working reagent was added to each well. The plate was then incubated for 2 hours at 37°C and the absorbance read at 562 nm using plate reader spectrophotometer. Linear regression analysis was performed using Prism 7.0 software to determine the concentrations of protein samples from the BSA standard curve (Figure 2.4)

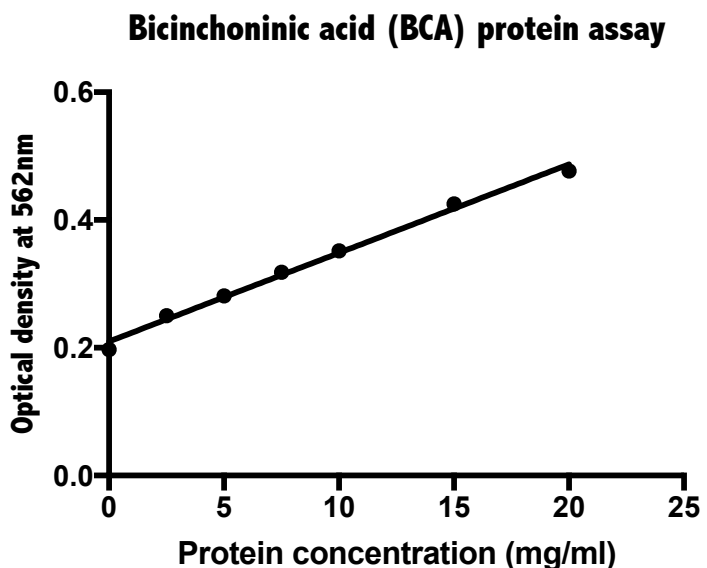


Figure 2.4: BCA standard curve example. The thick line is the linear regression curve for the entire set of standard BSA points.

Absorbance values of unknown samples are then interpolated onto the plot or formula for the standard curve to determine their concentrations (performed automatically using Graphpad Prism 7 software).

2.2.4.4 Sample preparation and loading

Samples were prepared by mixing 1 volume of the 2X Laemmli gel-loading solution and 1 volume of the protein sample and heating at 95°C for 10 minutes. The 2x Loading sample buffer contains:

| | |
|---|--|
| β-mercaptoethanol | To reduce the intra and inter-molecular disulphide bonds |
| 10% SDS (detergent) | To denature the proteins and subunits; bring the folded proteins down to linear molecules. Also coats the protein with a uniform negative charge so that each protein will separate based on size/molecular weight |
| 1% Bromophenol blue | Serves as a dye that facilitates sample visualisation during loading. Also, a dye front that runs ahead of the proteins |
| Glycerol | To increase the density of the sample so that it will layer in the sample well |
| 1M Tris-HCl (pH 6.8) and dH₂O | |

2.2.4.5 Protein Electrophoresis (SDS-PAGE)

After protein quantification and sample preparation, proteins were separated using gradient pre-cast gels (4-20% Mini-PROTEAN® TGXTM) on a Bio-Rad Mini-Protean 3 electrophoresis system. The predicted molecular weights for all the transporters investigated were between 50-65kDa. After careful removal of the comb, the plate was then placed in the gel running apparatus, making sure that the shorter plate was placed towards the centre of the tank, and the tank filled with 1X running buffer (25 mM Tris-base, 192 mM glycine, 20% methanol) until the wells were covered. The wells were rinsed out to ensure that they were free of any loose bits of acrylamide that would interfere with clean running of the samples. 20 µg of sample was added to each well, and 10 µl of the pre-stained protein marker was loaded in the first well as a reference. The gel was run at 100 V initially to allow the proteins to go through the stacking gel and then the voltage was turned up to 150 V for about 90 minutes until the tracking dye ran off the bottom.

2.2.4.6 Western blot

Following the SDS-PAGE, the proteins were then transferred to a PVDF membrane using a semidry blotter (Trans-Blot Turbo Transfer System, Biorad). The plates were removed from the gel running apparatus and opened carefully. The stacking gel was then removed from the resolving gel, which was subsequently washed 2 times in transfer buffer for 10 minutes. To create the transfer sandwich, a PVDF membrane was cut to suitable size (6.5X8.5 cm²) and activated by placing in 100% methanol for 5 minutes. The membrane was then rinsed in transfer buffer for another 5 minutes and the corner of the membrane was cut for orientation. Four pieces of filter paper were also soaked in transfer buffer for 2 minutes. The transfer sandwich (from the bottom to the top: 2 filter papers, PVDF membrane, gel, 2 filter papers) was loaded onto the semi-dry blotter cassette with air bubbles rolled out at every step (Figure 2.3). For efficient transfer, the machine was run for 7 minutes at 2.5 A; up to 25 V; using the pre-programmed Bio-Rad protocol for mixed molecular weight proteins (5-150 kDa). Once transfer had been confirmed by checking the molecular weight markers had transferred onto the membrane, the membrane was incubated in blocking solution (5% non-fat milk in 0.05% TBS-Teen) at room temperature for 1 hour to prevent non-specific binding of the antibodies. Following blocking, the relevant primary antibody, diluted as previously

stated in blocking solution, was added and incubated overnight at 4°C with gentle agitation (about 16 hour). The next morning, the membrane was washed three times for 10 minutes with 0.05% TBST to remove any residual antibodies. 10 ml blocking solution containing an appropriate dilution of the relevant horse radish peroxidase (HRP) secondary antibody was then placed on the membrane and incubated for 1 hour at room temperature, followed by a further three 10 minutes washes with TBST.

2.2.4.7 Chemiluminescence development

In the dark room under red light, the membrane was covered with 1ml of the enhanced chemiluminescence (ECL) blotting substrate for 5 minutes. The excess ECL was discarded and the membrane was wrapped in plastic and placed in a hypercassette container. A piece of film was placed over the membrane and exposed for a time ranging between 30 seconds and 1 hour depending on the band intensity. Once exposed, the film was placed in developing solution with a gentle rocking motion until bands were visible. The membrane was then washed in water before placing in the fixer solution for 30 seconds to avoid overdevelopment and then washed 5 times in tap water and allowed to dry. The exposure time, which is the most important parameter during membrane development, was carefully optimised for each antibody to avoid the risk of overexposure and/or underexposure, both of which can lead to inaccurate quantification.

2.2.4.8 Stripping and re-probing of membranes

Following confirmation of protein expression, the membrane was stripped using the stripping buffer, to ensure that the primary and secondary antibodies were removed, and re-probed for β -actin, which was used as a loading control. Loading controls such as β -actin are required to check that the lanes have been evenly loaded with equal quantities of sample, and to ensure proteins are transferred from the gel to the membrane with equal efficiency, in order to enable direct comparison of protein expression levels between different samples. Beta actin belongs to the actin family of proteins, which are expressed in all cell types and involved in cytoskeleton structure and muscle contraction. The β -actin sequence is highly conserved and identical across species (e.g human, mouse, rabbit), and the relative levels of β -actin are similar between different epithelial and cancer cells²⁶⁰.

In order to probe for β -actin, after development, the membrane was placed in a dish and rinsed with PBS. On a gentle shaker, 5 ml of stripping buffer was added to the membrane and kept for 15 minutes at room temperature, to allow the release of the first set of probes (i.e. the primary and secondary antibodies) from the membrane. Different proteins can now be detected using a second set of specific probes i.e. β -actin. The membrane was removed from the stripping buffer and washed 3 times with TBST and incubated in 10ml of blocking buffer for an hour at room temperature with shaking. The blocking buffer was removed and the membrane was given 3 washes of 10 minutes each with TBST. The TBST was discarded and 10ml of the blocking solution containing 1 μ l of anti- β -actin antibody was added and incubated for 2 hours. Afterwards, the membrane was washed 3 times for 10 minutes with TBST before the addition of the secondary antibody and incubated for 1 hour at room temperature. Following this, the membrane was again washed in TBST (4 X 5 minutes) and the expression of β -actin established following the membrane development protocol detailed in Section 2.2.4.7.

2.2.4.9 Analysis of Western blot

To allow semi-quantitative comparison of protein expression between various cell lines and antibodies used, the intensity of the detected bands were calculated as a proportion of the relevant β -actin band using ImageJ software; a densitometer programme. This allows direct comparison as well as confirming equal loading of the protein in the wells. Each of the detected protein bands was represented as a peak, the signal of which is proportional to the amount of the protein loaded.

2.2.5 Immunohistochemical staining for metformin-transporters expression in a breast tissue microarray

2.2.5.1 Principles of immunohistochemistry

The technique of immunohistochemistry was used to study the expression of metformin-transporters in a human breast tissue microarray with progressive changes from normal, premalignant and cancer tissues with progressive grades and stages. Immunohistochemistry (IHC) is the process of using antibodies to detect antigens (proteins) in cells within a tissue section. Therefore this method is used to localize specific antigens with labelled antibodies based on antigen-antibody interactions. The antibody-antigen binding can be visualized by using an enzyme such as horseradish

peroxidase (HRP), which is commonly used to catalyse a colour-producing reaction (Figure 2.5).

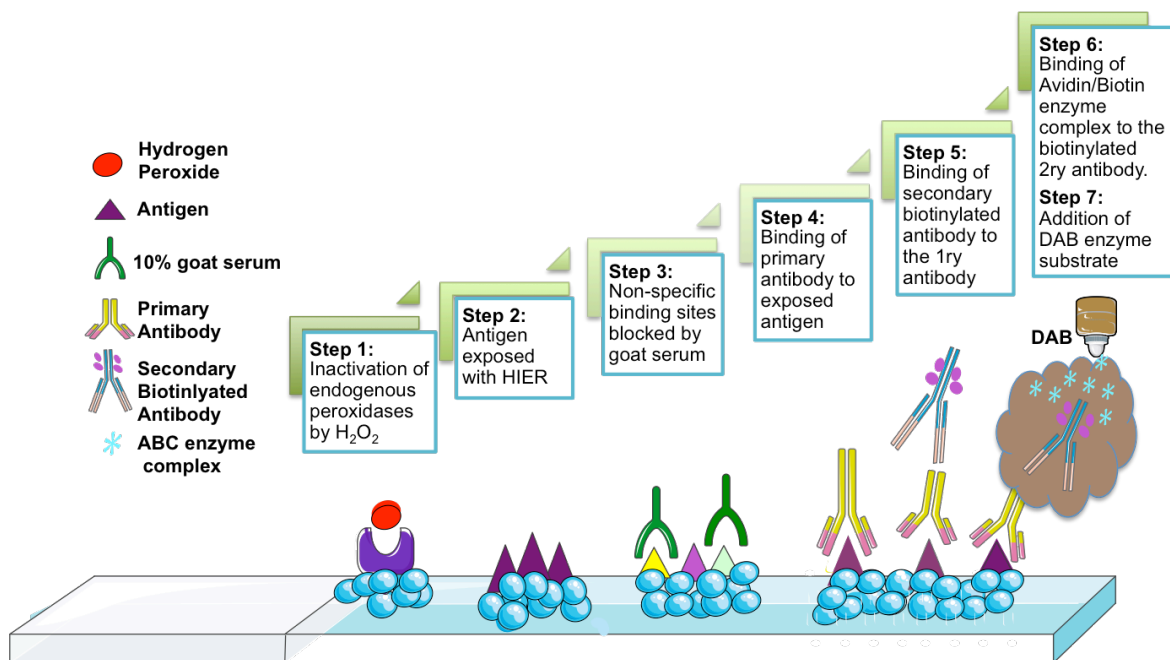


Figure 2.5: Principles of immunohistochemistry.

When the horseradish peroxidase (HRP) system is applied for IHC, activation of endogenous peroxidases enzymes should be blocked by H_2O_2 to avoid producing non-specific binding. The HIER is implemented to breaks the methylene bridges and exposes the epitope to allow subsequent binding to the specific antibodies. The unlabelled primary antibody binds to the antigen on the tissue section. The Labelled secondary antibody binds to the primary antibody. The enzyme attached to the secondary antibody acts as a substrate to deposit a coloured product where the antigen is located. H_2O_2 ; Hydrogen peroxide, HIER; heat-induced epitope retrieval, DAB; 3-Diaminobenzidine tetrahydrochloride, ABC; avidin–biotin enzyme complex (This figure produced using Servier Medical Art: <http://www.servier.com/Powerpoint-image-bank>).

2.2.5.2 Protocol for immunohistochemistry

The breast tissue microarrays (TMAs) were stained for the presence of metformin-transporters (Table 2.15). Prior to staining, the slides were baked at 60°C for 30 minutes in an oven, deparaffinised to remove the embedding wax and then rehydrated. The slides were dewaxed by immersion in 2 changes of xylene for 5 min each. Tissues were then rehydrated by immersion in absolute ethanol twice, then transfer once through 95%, 70% ethanol respectively for 3 minutes each.

Table 2.15: Total number of breast tissue cases from TMA slides used in this project

| Tissue type | Number of cases |
|---|-----------------|
| Normal Tissue | 34 |
| Fibrocystic Disease | 12 |
| Atypical Ductal Hyperplasia (ADH) | 11 |
| Ductal Carcinoma <i>in situ</i> (DCIS) | 13 |
| Invasive Ductal Carcinoma Grade I (IDC-I) | 9 |
| Invasive Ductal Carcinoma Grade II (IDC-II) | 38 |
| Invasive Ductal Carcinoma Grade III (IDC-III) | 7 |

Following rehydration, blockade of endogenous peroxidases was achieved by incubating the slides for 30 minutes in 3% hydrogen peroxide (H_2O_2) in methanol at room temperature. Following incubation, the slides were washed in running water for 5 minutes. To unmask the antigenic epitope, heat-induced epitope retrieval (HIER) took place using the citrate buffer method as follows. 100ml of sodium citrate buffer (10 mM sodium citrate, 0.05% Tween 20, pH 6.0) was poured onto the pre-arranged slides in the slide rack and incubated at 120 °C in a pressure cooker for 5 minutes. The slides were allowed to cool inside the antigen-retrieval solution for 2 hours. This was followed by three rinses in TBST of 5 minutes each, with gentle agitation at room temperature.

To block any non-specific proteins, the tissue slides were incubated for 30 minutes in 200 µl of blocking solution, consisting of 10% goat serum and 10% casein diluted in PBS. At the end of the incubation period, the excess fluid was drained and either a negative control or a primary antibody was added to the slides. 2% of blocking solution in 200 µl of PBS was applied to negative control slides. An appropriate dilution of primary antibodies (Table 2.10) was added to 2% blocking solution in 200 µl of PBS and applied to the relevant slide and incubated overnight at 4°C.

The following morning, slides were rinsed for 5 minutes in TBST 3 times with gentle agitation. 200 µl of the relevant biotinylated secondary antibody diluted in 2% blocking solution and PBS was then added to each slide and incubated for an hour at room temperature. While the secondary antibody incubated, the VECTASTAIN® avidin–biotin enzyme complex (ABC kit) solution was prepared and left to stand for an hour at room temperature. The solution is made up of 2 drops of reagent A and 2 drops of reagent B in 5 ml of PBS. 200 µl of this solution was added to each slide and incubated for 30 minutes after the secondary antibody had been washed off the slides

using three five minute washes of PBS as before. Excess fluid was then removed and further 3 rinsing steps in TBST were undertaken.

The 3-Diaminobenzidene tetrahydrochloride (DAB) substrate was then added to the slides. This solution is made up of 2 drops of buffer solution, 4 drops of DAB solution, 2 drops of H₂O₂ in 5ml of ddH₂O. Within 10 minutes of adding DAB, slides were examined under the light microscopy to assess colour development. Once the brown staining could clearly be seen the slides were rinsed in gently running water for 5 minutes to terminate the actions of the DAB solution.

Slides were then counterstained by immersion in a bath of Gill's haematoxylin for one minute to stain the nuclei. Again, the slides were rinsed in gently running water until the run-off water was clear. The tissues were then dehydrated through 5 changes of alcohol (70%, 95%, 95%, 100% and 100%) by incubating for three minutes in each. The final step of dehydration was performed by 2 changes of xylene for 5 minutes each. Finally, coverslips were secured to the stained tissue slides by using the DPX mounting solution. The mounted slides can then be permanently stored at room temperature.

2.2.5.3 Analysis of immunohistochemical staining

For the analysis of immunohistochemical staining, various human tissue sections were used as a positive control (Table 2.16). The quality control for the staining of all tissue sections was provided by Dr. P. Vergani; consultant histopathologist at Royal Hallamshire Hospital. A combined score of intensity and percentage of staining was performed and the staining was considered positive if greater than 10% of breast epithelium was stained brown²⁶¹. The staining was subjectively scored in order to semi-quantify the data (Figure 2.6). Based on the intensity of staining from light to dark brown the scores were given as the following:

0= no Staining, 1= weak Staining, 2= moderate Staining, 3= strong Staining

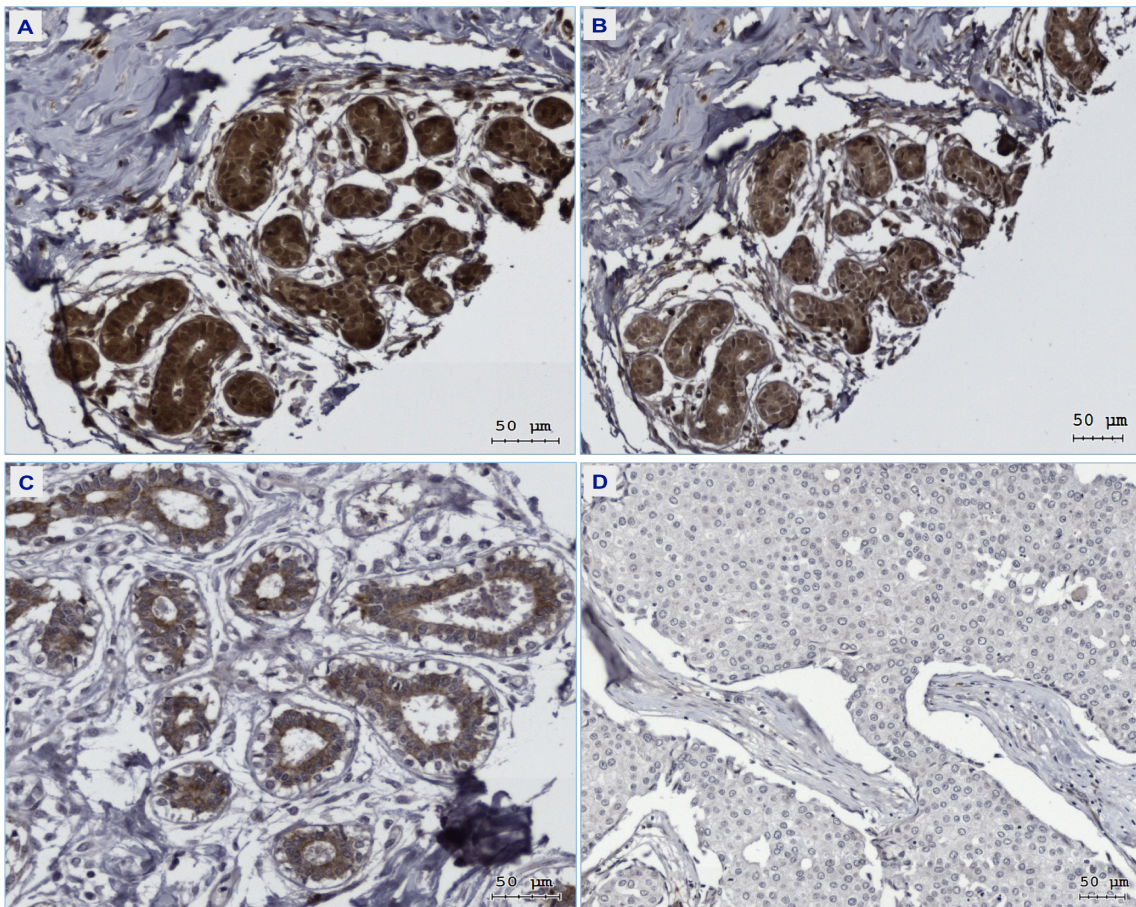


Figure 2.6: Immunohistochemical analysis of transporter proteins staining on normal breast tissues.

Representative images of immunoreactive staining, (A) Strong staining. (B) Moderate staining. (C) Weak staining. (D) Negative staining. The scale bar=50 μm .

Known protein positive tissues were used as positive controls in each run (summarised in table 2.16), negative controls (which had only 2% of goat serum) were used to confirm the validity of results.

Table 2.16: Positive tissue controls used for optimisation of the IHC assay.

| Transporter protein | Positive control (human tissue sections) |
|---------------------|---|
| OCT1 (SLC22A1) | Normal kidney and prostate |
| OCT2 (SLC22A2) | Normal kidney and skin |
| OCT3 (SLC22A3) | Normal kidney and prostate + colon adenocarcinoma |
| PMAT (SLC29A4) | Ductal carcinoma tissue section* |
| MATE1 (SLC47A1) | Normal kidney and prostate tissue sections |
| MATE2 (SLC47A2) | Normal kidney |

*The pre-invasive (DCIS) tissue slides were obtained from patients attending the Royal Hallamshire Hospital from 1995-2003 (Research Ethics: SSREC 98/137).

2.2.6 Assessment of breast cell proliferation and survival

Four independent methods were used to assess cell proliferation and survival which include: MTS assay, cell count and viability assay, BrdU incorporation assay and colony formation assay.

2.2.6.1 MTS cell proliferation assay

2.2.6.1.1 Principles of the MTS assay

To evaluate the sensitivity of different cell lines to metformin treatment, the MTS proliferation assay (3-(4,5-dimethylthiazol-2-yl)-5-(3-carboxymethoxyphenyl) -2-(4-sulfophenyl)-2H-tetrazolium, inner salt), an *in vitro* plate-based proliferation assay, was used to detect the approximate number of viable cells. The assay is based on the reduction of the tetrazolium salt, MTS, to a coloured soluble formazan compound mediated by mitochondrial-NADH or NADPH of the viable cells in culture and is therefore a measure of the mitochondrial function. The intensity of formazan can be quantified by reading the absorbance at 490nm in a 96 well plate reader. The MTS assay has the advantages of precision, ease of use, reagent solubility in culture media and elimination of the washing step, over the widely used MTT assay). The MTS assay was used initially as many previous publications investigating the effects of metformin have used either MTS or MTT^{165, 172}. However, as it has been shown that metformin may interfere with mitochondrial enzymatic activity²⁶² this may not be the most accurate assay for assessing the effects of metformin on cell growth so a simple trypan blue exclusion cell counting assay was also employed to confirm the results of the MTS assay.

2.2.6.1.2 Protocol of the MTS assay

When cells were 70% confluent they were trypsinized, counted and seeded at 5×10^3 cell/100 μ l/well in 96-well plates. For each experiment, a total of three 96-well plates were prepared; one for each time point (24, 48 and 72 hours). Each of the assay plates were set up, and then incubated for a period of 24 hours to allow the cells to equilibrate and begin to proliferate before discarding the media and adding 100 μ l of freshly prepared metformin-containing phenol red-free media (6 wells for each concentration excluding the wells that contained control cells only and media-only) (Figure 2.7). To eliminate the edge effect and maintain the well-to-well consistency throughout the entire plate, 150 μ l of PBS was used to surround the periphery wells and prevent evaporation.

The plates were incubated at 37°C, 95% O₂ and 5% CO₂ for 24, 48 and 72 hours post exposure to metformin. Three hours prior to each time point, 20 µl of MTS reagent was added directly to the wells of the relevant plate, the plate wrapped in foil and then incubated at 37°C for 3 hours. The MTS reagent is extremely light sensitive, so light was turned off in the hood before work started. Assessment of metabolic activity was established by measuring the colorimetric changes using absorbance at 490 nm recorded using a micro-plate reader. Data were analysed on Microsoft Excel by subtracting the background absorbance level of the media-containing wells. The results were graphically presented using Prism 7 software. Each experiment was performed at least 3 times.

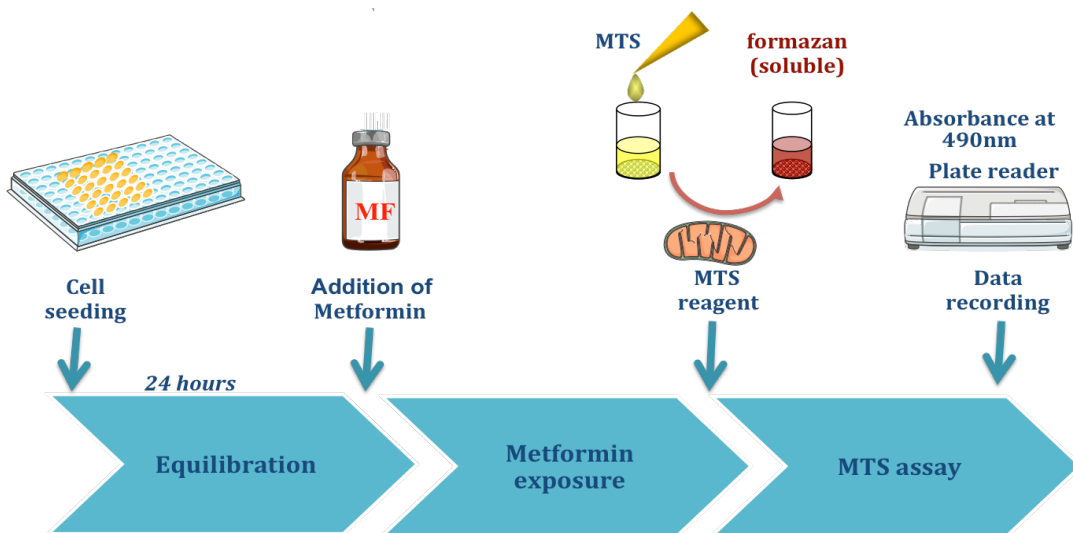


Figure 2.7: Generalized scheme of the MTS cytotoxicity assay.

Cells were seeded into 96 well plates and allowed to equilibrate for 24 hours prior to metformin exposure for 24-72 hours. MTS reagent was added 3 hours prior to each time point resulting in a coloured formazan product, which was read on the plate reader (This figure produced using Servier Medical Art: http://www.servier.com/Powerpoint-image_bank).

2.2.6.1.3 Optimization of the MTS assay

Initially, the seeding density for the MTS assay was optimized to avoid one of the most common limitations affecting MTS validity, which is cessation of cell growth due to depletion of media or cellular confluence during the time course. All cell lines were seeded at two different densities (5×10^3 and 1×10^4 cell/well) in a 96 well plate in the absence of treatment in order to determine the most appropriate seeding density for these experiments. At 5000 cell/well, a steady rate of growth was seen in all cell lines with very little difference in the growth speed between the premalignant and pre-invasive cells on one hand and the cancer cells on the other hand, except the T47D cells

which were slow growing (Figure 2.8A). At 10000 cell/well, a decrease in the growth rate was markedly seen after 48 hours in the premalignant and pre-invasive cells and 96 hours in the invasive cancer cells (Figure 2.8B). As a result of these data a density of 5×10^3 was used, where all cell lines continued to grow throughout the time course of the experiment (4 days).

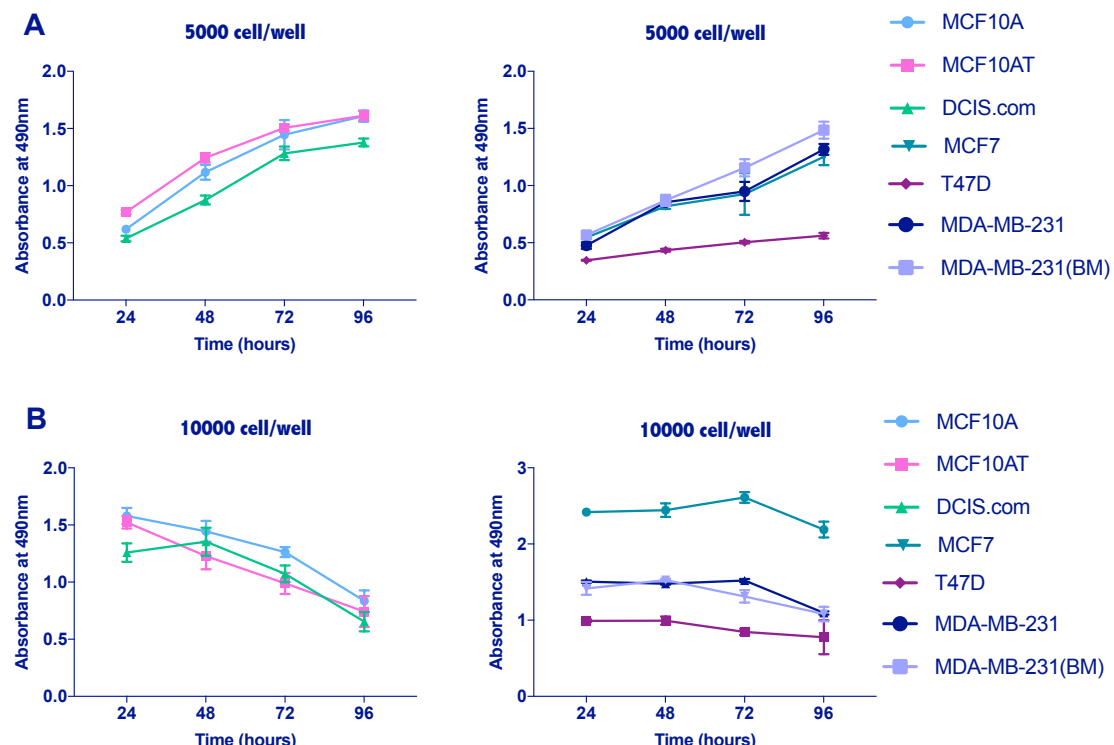


Figure 2.8: Optimisation of the MTS assay (n=3).

(A) Cells were seeded at 5000 cell/well in their assay media, and their proliferation measured by MTS assay. Under these conditions all cell lines continued to grow at different rates. (B) Cells were seeded at 10000 cell/well and their proliferation measured by MTS assay. Under these circumstances the premalignant cells slowed their growth at 48 hours, while the cancer cells slowed their growth at 72-96 hours depending on cell line. Data shown are the mean \pm SD of three independent experiments.

2.2.6.2 Viability assay using trypan blue cell counting

This method is based on the principle that viable cells do not take up trypan blue dye whereas non-viable cells do. However, it is important to note if cells are exposed to trypan blue for extended periods of time, both viable and non-viable cells may begin to take up dye so the assay must be performed promptly. As the results from the MTS assay demonstrated that the 72-hours time point was the one at which an effect of

metformin was most clearly visible, the following experiment was only performed at 72 hours. Cells to be assayed were recovered from a culture flask as described in Section 2.1.2. Cells were counted and the density adjusted to be plated at 5×10^3 cells/well in a 12-well plate (triplicate for each metformin concentration + triplicate for the control untreated cells). 1 ml of the cell suspension was added to each well and incubated for 24 hours at 37°C , following which the media was discarded and different concentrations of metformin were added to each triplicate and incubated for a further 72 hours in a 5% CO₂ incubator. After 72 hours of treatment, media were collected from each well into a corresponding pre-labelled tube. Each well was washed twice with 1ml PBS (also collected) before adding 0.5 ml of trypsin. After 2 minutes, the action of trypsin was neutralized by addition of 1.5 ml of fresh media, and the entire contents of the well (cells, trypsin and media) collected and transferred into the corresponding tube. Each well was then washed with 1 ml of media to ensure all cells were removed from the well and collected again. The collecting tubes were then centrifuged and the contents were re-suspended in 1ml of fresh medium before counting. Viability and total cell counts were then detected using TC20™ Automated Cell Counter as described in section 2.2.1.7.

2.2.6.3 BrdU (bromodeoxyuridine) proliferation assay

2.2.6.3.1 Principles of the BrdU assay

The BrdU cell proliferation assay was employed to detect the incorporation of 5-bromo-2'-deoxyuridine (BrdU) into cellular DNA during cell proliferation using an anti-BrdU antibody. The pyrimidine analogue (BrdU) is incorporated in place of thymidine into the newly synthesized DNA of proliferating cells. A BrdU mouse monoclonal antibody detects the incorporated BrdU after DNA denaturation; a necessary step to improve the accessibility of the incorporated BrdU to the detection antibody. The anti-mouse horseradish peroxidase (HRP)-linked antibody can then recognize the bound detection antibody. Finally, the HRP substrate, tetra-methylbenzidine (TMB), can then be added to generate a colour reaction. The intensity of the colour is proportional to the quantity of BrdU incorporated into cells, which is a direct indication of DNA synthesis and therefore cell proliferation (Figure 2.9).

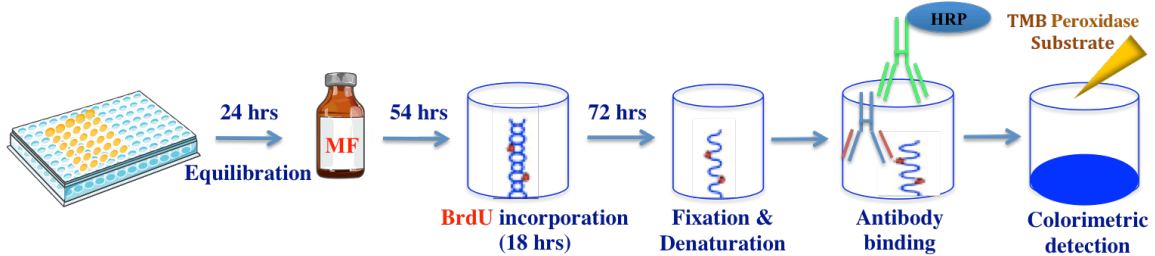


Figure 2.9: BrdU cell proliferation assay principles.

Cells are incubated with BrdU to allow its incorporation into the newly synthesized DNA in place of thymidine. Subsequently, anti-BrdU antibodies are used to detect the level of BrdU incorporation, an accurate indicator of cell proliferation (This figure produced using Servier Medical Art: <http://www.servier.com/Powerpoint-image-bank>).

2.2.6.3.2 BrdU assay protocol

5×10^3 cells were seeded in triplicates for each dose and control in 96 well plates in the respective assay media to a final volume of 100 μl /well and incubated overnight at 37°C . Three types of controls were used: Blank control, contains only culture media without cells or BrdU label; Background control, contains cells without BrdU and a positive control contains the untreated cells and the BrdU label. On the following day, the media were discarded before adding different doses of metformin to the corresponding wells and incubated for 72 hours at 37°C . 18 hours before the end of the 3-day incubation period, 20 μl of diluted BrdU label (diluted to 5-fold according to manufacturers instructions) was added to all wells except the blank and background controls. On the following day, the media was removed from the wells and the cells were fixed in 200 μl of the fixative/denaturing solution. After 30 minutes incubation at room temperature, the cells were then washed 3 times with 1X washing solution (prepared by diluting the 20X concentrated washing solution in deionised water). 100 μl /well of the anti-BrdU monoclonal detector antibody (prepared by diluting the antibody stock as 1:100 ratio in the supplied antibody dilution buffer) was added and incubated for 1 hour at ambient temperature. Each well was then washed three times with 1X washing solution before the addition of 100 μl /well of the 1X HRP-conjugated Goat Anti-Mouse secondary antibody and incubated for further 30 minutes at room temperature. The three washing steps were repeated for each well, followed by flooding the entire plate with distilled water. The water was removed and then 100 μl /well of the TMB Peroxidase substrate (tetra-methylbenzidine solution) was added and incubated for 30 minutes at ambient temperature in the dark. The population of BrdU positive

cells, which are actively synthesizing DNA will be visible as a blue colour with variable intensities based on the amount of incorporated BrdU in the proliferating cells. Finally, 100 μ l/well of the stop solution (2.5N Sulphuric acid) was added and the change of colour, from blue to bright yellow, was recorded immediately at A450 using a microplate reader.

2.2.7 Cell survival assay

2.2.7.1 Principles of the clonogenic assay

The clonogenic assay is a basic tool to study cell survival. It is different from the proliferation assays but complementary to them in terms of exploring the mechanism by which the cells can respond to an insult; and evaluate whether metformin is working differently in the different cell lines. It determines the ability of the cells to retain their reproductive ability, thereby to proliferate indefinitely and to form a large clone in the presence of an agent. It also defines the relationship between the dose of the agent used and the number of cells that were able to reproduce after drug exposure. Cell death, either by necrosis or apoptosis, is not the only parameter that confirms the cytotoxic effect of the drugs, because even the living cells with retained ability for DNA and protein synthesis are considered dead, if they lose their reproductive integrity and become unable to divide and produce colonies²⁶³, therefore, a clonogenic assay was employed to test this aspect of metformin activity. To assess the differences in reproductive capability between the untreated cells and metformin-treated cells (the capacity of cells to form a colony of 50 or more cells)²⁶⁴, clonogenic assays were performed using two different protocols. Namely, the traditional method whereby cells are treated with metformin then washed and placed into the assay in the absence of metformin exposure, or the method commonly reported in previous studies¹⁷² whereby metformin is present in the media throughout the assay (Figure 2.10). Using both methods is important to both confirm previous data, and to show whether metformin has a true effect on the clonogenicity of the breast cell lines.

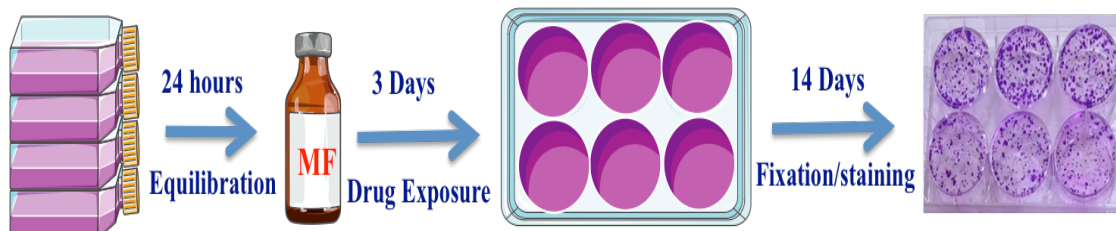


Figure 2.10: Traditional clonogenic assay setting up.

2.2.7.2 Clonogenic assay on adherent cells (traditional method)

Breast cancer cells (25×10^4) were seeded into T25 flasks and incubated overnight. After incubation, the cells were exposed to varying concentrations of metformin for a further 72 hours (consistent with the proliferation assay time point) before they were trypsinized, counted, syringed (to ensure that the suspension is really single cells) and plated in triplicates at a density of 50 cells/well. Plates were incubated for 10-14 days at 37°C at the back of the incubator without moving or replacement of media. After this time point when colonies had formed, the cells were fixed in 100% ice-cold methanol and incubated for at least 30 minutes in a spark proof freezer. Afterwards, the methanol was removed with care (as it is a neurotoxic substance) and the cells were stained with 0.25% crystal violet in 40% methanol (0.25g in a mixture of 40ml methanol and 70ml water; filtered through a funnel and Wattman filter paper). The stain was washed off after 10 minutes by immersing the plate several times in tap water. Plates were dried at room temperature and colonies consisting of 50 or more cells were counted under a light microscope.

A previously published metformin study¹⁷² has used a different protocol where cells were trypsinized, syringed and counted, then seeded into the 6-well plates at a density of 1000 cells/well and incubated at 37°C for 24 hour before replacing the media with metformin-containing media. Every 3 days, the media were changed with a fresh metformin-containing media. This method was trialled for direct comparison with the previous study, but the colonies in the control wells were impossible to count by the end of the experiment and so this method was not pursued (Figure 2.11).

2.2.7.3 Optimization of the plating densities for the clonogenic assay

In order for a clonogenic assay to yield meaningful data an appropriate seeding density must be established that will result in single discrete colonies for counting at the end point of the assay (after 2 weeks). Two different methods were trialled with

different seeding densities. Alimova and colleagues seeded the cells at 1000 cell per well and therefore utilized this protocol but the colonies in the control wells were impossible to count and therefore this method was not utilized further (Figure 2.11). The traditional method where 100 and 50 cells were seeded per well yielded much better results with clear, discrete colonies in the untreated wells at a seeding density of 50. Therefore, the traditional clonogenic assay protocol was employed to assess whether clinically relevant doses of metformin would alter the ability of BC cells to form colonies. While clonogenic potential of most cells was readily measured after 72 hours of metformin exposure, MCF10A and MCF10AT cells did not form colonies and were therefore excluded from clonogenic assays.

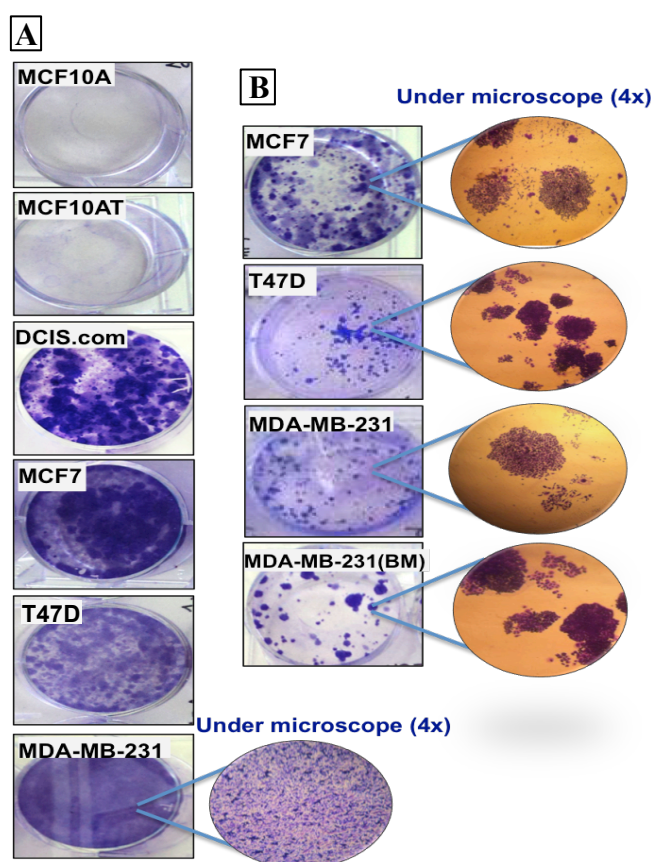


Figure 2.11: Plating densities for the clonogenic assay.

(A) Method adopted from Alimova *et al.*¹⁷². The MCF10A and MCF10AT cells did not form colonies at the higher density of 1000cells/well. (B) Traditional clonogenic assay method. Pictures of cells from the control wells in 6 well plates were taken by digital camera; Results show that untreated cells in Alimova method were coalesced together and difficult to count even under a microscope (4X magnification).

2.2.8 DNA cell cycle analysis

2.2.8.1 Principles of cell cycle analysis

Quantitation of DNA content in each phase of the cell cycle was evaluated by flow cytometry using propidium iodide, a DNA-binding dye. PI binding is proportional to the amount of DNA present in the cell. To allow easy access of PI to the cellular DNA, cells were fixed and permeabilized using alcohol. Cells in the synthesis phase (S phase) will have more DNA than cells in Gap1 phase (G1), and thus will take up more dye and will fluoresce more brightly. However, the G1 phase shows up as the largest peak as it is the most predominant phase of the cell cycle. The cells in G2 will be approximately twice as bright as cells in G1. The $G_1 \rightarrow S \rightarrow G_2 \rightarrow M \rightarrow G_1$ cycle is schematically shown in figure 2.12.

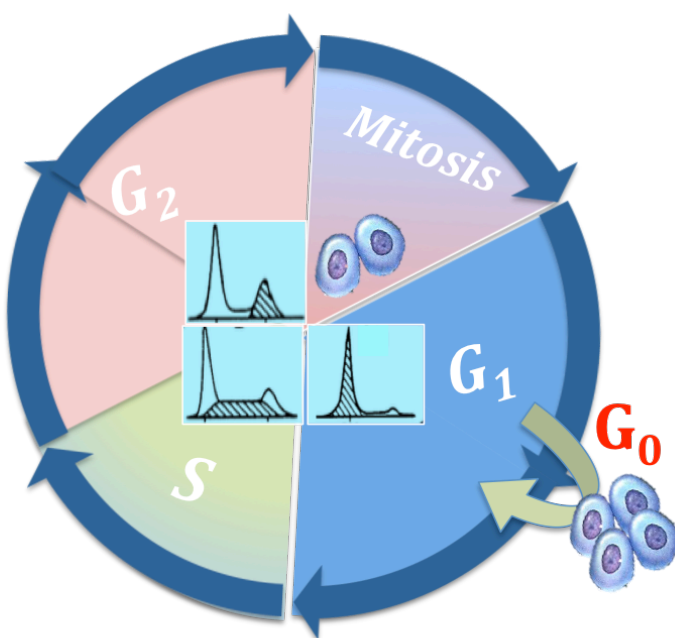


Figure 2.12: A schematic representation of the cell cycle, including the flow cytometric components of each phase.

Before cell division, the synthesis and duplication of the repository of the cell's genetic material, DNA, occurs during "S phase". G₁ represents the gap between mitosis and the onset of DNA synthesis where most of the RNA and protein molecules needed for DNA replication are synthesized. G₂ represents the gap between the completion of DNA synthesis and the onset of mitosis where the repair of any DNA damage from the preceding cell cycle phases takes place. The G₀ cells represent the quiescent cells that have yet to enter the cell cycle. Mitosis phase represents cellular division where DNA is divided equally between daughter cells.

2.2.8.2 Sample preparation

Cells were serum starved for 48 hours. Serum starvation was used to deplete the nutrient availability and therefore induce cell cycle synchronization to accumulate the cell population prior to G2/M, after which they were grown at a density of 5×10^5 cells in 100 mm culture dishes and were treated with or without metformin (0, 0.3, 1, and 5 mM) for 72 hours. The media were collected; the cells were then trypsinized, washed twice with cold PBS, and centrifuged with the collected media. 1 ml of 70% ice-cold ethanol (made with ddH₂O not PBS to avoid protein precipitation on fixation) was added drop wise to each pellet while vortexing, to ensure cell fixation and minimize clumping. The cells were then maintained at 4°C overnight or up to 2 weeks. 24 hours before evaluation by flow cytometry, the ethanol was washed off the cells using 2 ml of PBS. Cells were centrifuged at 850 x g for 5 minutes and the supernatant was discarded with extreme care to avoid cell loss. To ensure that only DNA, not RNA, is stained the cells were treated with 50 µl of ribonuclease (from 100 µg/ml RNase stock, 5 µg final volume) and incubated at ambient temperature for 30 minutes. For DNA staining, 200 µl of propidium iodide (from 50 µg/ml stock solution) was added and incubated overnight at 4°C before being analysed by flow cytometry for DNA content and cell cycle stage the next morning.

2.2.8.3 Flow cytometry analysis

The majority of dead cells and debris were excluded from the flow cytometry data acquisition by thresholding on forward scatter. Single cell populations were identified by forward scatter (FS) and side scatter (SS). For each sample, 10000 cells were evaluated for PI staining. Cells being evaluated for PI staining were acquired using a LSRII model flow cytometer equipped with a laser (488 nm) and a red diode laser (640 nm). PI was excited by the 488 nm laser with collection of PI emissions at 564-606 nm. Cell cycle analysis was carried out using the BD FACSDiva 8.0.1 software (Figure 2.13).

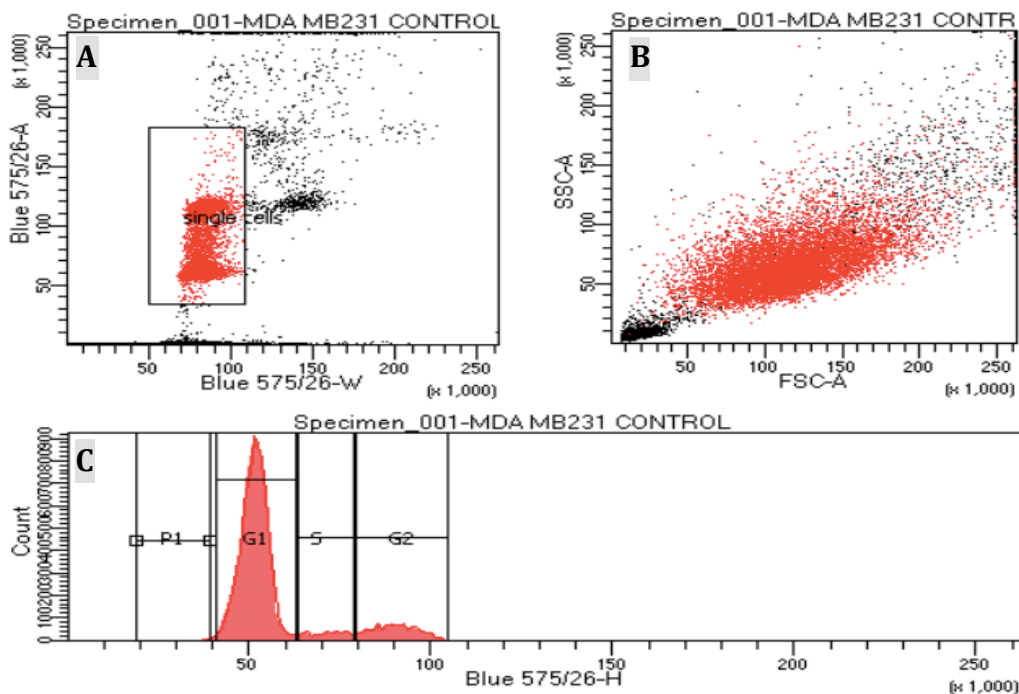


Figure 2.13: A representative cell cycle analysis of untreated MDA-MB-231 cells using FACSDiva 8.0.1 software.

Panel A shows the pulse width (X-axis) vs. pulse area (Y-axis) blot, used to gate on the single cell population. Panel B is an example of forward (X-axis) and side scatter (Y-axis) blot where the gate from panel A is applied to gate out obvious debris. Panel C shows the PI histogram plot, where the combined gates are applied (P1 represents the subG₁ or apoptosis phase).

2.2.9 Scratch wound-healing assay

One characteristic of tumour spread is the increased migratory ability of tumour cells. The inhibition of migration of the invasive and metastatic breast cancer cells by the clinically relevant doses of metformin was investigated using the scratch wound-healing assays. The scratch wound healing assay is a popular simple and cheap *in vitro* method to study cell migration by “wounding” a confluent monolayer of cells and observing the process of cell migration to close the gap.

2.2.9.1 Optimization of the scratch wound healing assay

In order to set up a reliable assay, various experimental conditions in 96-well plate needed to be optimised including the seeding density, starvation period prior to the assay and the duration of breast cancer cell migration as detailed below, although the scratch assay has been previously used for breast cancer cell migration in multiwall plates.

2.2.9.2 Optimization of the starvation period

Serum deprivation is a prerequisite step for the migration assay, as this step would synchronize the cells and arrest them at G0 phase of the cell cycle, thus, the cells would respond uniformly to metformin treatment. As a confluent cell monolayer is required for this assay, we therefore established whether the cells could maintain an adherent monolayer after 48 hours of starvation when compared to cells without starvation. We found that the starvation didn't affect cell attachment to the plate if the PBS washing was extremely gentle.

2.2.9.3 Optimization of the migration time period

To establish how long the cells take to close a wound made by 200 μ l pipette tip, different time points were required by different cells to migrate to close the gap. When confluent monolayers of cells were scratched, the MCF-7, T47D and MDA-MB-231 cells readily closed the gap at 24 hours. Both MCF10A and MCF10AT cells did not migrate over a 3 days time period. Similarly, DCIS.com and MDA-MB-231(BM) cells did not migrate after 5 days post scratch (Figure 2.14). Therefore, the cells that did not migrate were excluded from the final experiment. For the final experiment, the treated cells were not allowed to migrate for so long so that they will fully close the gap; this is to show any difference in migration speed relative to the untreated cells with one time point being chosen based on the subsequent optimisation steps (the 24 hours).

As the gap can potentially be filled by cell migration and cell proliferation, in order to avoid cell proliferation masking the effects of metformin on migration, 4 doses of mitomycin C (2-20 μ g/ml) were added to all cell lines in triplicates for 2-4 hours before scratching. Mitomycin C (MMC) is a cell cycle antagonist and DNA synthesis inhibitor, a commonly used inhibitor in cell migration assays²⁶⁵. However, mitomycin C caused cell death and disruption of cell monolayer at these concentrations and the scratch assay could not be performed without a confluent monolayer (Figure 2.15). There was a concern that in the absence of any proliferation inhibitory agent the results of this assay may be affected by breast cancer cells proliferation masking or enhancing the effects purely on migration. Therefore, in order to set up a reliable wound-healing assay in absence of mitomycin C, different measures were taken.

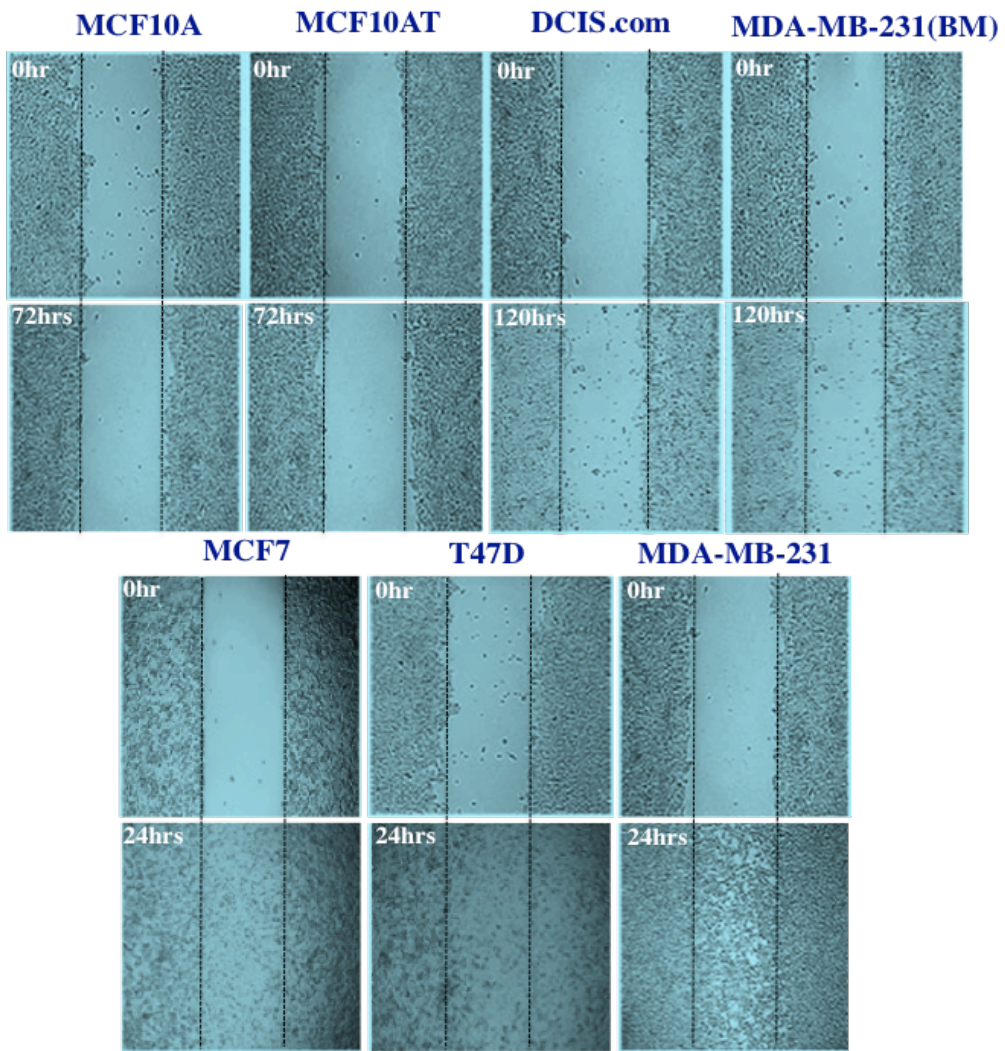


Figure 2.14: Optimisation of the migration time period. Images were taken at different time points post scratch of untreated cells.

The gap was almost closed by the MCF7, T47D and MDA-MB-231 at 24 hours. The MCF10A, MCF10AT, DCIS.com and MDA-MB-231(BM) did not migrate after 72 to 120 hours post scratch.

The cells were first synchronized by serum starvation prior to the assay, which would bring all cells to a phase of growth and proliferation arrest. Additionally, the EGF was removed from the pre-malignant cell assay medium and 1% FBS medium was used for the entire assay that may further help in reducing the proliferation over the time course of the assay. Furthermore, the assay time was set to be less than the invasive cells doubling time. Finally, to ensure that proliferation would not be taking place over the time course of the scratch assay, cellular proliferation was measured by MTS assay immediately after wounding and 24 hours later (the end point of the assay). This

enabled assessment of whether the wound-healing assay would only assess migration and not gap closure due to proliferation.

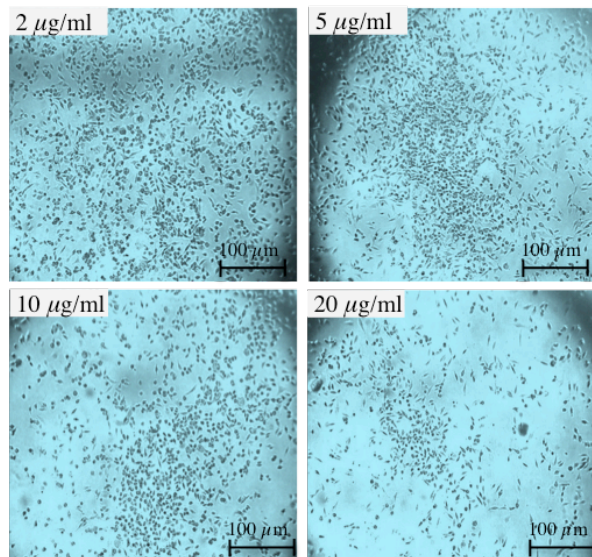


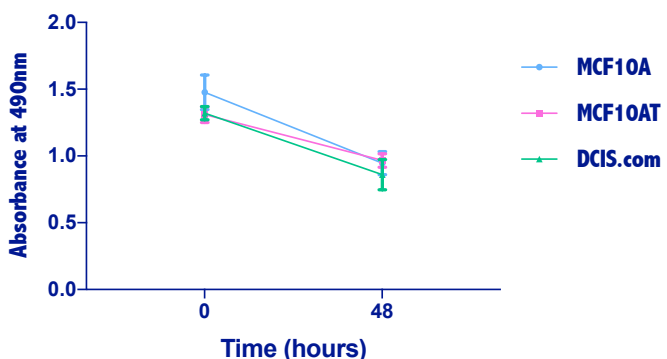
Figure 2.15: A representative picture of the effect caused by different doses of mitomycin C on MDA-MB-231 monolayers.

Cells were treated with 4 different doses of mitomycin C (2, 5, 10 and 20 µg/ml). Cells were less confluent and showed evidence of cell death at 2 hours with increased doses of mitomycin C. Scale bar represents 100 µm.

2.9.3.4 Control proliferation experiment

The proliferation results obtained by MTS assay clearly showed that the three invasive cell lines did not proliferate over the course of the assay (24 hours), however, the viability of the pre-malignant, pre-invasive and the bone-homed cells was markedly reduced consistent with the finding observed previously that these cell were unable to migrate and close the scratch (Figure 2.16). This might be due to the unfavourable culture conditions as the pre-malignant cells are both serum and growth factors dependent. Accordingly, the migration of the invasive breast cancer cells was analysed at 24 hours following wounding, confident that the majority of scratch closure will be due to migration and not proliferation of the cells.

Pre-malignant and pre-invasive cells



Invasive and metastatic cancer cells

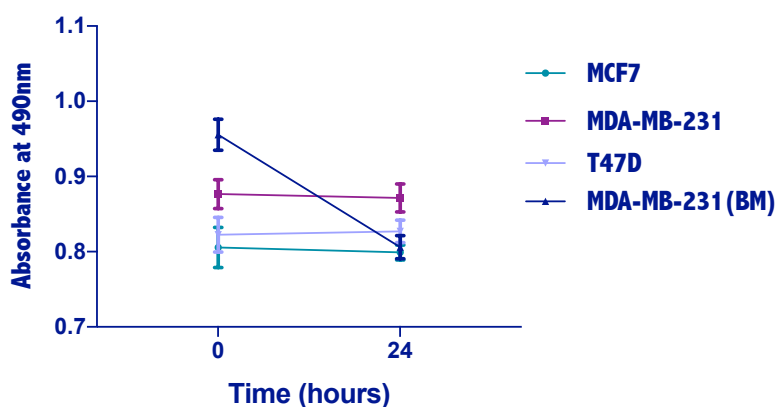


Figure 2.16: Control proliferation experiment.

Cells were seeded into the 96 well plates, left to become confluent, serum starved and the scratch generated. Cellular proliferation was then measured immediately and after 24 hours using the MTS assay and expressed as absorbance at 490nm. Results shown are the mean \pm SD of three independent experiments. The metabolic activity of the three pre-malignant cells was significantly affected at 48 hours; similarly the metabolic activity of metastatic bone-homed cells was markedly affected at 24 hours. Meanwhile the viability of the three invasive cells was not affected at the 24 hours time point.

2.2.9.5 Wound healing assay protocol

The ability of the invasive breast cancer cells to migrate into an empty space was evaluated by creating a scratch wound *in vitro*. The MCF7, T47D and MDA-MB-231 cells were firstly serum-starved for 48 hours. The following day, cells were seeded in triplicate in a 96-well plate at a density of 4×10^4 cells/well for the T47D cells and 3×10^4 for MCF7 and MDA-MB-231 cells in a low serum medium (1% FBS), to reduce their ability to proliferate during the assay, and allowed to settle for 4 hours. After this time the scratch wounds were created using a sterile 200 μ l pipette

tip. Cellular debris was removed by extremely gentle washing with PBS before four concentrations of metformin were added in 100 μ l of low serum medium, with 1% FBS medium only as a control. Images of the wounds were captured by a digital camera at 0 and 24 hours for the three cells. ImageJ software was used to analyse the results. 20 different random distances between the two edges of the wound were measured. The percentage of wound closure was calculated using the following equation:

$$\text{Percentage of wound closure} = \frac{(A-B)}{A} \times 100$$

Where A is the width of initial scratch wound and B is the width of scratch wound at time 24 hours (Figure 2.17).

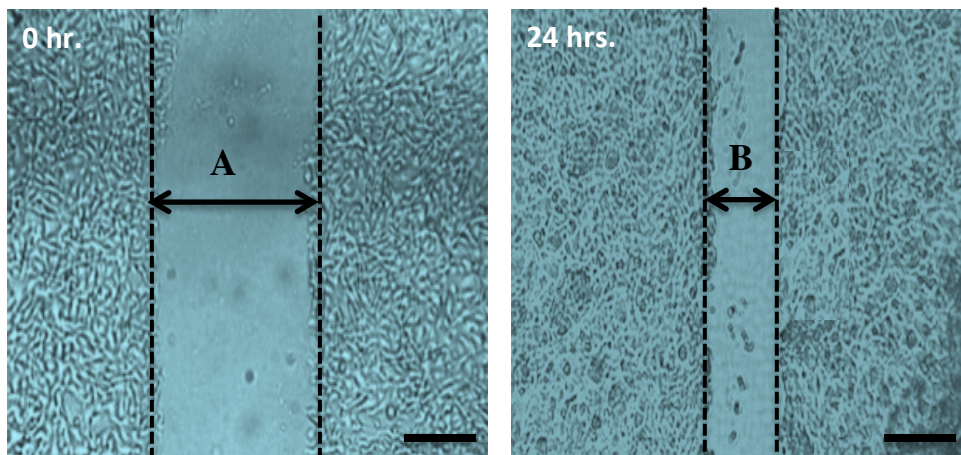


Figure 2.17: Calculation of the percentage of wound closure.

A representative of scratch closure by untreated MDA-MB-231 cells at 0 and 24 hours. The edges of the wound are emphasised by the dotted lines. Images were taken using Olympus digital camera. 20 points across the gap were assessed for each image. Scale bar represents 100 μ m.

2.2.10 Mass spectrometry-proteomic analysis

Two Mass spectrometry-proteomic analysis techniques were performed in this project, namely Label free quantification (LFQ) and Spike-in SILAC-based quantification (SIS). The details of the methodology used can be found in chapter 5.

2.2.11 Statistical analysis

The D'Agostino-Pearson omnibus test was first used to assess normality. This test computes the skewness of the data and quantifies how far the distribution is from the Gaussian, in terms of shape and asymmetry. It then calculates how far each of these values differs from the value expected with a Gaussian distribution, and computes a single P value from the sum of these discrepancies. Considering that the very large majority of data were not normally distributed, statistical comparisons were carried out using the non-parametric tests using Graphpad Prism software 7 for Mac and shown as mean \pm standard deviation (SD) in all graphs for all replicates.

Therefore, data were analysed using a non-parametric one-way ANOVA test to compare the means of data among each groups followed by Dunnett's post hoc test for multiple comparison. All P values are two-tailed. A P value < 0.05 was considered statistically significant.

Data for the analysis of qRT-PCR, Western blot and immunohistochemistry experiments was assessed using the same tests comparing each cell line/tissue to the normal non-tumorigenic MCF10A cells/normal breast tissue.

3. Chapter 3: Analysis of metformin-transporters expression, *in vitro*

3.1 Introduction

Although previous studies have suggested that breast cancer incidence and recovery may be influenced by metformin treatment in diabetics, there is still a question as to whether metformin will be taken into the cancer cells and gain access to the mitochondrial respiratory complex in order to mediate these effects or whether these effects are indirect. Metformin is highly hydrophilic and cannot readily cross the impermeable plasma membrane, thus to enter the cell, metformin trafficking across the cell membrane must be transporter-mediated¹²⁴. Four organic cation-transporters (OCTs) are actively involved in the cellular uptake of metformin and have been identified as putative determinants of metformin's pharmacokinetics in the main organs such as liver and small intestine, namely OCT1-3 and PMAT. If cancer cells were positive for those transporters it would strongly suggest that metformin could accumulate and exert its direct effect in these cells. The multidrug and toxin extrusion transporters (MATE1 and 2) can also mediate cellular extrusion of metformin and contribute to its excretion through urine and bile. With this in mind, reduced drug response cannot be solely attributed to reduced metformin uptake into cancer cells but also to increased efflux out of the cells, which is governed by the presence of two metformin extrusion proteins.

The expression of metformin transporters has been found to be extremely diverse in different tissues²⁶⁶ (Figure 3.1). In diabetic patients, alteration in metformin pharmacokinetics, disposition and side effects have been linked to single nucleotide polymorphisms affecting the functions of OCT1-2 and MATE1-2^{138, 267-277}, and these polymorphisms have also been identified in healthy subjects²⁷⁸. A detailed description of the localization and tissue distribution of these transporters can be found in the introduction chapter (section 1.3.2 and table 1.3).

To date, very little is known about the quantitative expression of metformin transporters in breast cancer settings. Only one study, by Cai and colleagues²⁷⁹, examined whether the expression of metformin transporter mRNAs differ significantly between basal and luminal breast cancer cells/tumour tissues. These authors found that the expression of cation-selective transporter is critical for the anti-proliferative effect of metformin in basal breast cancer cell lines²⁷⁹. However, no comprehensive description

of gene and protein expression in normal, pre-malignant, pre-invasive and tumour breast cells and tissues is available, to date.

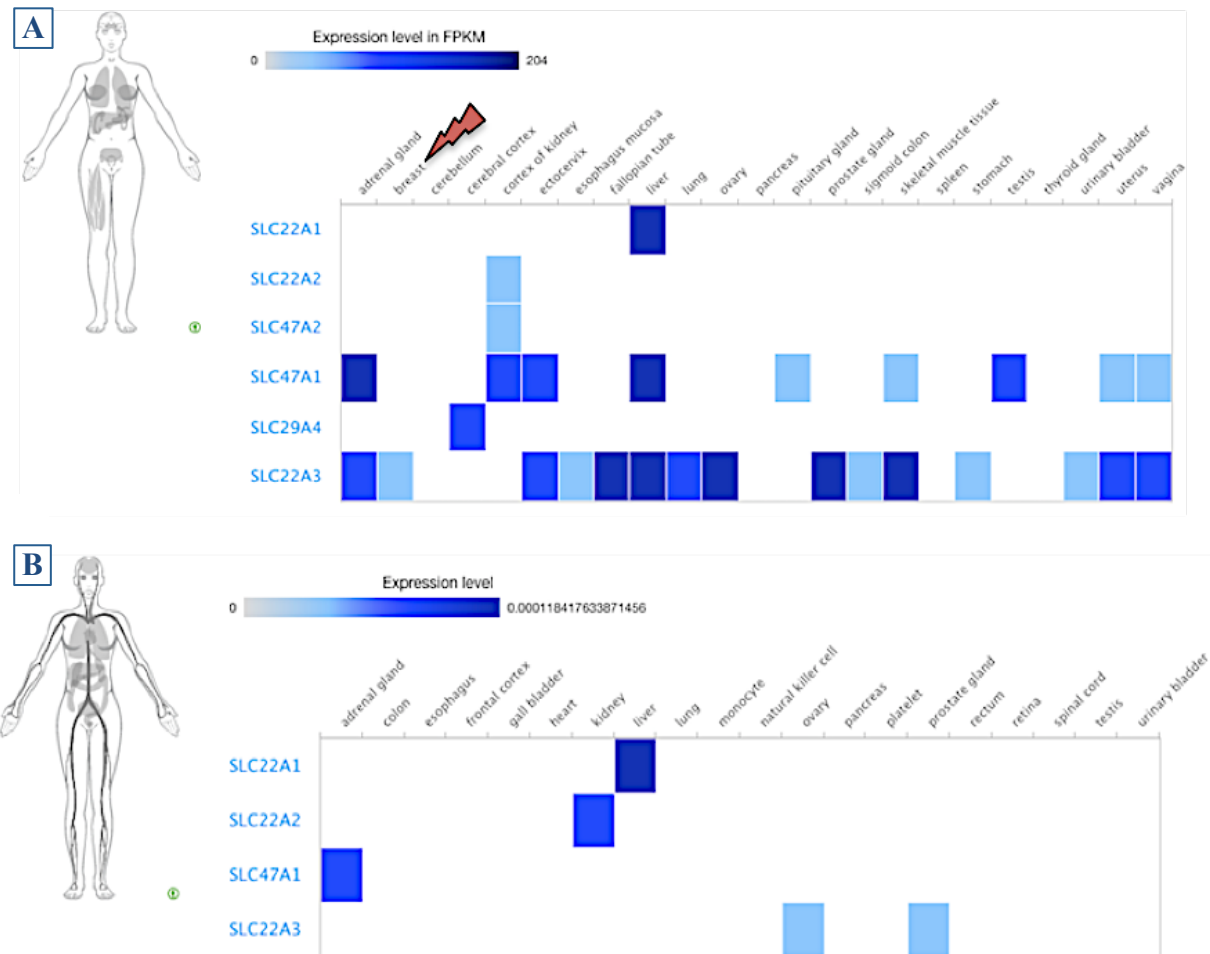


Figure 3.1: Baseline expression of metformin-transporter genes and proteins in normal organs and tissues.

(A) Transporter gene expression corroborating high level of OCT1, OCT3 and MATE1 expression in liver across GTEx (Genotype-Tissue Expression) studies with very little information about transporter expression in breast tissue. The unit used for reporting expression in RNA-seq studies is FPKM (fragments per kilobase of transcript per million). (B) Very little is known about transporter protein expression in the human protein atlas and human proteome studies, and it appears that normal breast tissue was not assayed in the given studies. Likewise there was no available information about PMAT and MATE2 expression in various normal tissues. Data obtained from Expression atlas website <https://www.ebi.ac.uk/gxa/> (accessed on 15-December-2017).

Therefore, to address this gap in knowledge, this study was designed to compare the expression of the six important metformin transporter genes and proteins (Table 3.1) in our representative *in vitro* model of breast cancer disease progression and to enable testing of the hypothesis that the expression of the solute carrier transporters is critical for the direct effect of metformin on breast cells, in the subsequent chapter.

Table 3.1: Metformin transporters

| Import transporters | Export transporters |
|-----------------------|------------------------|
| SLC22A1 = OCT1 | SLC47A1 = MATE1 |
| SLC22A2 = OCT2 | SLC47A2 = MATE2 |
| SLC22A3 = OCT3 | |
| SLC29A4 = PMAT | |

In an attempt to mimic the diversity of breast disease and carcinoma that is seen in the clinical population of patients, a panel of increasingly transformed breast cell lines were chosen to represent the graduated progress and evolution of breast carcinogenesis as described by Wellings and Jensen⁶. In this case, the MCF10A cell line was used to represent the non-transformed breast ductal epithelial cells, MCF10AT cells represent pre-malignant hyperplastic ductal epithelial cells and the DCIS.com cells represent pre-invasive ductal carcinoma *in situ*. Three immortalised human invasive breast cancer cell lines were chosen to represent a variety of hormone receptors status, variable invasive activity and metastatic potential. MCF7 (Luminal A) represents tumours with non-invasive and low metastatic potential, T47D (Luminal A) represents tumours with low invasive and low to moderate metastatic potential, while MDA-MB-231 (Basal/Triple negative) represents tumours with highly invasive and metastatic capacity²⁸⁰⁻²⁸³. For the sake of better comprehensiveness an end-stage metastatic bone-seeking cell line (MDA-MB-231(BM)) was also added to the previous spectrum (Figure 3.2).

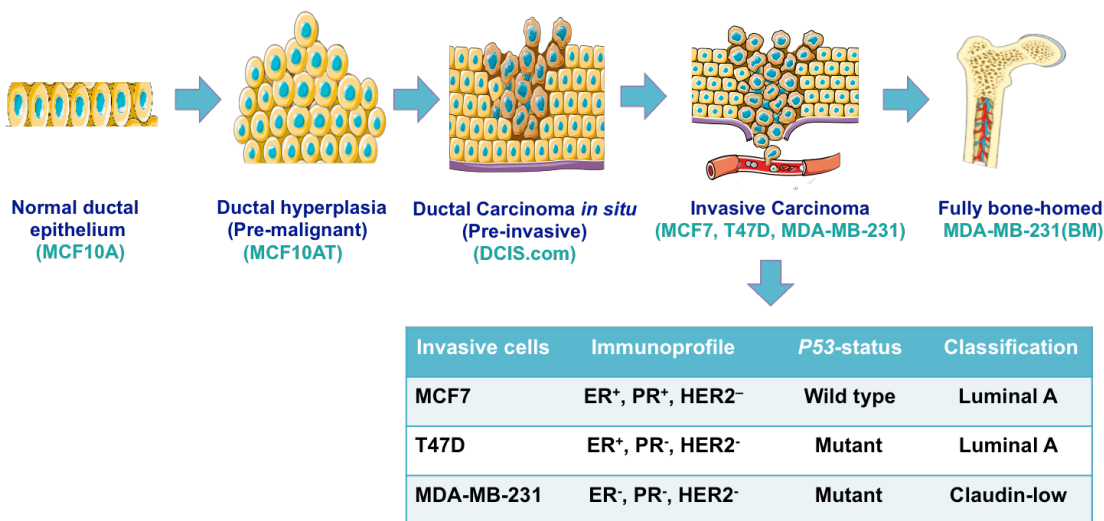


Figure 3.2: An *in vitro* model of breast cancer and disease progression.

The major aim of this chapter was to assess which of the metformin transporters are present in the different cell lines and whether transporter expression alters with increasing severity of the disease.

More specific aims were to:

1. Investigate gene expression of the endogenous solute carrier transporters *SLC22A1*, *SLC22A2*, *SLC22A3*, *SLC29A4*, *SLC47A1* and *SLC47A2* in human breast cell lines at various stages of BC disease progression.
2. Investigate the transporter protein expression in the representative human breast cell lines.
3. Evaluate the transporter expression in human breast tissues of similar morphology to the cell lines used.

3.2 Methods

- In order to investigate the expression of the putative metformin transporters in breast cancer, cell lines representing different severities of breast lesion were cultured as described previously (see section 2.2.1).
- To assess the transporter gene expression, mRNA was extracted from the cells (as described in section 2.2.3.1) and then converted to cDNA for use in a quantitative real-time polymerase chain reaction (qRT-PCR) (sections 2.2.3.3, 2.2.3.4). All the validated metformin-transporter qPCR Primers ID and sequences are listed in table 2.8.
- To assess the protein expression of the transporters, samples were prepared and resolved by SDS-PAGE (section 2.2.4.5), transferred to a PVDF membrane (section 2.2.4.6) and incubated with the corresponding primary and secondary antibodies (listed in table 2.10 and 2.11). The immune-reactivity was visualised by chemiluminescence (section 2.2.4.7). The transporter protein expression was semi-quantified using the ImageJ programme as described in section 2.2.4.9, then normalized to β -actin and presented as the percentage of β -actin expression.
- Immunohistochemical staining was performed to further characterize metformin-transporters expression in a total of 124 human tissue microarray sections per transporter representing a model of breast cancer progression (detailed in table 2.14), along with the positive controls listed in table 2.15. IHC was conducted according to normal laboratory routines (section 2.2.5.2) with commercially available antibodies (tables 2.10 and 2.11) and analysed as detailed in section 2.2.5.3.
- Each experiment was performed on at least three occasions and the graphs shown are the average of these data. All statistical analyses were performed comparing each cell line/tumour tissue to the non-tumorigenic MCF10A cells/normal tissue and the tests used were the non-parametric tests as advised by the Sheffield statistical services as detailed in statistical analysis, section 2.2.11. A P-value of <0.05 was taken to be significant.

3.3 Results

3.3.1 Evaluation of metformin-transporter genes expression in the tumour and non-tumour breast cell lines

In order to evaluate whether the development and progression of breast cancer from normal to pre-malignant, pre-invasive, invasive to a metastatic disease would be associated with changes in metformin-transporter expression at the gene level, quantitative real time polymerase chain reaction (qRT-PCR) was performed on the representative cell lines of breast disease progression. HepG₂, the human hepatocellular carcinoma cell line and a commonly used organotypic cell line for *in vitro* studies²⁸⁴, was used as a positive control for transporter gene expression and GAPDH (Glyceraldehyde 3-phosphate dehydrogenase) as an internal control gene. Consistent with the previous literature, the HepG2 cell line expressed all the investigated transporter mRNAs²⁸⁴ (Figure 3.3).

The relative expression of our genes of interest was quantified to determine the changes in steady-state mRNA levels across all cell lines and expressed relative to the level of GAPDH as an internal control as shown in Figure 3.3. Both cancer and non-cancerous breast cell lines were found to express a significant level of metformin-transporter mRNAs with PMAT being the predominant transporter in both the tumour and non-tumour cell lines except the MDA-MB-231 cells where OCT3 was the most predominant. MATE1 was the second most highly expressed transporter. OCT1, OCT2 and MATE2 were the third, fourth and fifth most highly expressed genes (Figure 3.3). The pattern of expression of each individual transporter mRNA across all cell lines is summarized in table 3.3.

Table 3.2: Analysis of metformin transporter gene expression relative to GAPDH

| | |
|----------------------------------|---|
| Importer genes expression | <p>OCT1 mRNAs: there was a tendency for the expression to increase slightly with increased cellular invasiveness and metastatic potential ($P=0.003$, One-way ANOVA test), however, a post hoc Dunnett's test revealed no significant difference in the expression of OCT1 between the non-tumorigenic MCF10A and other cell lines.</p> <p>OCT2 mRNAs were shown to have a relatively similar expression level across the representative cells of the breast disease spectrum ($P=0.1$, One-way ANOVA test). (Figure 3.3).</p> <p>OCT3 mRNA, most cell lines showed a similar level of expression, except the metastatic MDA-MB-231 that showed a relatively higher expression compared to the normal MCF10A cell ($P=0.001$, Dunnett's test). However, OCT3 expression was not detectable in MCF7 cell line (Figure 3.3).</p> <p>PMAT mRNA was found to present a similar pattern of expression to that of OCT1, with no statistically significant difference in the expression across the investigated breast cell lines ($P=0.05$, One-way ANOVA test) (Figure 3.3).</p> |
| Exporter genes expression | <p>MATE1 mRNA expression was unchanged between the normal, pre-malignant and pre-invasive cell lines whereas it was slightly decreased in MCF7 and MDA-MB-231 and slightly increased in T47D and MDA-MB-231(BM) cell lines ($P=0.008$, One-way ANOVA test). However, these differences between the tumorigenic cell lines and MCF10A cells were not significant (Figure 3.3).</p> <p>MATE2 mRNA analysis showed a slight increase in the expression with increased cellular atypia and invasiveness in the MCF10AT, DCIS.com and MCF7 cell lines compared to the normal MCF10A cell line. However, the expression was slightly reduced to a level similar to the MCF10A cells in the T47D, MDA-MB-231 and MDA-MB-231(BM) cell lines ($P=0.004$, by One-way ANOVA test). However, none of the pairwise comparisons to the normal cell line as a control were significant.</p> |

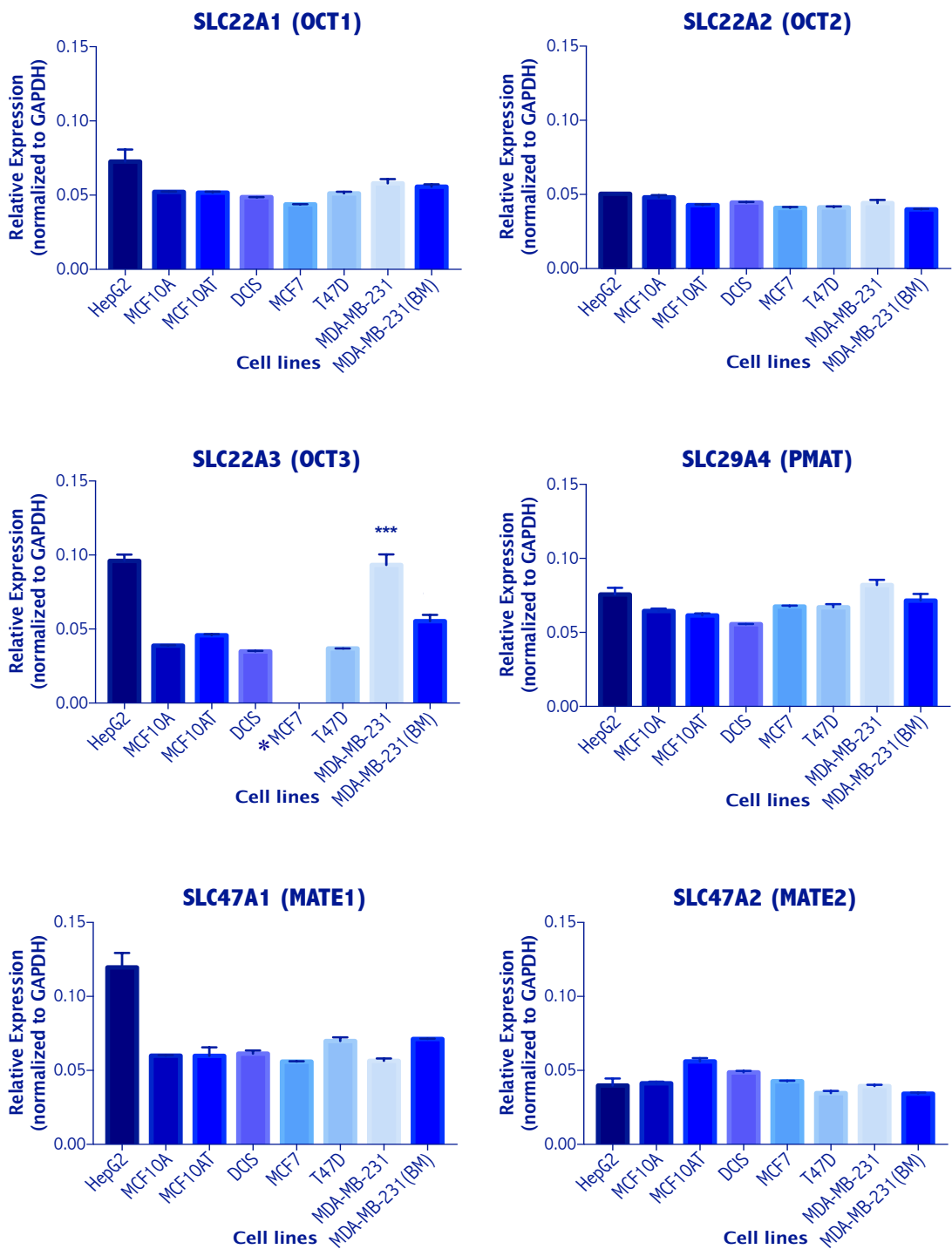


Figure 3.3: Expression profiling of the cation-selective transporters OCT1-3, PMAT, MATE1 and MATE2 mRNAs in various human breast cell lines.

Relative gene expression was determined by qRT-PCR and normalized to GAPDH. HepG2 cells were used as a positive control and GAPDH as an internal control gene. Values represent the mean of 3 duplicate repeats and error bars are SD. Cell line marked with an asterisk (*) indicates undetermined transporter expression in all biological replicates. For statistical analysis the cells were compared to the non-tumorigenic MCF10A cell as a control. $P<0.05$ was considered significant. $***P<0.001$. For raw data, see Supplementary material CD (S1).

3.3.2 Evaluation of metformin-transporter proteins in the tumour and non-tumour breast cell lines

To evaluate whether the transporter gene expression observations were translated to the protein level, Western blot analysis was carried out and protein expression of all cell lines was analysed and compared to the non-tumorigenic MCF10A cells. The cell lysates from three biological replicates per cell line were tested independently for the expression of human OCT1 (molecular weight 61kDa), OCT2 (molecular weight 63kDa), OCT3 (molecular weight 61kDa), PMAT (molecular weight 58kDa), MATE1 (molecular weight 62kDa), MATE2 (molecular weight 61kDa) and normalized to β -actin (molecular weight 42kDa). The results showed that the human hepatocellular carcinoma cell (HepG2), used as a positive control, expressed all the tested transporter-proteins in the cell lysates²⁸⁴. The percentage expression of band densities against β -actin in the above experiments was graphically plotted in figure 3.6. Semi-quantification densitometry was not possible for MATE2 due to non-detectable bands.

In the non-tumorigenic and pre-malignant human breast epithelial cells (MCF10A and MCF10AT), there was a strong expression of OCT1, OCT2, PMAT and MATE1; with PMAT being the predominant transporter followed by MATE1, OCT1 and OCT2 respectively. There was no expression of either OCT3 or MATE2 in these cell lines (Figures 3.4 and 3.5).

The pre-invasive DCIS.com cells demonstrated a strong expression of OCT2, PMAT and MATE1 but only minimal positivity for OCT1 and no expression of OCT3 and MATE2. A similar pattern of expression was found in the invasive MCF7, T47D, the metastatic MDA-MB-231 and the bone homed MDA-MB-231(BM) cells, with MDA-MB-231 being the only cells to express OCT3 protein (Figure 3.4).

There was not generally a good correlation between the gene and protein expression pattern for most transporters. OCT1 and PMAT proteins expression do not reflect the gene expression, while PMAT protein expression was elevated in the pre-invasive, invasive and metastatic breast cancer cells ($P<0.0001$, by One-way ANOVA test), OCT1 protein expression was reduced in these cells ($P<0.0001$, One-way ANOVA test) (Figure 3.5). No significant difference was observed in OCT2 and

MATE1 expression between all cell lines ($P=0.33$ and $P=0.2$ respectively, by One-way ANOVA test) (Figure 3.4), which is in agreement with gene analysis results.

The expression of OCT3 and MATE2 proteins was not detectable in all cell lines except the MDA-MB-231 cells, which expressed a significant level of OCT3 protein. This observation was not consistent with the gene expression data where these transporters were expressed at a higher level (Figure 3.4 and 3.5).

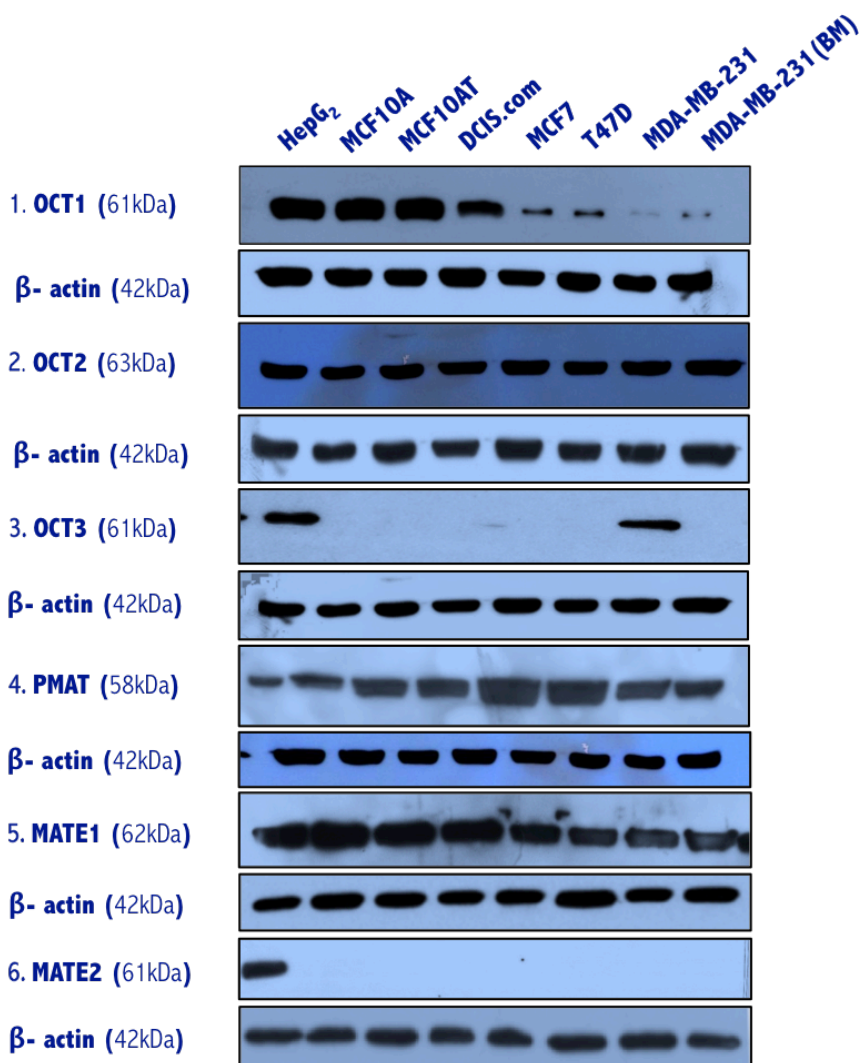


Figure 3.4: Representative cropped Western blots of transporter expression in normal, pre-malignant, pre-invasive, invasive, bone-homed breast cell lines and hepatoma cell control (HepG2).

The images represent the expression of metformin transporter proteins (OCT1-3, PMAT and MATE1-2) and their corresponding molecular weights are indicated in brackets. β -actin (42kDa) served as a loading control for comparison of expression levels for all proteins tested. 20 μ g of proteins (total cell lysate) were loaded into each lane. For full images of the three independent experiments, see Supplementary material CD (S2).

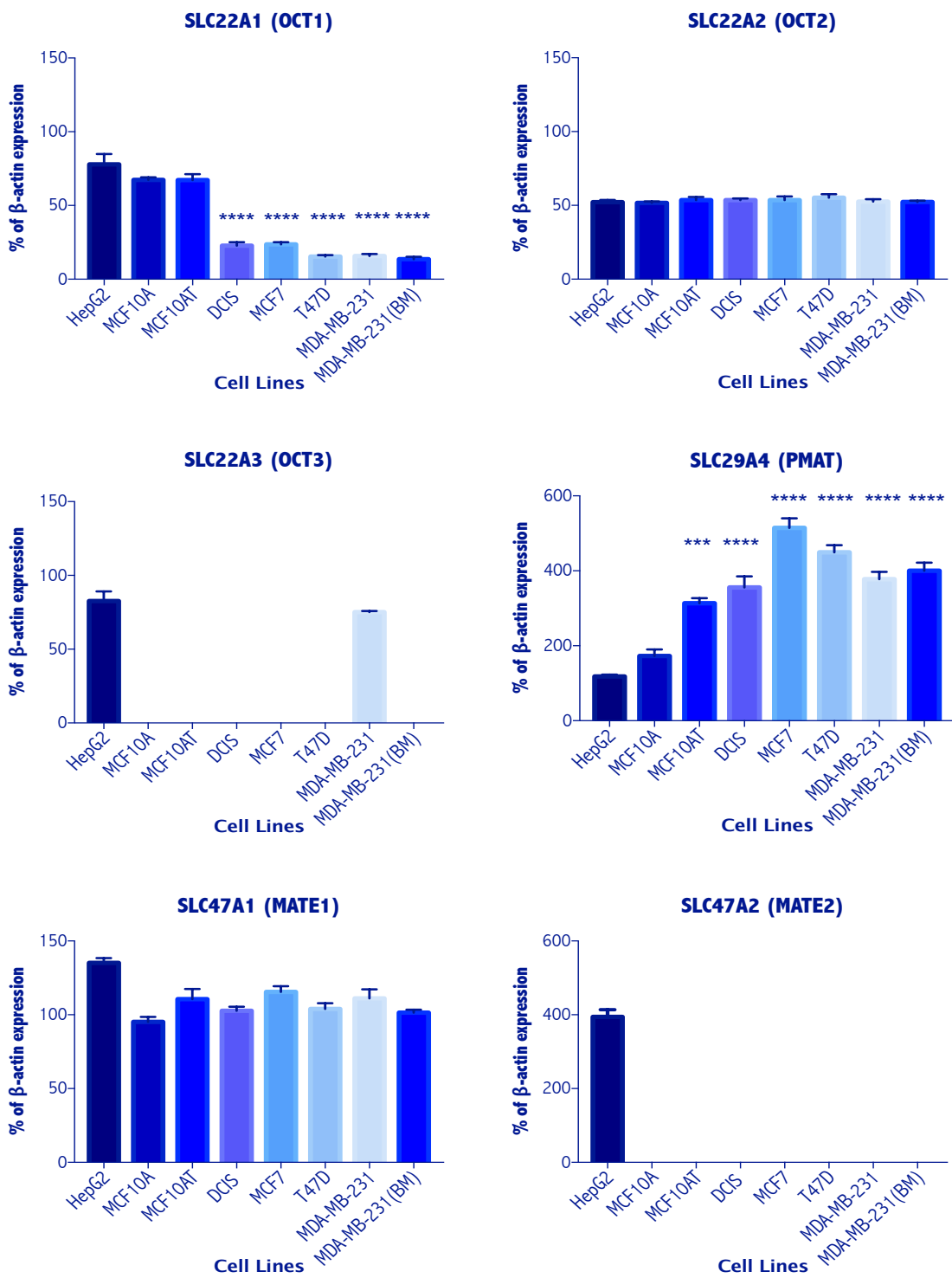


Figure 3.5: Representative Western blot analysis of metformin-transporter proteins expression (OCT1-3, PMAT and MATE1-2) by all breast cell lines.

The intensity of the different bands were determined by densitometry, normalized to β -actin, plotted as the percentage of β -actin expression and expressed as mean \pm SD from three independent experiments. For statistical analysis cells were compared to the non-tumorigenic MCF10A cells as a control. ***P<0.001 and ****P<0.0001.

3.3.3 Analysis of metformin-transporter expression in human breast tissues

Having determined the levels of metformin-transporter genes and proteins expression in the representative cell lines of breast cancer progression, immunohistochemical staining was performed to determine whether the transporters are expressed in human breast tissues of similar morphology to the cell lines. To correlate the findings of this experiment with the results of qRT-PCR and Western blot analysis, sections with fibrocystic disease were also analysed to represent the source from which the immortalized MCF10A cells were derived and to investigate if there is a difference in expression between them and the completely normal epithelial cells. The different grades of invasive ductal carcinoma (IDC I-III) were analysed and plotted separately owing to the fact that the degree of differentiation is a better clinical representative of disease severity rather than the tumour subtype (grade I, II and III represent well, moderately and poorly differentiated tumours, respectively). It is worth noting that there was no metastatic breast tissue available for use in this study.

Each tissue microarray slide was stained for metformin-transporters and scored under light microscope to evaluate the intensity and quantity of staining as described in section 2.2.3.3. Examples of the grades of staining intensity are shown in the materials and methods chapter figure 2.6. The pattern of staining in the ductal epithelial and tumour cells was observed to be uniformly membranous and cytoplasmic, occasionally nuclear (based on slides examination with higher magnification lenses). There was no staining observed in the surrounding stromal cells. Analysis is presented as the percentage of each tissue type scoring 0, 1, 2 or 3 for intensity of stain of the relevant metformin-transporter, as shown in figure 3.6. A proportion of the scoring was confirmed by a histopathologist (Patricia Vergani) and double assessed by another scorer (Nashwa Shesha). The kappa coefficients for inter-observer error scores were OCT1, 0.93; OCT2, 0.84; and OCT3, 0.95, PMAT, 0.89; MATE1, 0.83 and 0.91 for MATE2, showing a high level of agreement.

Moderate to strong membranous and cytoplasmic expression of OCT1 was detected in 70% of normal ductal epithelial cells. This was significantly reduced to 40 % in the non-tumorigenic fibrocystic disease sections (FCD), 58% in the pre-malignant atypical ductal hyperplasia (ADH) and 69.3% in ductal carcinoma *in situ* (DCIS). Statistical analysis indicated that the expression of OCT1 decreased in disease

compared to normal breast epithelial cells ($P<0.004$, One-way ANOVA test) with post hoc test indicating that invasive carcinoma had a significantly reduced expression compared to normal epithelial cells ($P=0.0001$, Dunnett's test) (Figure 3.6).

High levels of OCT2 expression were seen with moderate to strong membranous and cytoplasmic staining in 100% of ductal epithelial cells in normal breast, 80% in the non-tumorigenic epithelium (Fibrocystic disease), 90% in the dysplastic epithelium (ADH) and 85% in the pre-invasive ductal carcinoma cells (DCIS). The expression did not change significantly with increasing severity until invasive ductal carcinoma where it decreased significantly to 20% compared to normal breast epithelial cells ($P=0.002$, Dunnett's test) (Figure 3.6 and 3.7). The observation that there was no statistical difference in the normal, pre-malignant and pre-invasive breast tissues stained for OCT2 expression is in agreement with both gene and protein cell line expression results.

Moderate to strong expression of OCT3 was identified within the cytoplasm and membrane of 37% of normal ductal epithelium, 42% of fibrocystic disease and 33% of ADH tissues. Similarly, moderate to strong expression was also detected in 31% and 40% of DCIS and grade-I IDC cells, respectively. 85% of the grade-III IDC cells stained negative for OCT3. There was no statistically significant difference between tissues stained for OCT3 expression across the range of normal to grade I IDC, even though there was a small tendency of decreased strong staining intensity with increased lesion severity (Figure 3.6 and 3.8). Results presented here correlate well with the gene expression findings but not with the non-detectable proteins on Western blot.

Moderate to strong PMAT cytoplasmic and membranous expression was seen in 83% of the normal breast epithelium with a significant decrease in expression to only 20% of fibrocystic disease tissues compared to normal breast epithelial cells ($P=0.0001$, Dunnett's test) and 60% of ADH. Moderate to strong expression was also observed in the cytoplasm of 100% of DCIS cells while 60% and 40% of grade I-II invasive carcinoma cells expressed PMAT and this was significantly reduced to 10% in grade III IDC compared to normal breast epithelial cells ($P=0.0001$, Dunnett's test) (Figure 3.6). Although tissue expression of PMAT did not correlate with gene expression in terms of being the predominant transporter in all cell lines, PMAT is expressed in all stages at different degrees in both cell lines and tissues.

There was moderate to strong expression of MATE1 in the cytoplasm and membranes of 100% of epithelial cells in normal breast ducts and this expression reduced slightly but non significantly in fibrocystic disease sections (90%) and in ADH (66%), whereas it was 100% in DCIS and then 80-71% among the progressive grades of invasive ductal carcinoma tissues from I to III respectively. This is also consistent with gene and protein expression findings (Figure 3.8 and 3.9).

There was generally weak cytoplasmic expression of MATE2 in 36% of the normal breast ductal epithelium and atypical ductal hyperplasia. Moderate to strong expression was only observed in 41% of fibrocystic disease sections. The weak expression was significantly decreased with increasing lesion severity ($P= 0.0009$, One-way ANOVA test); with no expression detected in grade-III invasive ductal carcinoma cells (Figures 3.9). The very low to no expression pattern of MATE2 in different breast tissues is consistent with the protein expression findings.

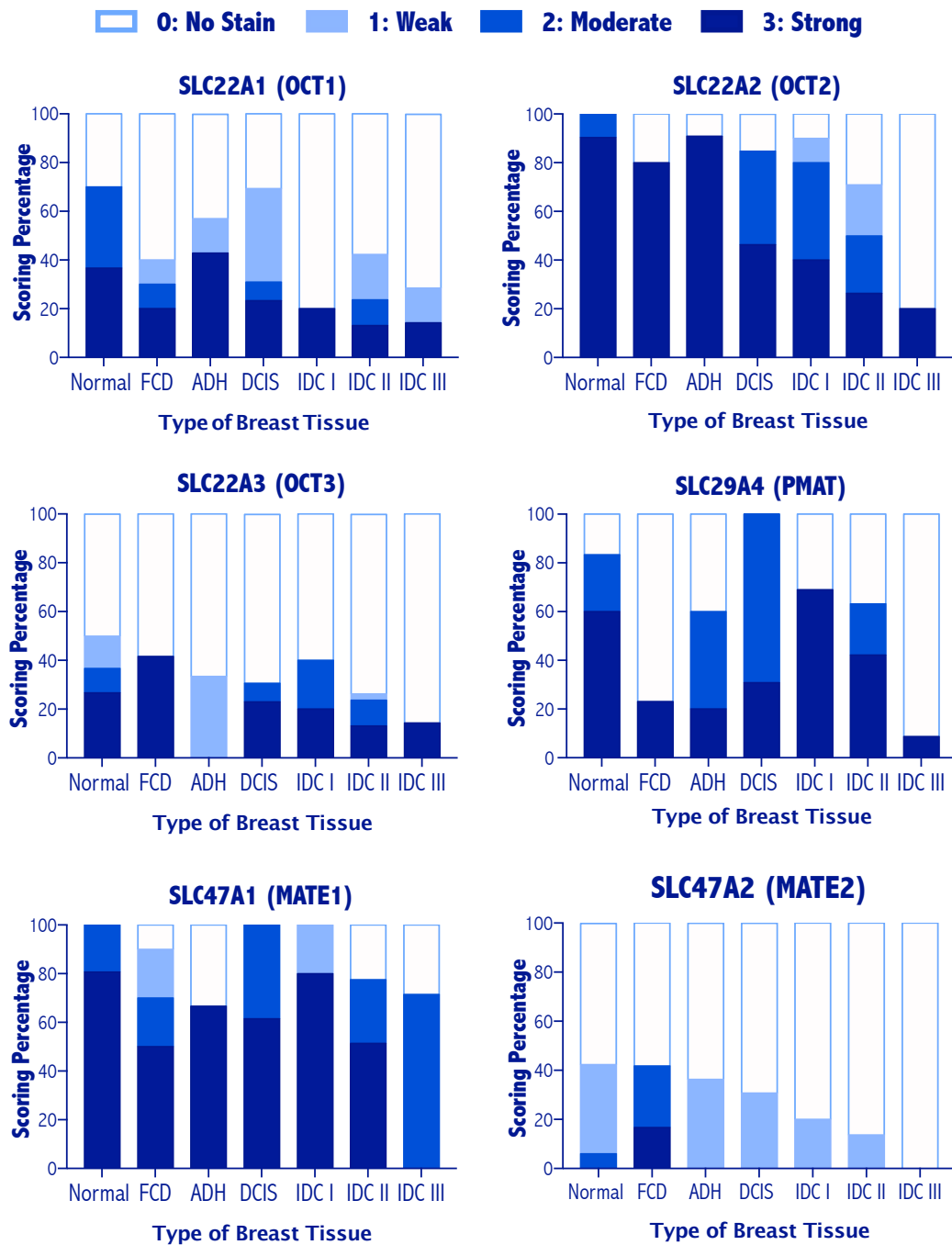


Figure 3.6: Expression of metformin transporters OCT1-3, PMAT and MATE1-2 in a spectrum of breast tissue lesions.

Percentages of staining intensity in different cases with varying epithelial/tumour cell transporter expression. There is a significant decrease in the expression of some uptake transporters, such as OCT2 and OCT3, with increased severity and grade of invasive ductal carcinoma. Low expression of MATE2 transporter was evident among most types of breast tissues. Normal: Normal breast tissue, FCD: Fibrocystic disease, ADH: Atypical ductal hyperplasia, DCIS: Ductal carcinoma *in situ*; IDC: Invasive ductal carcinoma grade I-III.

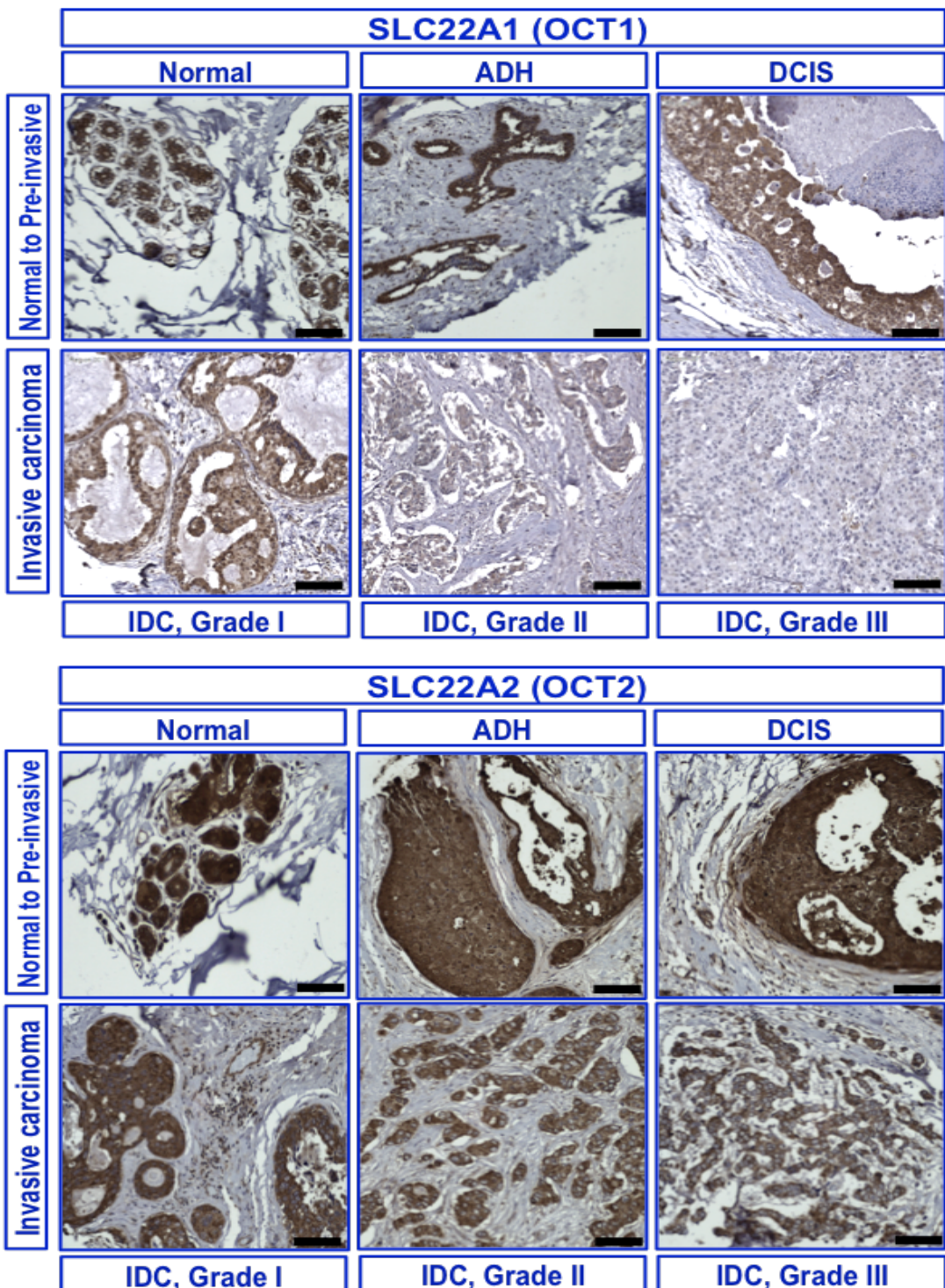


Figure 3.7: Examples of metformin uptake transporters staining (OCT1 and OCT2) in human breast tissues.

The images show sections of a range of breast tissues, which are positively or negatively stained for OCT1 and OCT2. Membranous and cytoplasmic staining of ductal and tumour cells indicate positivity (scale bar: 50 µm)

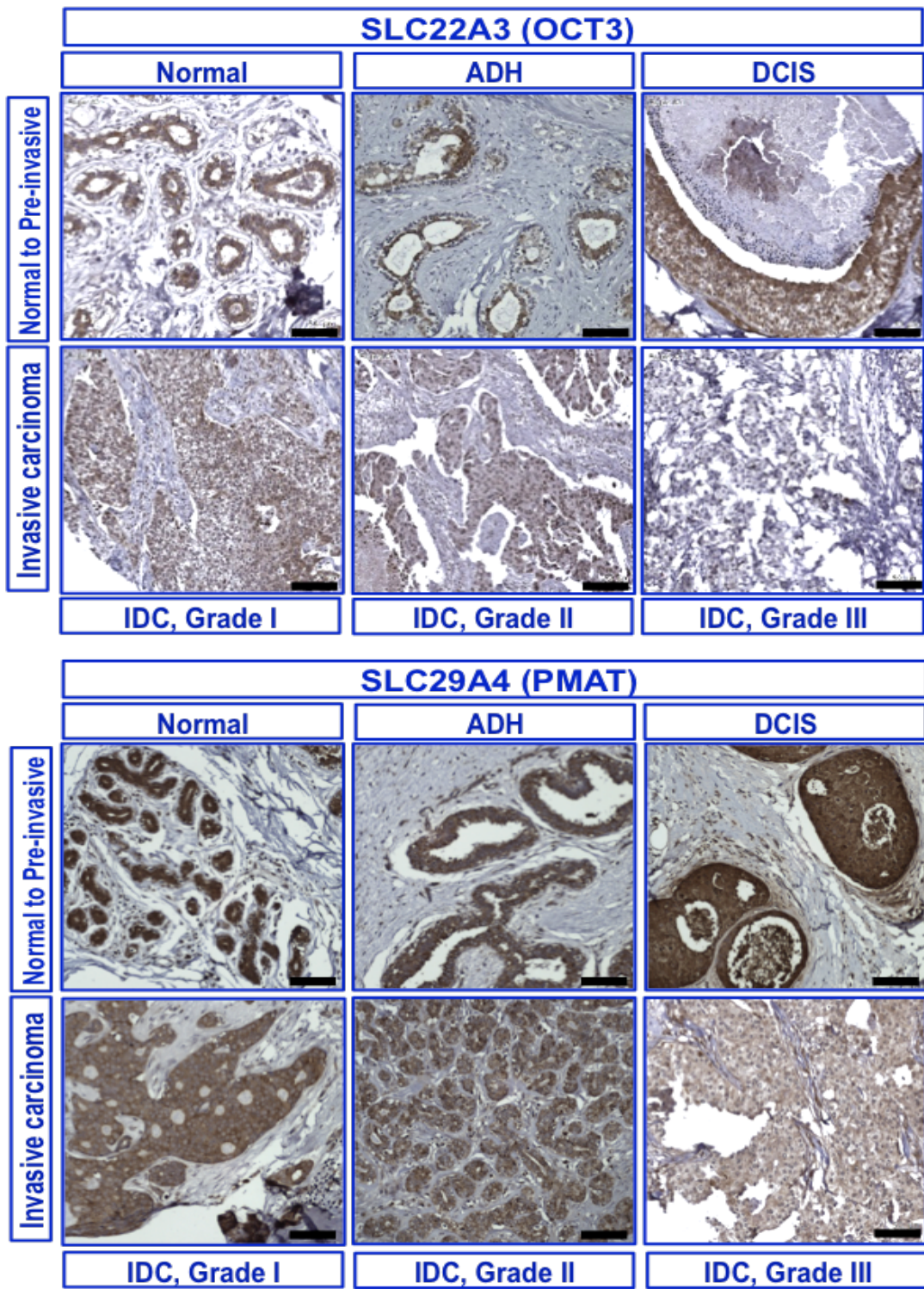


Figure 3.8: Examples of metformin uptake transporters staining (OCT3 and PMAT) in human breast tissues.

The images show sections of a range of breast tissues, which are positively or negatively stained for OCT3 and PMAT. Membranous and cytoplasmic staining of ductal and tumour cells indicate positivity (scale bar: 50 µm).

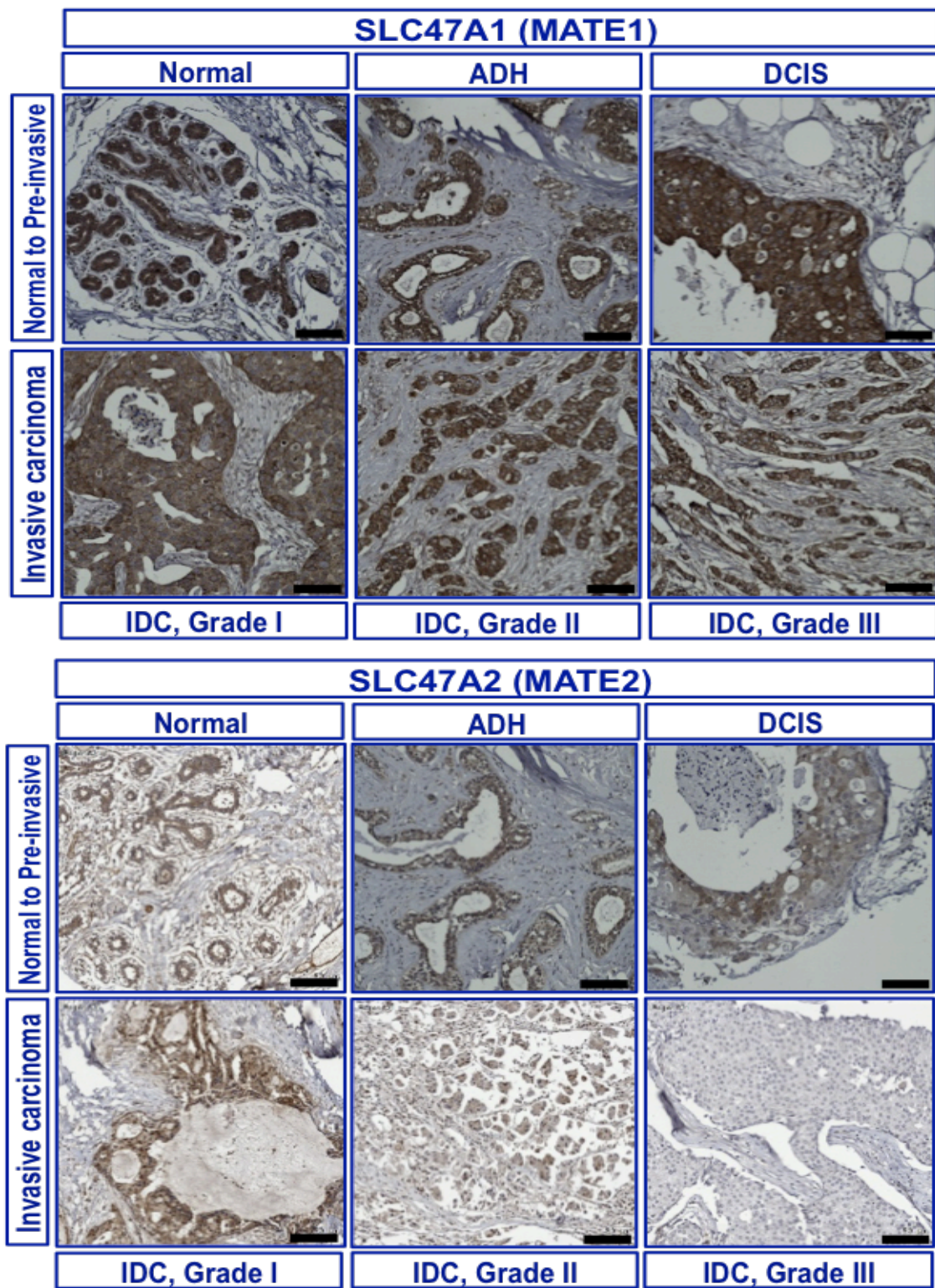


Figure 3.9: Examples of metformin extrusion transporters staining (MATE1 and MATE2) in human breast tissues.

The images show sections of a range of breast tissues, which are positively or negatively stained for MATE1 and MATE2. Membranous and cytoplasmic staining of ductal and tumour cells indicate positivity (scale bar: 50 µm).

4.4 Discussion

Previous studies have suggested that OCT1 and OCT2 expression is highly restricted to liver and kidney respectively, whereas OCT3 was found to be more widely distributed across several human tissues, and the efflux transporters MATE1-2 are predominantly expressed in the kidney²⁶⁶, but not according to the Genotype-Tissue Expression (GTEx) project and RNA sequencing (RNA-seq) results mentioned earlier in this chapter. The present study is the first comprehensive evaluation of all these putative metformin transporters in breast epithelial and cancer cells. To our knowledge, none of the previous investigators have examined metformin transporter expression using human breast tissue specimens and there is no published literature investigating the expression profile of metformin-transporters in the MCF10A, MCF10AT, DCIS.com, T47D and MDA-MB-231(BM) cell lines.

In the present study, three techniques have been used to investigate the expression of the solute carrier transporters (OCT1-3, PMAT, and MATE1-2) in human breast cell lines (using qRT-PCR and Western blot) and tissues (using immunohistochemistry).

Our results showed that the expression of metformin transporters varies across the different cell lines and tissues and provide convincing evidence that at least one importer and one exporter is present on each cell line and in each tissue. These data therefore suggest that metformin could act on all cell lines and in all breast cancer tissues. However, the immunohistochemistry data seem to suggest that there is a decrease in expression of all of the transporters in stage III breast cancer, suggesting that metformin may be transported to a lesser degree into these tissues and have less beneficial effects in patients with advanced breast cancer.

We firstly aimed to determine metformin transporter expression in human breast cell lines and explore whether there is a differential expression between malignant and non-malignant cells. We found that all cell lines expressed all candidate cation-selective transporter genes. However, at the protein level, OCT1 and PMAT were the predominant transporters in the normal and pre-malignant cells while PMAT was the predominant transporter in the pre-invasive and invasive malignant cells. OCT2 and MATE1, which are involved in metformin uptake and excretion respectively, were abundantly expressed in all cell lines. OCT3 appears to be important for metformin uptake by the triple-negative cells as these were the only cells expressing this transporter. However, although the pre-malignant and malignant cells expressed low level of PMAT and OCT1 respectively, this does not

exclude the possibility that they might have an important role in metformin uptake too. Therefore, the data in this chapter suggests that metformin transport is multi-transporter dependent in breast cell lines.

Quantitative RT-PCR was used to identify the cell lines with high, low or no expression of OCTs and MATEs genes in order to explore potential correlation with metformin response, as described in the next chapter. Thus, to quantify the relative expression difference between samples in all biological replicates (n=3), comparative Ct measurements were used. The Ct value (the threshold cycle) indicates the cycle at which the fluorescent signal first shows significant difference with respect to the background where a lower Ct value means greater expression and vice versa. In our study, OCT1-3, PMAT and MATE1-2 were amplified between 14-29 cycles, which indicates high expression of these genes. The findings presented here add to and expand the previous study by Cai and colleagues as it is currently the only published study which investigated the transporter expression in a panel of 13 basal and luminal breast cancer cell lines including MCF7 and MDA-MB-231²⁷⁹. However, in contrast to our findings they suggest that the expression of most transporter mRNAs was negligible in MCF7 cells while we showed a sufficient amount of expression of all investigated transporter mRNA except OCT3 in this cell line. We have also reported the same finding that multiple transporters are expressed by the MDA-MB-231 and showed for the first time that the OCT2 and PMAT uptake transporter genes were also expressed in a significant amount. Generally, the normalized gene expression values in the Cai *et al.* study were relatively lower than our expression values and their data were normalized to the 18s as a reference gene, which might be a possible reason for the discrepancy in the results. In addition, variation in the results obtained by different laboratories using the same cell lines, may also be attributed to genotypic drift caused by high passage number, or cross-contamination with another cell line²⁸⁵. In this study, fresh cells (bought from the ATCC) with low passage number were used to overcome this limitation including the non-tumorigenic MCF10A and the three invasive breast cancer cell lines.

Metformin transporter gene expression have also been previously demonstrated in a study that used a panel of cancer cell lines including colorectal, pancreatic, lung, prostate, liver and cervical carcinomas. This study detected a relatively low and uniform expression of OCT1-2 and higher variability in OCT3 and MATE1-2 expression among the cancer cell lines with OCT3 showing the highest overall expression²⁸⁶. Generally, the pattern of transporter genes expression seen in the breast cancer invasive cell lines in this study is

different, suggesting a low expression of OCT2, high expression of OCT1 and PMAT, and variability in OCT3, MATE1-2 expression, indicating that the breast cancer cell lines are likely to react in a different way to other cancer cells in response to metformin. However, the gene expression findings of this study are generally in concordance with the microarray data published in the cancer cell line encyclopedia, which indicates high expression of PMAT and MATE1 genes, and a low expression of OCT1-3 and MATE2 genes across breast cancer cell lines (includes MCF7, T47D and MDA-MB-231)²⁸⁷.

One of the possible limitations of the RT-qPCR approach is improper use of the internal control gene where careful normalization is an essential step for accurate quantification of mRNA levels. To avoid these issues in this study GAPDH was used as a normalizing gene, as it has been identified previously as the most stable reference gene, along with ACTB gene (β -actin), in both basal (MDA-MB-231) and ER+ (MCF7 and T47D) as well as MCF10A cell lines^{288, 289}. Furthermore, variation of GAPDH mRNA expression within the same tissue, such as breast tissue, was also demonstrated to be relatively small when compared to other housekeeping genes²⁹⁰. Indeed, the GAPDH Ct values in this chapter strongly suggest the stability of GAPDH expression in all cell lines investigated (see supplementary material CD, S1). Although the compact error bars observed in this experiment minimize the possibility that a significant expression of metformin transporters was obscured by outlying results, as only duplicates of three biological replicates were used, the data may potentially be improved by repeating the experiment with more replicates but time constraints prevented this.

Indeed, the detection of the transporter expression at mRNA level provides a good indication of their presence or absence in a given biological sample. However, a good correlation between the mRNA transcript level and the protein level does not always exist in the same tissue, therefore, the confirmation of expression is required at the protein level²⁹¹. Additionally, protein expression is expected to correlate better with transporter function than mRNA expression and so Western blot analysis was performed to establish transporter protein expression in these cell lines.

Using Western blotting, OCT1, OCT2, PMAT and MATE1 proteins were all detected in the cell lysates of all the cell lines. In contrast the extrusion protein, MATE2, was not seen in any of the cells at the protein level and OCT3 expression was only detected in the MDA-MB-231 cells (Figure 3.6). To confirm that the results were not a consequence of absent or

unequal protein loading, β -actin was used as a loading control where the presence of equivalent bands confirmed equal protein loading. Generally, there was no exact correspondence between the transporter gene and transporter protein expression in the human breast cell lines analysed, however, the OCT2, PMAT and MATE1 gene and protein expression have all followed similar patterns. This poor correlation between the gene and its relevant protein level can be attributed to several different reasons, including post-translational modification involved in translating the mRNA into protein, the stability of the mRNA, low level of protein expression, differential *in vitro* half-lives of the proteins and protein modification. Interestingly, our findings of transporter protein expression by MDA-MB-231 cell are consistent with the Cai *et al.* study (including OCT1, OCT3 and MATE1) and in addition showed for the first time that OCT2 and PMAT uptake proteins are also highly expressed by MDA-MB-231 cells. In contrast to the finding by Cai and colleagues that expression of all transporter proteins was undetectable in the MCF7 cell line, this study showed for the first time that MCF7 cells actually abundantly express OCT1-2, PMAT, MATE1 but not OCT3 and MATE2. The investigators in Cai study have obtained their MCF7 cells from their local tissue culture facility, while the MCF7 cells used in this project were freshly bought from the ATCC, this can explain the remarkable difference in the expression data between the two studies. It is well known that MCF7 cell lines used by various laboratories may exhibit a fundamental difference in their biological properties, despite having a similar karyotype, and this difference is related to the number of passages and the culturing conditions before storage^{292, 293}.

Previous studies have shown that high expression of OCT3 was associated with increased intracellular concentration of metformin and improved cellular response in terms of inhibition of proliferation in breast²⁷⁹ (MDA-MB-231) and prostate (LNCaP) cancer cell lines²⁸⁶. OCT3 expression was also shown to be a critical determinant of metformin uptake in breast cancer cells where metformin uptake was negligible in the OCT3-deficient BT20 cells and high in OCT3-competent MDA-MB-231 cells²⁷⁹. In contrast, positive expression of MATE2 correlated with resistance to antineoplastic activity of metformin in some cancer cell lines such as prostate (LNCaP) and small cell lung cancer (A549) cells²⁸⁶. This correlation was in the expected direction given the role of OCT3 and MATE2 as metformin importer and exporter respectively. Our findings might suggest that the transporters identified in other cancers may not be as relevant for metformin action in breast cancer where OCT3 appears to be the least likely to be involved while other transporters such as PMAT and OCT2 are more

likely to be involved in metformin translocation into the invasive and metastatic cancer cell lines and MATE1 in the extrusion of the drug, however, further cellular uptake experiments should be performed before such a conclusion can be reached.

Finally this chapter investigated transporter expression in the non-tumour and tumour breast tissues using immunohistochemical staining, a reliable method of testing for protein expression status in breast cancer patients. To date, little is known about the expression and localization of metformin transporters in human breast tissue and this was the first study to explore this. OCT1-2, PMAT and MATE1-2 proteins were predominantly localized to the plasma membrane but also found in the cytoplasm and intracellular organelles of the ductal epithelial and tumour cells but not the stromal cells. Generally, there is a consistency in expression data between the normal and the fibrocystic disease tissues with a few discrepancies, which might be explained by the difference in the number of tissue sections analysed (n=34 and n=12, respectively). The results obtained from breast tissue immunostaining suggest that, OCT1 is down-regulated with increased disease severity, MATE1 is highly expressed, while OCT3 and MATE2 are the least expressed, which correlate well with the protein expression study of the cell lines. All breast tissue subtypes abundantly expressed OCT2, however, Western blotting revealed no change in the expression of OCT2 among the cell lines while the immunostaining showed down-regulation of the expression with increased stage of BC disease. Unlike the cell line expression findings, PMAT tissue expression was reduced with advanced stages of the breast cancer disease.

The data might suggest a possible role for OCT1-3, PMAT and MATE1 in breast tissue response to metformin; however, this remains inconclusive unless further uptake studies are performed. The data also demonstrate a clear pattern of decreasing OCTs and PMAT expression with an increasing severity of breast disease, with grade III having the lowest. This suggests that metformin may be transported into breast cells at all stages of cancer progression, but least at stage III and therefore if a patient has stage III cancer they are less likely to respond to metformin, and analysis of the transporter expression would be necessary to identify patients who are likely to respond to metformin treatment. Although it would be interesting to identify the hormonal receptor status of the different grades of IDC tissue section used in our study, they were all commercially available TMAs and this data was not available. To date there are no studies that have looked at a correlation between breast cancer stage and metformin response in established disease.

The expression of OCTs and MATEs genes in human breast tumour tissues, and their corresponding adjacent normal and non-malignant tissues has been previously assessed using RT-qPCR. In the three tissue types examined in this study, OCT3 and PMAT genes were the predominant transporters expressed using PCR²⁷⁹. The study also detected a lower expression of OCT1 and MATE1 genes and negligible expression of the OCT2 and MATE2 genes. Similarly to the protein immunohistochemistry results presented here, the analysis of OCT1, OCT3, PMAT and MATE1 gene expression revealed a down regulation of these transporters in all the breast tumour tissues analysed compared to the adjacent non-malignant tissues, although this decrease was not statistically significant. However, considering that the RT-PCR and immunohistochemistry techniques are totally different (targeting RNA and proteins respectively), the results, although similar, are not fully comparable, which may explain some of the subtle differences between them. Sample size and preparation are also likely to make a difference.

To complement this work, future experiments might include a mass spectrometry analysis to determine the relative importance of how the expression of these transporters can affect intracellular uptake of metformin. This would be followed by a knockdown experiment of these transporters to determine whether this would alter sensitivity to metformin (in terms of proliferation) and metformin uptake. Moreover, it remains to be determined whether the transporter expression would change with prolonged exposure to metformin and hence this could be a mechanism of acquired resistance. However, due to time and money constraint these experiments were not performed.

To conclude, in this study, OCTs, PMAT and MATE1 were all detected in normal, pre-malignant, pre-invasive and invasive human breast cell lines and tissues. These findings suggest that multiple transporters are likely to be involved in metformin transport in breast cell lines and tissues and there might be an overlap between them. Therefore, metformin is likely to enter and leave all the breast cells in our model of breast disease, as the majority of our cell lines are positive for at least one influx and one efflux transporter. Furthermore, data in this chapter have demonstrated that there is an altered expression of metformin transporters in disease states, with the majority decreasing with increasing lesion severity. The next chapter will now investigate whether clinically relevant doses of metformin will be efficacious in these models of increasing severity of breast disease. The data will also identify whether there is a correlation between transporter expression and metformin response in these cells.

4. Chapter 4: Evidence of anti-Cancer effects of clinically relevant doses of metformin, *in vitro*

4.1 Introduction

Recently, the bench-to-clinic scenario for metformin as a potential treatment for non-diabetic breast cancer patients has received considerable critical attention. Population-based observational studies indicate that metformin might reduce breast cancer risk and mortality in diabetic patients. Metformin might protect against breast cancer indirectly by ameliorating insulin resistance and systemic glucose homeostasis. Alternatively, metformin might directly target breast cancer cells through a series of events resulting in decreased protein translation, inhibition of cell proliferation and increased apoptosis.

Indeed, a considerable number of preclinical studies have also suggested a wide range of anti-cancer effects of metformin, including the inhibition of cell proliferation, cell cycle progression and apoptosis *in vivo* and *in vitro* cell line model systems of various breast cancer subtypes, and have attempted to identify the potential mechanisms of action. Moreover, considerable attention has been paid to the role of altered metabolism in breast cancer and the ability of metformin to significantly affect several metabolic pathways that suggests that it could be effective at preventing the development and progression of this disease. However, an important shortcoming of most previous *in vitro* studies is the use of supra-pharmacological doses of the drug and supra-physiological glucose concentrations in culture. Consequently, the clinical relevance of the data obtained using doses higher than 10mM metformin has been questioned with growing concerns that the inhibitory effects seen with higher metformin doses are likely to be off-target effects which are not reflective of *in vivo* events; this remains a contentious issue which limits the translation of published preclinical data into the clinical setting.

Despite the wealth of information presented in chapter one, we are still far from a clear, consistent picture that could support the rational for metformin to be used in either breast cancer prevention or treatment. Additionally, there is still a concern that not all breast cancer cell lines responded to metformin treatment, so it could therefore potentially be more effective on specific subtypes of breast cancer such as luminal A, and as yet it is not clear why some respond while others do not. What is clear is that metformin does have a great impact on breast cancer growth both directly and indirectly *in vitro*, at least at supra-physiological doses.

The data in the previous chapter demonstrated that there is at least one importer and one exporter protein on each breast cell type that could potentially allow metformin to accumulate in the non-tumour and tumour breast cells, suggesting that metformin would directly enter the cells and has the potential to enter the mitochondrion where it can inhibit complex 1, which would result in growth and survival inhibition of the breast cells. In addition, the previous observations from the literature that metformin inhibits the growth and proliferation of breast cancer cells in culture, suggests that the antineoplastic action of metformin could be mediated, at least in part, through a direct effect on cancer cells. Therefore, this project tests the hypothesis that clinically relevant doses of metformin would inhibit the growth and survival of breast cancer cells. Accordingly, our panel of increasingly malignant cell lines would be expected to demonstrate potential variability in their response to the clinically relevant doses of metformin, due in part to the heterogeneity in their OCTs and MATEs metformin transporter expression.

As data on the effect of the therapeutically relevant doses of metformin on breast cancer is extremely limited, this study aimed to assess the direct anti-proliferative and cytotoxic effects of metformin at increasing doses including those which are clinically relevant plasma doses (0.03-0.3 mM) close to those found in the plasma of type 2 diabetic patients treated with this drug, potential tissue accumulated doses (1 mM and 5 mM), as well as using higher concentrations corresponding to the toxic supra-pharmacological doses (10 mM and 20 mM) in certain assays to confirm the previous literature, against a panel of breast cell lines. The cell lines were chosen as a representative sequence in the tumourigenesis of breast cancer, with cell lines corresponding to non-tumorigenic (normal epithelial), hyperplastic tissue, *in situ* carcinoma, 3 molecular subtypes of invasive carcinomas (with different hormonal status) and the fully bone-homed metastatic breast cancer cells in order to mimic a more clinically relevant breast cancer model system, *in vitro*. The luminal cell lines A (MCF-7 and T47D) have molecular signature of epithelial phenotype, while the basal cell line (MDA-MB-231) is molecularly mesenchymal-like. It is hoped that this will be useful in identifying any subpopulation that are more responsive to metformin treatment.

This work therefore aimed to provide insight into whether metformin may act as a chemotherapeutic drug in different breast cancer subtypes by affecting cell viability, metabolic activity, DNA replication and cell cycle and migration at clinically relevant doses *in vitro*. Additionally, the work in this chapter aimed to see whether there is a possible correlation between the sensitivity to metformin and metformin-transporter expression.

4.2 Methods

- In order to investigate the effects of the clinically relevant doses of metformin in breast cancer, cell lines representing different severities of breast lesion were cultured as described previously in section 2.2.1.
- MTS assay was used to assess the effect of the pharmacologically relevant doses of metformin on the metabolic activity of breast cells, following the protocol in section 2.2.6.1.2.
- Trypan blue exclusion assay was used to investigate the effect of the clinically relevant doses of metformin on viability and total cell count of the breast cells, as in section 2.2.7.2.
- BrdU incorporation assay, a DNA synthesis-based cell proliferation assay, was used to explore the effect of the clinically relevant doses of metformin on the proliferation of breast cells, following the protocol in section 2.2.8.4.
- Clonogenic assays were used to assess the influence of the clinically relevant doses of metformin on cell survival and reproductive capabilities, following the protocol in section 2.2.7.2.
- Flow cytometry analysis was used to explore the effect of metformin on cell cycle progression as detailed in sections 2.2.8.2 and 2.2.8.3.
- Wound healing scratch assay was used to assess the effect of metformin on the migration of breast cancer cells following the protocol in section 2.2.9.4.
- Each experiment was performed on at least three occasions and the graphs shown are the average of these data. Statistical analysis was performed with advice from the Sheffield statistical services and the tests used were the non-parametric tests as detailed in Statistical analysis, section 2.2.11, and a P-value of <0.05 was taken to be significant.

4.3 Results

4.3.1 Comparison of growth rate between tumour and non-tumour breast cell lines

Before assessing the anti-proliferative effect of metformin on different cells, cellular-growth curves for all cell lines were established to compare the growth patterns and rates between different human mammary cells and define the baseline growth characteristics of cells. Proliferation was quantitated and expressed as population-doubling time. Cell line population doubling times (PDTs) were determined by plating 2×10^4 cells of three biological replicates as triplicates in a 6-well plate in their respective assay media. Four plates per cell line were counted at 24, 48, 72 and 96 hours after plating and cellular proliferation was analysed by counting the viable cell number. The PDT for each cell line was calculated using the following equation (doubling time computing tool at <http://www.doubling-time.com/compute.php> was employed):

$$\text{Doubling time} = \frac{\text{duration} \times \log(2)}{\log(\text{FinalConcentration}) - \log(\text{InitialConcentration})}$$

Where "log" is the logarithm to base 10 (as automatically calculated).

The growth curves, illustrated in figure 4.1, showed that the malignant cells divided at a slower rate than normal, premalignant and pre-invasive cells and population-doubling time values of malignant cells were more heterogeneous than those of the normal cells. Our findings demonstrate that the MCF10A and MCF10AT cell lines had the highest growth rate and T47D cells were the slowest; PDTs were 19.02 hours, 19.12 hours and 45.87 hours, respectively. For the rest of cell lines, the doubling time was in the following order: DCIS.com (21.19 hours) > MDA-MB-231(BM) (36.49 hours) > MDA-MB-231 (37.15 hours) > MCF7 (40.26 hours), PDTs are summarized in table 4.1.

It should be noted that the media in which MCF10A, MCF10AT and DCIS.com were growing contains more growth stimulatory factors than the media in which the breast cancer cells were grown, which may account for some of the differences seen.

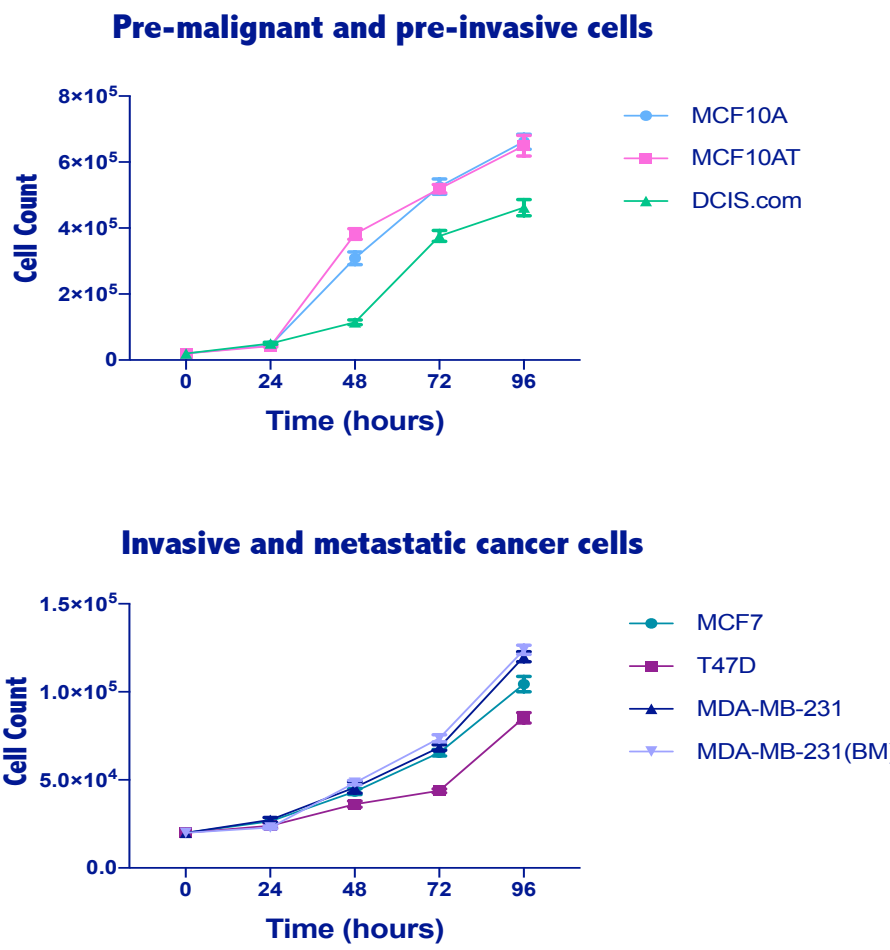


Figure 4.1: The growth curves of normal, premalignant, pre-invasive, invasive and the fully bone-homed human breast cells.

The numbers of viable cells were counted for 4 days. Data represent the mean \pm SD of three independent experiments.

Table 4.1: Summary of the cell lines used in this chapter and their population doubling times (PDTs)

| Cell line | Classification | PDT (hours) | PDT from the ATCC website |
|----------------|--|-------------|---------------------------|
| MCF10A | Non-tumorigenic normal epithelium | 19.02 | 16 hours |
| MCF10AT | Pre-malignant ductal hyperplasia | 19.12 | Not available |
| DCIS.com | Pre-invasive ductal carcinoma <i>in situ</i> | 21.19 | Not available |
| MCF7 | Invasive BC, luminal A | 40.26 | 38 hours |
| T47D | Invasive BC, luminal A | 45.87 | 43 hours |
| MDA-MB-231 | Invasive BC, Claudine low (triple negative) | 37.15 | 38 hours |
| MDA-MB-231(BM) | Metastatic bone-seeking | 36.49 | Not available |

4.3.2 Assessment of the anti-metabolic effect of metformin using MTS assays

Initially, in order to compare our findings with those of the literature^{152, 173, 294}, the post-treatment cellular viability and metabolic activity were assessed using the colorimetric MTS assay. Following assay optimisation (section 2.2.6.1.3), the anti-proliferative effect of metformin was then evaluated by treating all cell lines with increasing concentrations (0.03-20 mM). Cellular responses in terms of metabolic activity were measured at 3 time intervals (24, 48 and 72 hours) (Figure 4.2).

Following 72 hours of treatment, the clinically relevant doses of metformin did not inhibit the proliferation of the invasive breast cancer cell lines, but significantly reduced the cellular metabolic activity of the pre-invasive MCF10A (by 11.8% of the untreated control), MCF10AT (by 8.3% of the untreated control) and DCIS.com (by 41.6% of the untreated control) cells at a dose equal to or greater than 0.03 mM ($P<0.001$, $P<0.001$ and $P<0.0001$, Dunnett's test, respectively, compared to the untreated controls), the same effect was observed at 0.3 mM in the metastatic bone-homed cells (by 20% of the untreated control) ($P=0.01$, Dunnett's test, compared to the untreated control).

A significant inhibition was only achieved at 20 mM concentration resulting in 19% ($P=0.01$), 13% inhibition ($P=0.04$) and 10% ($P=0.03$) in the MCF7, T47D and MDA-MB-231 cells respectively; assessed using the Post hoc Dunnett's test compared to the untreated controls. Percentages of inhibition are summarized in Table 4.2.

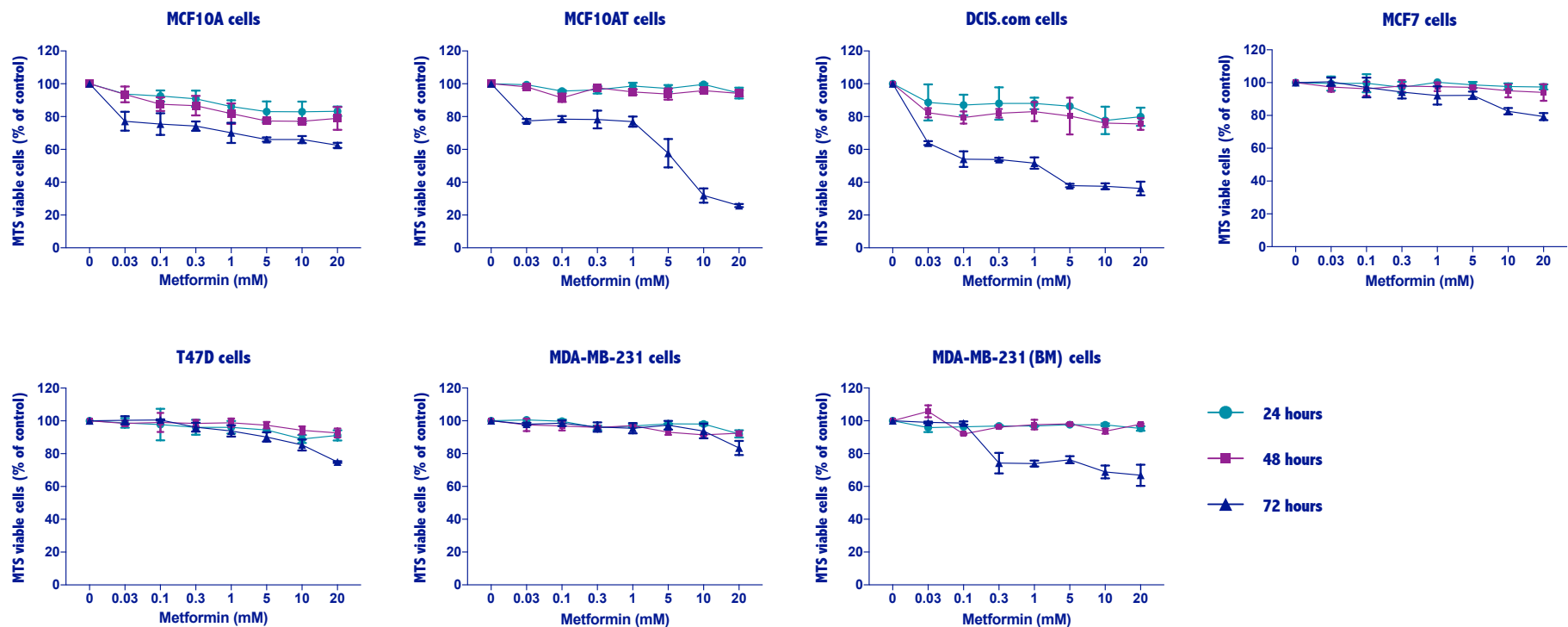


Figure 4.2: Clinically relevant concentrations of metformin reduced the viability of the non-tumorigenic (MCF10A), premalignant (MCF10AT) and pre-invasive (DCIS) cells.

Cellular metabolic activity was measured using the MTS assay and the percentage of cell viability was calculated relative to control wells (no treatment) designated as 100% viable cells. Metformin inhibited all the pre-malignant and pre-invasive cell lines in a significant dose dependent manner achieving significance at 0.03 mM and 0.3 mM in the metastatic bone-derived cells. The metabolic activity of the three invasive cells was inhibited at 20 mM. The values are presented as mean \pm standard deviation (SD) from three independent experiments.

Table 4.2: Analysis of the inhibition in cellular metabolic activity following 72 hours of metformin treatment

| Cell line | Percentages of inhibition | | | | | | | P-values | | IC50 | |
|----------------|---------------------------|---------|---------|-------------------------------------|---------|-------------------------------------|---------|--------------------|---|-------------|--|
| | Clinically relevant doses | | | Potential tissue accumulation doses | | Supra-pharmacological (Toxic) doses | | One-way ANOVA test | Post hoc Dunnett's test | | |
| | 0.03mM | 0.1mM | 0.3mM | 1mM | 5mM | 10mM | 20mM | | | | |
| MCF10A | (11.8%) | (14.7%) | (16%) | (20.6%) | (24.5%) | (24.6%) | (25%) | P<0.001 | Achieved significance at 0.03 mM (P=0.001) | >20mM | |
| MCF10AT | (8.3%) | (11.4%) | (9.3%) | (9.7%) | (41%) | (70.2%) | (75.5%) | P<0.003 | Achieved significance at 0.03 mM (P=0.002) | 5.7mM | |
| DCIS.com | (41.6%) | (46.4%) | (45.3%) | (49.7%) | (61.7%) | (63.2%) | (63.1%) | P<0.001 | Achieved significance at 0.03 mM (P=0.0001) | 1.8mM | |
| MCF7 | (0.9%) | (2.3%) | (3.5%) | (3.3%) | (3.9%) | (5.2%) | (19.7%) | P<0.01 | Achieved significance at 10 mM (P=0.01) | >20mM | |
| T47D | (0.8%) | (0.8%) | (3.1%) | (3.7%) | (6%) | (4.4%) | (13.7%) | P<0.05 | Achieved significance at 10 mM (P=0.03) | >20mM | |
| MDA-MB-231 | (4.3%) | (4.9%) | (10%) | (9.5%) | (7.7%) | (8.8%) | (10.6%) | P<0.05 | Achieved significance at 20 mM (P=0.04) | >20mM | |
| MDA-MB-231(BM) | (0.2%) | (4%) | (20%) | (20.5%) | (19.3%) | (23.2%) | (25.3%) | P<0.002 | Achieved significance at 0.3 mM (P=0.01) | >20mM | |

4.3.3 The effects of metformin on viable cell numbers and viability as assessed by trypan blue exclusion assay

As the MTS assay relies on the activity of mitochondrial dehydrogenase and there is some evidence that metformin may alter the activity of mitochondrial enzymes²⁹⁵, the data needed confirming in an alternative assay. Using a trypan blue exclusion assay it was possible to both confirm the MTS assay data and to evaluate whether clinically relevant doses of metformin have an effect on both on both the viability and viable cell counts 72 hours after treatment. This time point was used, as this is the point at which maximum inhibition was seen in the MTS assay for all cell lines.

The data clearly demonstrate a significant decrease in cell number in all cell lines in a dose dependent manner (Figure 4.3A and Table 4.3) as assessed by the One-way ANOVA test. The reduction in viable cells count was significant at doses equal to or greater than 0.03 mM ($P=0.0001$, Dunnett's test, compared to the untreated controls) in MCF10A, MCF10AT, DCIS.com (to 42%, 58% and 78% of the untreated controls, respectively) and achieved significance at 0.3 mM in T47D, MDA-MB-231 and its bone-homed variant cells to 19%, 36% and 39% of the untreated controls respectively ($P=0.0001$, Dunnett's test, compared to the untreated controls) (Table 4.3). In contrast the MCF7 cells only achieved significant inhibition in cell number (36% of the untreated control) when treated with 5 mM metformin ($P=0.0001$, Dunnett's test, compared to the untreated controls).

However, unlike in the MTS assay, among cancer cells the invasive T47D, MDA-MB-231 and the fully bone-homed cells were responsive to the highest dose in the clinically relevant doses range, namely 0.3 mM, as well as to the potential tissue accumulation doses of metformin (1-5 mM). MCF7 cells have also significantly responded to a dose of as low as 5 mM. The results from all other cells were in line with the MTS assay.

Interestingly the pre-malignant and pre-invasive cell lines showed a clear dose dependent inhibition in cell viability at all doses (Figure 4.3B), achieving significance at 0.03 mM ($P=0.0001$) in the MCF10AT and DCIS.com and 0.1 mM ($P=0.0001$) in the MCF10A cells; assessed by post hoc Dunnett's test compared to the untreated controls.

In contrast, there was only a slight reduction in the viability of the invasive breast cancer cells in response to metformin treatment. Indeed, T47D cells were the most responsive showing a significant inhibition in viability in response to 5 mM metformin treatment ($P=0.0001$), whereas MCF7 and MDA-MB-231 cell viability was only significantly affected at the highest tested dose; 20 mM ($P=0.0012$). In contrast the viability of the fully bone-homed cells was not significantly affected at any tested dose ($P=0.109$); Dunnett's test compared to the untreated controls (Figure 4.3B). Percentages of inhibition are summarized in Table 4.3.

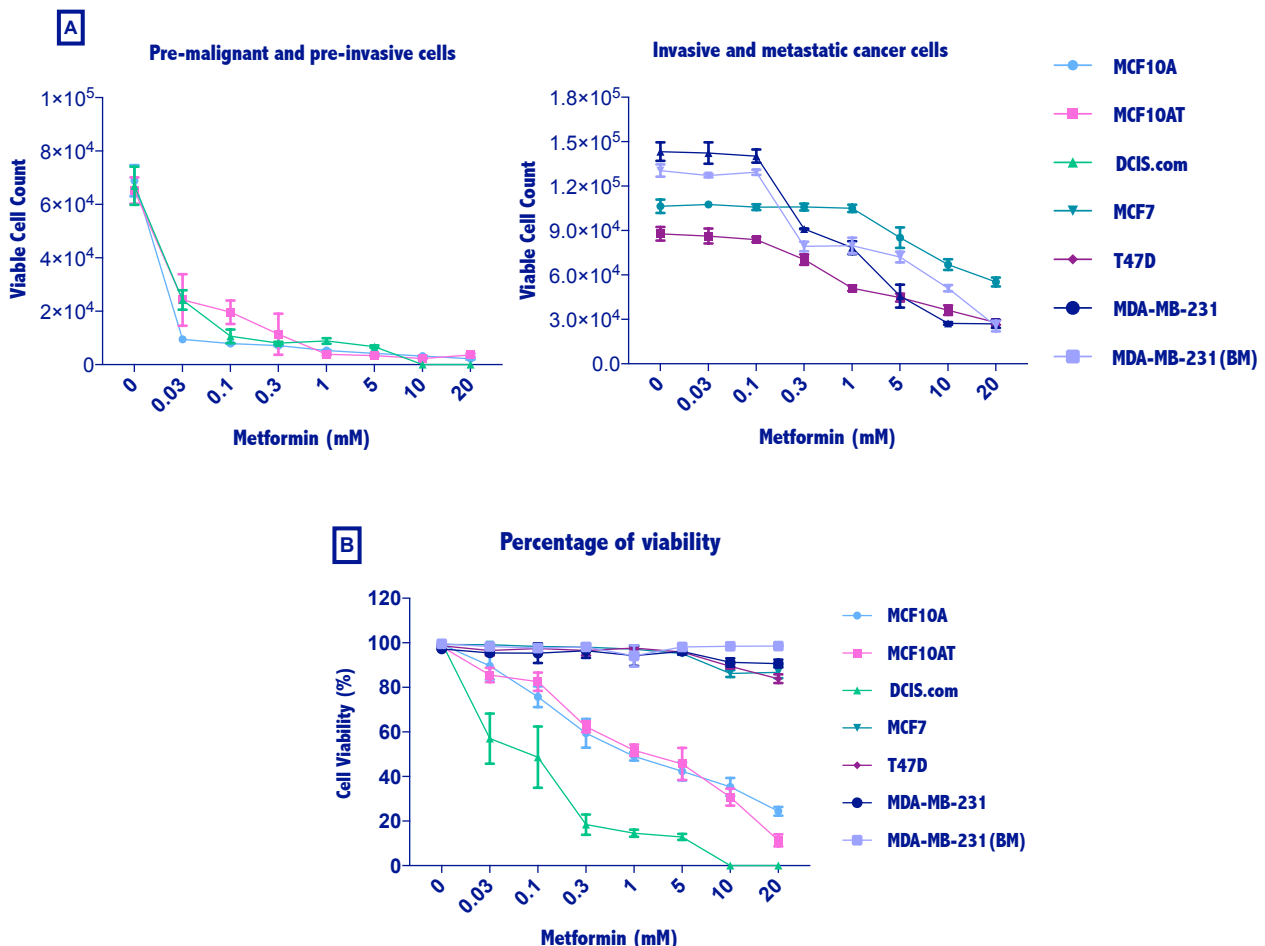


Figure 4.3: Clinically relevant doses of metformin reduce the growth and viability of the premalignant cells and suppress the proliferation of invasive cells without affecting their viability.

Cells were treated with increasing doses of metformin and the cell number and viability established following 72 hours of treatment. (A) The growth inhibitory effect of metformin was noticeable at lower doses than the MTS assay in all cancer cells. MCF10A, MCF10AT and DCIS.com cellular proliferation were inhibited at the lowest dose of 0.03 mM. (B) In contrast to the invasive cells, in which the effect on viability was limited, the viability of MCF10A, MCF10AT and DCIS.com was significantly reduced at 0.03 mM ($P=0.0001$; Dunnett's test). Data is presented as mean \pm SD of the viable cell counts and percentage of viability from three independent experiments.

Table 4.3: Analysis of the reduction in viable cells number following 72 hours of metformin treatment

| Cell line | Percentages of inhibition | | | | | | | P-values | | IC50 | |
|----------------|---------------------------|---------|---------|-------------------------------------|---------|-------------------------------------|----------|--------------------|---|---------|--|
| | Clinically relevant doses | | | Potential tissue accumulation doses | | Supra-pharmacological (Toxic) doses | | One-way ANOVA test | Post hoc Dunnett's test | | |
| | 0.03mM | 0.1mM | 0.3mM | 1mM | 5mM | 10mM | 20mM | | | | |
| MCF10A | (42.2%) | (52.4%) | (56.8%) | (67.7%) | (74.3%) | (80.2%) | (86.8%) | P<0.001 | Achieved significance at 0.03 mM (P=0.0001) | 0.05mM | |
| MCF10AT | (58.2%) | (74.6%) | (90.4%) | (91.4%) | (94.4%) | (96.71%) | (96.8%) | P<0.001 | Achieved significance at 0.03 mM (P=0.0001) | <0.03mM | |
| DCIS.com | (78.0%) | (82.4%) | (82.9%) | (83.2%) | (88.8%) | (100%) | (100%) | P<0.0001 | Achieved significance at 0.03 mM (P=0.0001) | <0.03mM | |
| MCF7 | (1.6%) | (0.8%) | (1.3%) | (3.5%) | (36.5%) | (37.3%) | (48.4%) | P<0.003 | Achieved significance at 5 mM (P=0.0001) | >20mM | |
| T47D | (1.7%) | (4.3%) | (19.7%) | (41.7%) | (48.7%) | (58.6%) | (68.0%) | P<0.001 | Achieved significance at 0.3 mM (P=0.002) | 5.7mM | |
| MDA-MB-231 | (0.7%) | (2.0%) | (36.3%) | (45.2%) | (67.9%) | (80.93%) | (81.12%) | P<0.0001 | Achieved significance at 0.3 mM (P=0.0001) | 1.4mM | |
| MDA-MB-231(BM) | (2.5%) | (0.8%) | (39.1%) | (38.7%) | (44.7%) | (60.8%) | (80.5%) | P<0.0001 | Achieved significance at 0.3 mM (P=0.0001) | 7.8mM | |

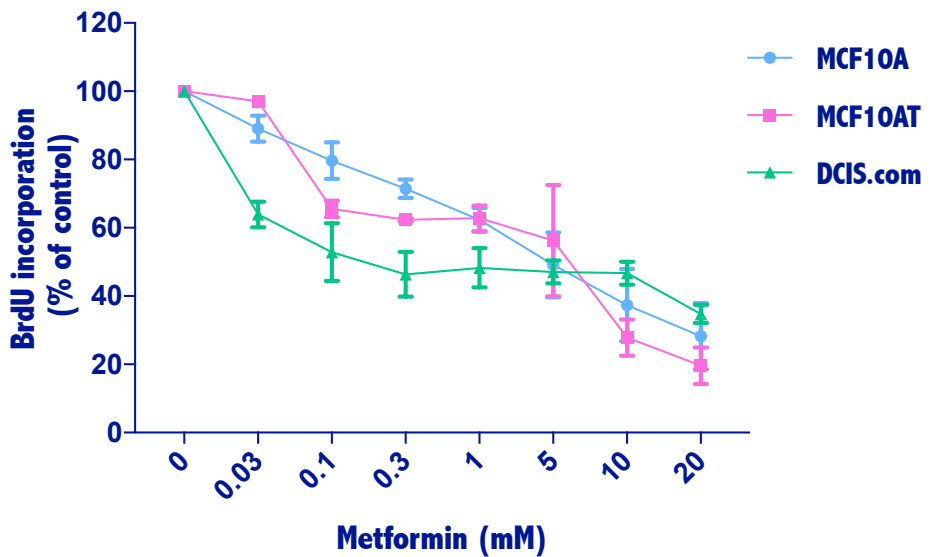
4.3.4 The effects of metformin on DNA replication activity of the breast cells as measured by the BrdU assay

As the MTS assay measures metabolic activity and the trypan blue exclusion assay simply measures cell number and viability, it was decided to use the BrdU incorporation assay to measure DNA replication as a further measure of proliferation, again after 72 hours treatment with increasing doses of metformin. The change in DNA synthesis was calculated by comparing BrdU signals of metformin-treated cells to that of the BrdU-labelled control untreated cells.

Proliferation of cell lines as measured using the BrdU assay was significantly inhibited in a dose dependent manner (Figure 4.4). Metformin treatment of the immortalised normal breast epithelial cells (MCF10A) resulted in a significant inhibition at a dose of 0.3 mM achieving 37% inhibition. In contrast the premalignant, MCF10AT, and pre-invasive, DCIS.com, cells were more sensitive to metformin treatment, achieving significance at 0.1 mM (34.4%, P=0.0019) and 0.03 mM (36%, P=0.0001), respectively; assessed by Dunnett's test compared to the untreated controls. The less invasive breast cancer cell lines were less sensitive with inhibition achieving significance at 1 mM (MCF7 = 43.3%, P=0.0008; T47D = 41%, P=0.0018, Dunnett's test, compared to the untreated controls). In contrast the highly aggressive MDA-MB-231 and the metastatic bone-homed variant MDA-MB-231(BM) cells were more sensitive with significance seen at lower doses; 0.3 mM and 0.03 mM, respectively (26.2%, P=0.0024 and 27.6%, P=0.004, respectively, Dunnett's test, compared to the untreated controls) (Table 4.4).

However, metformin at concentrations of 10-20 mM inhibited BrdU incorporation by 71%-90% in MCF10A, MCF10AT, MCF7, MDA-MB-231(BM) and T47D (Figure 4.4). Metformin at 20 mM inhibited 65% and 47% of the DCIS.com and MDA-MB-231 cells proliferation.

Pre-malignant and Pre-invasive cells



Invasive and metastatic cancer cells

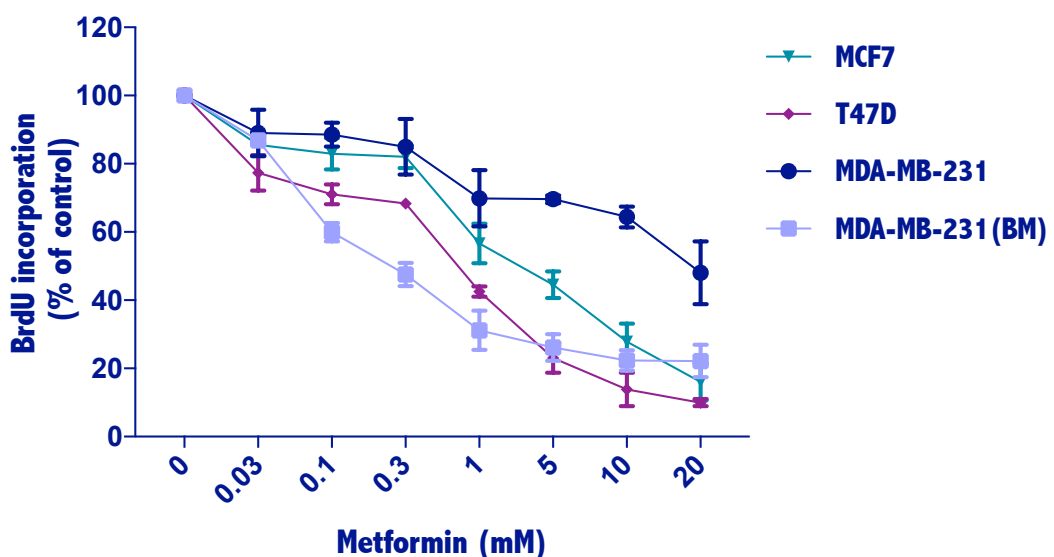


Figure 4.4: Experimentally relevant doses of metformin significantly reduced the proliferation in all cell cultures after 72 hours of treatment.

Cell proliferation was evaluated by BrdU incorporation assay. Three individual experiments were performed in triplicates. Graphs represent the percentage of BrdU positive cells relative to the BrdU-labelled control cells. The data are expressed as mean \pm SD. Metformin inhibited all cell lines in a significant dose dependent manner achieving significance at 0.1 mM in the pre-malignant and pre-invasive cells and 1 mM in invasive cells and 0.1 mM in the metastatic bone-derived cells.

Table 4.4: Analysis of the inhibition in BrdU incorporation in breast cells following 72 hours of metformin treatment

| Cell line | Percentages of inhibition | | | | | | | P-values | | IC50 | |
|----------------|---------------------------|---------|---------|-------------------------------------|---------|-------------------------------------|----------|--------------------|---|--------|--|
| | Clinically relevant doses | | | Potential tissue accumulation doses | | Supra-pharmacological (Toxic) doses | | One-way ANOVA test | Post hoc Dunnett's test | | |
| | 0.03mM | 0.1mM | 0.3mM | 1mM | 5mM | 10mM | 20mM | | | | |
| MCF10A | (20.3%) | (28.5%) | (37.6%) | (50.8%) | (62.6%) | (71.7%) | (75.0%) | P<0.002 | Achieved significance at 0.3 mM (P=0.001) | 0.97mM | |
| MCF10AT | (2.9%) | (34.4%) | (37.6%) | (37.1%) | (43.7%) | (72.13%) | (80.36%) | P<0.001 | Achieved significance at 0.01mM (P=0.0019) | 6.1mM | |
| DCIS.com | (36.0%) | (47.1%) | (53.6%) | (51.7%) | (52.9%) | (53.2%) | (65.2%) | P<0.0001 | Achieved significance at 0.03 mM (P=0.0001) | 0.29mM | |
| MCF7 | (14.4%) | (17.0%) | (17.9%) | (43.3%) | (55.4%) | (72.1%) | (83.9%) | P<0.002 | Achieved significance at 1 mM (P=0.0008) | 4.1mM | |
| T47D | (19.0%) | (28.9%) | (31.6%) | (41.4%) | (76.9%) | (86.15%) | (90.02%) | P<0.005 | Achieved significance at 1 mM (P=0.01) | 2.5mM | |
| MDA-MB-231 | (11.9%) | (15.4%) | (26.3%) | (30.3%) | (30.3%) | (35.5%) | (47.5%) | P<0.001 | Achieved significance at 0.3 mM (P=0.0024) | >20mM | |
| MDA-MB-231(BM) | (27.6%) | (40%) | (52.4%) | (68.8%) | (73.8%) | (77.62%) | (77.8%) | P<0.0001 | Achieved significance at 0.03 mM (P=0.004) | 0.91mM | |

4.3.5 Assessment of the anti-survival effect of metformin using clonogenic assays

As previous studies have used clonogenic assays to investigate the effects of high doses metformin on the ability of the breast cancer cells to form colonies, it was decided to study the ability of the breast cancer cells to form colonies after exposure to the pharmacologically relevant doses of metformin using a traditional clonogenic assay. In this assay cells were exposed to various concentrations of metformin for 72hrs before being collected by gentle trypsinization and seeded onto the assay plates and incubated for 14 days before they were stained with crystal violet and the number of colonies counted. It should be noted that while the majority of the cell lines readily formed colonies, MCF10A and MCF10AT cells did not form colonies in the absence of treatment and were therefore not able to be investigated in these assays.

Metformin induced a significant reduction in colony formation in a dose-dependent manner in all cell lines tested (Figure 4.5). In contrast to the data seen with the cell counting assays, the clinically relevant doses of metformin induced a significant reduction of the reproductive capability of all invasive cell lines ($P < 0.0001$, by One-way ANOVA test). At 0.03 mM, all cell lines lost a significant percentage of their reproductive ability; DCIS.com (by 57% of the untreated control, $P < 0.0001$), MCF7 (by 39% of the untreated control, $P < 0.0019$), T47D (by 48% of the untreated control, $P < 0.0001$) and MDA-MB-231 (by 37.4% of the untreated control, $P < 0.0116$), MDA-MB-231(BM) (by 44.7% of the untreated control, $P = 0.0008$) measured by Dunnett's test.

At higher doses (10-20 mM) the colony formation ability was markedly impaired and frequently no colonies were observed (reduced to <5% as compared to the controls in all cell lines) (Figure 4.5).

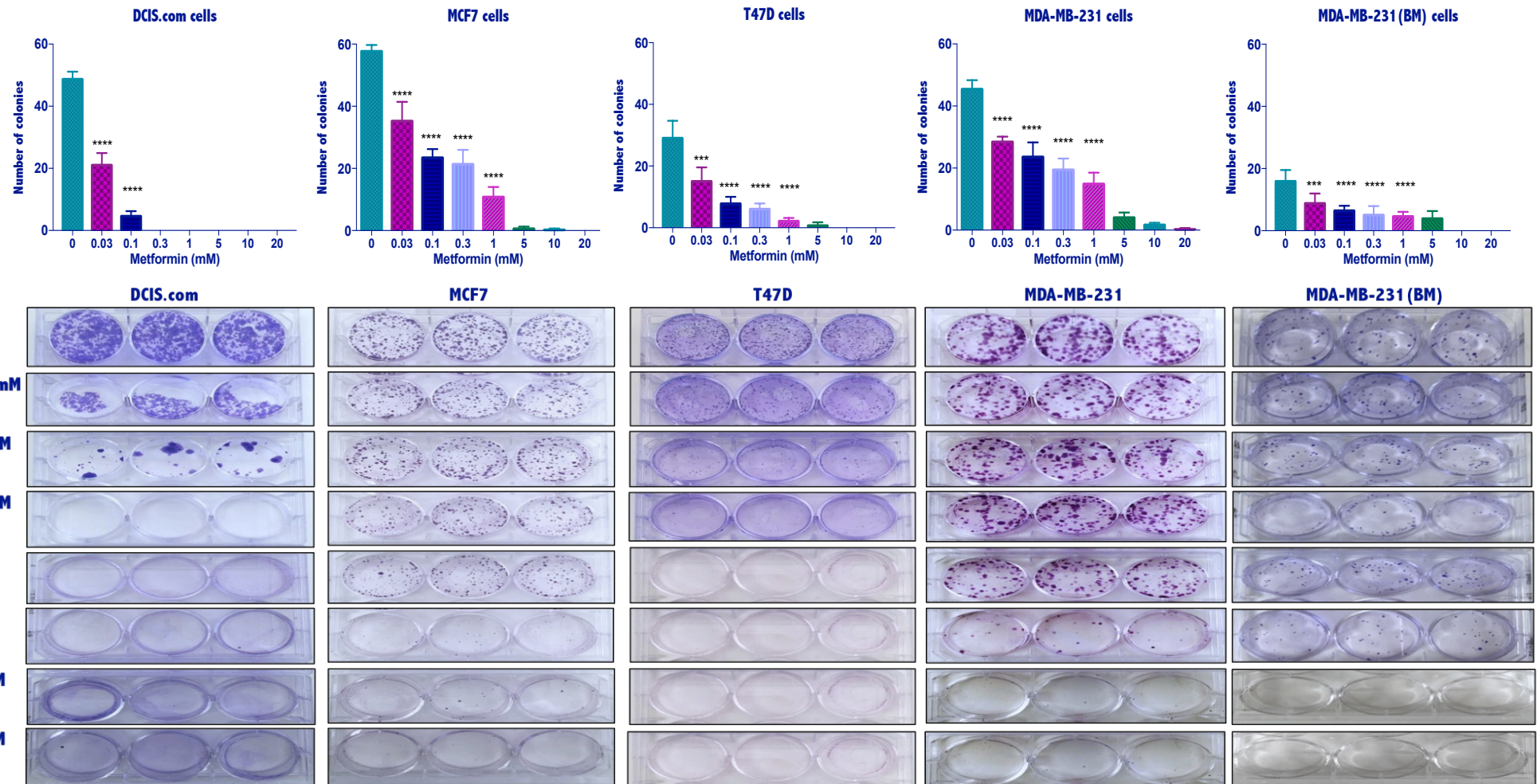


Figure 4.5: Metformin is able to significantly suppress colony formation at the lowest concentration of 0.03 mM in all cell lines tested.
The bar graphs represent the mean of 3 independent experiments +/- SD. P-value of each dose versus control was measured by Dunnett's test.
Representative pictures of the crystal-violet stained colonies were taken on day 14 using a digital camera. ***P<0.001 and ****P<0.0001.

4.3.6 The effects of metformin on cell cycle progression in breast cells

As the different assays described demonstrated an inhibition in proliferation in all the cell lines, flow cytometric cell cycle analysis was performed to determine whether the results of these proliferation assays were a reflection of cytostatic or cytotoxic effects due to cell cycle arrest or apoptosis. Since the inhibition of cellular proliferation may be mediated by the regulation of cell cycle, we examined the effect of three doses of metformin (0.3, 1 and 5 mM) on cell cycle perturbations; these were the doses that were significant in all the cell lines in most of the assays and represent both plasma and tissue achievable doses of metformin.

Compared with untreated controls, more cells had accumulated in G₀/G₁ phase in MCF10A, DCIS.com, MCF7, T47D and MDA-MB-231 cell lines after 72 hours of metformin treatment in a dose dependent manner; the higher the dose the more cells accumulated (98%, 94%, 98%, 97%, 80% at 5 mM compared to 91%, 80%, 78%, 70%, and 73% in the control cells; P<0.0001, respectively), as shown in figures 4.6 and 4.7.

In contrast, a significant reduction in the number of cells present in the G₀/G₁ phase was observed in MCF10AT cells at all tested concentrations (67%, 61% and 66% at 0.3, 1 and 5 mM, compared to 74% in the control untreated cells, P<0.0001) and there was a significant accumulation of cells in the G2/M phase at all tested doses (27%, 34% and 25%, compared to 21% in the control untreated cells, P<0.0001), as shown in figure 4.6.

In contrast to the other cell lines the MDA-MB-231(BM) cells did not show a consistent pattern with the number of cells in G0/G1 phase increased significantly when treated with 5 mM metformin (97%, compared to 73% in the control untreated cells, P<0.0001), but significantly reduced alongside a significant increase in the number of cells in G2/M phase at the 0.3 and 1 mM doses (23% and 26.6%, respectively, compared to 21% in the control untreated cells ; P<0.0001), as shown in figure 4.7.

There was no significant change in the number of S phase cells throughout all concentrations in all cell lines tested, suggesting that the cells were arrested at either

G0/G1 or G2/M phase. Importantly there were no cells in the sub-G1 phase indicating that the tested concentrations did not induce cell apoptosis.

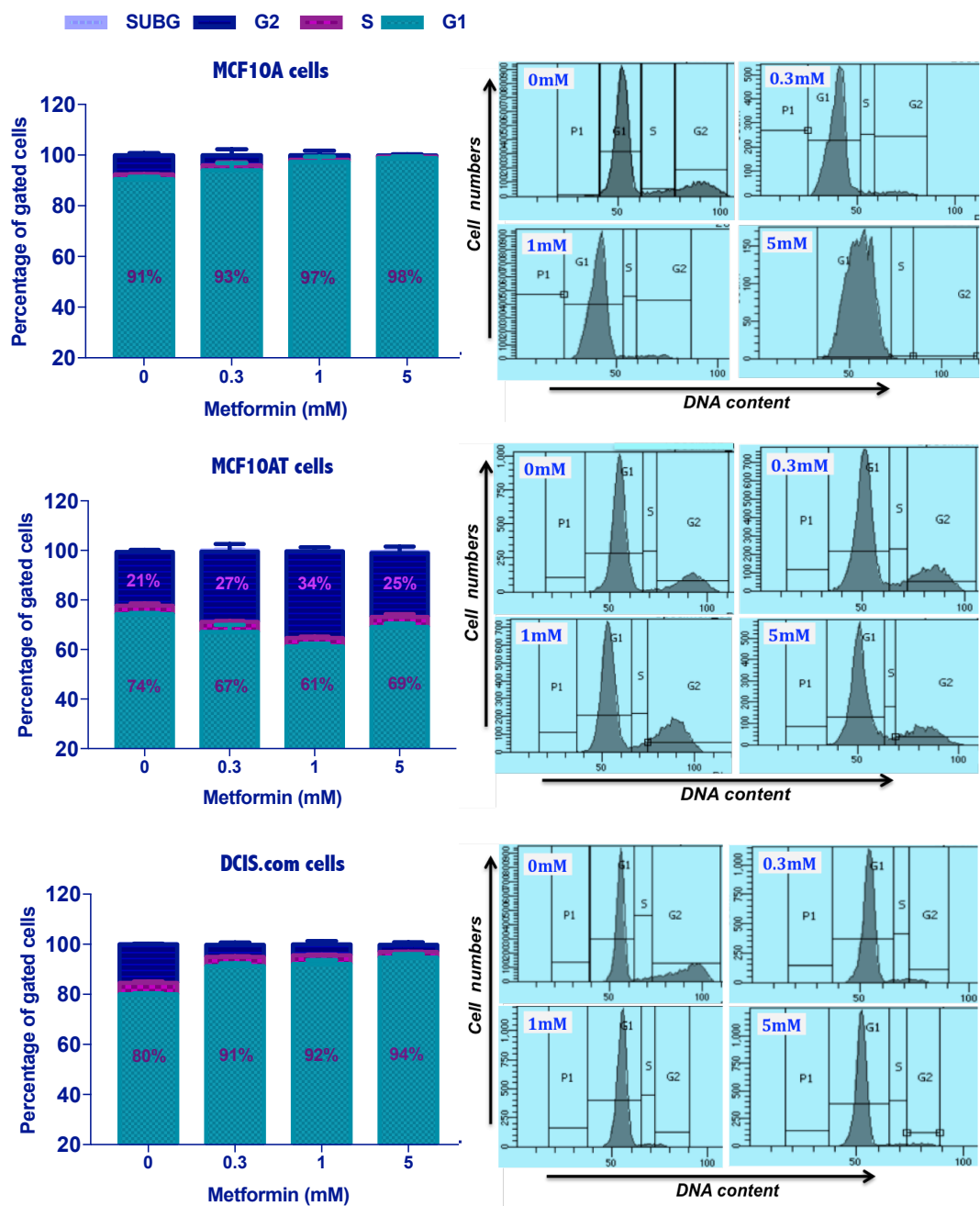


Figure 4.6: Metformin induced cell cycle arrest in the premalignant and pre-invasive breast cells.

Cells were treated with 0.3, 1 and 5 mM of metformin for 72 hours, stained with PI, and analyzed by flow cytometry. Stacked bar graphs represent the percentage of cells in each cell cycle phase for MCF10A, MCF10AT and DCIS.com cells respectively. Histograms represent the distribution of cells in each cell cycle phase; P1 represents the Sub-G1 or apoptosis phase. Data are presented as the means \pm SD from three independent experiments.

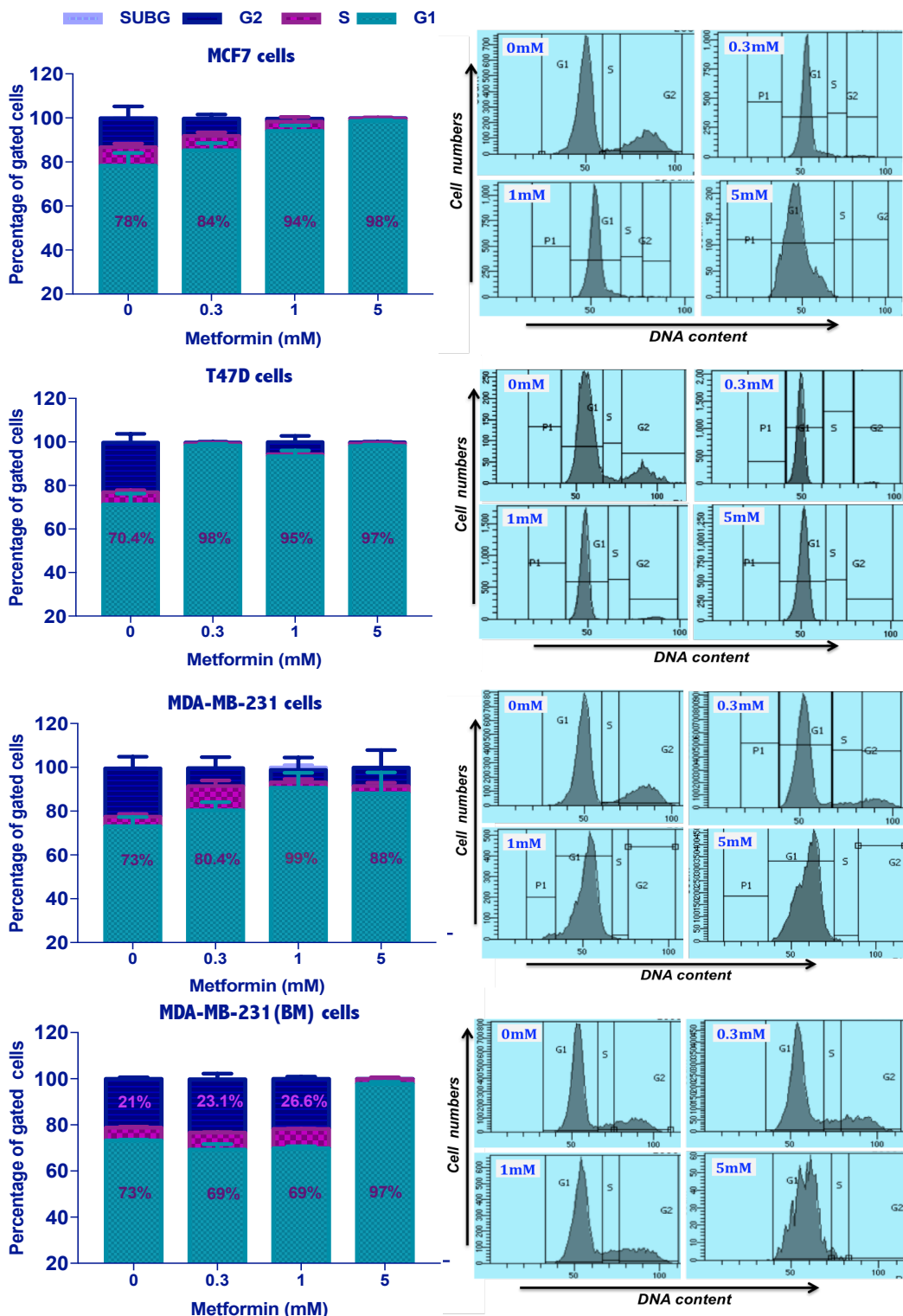


Figure 4.7: Metformin induced cell cycle arrest in the invasive and fully bone-homed breast cancer cells.

Stacked bar graphs represent the percentage of cells in each cell cycle phase for MCF7, T47D, MDA-MB-231 and MDA-MB-231(BM) cells respectively. Histograms represent the distribution of cells in each cell cycle phase. Data are presented as the means \pm SD from three independent experiments.

4.3.7 Assessment of the anti-migration effect of metformin as measured by in vitro scratch wound healing assay

To investigate the effects of the clinically relevant and potential tissue accumulation doses of metformin on cell migration; an important part of the metastasis pathway, a wound-healing assay was performed. As discussed in section 2.2.9, it was only possible to perform this experiment in the non-aggressive MCF7, less invasive T47D and the highly aggressive MDA-MB-231 human breast cancer cells, as the other cell lines did not migrate in this assay (Section 2.2.9.3).

Cells were incubated with different concentrations of metformin and their ability to fill the scratch by migration assessed over 24 hours (Figure 4.8). In all the cell lines where migration occurred, metformin doses equal to or greater than 0.03 mM caused a significant, concentration-dependent inhibition in migration, with the exception of the MDA-MB-231 cells where inhibition became significant at 0.3 mM but not 0.03 mM. The T47D cells showed a 50% inhibition in migration following 0.03 mM metformin treatment, while MCF7 cells showed a 37% decrease in migration at the same dose; compared to the untreated control cells. The migration ability of the highly metastatic MDA-MB-231 cells was reduced to 47% at 0.3 mM, compared to the untreated control cells. At the highest dose tested, 5 mM, the inhibition ranged between 50% for MCF7 cells and 60% for T47D and MDA-MB-231 cells.

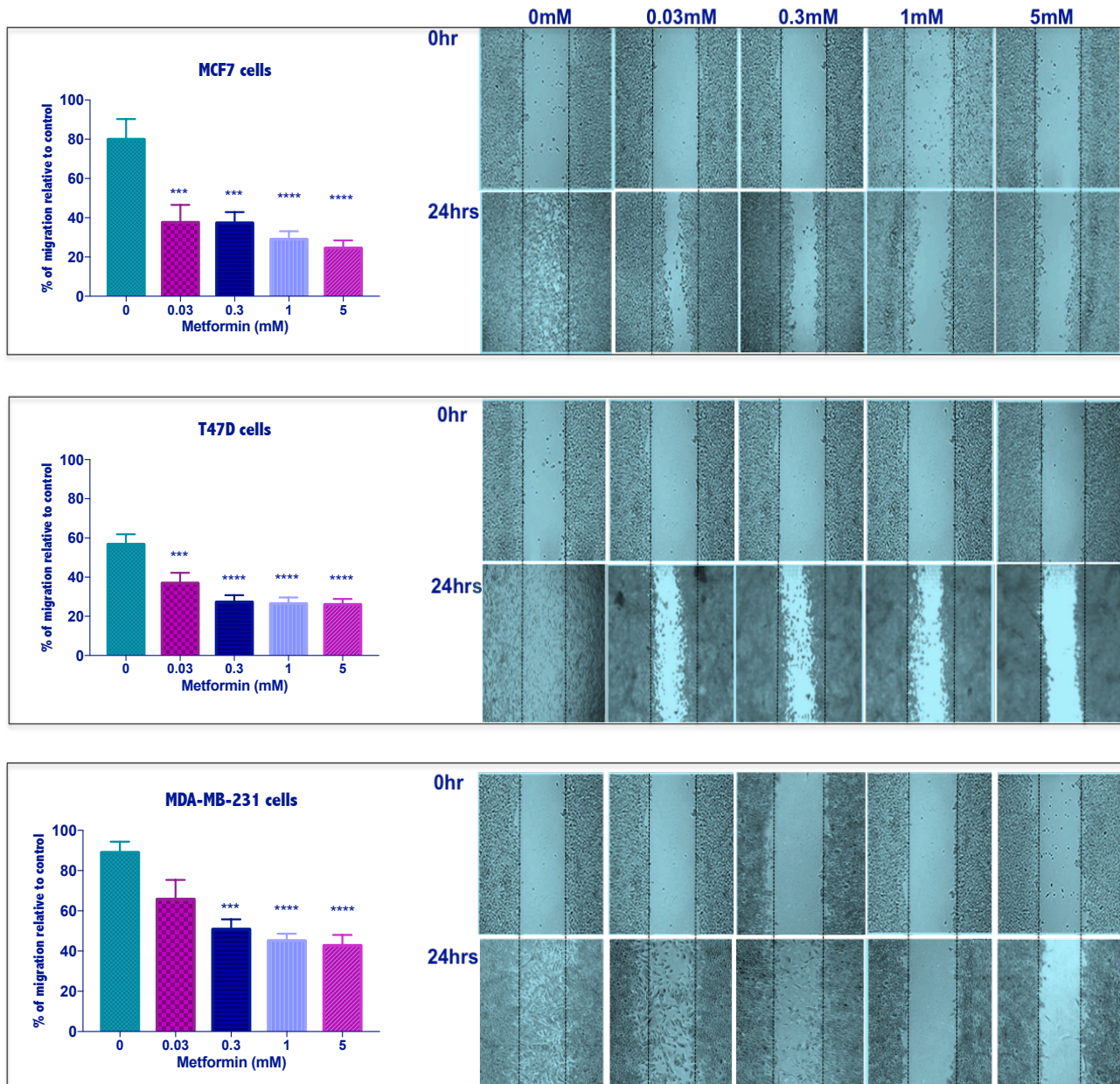


Figure 4.8: The migration of invasive breast cancer cells is reduced by metformin treatment.

Cell migration was detected by wound scratch assay. In all cell lines, untreated cells had completely closed the gap by 24 hours. The quantitative effect of metformin treatment on wound closure at 24 hours was used to compare cell motility, represented by the bar graphs. Cell migration was calculated and expressed as the percentage of migration relative to the untreated control cells. Statistical significance of differences was assessed by Dunnett's test. Values are presented as means \pm SD of three independent experiments, ***P<0.001 and ****P<0.0001. Representative wound closure images from three experiments are shown. The photographs represent images obtained at zero time, and at 24 hours after scratch formation.

4. Discussion

To date, despite strong evidence from *in vitro* studies supporting the role of metformin in treating most, if not all, molecular subtypes of breast cancer, there is no consensus regarding which molecular subtype would, more likely, respond better than others. The data demonstrate variability in proliferation and cytotoxic sensitivity between breast cancer cells in response to different concentrations and different exposure time-points. However, when reviewing the literature it becomes increasingly obvious that all the evidence about the cytotoxic effect of metformin in pre-clinical studies was obtained by exposing the *in vitro* cultured cells to supra-pharmacological concentrations of metformin (5-50 mM)^{156, 176, 177, 179, 243, 296}. Therefore, the anti-proliferative effect seen at these supra-clinical doses might be considered as a general response to metformin toxicity with no clinical value. In order to understand the anticancer mechanism of this anti-diabetic drug, it is important to clarify whether metformin can exert direct effects on breast cancer cells at the recommended clinical doses (850-2250 mg).

In the present study, six *in vitro* techniques have been used to evaluate the effects of clinically and experimentally (probable tissue accumulation concentrations) relevant doses of metformin^{244, 248, 249} on the proliferation, survival, cell cycle progression and migration of various breast cell lines. Metformin was tested at concentrations within the therapeutic range (0.03-0.3 mM) that were 10-100-fold lower than those used in most previous reports in order to overcome the limitations of those studies, as well as using higher concentrations (10-20 mM), in certain assays, to confirm the previous literature.

To account for the variability in cell culture and to enable comparison between groups of cell lines we used the same assay media for all the non-transformed, premalignant and pre-invasive cells (MEGM). Similarly, all the invasive and metastatic breast cancer cells were assayed in the same media (RPMI-1640).

Our finding that the invasive malignant breast cells doubled, on average, more slowly than the non-transformed, premalignant and pre-invasive cells, may appear surprising. However, a number of previous *in vitro* studies have shown very similar growth rates to the data shown in our study^{255, 297}. This increase in growth potential is conferred by the presence of human epidermal growth factor and cholera

toxin in the Mammary Epithelial Cell Growth Medium (MEGM) used to grow the MCF10A, MCF10AT and DCIS.com cells. The addition of EGF, hydrocortisone and insulin supplements to the MEGM assay medium is known to stimulate the growth and proliferation of the mammary epithelial cells^{298, 299}. In addition, cholera toxin is also known to increase the intracellular cyclic adenosine monophosphate (cAMP) levels caused by continuous stimulation of adenylate cyclase in the mammary epithelial cell culture system, which has a growth stimulatory effect³⁰⁰⁻³⁰². The heterogeneity of the doubling time values among the invasive malignant cells may indicate a high degree of individuality between the breast cancer subtypes, and are consistent with previous studies showing that T47D cells grow more slowly than MCF7, which grow more slowly than MDA-MB-231 cells^{303, 304}.

MTS, trypan blue and BrdU incorporation assays of viability and proliferation

One cellular metabolic assay employed in this chapter was the MTS assay to measure the cytotoxic/static effect of metformin exposure in different breast cell lines for comparison with the previous literature. In addition two alternative independent measures of viability/proliferation, that of trypan blue exclusion and BrdU incorporation, were used to directly compare the measurements obtained by MTS, as there is a theoretical risk that metformin may falsely lower the measure of viability due to mitochondrial effects which may influence the MTS results^{252, 295}. MTS assay measures cellular metabolic activity of various dehydrogenase enzymes such as NAD(P)H-dependent oxidoreductases found in the mitochondria of cells by measuring the reduction of a tetrazolium component (3-(4,5-dimethylthiazol-2-yl)-5-(3-carboxymethoxyphenyl)-2-(4-sulfophenyl)-2H-tetrazolium, inner salt) to yield a formazan product. As metformin is thought to potentially affect this and other mitochondrial enzymes, data from the MTS assay may be lowered as a result of this, rather than a decrease in the number of metabolically active cells³⁰⁵, and may therefore underestimate the cell viability. However, the tetrazolium ring is not only cleaved in the mitochondria, but it may also cleaved in the presence of non-mitochondrial pyridine nucleotide-dependent enzymes³⁰⁶, this suggests that, despite the theoretical concerns, MTS assay might still be used as a relevant metabolic measure of metformin activity. In addition to the MTS assay, the BrdU assay, which measures replicating DNA in the proliferating cells, and would not be similarly affected by metformin exposure, was also utilised. Similarly, the trypan blue

exclusion assay was utilized, but in this case as only one time point was assessed (72 hours), it was used as a measure of viability, and not specifically cellular proliferation. Trypan blue is a dye that is excluded from viable cells due to an impermeable intact plasma membrane³⁰⁷.

In the MTS assay, metformin demonstrated a time and dose dependent reduction in the metabolic activity to a greater or lesser extent after 72 hours of treatment. Interestingly our data demonstrate that actually the pre-malignant and pre-invasive cells (MCF10AT and DCIS.com) may be more responsive to metformin treatment than the invasive cancer cells. This is an interesting finding that has potential implications for clinical use of this drug. However, there is no previous literature to compare these results to, and it may simply be a result of these cells proliferating faster than the other cell lines in the absence of metformin treatment (Figure 4.1), and therefore being more metabolically active in the first place. Further work is required to assess whether proliferation rate will dictate how well cells respond to metformin.

A significant effect was observed at 72 hours following 20 mM metformin treatment in all the invasive cell lines. With regard to MCF7 cells, our findings correlate well with previous studies using both MTT¹⁸⁰ and MTS¹⁷² assays which reported the same effect at the same concentration and the same time point. However, the literature has reported inconsistent results from experiments using MDA-MB-231 cells, when assessing the effectiveness of metformin as a direct anti-cancer agent. In our MTS assay, although our data demonstrate similar findings to those reported by Wang and colleagues²⁹⁴, reported the same effect at 20 mM concentration after 72 hours, they are inconsistent with the majority of *in vitro* work that have reported that the MDA-MB-231 cells were the more responsive to the cytotoxic effects than other breast cancer cells^{152, 176, 296} using the same assays. For example, Liu and colleagues¹⁵², using MTS assay, reported a significant inhibition of metabolic activity at a dose as low as 10 mM from a range of 1-40 mM. However, in our assay we did not observe a difference between the three invasive cell lines in response to metformin. This is surprising as there was no obvious difference in the protocol used for this assay, so it may be due to confluence of the cells prior to the experimental set up (i.e. were they in the exponential phase of growth or the lag phase).

Additionally, a recent study has recently investigated the effects of clinically and experimentally relevant doses (6-30 μ M and 1000-5000 μ M) of metformin using MTT assay³⁰⁸, and showed that the reduction in both the proliferation and metabolic activity was observed at the clinically relevant doses in the MCF7 cells and at the experimental relevant concentrations at the MDA-MB-231 after 24 hours of treatment. However, in our assay we have neither observed an inhibitory effect at the 24 hours time point nor a positive effect at the mentioned concentrations after 72 hours of drug exposure. This may be attributed to the difference in the protocol as they serum starved the cells prior to the assay.

Data from the trypan blue exclusion assay further confirms the proliferation-curtailing activity of metformin after 72 hours of exposure. Consistent with the MTS data, the clinically relevant concentrations of metformin were able to reduce the survival of all the pre-malignant and pre-invasive cells. Our results demonstrate for the first time, a significant inhibitory effect on the premalignant, pre-invasive, T47D, triple negative cells and its bone homed variants at the therapeutic doses of metformin. Additionally, the MCF7 cell line has also responded to the potential tissue relevant dose of 5 mM, which although higher than the other cell lines, is lower than the previously reported doses in the literature.

The viable cell counts of T47D, MDA-MB-231 and its bone-homed variant cells were significantly reduced at 0.3 mM, whereas the MCF7 required higher doses, within the experimentally relevant range, for inhibition (5 mM). These data are in line with a study by Queiroz and colleagues who treated MCF7 cells for 24, 48 and 72 hours with single dose of metformin (10 mM) and also reported a significant inhibition of cellular growth and proliferation¹⁸⁰. In contrast to our data, a similar study by Zhuang and co-workers who used a single drug concentration (8 mM) for 3 days, demonstrated that the MDA-MB-231 were the least responsive to metformin treatment when compared to MCF7 and T47D¹⁷³. However, it was not clear in their protocols if they have renewed the metformin-containing medium every 24 hours or not as it has been recently suggested that medium renewal can block the anti-proliferative effect of metformin even if a low glucose-containing medium was used. This is because the glucose concentration in the medium is likely to be markedly reduced during a 72-hours experiment if the medium was not renewed, and therefore

the sensitivity to metformin under these conditions is likely to increase. The other key determinant of cellular response to prolonged metformin treatments besides the medium renewal protocol is the cell density that can also determine metformin sensitivity. Low cellular density cultures can be resistant to metformin treatment even if medium is not renewed, while high-density cultures consume more nutrients and have elevated rate of glucose consumption, which in turn sensitizes the cells to metformin action due to earlier glucose depletion³⁰⁹.

Despite the sensitivity of all the invasive and metastatic cells to doses lower than the supra-pharmacological doses (10-20 mM) previously reported, in terms of the cell number, survival data indicate that the viability of invasive cells was not affected even at 20 mM. In general, the viability data points towards cytostatic but not cytotoxic effects of metformin against the invasive and metastatic cells. However, there was a significant cytotoxic effect on all premalignant and pre-invasive cells, observed at all the clinically relevant doses, suggesting that these cells are more sensitive to metformin treatment. Since the viable cell count was significantly reduced at lower doses in all cells than that of the MTS assay, it appears that the MTS assay overestimated cell viability and/or failed to accurately detect the reduction in invasive cancer cells number at all tested concentrations. Therefore, an additional proliferation assay would potentially be beneficial to validate the MTS and trypan blue exclusion assay results, and therefore BrdU incorporation into all cells was measured (Figure 4.4).

After 72 hours treatment, incorporation of BrdU was reduced significantly by the clinically relevant doses in the premalignant, pre-invasive and the fully bone-homed cells. All the experimentally relevant concentrations of metformin also altered BrdU incorporation in all the pre-invasive, invasive and the fully bone-homed cells. To our knowledge, there has been no previous work in the literature using the BrdU assay to compare our data with. Collectively, as shown in figures 4.2, 4.3 and 4.4, the proliferation measured after 72 hours in the presence of 0.03-20 mM metformin is not significantly different between the three assays for the normal, pre-malignant and pre-invasive cells. However, the results were very different between the MTS and the other two assays, supporting our use of three different assays to evaluate the effects of the clinically relevant concentrations of metformin and suggesting that the MTS assay might not be the relevant assay to be used when evaluating the anti-proliferative effect

of metformin where the direct and off-target effects of metformin can result in over/underestimation of cell viability. This can be attributed to the ability of metformin to work as a weak mitochondrial “poison”, an effect that has been recently shown to be enough to reverse the resistance to tamoxifen in MCF7 cells, where the mitochondrial activity was responsible for the development of tamoxifen resistance and the use of metformin to block mitochondrial function and reversed this effect³¹⁰. Additionally, there is also the possibility that presence of phenol red in the assay medium interfered at the wavelength most suitable for the MTS formazan measurement, and this may have affected published results in the literature. This was excluded in the present study as a phenol red free media were used for this assay.

Metformin and breast cells survival

As all the previous data demonstrated that metformin inhibited cell growth a clonogenic assay was employed as an alternative method to study the effect of metformin on the survival of the pre-malignant, pre-invasive, invasive and metastatic breast cancer cells. This method involved treating the cells with metformin once, then seeding them in fresh media without metformin and not changing the media during the 14 days period. In all the breast cancer cell lines, the lowest dose of metformin (0.03 mM) had a significant effect on colony forming ability. Unlike our approach, all previous studies performed the assay by exposing the cells to fresh metformin-containing media every 72 hours for 14-21 days¹⁷². Data from previous literature using a wider range of supra-pharmacological doses (2, 10 and 50 mM) for 21 days have shown that concentrations as low as 2 mM and 5 mM inhibited colony formation in MCF7 and MDA-MB-231 respectively^{152, 172} which are in agreement with the data presented in this chapter. The clonogenic ability of T47D and the fully bone homed triple-negative cells in response to metformin has not been studied before. Thereby, we demonstrate here for the first time that colony-forming ability was markedly impaired by the clinical relevant doses of metformin and no colonies were observed at the potential tissue accumulation doses in the DCIS.com, MCF7, T47D and MDA-MB-231 and MDA-MB-231(BM) cell lines, confirming the previous proliferation data. As the clonogenicity is a property that frequently correlates with tumorigenicity, neither the MCF10A nor the MCF10AT were able to form colonies,

which is in agreement with the literature that states they cannot form colonies unless they are induced to produce colonies by expression of strong oncogenes³¹¹.

Metformin and cell cycle progression in breast cells

As the data in this chapter clearly show that proliferation is affected by metformin in all the cell lines and the effect was dose and cell line dependent, flow cytometry was used to characterize the cell cycle progression and establish whether metformin caused cell cycle arrest. The data indicate that both clinically and experimentally relevant doses of metformin arrest the cell cycle in the G0/G1 phase, thus inhibiting the proliferation of the pre-invasive and invasive breast cancer cells, suggesting that the growth inhibitory effects of metformin on the all cell lines tested might be caused by induction of cell cycle arrest rather than cell death. A different pattern of cell cycle arrest was observed in the MCF10AT and MDA-MB-231(BM) cells with cells accumulating mostly in the G2/M phase. These data are in agreement with previous studies, which demonstrated that the anticancer property of metformin is a consequence of cell cycle perturbation and that exposure to metformin induced cell cycle arrest in G0/G1 and G2/M phases in different cancer types, including breast cancer. Indeed, several studies reported similar pattern of cell cycle arrest in the invasive breast cancer cells (MCF7 and MDA-MB-231) at supra-pharmacological concentrations^{172, 173, 179, 180} although none of the studies have looked at pharmacologically relevant concentrations. As several other studies have demonstrated that the effects of metformin on cell cycle were mediated by the activation of AMPK and inhibition of mTOR signalling pathway in several human cancer cell lines including the breast^{177, 182, 185, 188, 190, 296, 312, 313}, we have not further evaluated the mechanism of action as the main focus of this project was to confirm the end result and explore if the phenotypic effect would occur at lower doses than those previously investigated. It is noteworthy however that although there was no sub-G₀ cell population suggesting that metformin did not induce apoptosis, future studies could include flow cytometric analysis using annexin-V to confirm the absence of cell death; by measuring both apoptosis and necrosis.

Metformin and tumour cell migration

Cellular migration is a crucial initial stage in the breast cancer metastatic process which is associated with a loss of cell–cell adhesion, increased migration as well as invasion of cancer cells. This study demonstrated that clinical and potential tissue accumulation doses of metformin suppressed the migration of the three invasive breast cancer cell lines (MCF7, T47D and MDA-MB-231). This finding suggests that the clinical doses of metformin might be considered in preventing the invasion and metastasis of some subtypes of malignant breast tumours. Our findings might add to and expand the results of a recent study by Zhang and colleagues where metformin treatment for 48 hours significantly inhibited the migration of MCF7, T47D and MDA-MB-231 at a concentration of 5 mM, 10 mM and 20 mM³¹⁴. However, our findings are not directly comparable with Zhang's study where a different migration assay was used, namely the Boyden transwell chamber, as well as prolonged time points (48 hours) and supra-pharmacological doses of metformin.

Our findings that the non-tumorigenic mammary epithelial cells (MCF-10A), the hyperplastic MCF10AT and the pre-invasive DCIS.com do not migrate is in line with their reported lack of invasive and metastatic capacity and their expression of high levels of the epithelial biomarker E-cadherin³¹⁵⁻³¹⁸. At the same time, cells with the highest colony-forming ability such as MDA-MB-231 are characterized by low expression of E-cadherin, which promote their migratory and invasive capacity. Furthermore, the inability of the bone-homed cells to migrate is consistent with a previous report showing that the MDA-MB-231(BM) cells exhibited significantly decreased migration in a wound-healing assay compared with the parental MDA-MB-231 cells suggesting that the alterations between the parental and bone-homing variants of MDA-MB-231 cells are likely to be clinically relevant to breast cancer patients²⁵⁶.

In conclusion, the data show for the first time that metformin treatment at clinically relevant doses inhibits proliferation via cell cycle arrest in breast epithelial cells, hyperplastic, pre-invasive (DCIS.com), invasive and metastatic breast cancer cells regardless of their receptor status and aggressiveness.

These data therefore give further support to the theory that metformin can directly affect the phenotype of human breast cancer cells. Moreover, the data demonstrate that metformin can inhibit migration of the invasive breast cancer cells, suggesting that metformin may potentially inhibit breast cancer invasion and metastasis. Interestingly, unlike other commonly used therapeutic drugs, metformin does not appear to exhibit a direct cytotoxic effect against the breast cancer cells, although it does against the pre-malignant cell line.

The data also suggest a strong effect against the pre-malignant and the pre-invasive cells, a finding that might correlate well with the findings arising from the observational studies in diabetic populations showing lower incidence of breast cancer in patients on long-term metformin treatment. However, in order to confirm this a transgenic mouse model would need to be employed whereby mice are treated with metformin from an early age and the age of onset of mammary cancer is established compared to those which are not treated.

To correlate between cellular response to metformin and the expression of cation-selective transporters, this study demonstrated that the triple negative BC cells (MDA-MB-231) express all the relevant transporters but is still less responsive to the effect of clinically relevant doses of metformin when compared to the DCIS.com; the most responsive cell line in all our *in vitro* assays in which PMAT was the predominant influx transporter; suggesting that metformin action does not solely rely on the transporter expression and its intra-cellular accumulation but several other factors are involved in the differential response, which include genetic variability, the dosage used, duration of treatment and the presence of competent LKB1/AMPK pathway in these cells; AMPK pathway was reported to be incompetent in the MDA-MB-231 due to an intrinsic deficiency in LKB1 kinase thus attenuating the anti-proliferative effect of metformin²⁰⁶. The data also emphasize that one needs to use caution in choosing a relevant *in vitro* cell model for investigating anticancer efficacy of metformin whose uptake is transporter-mediated and its action is LKB1-dependent.

However, another interesting extension to the assays used in this chapter is by culturing the breast cancer cells in 3D (eg spheroids constructed from immortal breast cell lines) and determine how this will impact on toxicity and other data. Once this was achieved, the IC₅₀ for metformin can be determined to evaluate whether the values obtained using 3D spheroids could be compared with those obtained *in vitro* in the classical proliferation assays used and with *in vivo* observations published elsewhere in the literature. This would represent a more clinically relevant assay; than the *in vitro* assays used in this project, to screen the effect of the clinically relevant doses of metformin.

In this chapter, we found that the parental MDA-MB-231 cells and its metastatic bone-homed variant were the most sensitive to the clinical doses of metformin of the invasive cell lines, however, the pre-invasive and pre-malignant cell lines were more sensitive. Although the ductal carcinoma *in situ* (DCIS) represents 20–25% of all breast neoplastic lesions, it is currently cured by complete surgical resection and the majority of the pre-cancerous and pre-invasive lesions will never progress to an invasive disease. In contrast, the triple negative breast tumours are more aggressive and harder to treat. Also, they are more likely to spread and recur and therefore identifying a new better treatment for these patients may be advantageous and is urgently needed. Thus, the next chapter will now focus on these cells (MDA-MB-231 and MDA-MB-231(BM)) in particular to profile the global proteomic response to metformin treatment.

5. Chapter 5: Comparative proteomic analysis of differentially-expressed proteins in response to metformin in metastatic breast cancer cell lines

5.1 Introduction

Data presented in the previous chapter demonstrate that although the clinically relevant doses of metformin were more efficacious against the normal epithelial, premalignant and pre-invasive cell lines, the triple negative MDA-MB-231 cells and their bone-seeking variant were the most sensitive of the invasive breast cancer cell lines to the anti-proliferative effect of these doses. Our data also suggest that the effects of metformin on parental MDA-MB-231 are distinct from the bone-homing metastatic cells. Indeed, metformin inhibits the migration of the wild-type triple-negative cells and reduces the number of viable cells as well as the BrdU-labelled cells at the highest dose in the clinically relevant range (0.3 mM), whereas the bone-homing cells were more responsive to doses as low as 0.03 mM and 0.1 mM in the cell counting and BrdU assays respectively. Metformin also induces G1 and G2 cell cycle arrest without apoptosis in the wild-type and the bone-homing cells respectively, at 0.3 mM. However, both cells were equally responsive to the lowest dose of 0.03 mM in the clonogenic assay. This indicates that both cells are differentially responding to metformin exposure.

Triple-negative/basal breast cancers (TNBCs) occur in a minority of patients compared with other molecular subtypes of breast cancer (15%), however, despite this fact triple-negative tumours are particularly aggressive and result in a disproportionately high morbidity and mortality due to their rapid proliferation rate, high metastatic potential and frequent chemo-resistance³¹⁹⁻³²¹. While triple negative cancers fail to express oestrogen, progesterone or HER-2 receptors, they express basal cytokeratins and the epidermal growth factor receptor (EGFR) and have a predominant subpopulation of stem-like cells or mesenchymal features and the latter feature would enhance tumour cell dormancy and therapeutic resistance³²². TNBCs are also known for some unique features, which include p53 mutations, activation of the cell surface receptor tyrosine kinase EGFR, up-regulation of interleukin-6 (IL6) expression and janus kinase-2/signal transducer and activator of transcription 3 (JAK2/STAT3) signalling pathways, as well as their dependence on both aerobic

and anaerobic glycolysis to derive energy and sustain cell growth (the Warburg effect)^{323, 324}.

Distant relapse remains a substantial risk for patients with all types of BC, with >75% of advanced breast cancer patients developing bone metastasis, resulting in skeletal complications which have a major negative impact on survival and quality of life, as well as incurring a high economic burden. Bone targeted agents such as the bisphosphonate drugs including zoledronic acid, and monoclonal antibody-based therapeutics (e.g Denosumab), have reduced the incidence of skeletal-related events (SREs) within BC patients, however these treatments are not without side-effects and only a proportion of patients will benefit³²⁵⁻³²⁷. In contrast to bone metastasis that occurs more frequently in patients with ER-positive tumours, lung metastasis; the second most frequent site for BC relapse, is more frequently diagnosed in patients with ER-negative tumours. Thus far, there remains a significant unmet clinical need to develop effective, safe and more specific systemic therapy options for the prevention and treatment of metastatic bone and lung spread, and in particular for the development of biomarkers that will predict those patients at highest risk of developing relapse. Current technological advances in the fields of genomics, proteomics and metabolomics approaches can potentially provide a major contribution to meeting this need by identifying novel target molecules as well as new therapeutic options.

Although the anti-cancer properties of metformin have been well-studied and it is now well known that metformin acts on cell metabolism and suppresses breast cancer cell proliferation by a number of different mechanisms, including cell-growth inhibition mediated via effects on IGF1 and downstream PI3K/AKT/AMPK signalling pathways, other mechanisms may also occur, including direct modulation of protein synthesis. To date there have been few studies of the global proteomic effects of metformin within TNBC. To our knowledge no previous attempt has been made to explore the global proteomic effects of metformin exploring whether metformin plays a potential therapeutic role in BC metastasis particularly to bone and lung.

Therefore, we hypothesize that metformin might have a potential anti-metastatic effect within breast cancer via differential targeting of signalling pathways,

or altering protein expression differentially between the wild-type triple negative and the two aggressive end-stage bone- and lung-derived breast cancer cell lines.

In this project, we had a useful opportunity to test our hypothesis by comparing the effects of metformin on the proteome of the relevant metastatic breast cancer cell models. This work has potential to not only identify possible biomarkers of metformin action but also to identify possible drug targets of interest within breast cancer metastatic spread. The spike-in SILAC method is suitable for this type of experiment and this method has been successfully used before for proteomics-based identification of biomarkers of bone-metastasis within the laboratory of Professor Janet Brown^{256, 328-330}. The major aim of this study was to identify additional unknown mechanisms by which metformin impacts metastatic breast cancer cell lines and to validate these changes by Western blot in metformin treated and untreated cells.

A three-cell line experiment was conducted utilising three biological replicates of each cell-type using heavy SILAC-labelled parental MDA-MB-231 as an overall control.

5.2 Methods

5.2.1 Label-free quantification (LFQ) proteomics

An initial small-scale pilot experiment testing the effect of both the clinically relevant (0.3 mM) and the potential tissue accumulated (5 mM) doses of metformin on the 'parental' MDA-MB-231 (PCC) cells and the fully bone-homed variant (MDA-MB-231(BM)) was carried out using a label-free quantification method. This small experiment was designed to assess any evidence of change in protein expression profiles in response to the different metformin doses to establish whether or not a subsequent proteomics experiment should be based on the clinically relevant or the potential tissue accumulated dose of metformin. The proposed larger proteomics experiment involved the use of the 'spike-in' SILAC method analysing PCC, bone- and lung-homed breast cancer cell types with and without the chosen dosage of metformin to enable comparison of protein expression across multiple replicates. For the initial pilot experiment, the following samples were generated, without sample mixing or isotopic labelling, where the cells were treated with the stated doses of metformin for 72 hours.

- PCC no drug (control)
- PCC + 0.3 mM of metformin
- PCC + 5 mM of metformin
- MDA-MB-231(BM) no drug
- MDA-MB-231(BM) + 0.3 mM of metformin
- MDA-MB-231(BM) + 5 mM of metformin

Samples were run into the top of a 4-20% SDS-PAGE gradient gel (For a maximum 20 minutes running time), to concentrate the protein samples into one tight band, in order to aid subsequent buffer exchange steps. The samples were then digested and processed as per figure 5.1 (Sample preparation workflow, without the heavy and light-labelled mixing step) and figure 5.2 (Experiment 1), the extracted tryptic peptides were sent for mass-spec analysis and label-free quantification (using 1 µg of peptide injections per run and duplicate injections performed for each sample to ensure greater confidence with the MS-based identifications and quantifications). Dr. Caroline Evans operated the mass spectrometer in a data dependent acquisition mode (DDA) as follows: liquid chromatography (LC) peptide separation was coupled online to MS using a data-dependent LFQ method on a Q Exactive™ HF hybrid quadrupole-Orbitrap mass spectrometer. Full-scan MS spectra (375-1500 m/z) were acquired at a resolution of 120,000 after accumulation to an automated gain control (AGC) target value of 1e6 or maximum injection time of 60 ms. MS2 spectra were obtained at a resolution of 30,000, with an AGC target value of 1e5 or maximum injection time of 60 ms. Higher-energy C-trap dissociation (HCD) was performed with a normalised collision energy of 27 and an underfill ratio of 2%. Dynamic exclusion was set to 20 s, charge state screening was enabled and unassigned charge states and singly charged precursors were excluded. MS performance was verified by running complex cell lysate quality, 400ng Hela protein digest (Pierce, P/N 88328 for quality control). The downstream data analysis steps were performed as described in the data analysis workflow in figure 5.1.

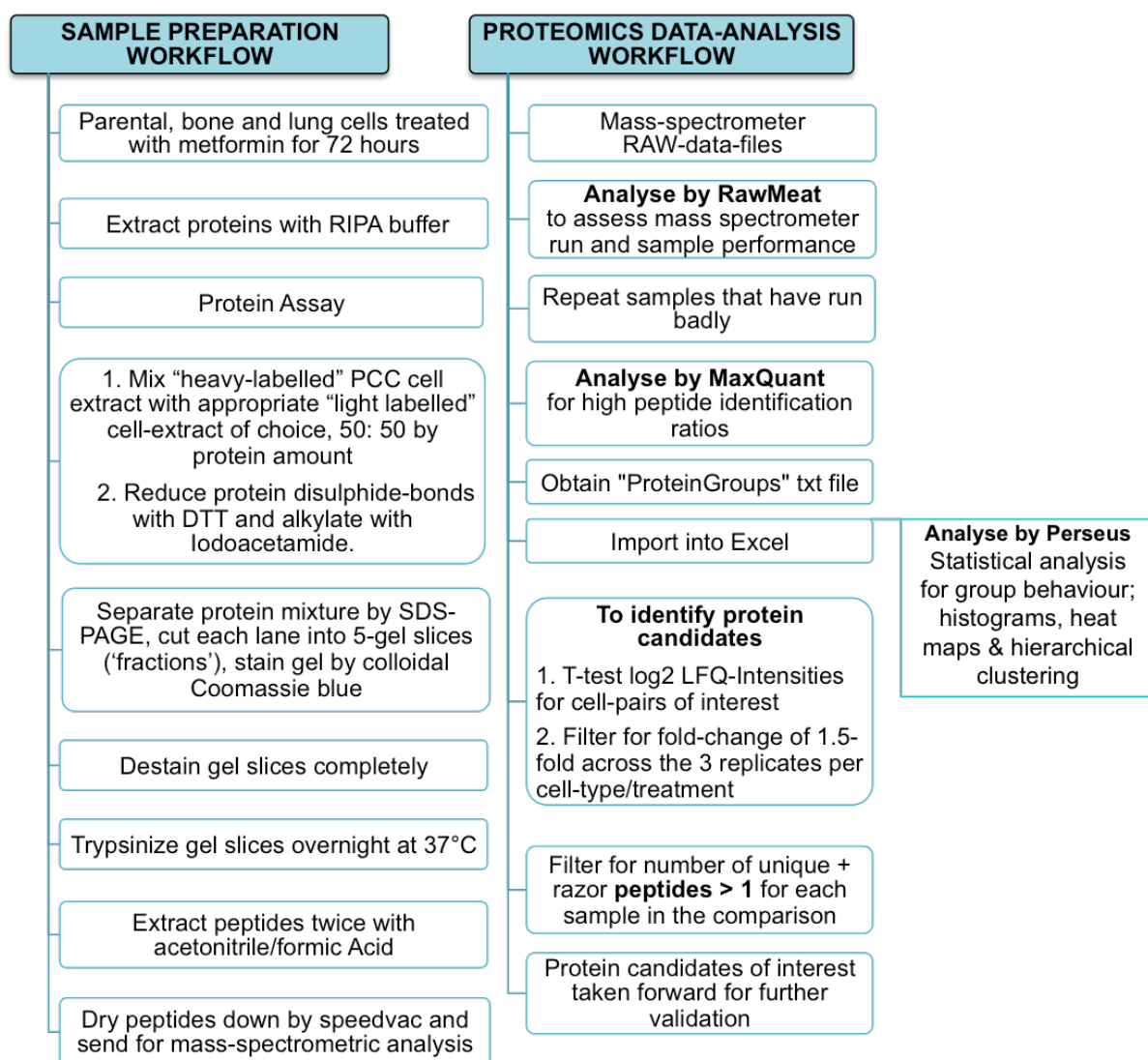


Figure 5.1: Schematic workflow of the mass spectrometry method.

Illustration of the experimental procedures: sample preparation and data analysis workflow.

5.2.2 SILAC-based quantitative proteomics

Metastatic variants of the human triple negative breast cancer cell (TNBC) line MDA-MB-231 which home to bone (BM) or lung (LM) produced by repeated intra-cardiac injection within an immunocompromised mouse²⁵⁷, were used alongside the parental MDA-MB-231 (PCC) cells. The parental PCC cells and the different metastatic variants were then used to explore differences in the proteomes between metformin-treated and untreated cells, and to identify any differences to metformin treatment between the cell lines. The idea is that analysis of the cellular proteomes would allow to infer network information that may complement the previous work in this thesis on the efficacy of metformin, the expression of metformin transporters, and any published literature on cellular mechanisms of action of metformin in triple negative breast cancer and their metastases.

Based on preliminary data from our small-scale experiment (Section 5.3.1.2), a 5 mM concentration of metformin was chosen as the validated test concentration. To account for any technical and biological variability within the cell system studied, for each cell type, three aliquots of a frozen stock were revived and cultured independently. Differential protein expression between the three independent cultures of these three cell lines was quantified by concentrating the proteins present within cell-lysates using SDS-PAGE followed by in-gel tryptic digestion and protein identification using an orbitrap-mass spectrometer (gel-LC-MS/MS) (Figure 5.1, Sample preparation workflow).

Comparative quantitative analysis of global-protein expression between the replicate cultures was facilitated by use of the spike-in-SILAC (SIS) method^{328, 329}, since it offers accurate and sensitive quantification of protein expression between replicate samples via the use of a spike-in heavy-labelled internal standard sample. Spike-in SILAC is also a cost-effective way to enable comparison of the 5 treatment combinations in 3 biological replicates. The use of triplicate biological repeats is a common approach used within the proteomics analysis of cell-lines as these display lower variability than patient-derived biological samples such as blood and urine. We analysed 15 samples in total, each containing 50 microgram of total protein pooled from each group (i.e. 25 µg of control (P-SIS) protein and 25 µg of metformin treated

protein). Three independent cultures from each of the cell lines/treatment combinations of 2-6 were used, as listed below (See figure 5.2 for the experimental setup).

| | |
|--------------------------|---|
| 1. P-SIS | Parental cell line cultured in ‘heavy’ SILAC medium |
| 2. PCC+5 mM of Metformin | Parental cells treated with metformin |
| 3. BM | Bone-homed variant of MDA-MB-231 |
| 4. BM+5 mM of Metformin | Bone-homed variant of MDA-MB-231 (treated) |
| 5. LM | Lung-homed variant of MDA-MB-231 |
| 6. LM+5 mM of Metformin | Lung-homed variant of MDA-MB-231 (treated) |

All cell lines (except P-SIS) were grown in standard “light; isotopically normal” (Lys0) (SILAC-control) medium containing 10% dialyzed FBS, 2 mM L-glutamine, 0.1mg/mL streptomycin and 0.2U/ml penicillin. The parental cell line (PCC) was grown in “heavy” SILAC medium Containing ¹³C and ¹⁵N-labelled variants of Lysine and Arginine, 10% dialyzed FBS, 2 mM L-glutamine, 0.1mg/mL streptomycin and 0.2U/ml penicillin, for at least six cell-doublings prior to use, so that the cells fully incorporated the labelled amino acids. When the cells have been passaged this way they are ready for treatment with metformin for 72 hours.

After metformin exposure, the protein samples were prepared in standard RIPA lysis buffer, homogenized and cleared of nuclei and cellular debris by centrifugation as described previously (Section 2.2.8), and assayed for protein content using the BCA protein assay kit. Protein extracts thus prepared were mixed with the heavy-labelled PCC-protein sample and the proteins from each of the light labelled samples forming a 1:1 mix (Summarized in table 5.1). The protein samples were then reduced with 10 mM dithiothreitol (DTT) (0.1 M final concentration) for 5 minutes at 60°C. Reduced cysteines were then alkylated with 50 mM iodoacetamide (IAA) (10 mM final concentration) by incubation for 30 minutes at room temperature in the dark, as the IAA is light sensitive.

The combined samples were run on a 4-20% SDS-PAGE gradient gel for approximately 45 minutes until the dye front reached the end of the gel. The gels were briefly stained with colloidal coomassie-G250 brilliant blue gel-stain for the shortest amount of time which allowed protein visualization, and then the concentrated gel-

bands from each lane were individually excised into 5 equal slices with a scalpel and each slice cut into cubes (approximately 1mm³). All gels were kept hydrated with distilled water to prevent shrinkage during cutting.

The proteins within the cubes obtained from each gel slice were once again reduced with DTT and alkylated with IAA to ensure complete reaction followed by extensive gel-destaining with 50 mM ammonium bicarbonate, 50% (v/v) acetonitrile (ACN) and vortexed briefly, to get rid of the negatively charged coomassie blue dye that can interfere with trypsin digestion, followed by gel-dehydration with acetonitrile. The reduced, alkylated, destained and dehydrated gel-cubes were then subjected to overnight tryptic digestion using a 1:25 trypsin:protein ratio.

The following day peptides were extracted twice from the gel cubes using sequential treatment with 1% (v/v) formic acid (FA) and acetonitrile and the combined extracts dried down for mass-spectrometric analysis using a speedvac concentrator. The dried down peptides were stored at -80°C. Individual samples were then analysed using the orbitrap-mass spectrometer using triplicate injections of each sample.

Table 5.1: An illustration of the sample mixing.

Five cell line/treatment combinations samples prepared by mixing with an equal concentration of the spike-in SILAC control cell protein.

| Sample number | Heavy-labelled sample (25 microgram) | Light-labelled sample (25 microgram) |
|---------------|--------------------------------------|--------------------------------------|
| 1. | SILAC-labelled PCC | PCC+ 5mM metformin |
| 2. | SILAC-labelled PCC | Untreated BM |
| 3. | SILAC-labelled PCC | BM+ 5mM metformin |
| 4. | SILAC-labelled PCC | Untreated LM |
| 5. | SILAC-labelled PCC | LM+ 5mM metformin |
| 6. | SILAC-labelled PCC | PCC+ 5mM metformin |
| 7. | SILAC-labelled PCC | Untreated BM |
| 8. | SILAC-labelled PCC | BM+ 5mM metformin |
| 9. | SILAC-labelled PCC | Untreated LM |
| 10. | SILAC-labelled PCC | LM+ 5mM metformin |
| 11. | SILAC-labelled PCC | PCC+ 5mM metformin |
| 12. | SILAC-labelled PCC | Untreated BM |
| 13. | SILAC-labelled PCC | BM+ 5mM metformin |
| 14. | SILAC-labelled PCC | Untreated LM |
| 15. | SILAC-labelled PCC | LM + 5mM metformin |

Dr. Caroline Evans performed the mass spectrometry as follows: A U3000 nano-flow high performance chromatography system (Thermo, Hemel Hempstead, UK) was employed with peptide separation using a 50cm C18 reverse-phase analytical column (Thermo Easy-spray P/N ES803) at 40 °C. A 300µm i.d x 5cm trap column packed with C18, 5µm, 100 Å particles (LC Packings P/N 160454) was used for sample loading. The buffers used were loading buffer (97% (v/v) water, 3 % (v/v) acetonitrile with 0.1% (v/v) trifluoroacetic acid (TFA)), buffer A (100% (v/v) water, 0.1% (v/v) FA) and buffer B (80% (v/v) acetonitrile, 20% (v/v) water with 0.1% (v/v) FA). Peptides were eluted over 3-10% buffer A for 30 minutes, then 10 to 50% buffer B gradient over 75 minutes for a total run time of 105 minutes.

The mass spectrometer was operated in a data dependent acquisition mode (DDA) as follows: LC peptide separation was coupled online to MS using a data-dependent Top15 method on a Q Exactive™ HF hybrid quadrupole-Orbitrap mass spectrometer (Thermo Scientific, Bremen, Germany). Full-scan MS spectra (375-1500 m/z) were acquired at a resolution of 120,000 after accumulation to an automated gain control (AGC) target value of 1e6 or maximum injection time of 60 ms. MS2 spectra were obtained at a resolution of 30,000, with an AGC target value of 1e6 or maximum injection time of 60ms. Higher-energy C-trap dissociation (HCD) was performed with a normalised collision energy of 27 and an underfill ratio of 2%. Dynamic exclusion was set to 20 seconds, charge state screening was enabled and unassigned charge states and singly charged precursors were excluded. MS performance was verified by running complex cell lysate quality; 400 ng Hela protein digest (Pierce, P/N 88328 for quality control).

5.2.3 Data analysis and statistical methods

Proteins within the final data set were prioritized as follows: proteins were selected which had at least 1 razor and unique peptide within all 5 samples in a replicate (i.e the 5 gel slices of each individual lane); this ensures high quality mass-spectrometric protein identifications across each sample set to be analysed. A razor peptide is a peptide that has been assigned to the protein group with the largest number of total peptides identified, if unique, the razor peptide only matches to this single protein group and if not unique, the razor peptide will only be a razor peptide for the group with the largest number of peptide IDs.

Proteins were then selected based upon a significant fold change within the light labelled cells compared to the heavy-labelled PCC-cells (light labelled / PCC = 1.5-fold or greater for increased expression or 0.7-fold or lower for decreased expression); these are standard cut-offs used to define up and down-regulated proteins within discovery proteomic experiments (reference).

The LFQ-intensity of the light peptide in each sample was normalized to the intensity of the identical heavy-labelled peptide spiked in as an internal standard within the sample, for the LFQ experiment the LFQ-intensity of the treated samples were normalized to the intensity of the control untreated samples. Upon Log2 transformation of these normalised LFQ-intensities a two-tailed parametric t-test was used to assess the statistical significance of any difference in expression observed across the three replicate injections of each sample. Proteins which survived these tests with a statistically significant difference in log2-LFQ-Intensity between metformin-treated bone or lung metastatic cell lines and the heavy-labelled control cell line (PCC), were assessed for relevance in breast cancer and/or bone/lung metastasis using published literature. The relevant protein candidates were then taken forward for verification by Western blotting (Figure 5.1, Data analysis workflow).

5.2.4 Determination of the labelling efficiency with heavy-SILAC-labelled MDA-MB-231

In order to test the quantitative accuracy of mass spectrometry for quantification of SILAC- labelled proteins, it was necessary to determine the percentage incorporation of heavy L-¹³C₆¹⁵N₄-arginine and L-¹³C₆¹⁵N₂-lysine into proteins synthesized in the MDA-MB-231 parental cell line, an important quality control step for checking the efficiency of cell labelling. Proteins from control MDA-MB-231 cells grown in labelling medium were tested for efficiency of incorporation of stable isotope-labelled amino acids after 6 doublings (following the same sample preparation and data analysis workflow in figure 5.1). We found that within all proteins the proteins identified from whole cell lysates significantly greater than 93% levels of label incorporation were achieved. However, the fact that some very stable proteins have slow turnover within the cell and their replacement by heavy-labelled versions during the SILAC-labelling may not have been complete may account for the 7% poorly labelled proteins found.

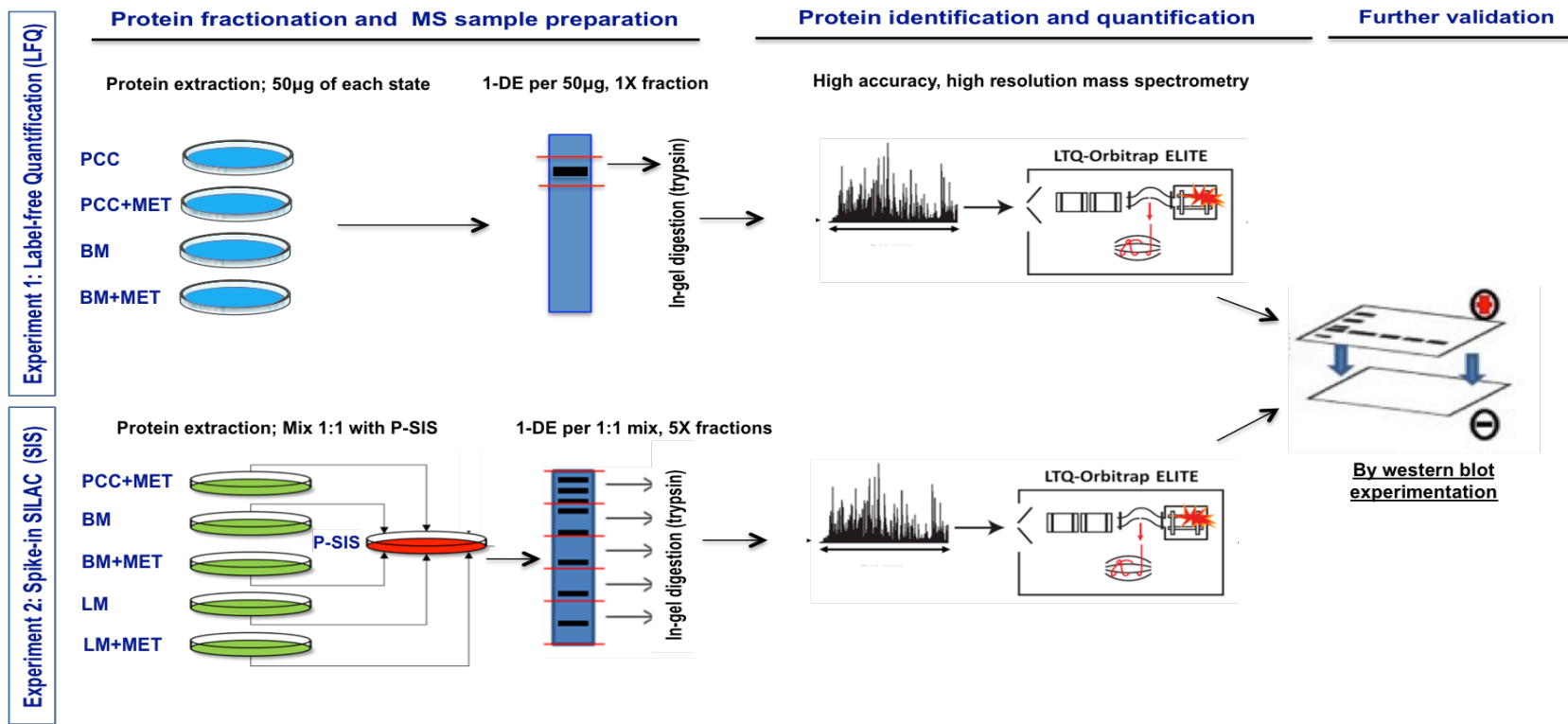


Figure 5.2: Schematic depiction of the experimental setup and subsequent workflow used for proteomic analysis of cell lines of interest.

Two separate experiments were conducted in the current study. In experiment 1, proteins from cells grown in standard culture media were extracted, concentrated briefly on 1D 4-20% gradient gel, digested, and subsequently analysed by LC-MS/MS. In experiment 2, proteins were extracted from both heavy-labelled spike-in SILAC standard and the light-labelled cells for comparison. Proteins from cells grown only in $^{13}\text{C}_6$ $^{15}\text{N}_4$ -Arginine and $^{13}\text{C}_6$ -Lysine containing medium, were mixed 1:1 (25 µg:25 µg) with proteins extracted from the cell lines of interest. Each 1:1 protein sample mix was separated according to molecular weight by 1-DE SDS-PAGE. The entire 1-D gel lane was fractionated into five equal ‘slices’, and the proteins within each slice were digested using trypsin before peptides were extracted from the gel matrix. The five-peptide samples for each 1:1 protein mix were subsequently analysed using mass spectrometry (MS). PCC: Parental MDA-MB-231 cell line, BM and LM bone and lung-seeking metastatic cell lines.

5.3 Results

5.3.1 Metformin action- label free quantification; proteomics pilot-experiment

5.3.1.1 Label free quantification's data correlation and quality check

Prior to protein identification and quantification by MaxQuant the mass-spec RAW files were first analysed via the RawMeat software package (freeware: <http://rawmeat.software.informer.com/2.0/>). RawMeat is used to compare the LC-MS run quality so poor or aberrant runs can have samples re-injected. Key parameters from the RawMeat analysis include “TopN” (the number of MS/MS scans triggered during each MS time window and thus the number of co-eluting peptides which the mass spectrometer can attempt to sequence and quantify). Next, RAW files were then analysed using MaxQuant for spectral alignment, normalization, peak matching, protein-identification and label-free quantification. MaxQuant-analysis provides many data outputs. The stated label-free quantification (LFQ) value for each identified protein was used as this is considered to be the most robust, quality controlled and normalized value for protein quantification provided by the analysis software. Once the LFQ-intensities were log2-transformed and valid protein entries were filtered for number of unique and razor peptides, the degree of correlation was estimated between the different samples to illustrate the reproducibility of the replicate samples and to eliminate possible outliers.

Then the outputted “ProteinGroups”.txt file from MaxQuant was analysed using the Perseus software package for statistical analysis of samples in terms of their group behaviour and large-scale data structure, including output of histograms, heat maps and hierarchical clustering identification (freeware available from the MaxPlanck Institute; <http://www.biochem.mpg.de/5111810/perseus>). The results of this quality check are presented in figure 5.3.

In this pilot study, none of our samples had to be re-injected. The three different bone-homing samples cluster together, as do the PCC samples (Figure 5.3B), but not to the same extent (Figure 5.3A). The data were normally distributed (Figure 5.3C) and meet the assumption of the parametric test, therefore, the parametric t-test was used to statistically compare between the groups (Figure 5.3C). The scatter plot (Figure 5.3D) shows the relationship between two quantitative variables measured for the same replicate. The values of one variable appear on the horizontal axis, and the values of the

other variable appear on the vertical axis. Each individual in the data appears as a point on the graph. The correlation r values are all around 0.9, which indicates a strong, positive, linear relationship between the variables. Generally, all the quality check parameters of the duplicate samples suggest good reproducibility as well as good data quality.

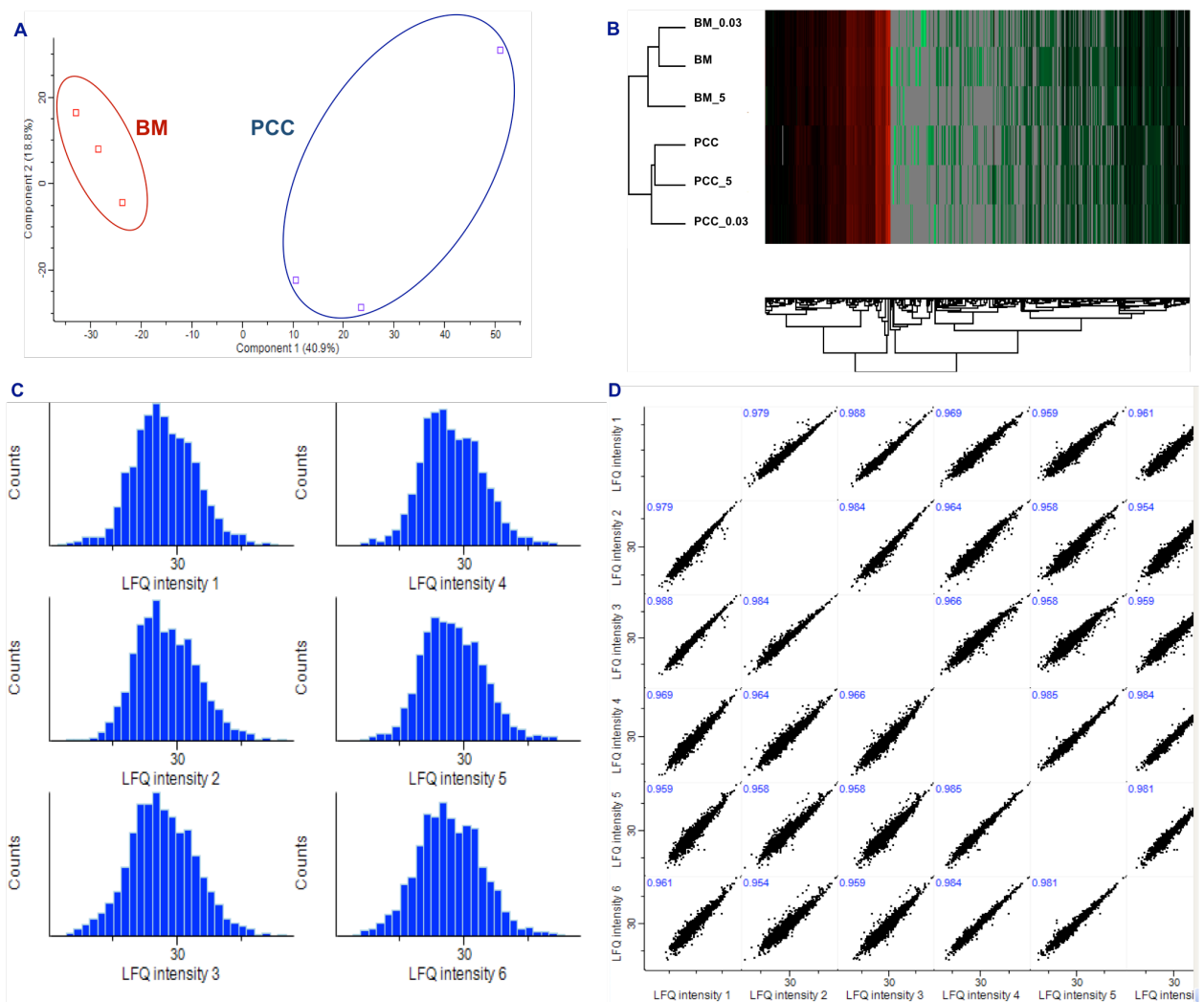


Figure 5.3: Reproducibility assessment of the label-free quantification data.

(A) A dendrogram shows clustering of the replicates from the bone-homed cells (BM) (red), while the PCC replicates (blue) have clustered separately, indicative of underlying cell type-specific differential protein expression. (B) Unsupervised hierarchical clustering based on label-free quantification of duplicate samples with all identified proteins; data from all contributing peptides were used to calculate protein abundance. Protein abundance values are indicated colorimetrically for each protein in each sample; indicating a good correlation of proteins expression; red=high, black=mean value, green=low. (C) LFQ-intensity plots for each sample. In each case the curve is symmetric at the centre suggesting that the mean, mode and median are all equal and indicates a normal distribution within all samples, (D) Representative scatter plots of all correlated LFQ-intensities for peptides quantified within pairwise sample comparisons. Intensities from paired samples; of the median of the duplicate, show inter-sample correlation, units of X- and Y-axes both represent LFQ intensities. LFQ intensities represent: LFQ-1: PCC+no drug, LFQ-2: PCC+0.3 mM, LFQ-3: PCC+ 5mM, LFQ-4: BM+no drug, LFQ-5: BM+ 0.3mM, LFQ-6: BM+ 5mM.

5.3.1.2 Proteins identified and candidate selection

A total list of 4070 proteins were identified and quantified within the complete output data set from MaxQuant, however, this figure is before data-filtering for reverse hits, proteins which do not have at least 1 razor + unique peptide in all samples analysed, potential contaminants and components of the serum used within the cell-culture media. Upon removal of proteins which did not satisfy these filters 2909 proteins remained which had ≥ 2 razor + unique peptides per ID (of which ≥ 1 was a unique peptide). A full list of proteins detected is provided in the supplemental CD table S5. Within these output proteins, 44 proteins were down-regulated with metformin when used at both concentrations in both cell-types. This number of proteins reduced still further to 27 proteins when a 1.5-fold change cut-off was applied (comparing between the untreated and 5 mM treated cells). 112 proteins were differentially regulated depending upon the cell type i.e. these proteins were up-regulated with metformin in the bone-homed BC cell line and down-regulated with metformin within PCC. Further filtering of these differentially regulated proteins returned 4 proteins when a 1.5-fold change cut-off was applied. In a similar way, looking for differentially regulated proteins between PCC and BM cells, 53 proteins were down-regulated with metformin in the bone-homed BC cell line and up-regulated with metformin within the parental cell line. This number of proteins reduced to 3 proteins when we applied the 1.5-fold change cut-off.

Several criteria were taken into consideration when selecting potential candidates for further validation, such as the fold difference with metformin treatment in both the PCC and BM cell lines, relative to the untreated cells (>1.5 fold for up-regulation and <0.71 -fold for down-regulation), statistical P-values ($P<0.05$ by the parametric t-testing or Dunnett's test as appropriate) and mean normalized LFQ-intensity values. The potential candidates were also assessed on the basis of their likely biological relevance to breast cancer initiation, progression and/or metastasis using published literature. Additionally, the commercial availability of the antibodies was also investigated and taken into account when selecting candidates for further analysis.

In total 34 candidate proteins were selected which demonstrated alterations in expression level that were potentially of interest. Table 5.2 summarizes the key proteomic results. Proteins in the “Up and Down proteins” categories are the proteins up- or down-regulated in both cell lines by increasing metformin dosage (green highlighted) and

differentially up- or down-regulated by metformin within the two cell lines (blue and pink highlighted) with increasing doses of metformin. The fold changes listed in the last two table columns are the ratios of protein level with 5 mM metformin compared to untreated controls. Proteins of interest with significant alterations in their quantifications, and more than 2 unique + razor peptides (of them at least 1 razor peptide) in both duplicates all are bold highlighted.

These proteins include members that differed in terms of their direction of change in protein abundance between the parental (PCC) and bone-homed (BM) cells, or showed similar changes in both cell types (using both concentrations of metformin).

Taken together, these considerations led to the selection of 5 prioritized proteins for further validation by Western blotting. These proteins are: tumour necrosis factor alpha-induced protein 8 (TNFAIP8), growth factor receptor-bound protein 2 (GRB2), signal transducer and activator of transcription 3 (STAT3), translocator protein (TSPO) and calmodulin.

However, it is noteworthy that most of the protein-abundance effects observed within this study were subtle, there was no strong on or off effect between the treated and untreated samples using both concentrations of metformin as reflected by the protein-expression fold-differences, and this seems to be the case for the majority of proteins identified (Table 5.1). This may be because most of metformin effects on signalling pathways are exerted via phosphorylation and not via global proteomic changes. For this reason, the 5 mM dose of metformin was chosen as the optimal dosage for the large-scale proteomics experiment, namely the SILAC-based quantification experiment. The choice of this dose was also based on the fact that the cells were more sensitive to this dose of metformin but their viability was not affected (as shown in the proliferation assays used in Chapter 4). Since this concentration of metformin was not yet cytotoxic, we can therefore rule out the possibility of radical alteration in protein levels that could be linked to the toxicological responses. The 72-hour time point was also chosen based on the previous proliferation and cell cycle assays where the effect of metformin was most notable.

Table 5.2: Proteins identified as significantly differentially expressed within the parental MDA-MB-231 PCC cell-line and its bone homed (BM) variant from pilot the Label-free quantification (LFQ) study.

Proteins here are progressively up- or down- regulated with increasing metformin dose and have a least a 1.5-fold increase (or 0.71-fold decrease) between the untreated cells and cells treated with 5 mM metformin. Fold change (FC) was calculated by comparing mean normalized LFQ intensity values between samples. Status indicates the direction of the differential expression and in which cell types: PCC= Parental MDA-MB-231, BM = bone homing cells. Entry refers to UniProt entry <http://www.uniprot.org/>.

| Entry | Protein names | Biological Function | Status | FC in PCC+5mM | FC in BM+5mM |
|-------|---|---|------------------|---------------|--------------|
| 1. | Q06481 Amyloid-like protein 2 | Cellular protein metabolic process, G-protein coupled receptor signalling pathway, post-translational protein modification | Down in PCC & BM | 0.59 | 0.50 |
| 2. | P63165 Small ubiquitin-related modifier 1 | DNA repair, positive regulation of calcium-transporting ATPase activity, positive regulation of proteasomal ubiquitin-dependent protein catabolic process, positive regulation of protein complex assembly, protein stabilization | Down in PCC & BM | 0.58 | 0.57 |
| 3. | P63165 Small ubiquitin-related modifier 1 | DNA repair, positive regulation of calcium-transporting ATPase activity, positive regulation of proteasomal ubiquitin-dependent protein catabolic process, positive regulation of protein complex assembly, protein stabilization | Down in PCC & BM | 0.58 | 0.57 |
| 4. | Q9BT0 Acidic leucine-rich nuclear phosphoprotein 32 family member E | Histone exchange, nucleocytoplasm transport and regulation of apoptosis | Down in PCC & BM | 0.56 | 0.55 |
| 5. | Q13283 Ras GTPase-activating protein-binding protein 1 | Negative regulation of canonical Wnt signalling pathway | Down in PCC & BM | 0.56 | 0.54 |
| 6. | Q15021 Condensin complex subunit 1 | Cell division, chromosome separation, meiotic and mitotic chromosome condensation. | Down in PCC & BM | 0.54 | 0.50 |
| 7. | Q8NBT2 Kinetochore protein Spc24 | Cell division and sister chromatid cohesion | Down in PCC & BM | 0.51 | 0.56 |
| 8. | P40763 Signal transducer and activator of transcription 3 | Acute phase response, cell proliferation, cytokines-mediated signalling pathway, energy homeostasis, glucose homeostasis, growth hormone receptor signalling, negative regulation of apoptosis, positive regulation of cell proliferation, negative regulation of glycolytic process, positive regulation of ATP biosynthesis, regulation of cell cycle and mitochondrial membrane permeability | Down in PCC & BM | 0.47 | 0.51 |

Table 5.2: continued (legend on previous page)

| | | | | | | |
|-----|--------|--|---|------------------|------|------|
| 9. | P04637 | Cellular tumour antigen p53 | Tumour suppressor, positive regulation of cell cycle arrest and intrinsic apoptotic signalling pathway, autophagy and cellular response to DNA damage | Down in PCC & BM | 0.47 | 0.54 |
| 10. | P02794 | Ferritin heavy chain; N-terminally processed | Cellular iron homeostasis, negative regulation of cell proliferation and immune response | Down in PCC & BM | 0.46 | 0.59 |
| 11. | P00403 | Cytochrome c oxidase subunit 2 | ATP synthesis coupled electron transport | Down in PCC & BM | 0.46 | 0.57 |
| 12. | O00217 | NADH dehydrogenase iron-sulfur protein 8 | Mitochondrial respiratory chain Complex I assembly, mitochondrial electron transport and response to oxidative stress | Down in PCC & BM | 0.46 | 0.54 |
| 13. | Q8TCF1 | AN1-type zinc finger protein 1 | Zinc ion binding | Down in PCC & BM | 0.46 | 0.56 |
| 14. | Q9BQ69 | O-acetyl-ADP-ribose deacetylase MACROD1 | Cellular response to DNA damage | Down in PCC & BM | 0.45 | 0.55 |
| 15. | P35222 | Catenin beta-1 | Androgen receptor signalling pathway, regulation of apoptosis, cell adhesion, cell differentiation, epithelial to mesenchymal transition, negative regulation of angiogenesis, negative regulation of cell death and proliferation, positive regulation of I-kappaB kinase/NF-kB signalling, positive regulation of MAPK cascade, positive regulation of osteoblast differentiation | Down in PCC & BM | 0.44 | 0.48 |
| 16. | P62158 | Calmodulin | Negative regulation of ryanodine-sensitive calcium-release channel activity, calmodulin-calcium complex stimulate kinases and phosphatases enzyme. | Down in PCC & BM | 0.43 | 0.41 |
| 17. | P33993 | DNA replication licensing factor MCM7 | DNA replication initiation, cellular proliferation, response to DNA damage and G1/S transition of mitotic cell cycle | Down in PCC & BM | 0.43 | 0.41 |
| 18. | O60493 | Sorting nexin-3 | Protein transport and regulation of Wnt pathway | Down in PCC & BM | 0.40 | 0.56 |
| 19. | P50454 | Serpin H1 | Collagen biosynthesis | Down in PCC & BM | 0.40 | 0.58 |
| 20. | P45974 | Ubiquitin carboxyl-terminal hydrolase 5 | Protein ubiquitination and deubiquitination | Down in PCC & BM | 0.39 | 0.57 |
| 21. | P49327 | Fatty acid synthase (FASN) | Fatty acid biosynthetic process, acetyl-CoA metabolic process, fatty-acyl-CoA metabolic process, positive regulation of cellular metabolic response and regulation of cholesterol biosynthesis | Down in PCC & BM | 0.38 | 0.58 |
| 22. | O75607 | Nucleoplasmin-3 | rRNA processing and transcription | Down in PCC & BM | 0.37 | 0.51 |
| 23. | Q96PU8 | Protein quaking | mRNA processing and stabilisation, positive regulation of gene expression and long-chain fatty acid synthesis. | Down in PCC & BM | 0.34 | 0.40 |
| 24. | P07339 | Cathepsin D | Proteolysis, autophagy protein catabolic process involved in the pathogenesis of breast cancer | Down in PCC & BM | 0.31 | 0.50 |

Table 5.2: continued (legend on previous page)

| | | | | | | |
|-----|--------|--|--|------------------------|------|------|
| 25. | Q56VL3 | OCIA domain-containing protein 2 | Unknown function | Down in PCC & BM | 0.30 | 0.40 |
| 26. | Q5JRX3 | Presequence protease, mitochondrial | Degradation of mitochondrial transit peptides after their cleavage | Down in PCC & BM | 0.29 | 0.56 |
| 27. | Q9P0S9 | Transmembrane protein 14C | Heme biosynthesis | Down in PCC & BM | 0.26 | 0.56 |
| 28. | P62993 | Growth factor receptor-bound protein 2 | Cell-cell signalling, cell differentiation and migration, EGFR signalling pathway, ERBB2 signalling pathway, insulin receptor signalling pathway, regulation of MAPK cascade, phosphatidylinositol-mediated signalling, signal transduction in response to DNA damage | UP in PCC & down in BM | 1.76 | 0.40 |
| 29. | P56134 | ATP synthase subunit f, mitochondrial | ATP biosynthesis, mitochondrial ATP synthesis and coupled proton transport | UP in PCC & down in BM | 1.60 | 0.71 |
| 30. | P30536 | Translocator protein | Anion transport, cell proliferation, contact inhibition, heme biosynthesis, negative regulation of ATP metabolic process, negative regulation of TNF production, positive regulation of apoptosis and necrotic cell death, positive regulation of calcium ion transport, positive regulation of reactive oxygen species metabolic process, regulation of cholesterol transport, regulation of steroid biosynthesis and metabolism, response to progesterone and testosterone | UP in PCC & down in BM | 1.55 | 0.48 |
| 31. | Q9NPA0 | ER membrane protein complex subunit | Carbohydrates binding | UP in BM & down in PCC | 0.58 | 1.83 |
| 32. | Q96TC7 | Regulator of microtubule dynamics protein 3 | Negative regulator of apoptotic process, cell differentiation and calcium ion homeostasis | UP in BM & down in PCC | 0.55 | 1.50 |
| 33. | O95379 | Tumour necrosis factor alpha-induced protein 8 | Negative mediator of apoptosis and play a role in tumour progression | UP in BM & down in PCC | 0.51 | 1.79 |
| 34. | Q96A33 | Coiled-coil domain-containing protein 47 | Calcium ion homeostasis, osteoblast differentiation | UP in BM & down in PCC | 0.50 | 1.65 |

5.3.1.3 Global pathway regulation in response to metformin treatment

In addition to the analyses performed to select candidate targets for further verification, all the proteins identified in Table 5.2 were uploaded into STITCH chemical association network (<http://stitch.embl.de/>) to characterize metformin's global effects on protein levels, cellular pathways and to identify possible direct and indirect interactions between the target proteins. The Uniprot identifiers of the 33 proteins identified in table 5.2 were uploaded to the STITCH website and up to 15 interaction networks were generated when the species was restricted to human only.

The output from the STITCH website allows examination of the biological, cellular and molecular functions represented, predicts upstream regulators of target proteins, as well as putative networks of interaction for specific molecules of interest. Moreover, by exploring the potential of the KEGG pathways; Kyoto Encyclopedia for Gene and Genome (which is a reference database for pathway mapping, representing up to date knowledge on the molecular interactions, reaction and relation networks for metabolism, cellular processes, human diseases and drug development) more can be learnt about metformin's actions on the global protein network within the two cell-types.

At least 14 proteins from the panel formed more than 7 interactions within the network (Figure 5.4). Thus the identified proteins have more interactions among themselves than would be expected for a random set of proteins of similar size, drawn from the genome. Such enrichment indicates that these proteins are at least partially biologically connected as a group, and may function together. The majority of the highly interconnected proteins are down-regulated in one or both of the metformin conditions (compared to untreated cells). In this network, most of our candidate proteins selected were centred on the epidermal growth factor receptor (EGFR). EGFR is known as an upstream transmembrane regulator, the phosphorylation of which can initiate an intracellular signalling cascade linked to versatile cellular responses including cell proliferation, differentiation, adhesion, migration, anti-apoptotic survival mechanisms and induction of angiogenesis. EGFR can also mediate several downstream signalling pathways including the MAPK and PI3k/Akt signalling pathways. Furthermore, at least 3 of the candidate proteins (STAT3, GRB2 and TSPO) were also connected to TP53 (tumour protein *p53*); which acts as a tumour suppressor in several tumour types by

inducing growth arrest or apoptosis depending on the cell type and physiological circumstances.

The main molecular and cellular functions identified as differentially regulated were cell growth and proliferation, cell migration, intracellular signal transduction, cell-to-cell communication, regulation of metabolic processes, DNA replication, cell cycle, cell death and apoptosis, response to insulin, protein binding, enzyme binding, response to stress, protein phosphorylation and membrane transport. The first nine of these were consistently the top functions identified in all treated groups. The biological functions for each individual protein identified are listed in table 5.2.

The major canonical KEGG pathways identified were: focal adhesion, pathways in cancer, apoptosis, insulin and insulin-like growth factors signalling, EGFR signalling, ErbB signalling, PI3K-Akt signalling, JAK-STAT signalling and MAPK signalling pathways (Figure 5.5). Other less statistically significant pathways related to Ras, FoxO, oestrogen, growth hormone, HIF-1 and calcium signalling have been also identified.

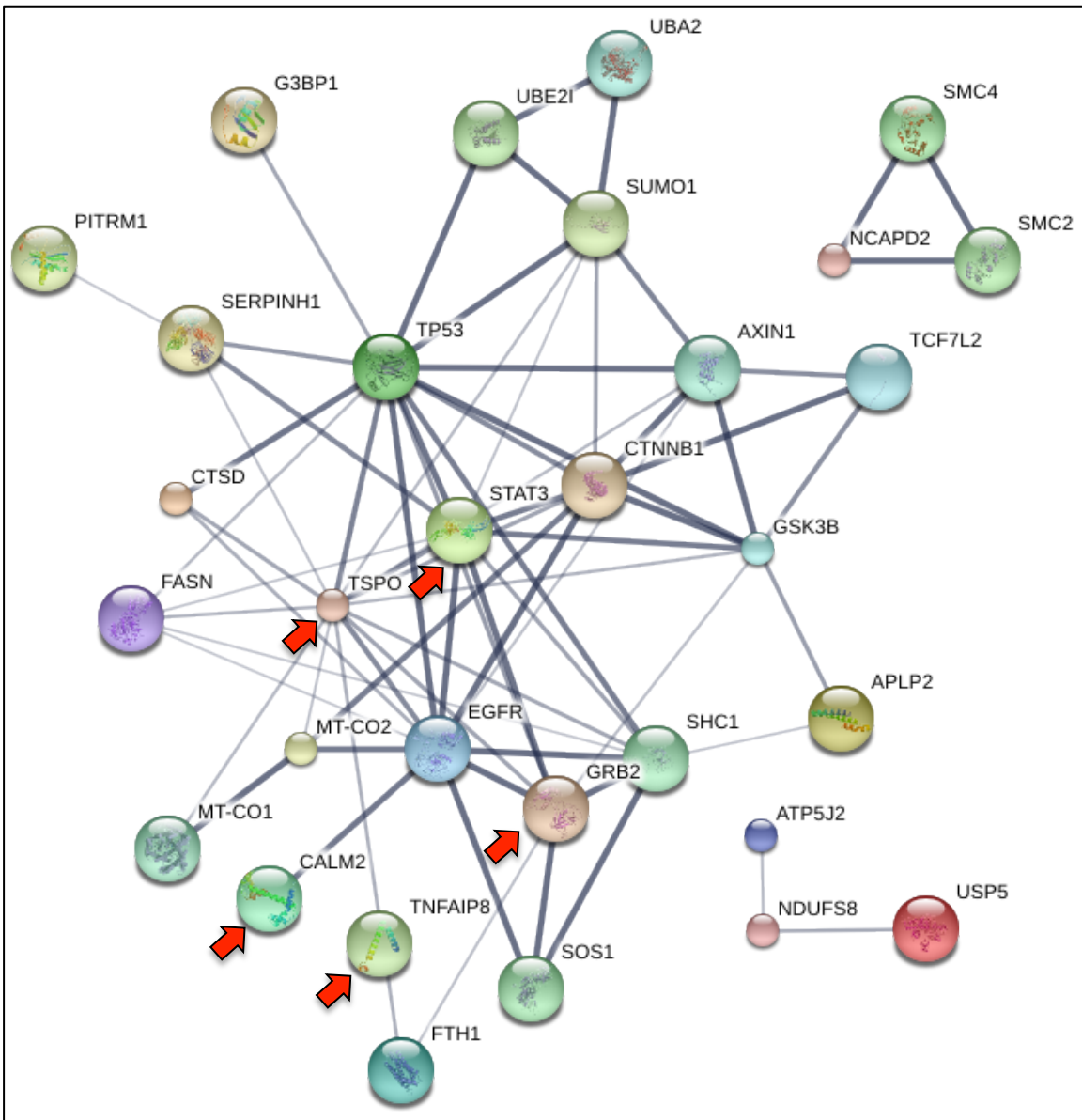


Figure 5.4: Networks identified by STITCH analysis and the patterns of interaction between the proteins up and down-regulated by metformin, with non-connected nodes removed.

Protein-protein interactions are displayed in confidence view. Each coloured circle represents a node; the node refers to when the protein is making or receiving a connection. The edges between the nodes that represent protein-protein associations reflect the reliability and confidence of the interaction evidence; thicker lines represent stronger associations. In the network image, most of the identified proteins have an established confident link with each other in the interaction network. Standard nomenclature gene name abbreviations were used to annotate individual proteins (this can be searched on www.Uniprot.org for more details). Red arrows highlight the proteins chosen for further analysis.

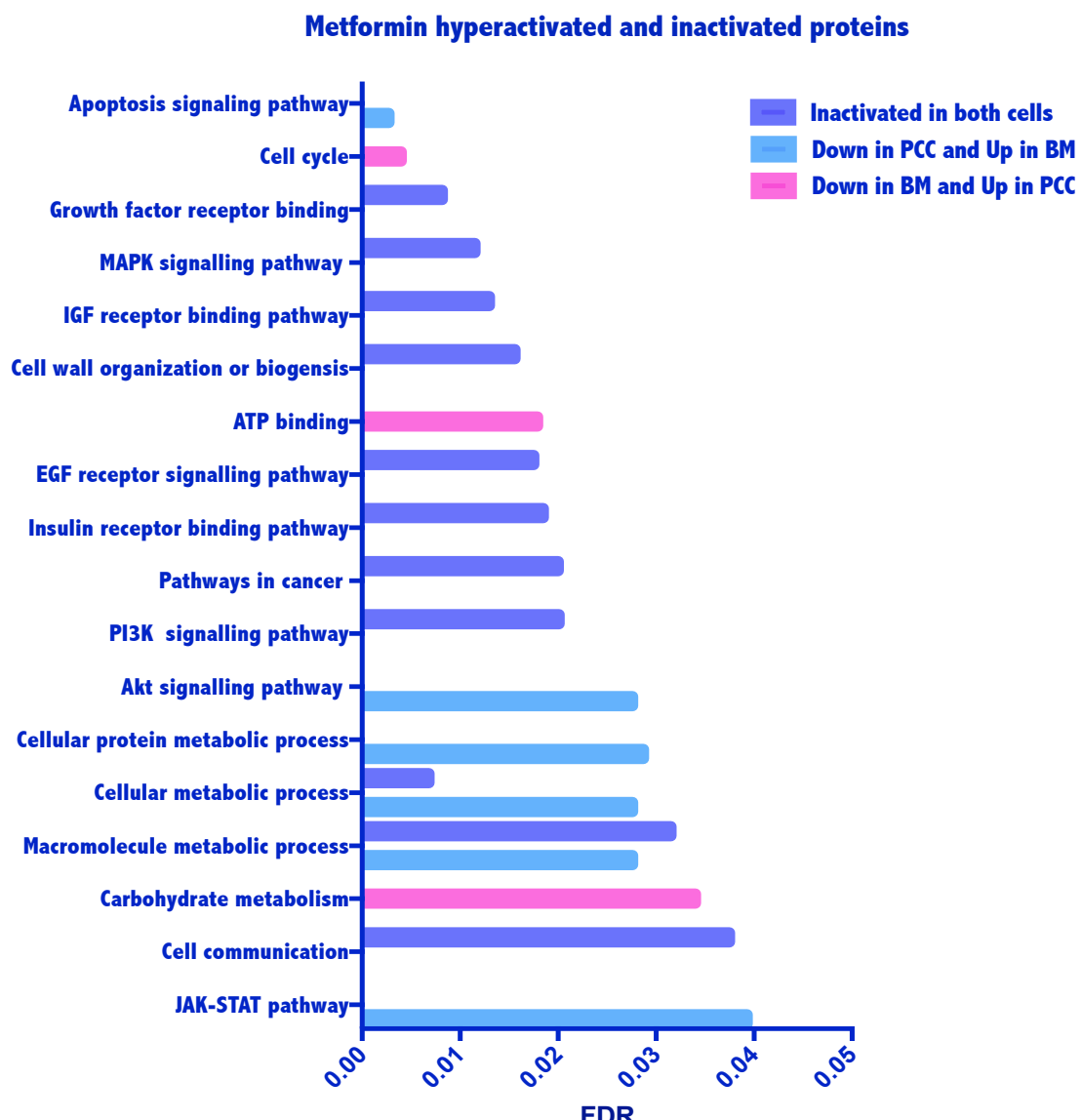


Figure 5.5: Metformin modulates key biological processes and pathways in metastatic breast cancer cells.

A bar graph shows the biological (BP) and KEGG pathways significantly overrepresented in hyper-activated and inactivated proteins (Benjamini-Hochberg FDR < 0.05) following exposure to 5 mM of metformin in the MDA-MB-231 (PCC) and the bone-homing MDA-MB-231(BM) cells. In the x-axis, the false discovery rate of each category is plotted.

5.3.1.4 Verification of protein expression for selected targets using Western blotting

In order to confirm that the mass spectrometry results were consistent and accurate, the differential expression of the selected proteins was assessed in cell lysates of three biological replicates of the parental cell line, MDA-MB-231, along with the bone (BM) and lung homed (LM) metastatic cell lines. These lysates were prepared for the large-scale proteomics experiment and in parallel employed within the Western blotting verification. Similar to the pilot experiment, both the clinically relevant dose (0.3 mM) and the potential tissue accumulated dose (5 mM) of metformin were used.

These experiments verified decreased TNFAIP8 expression ($P<0.002$, One-way ANOVA test) (Figure 5.6 and 5.7) in response to both 0.3 mM and 5 mM metformin in the wild type PCC (to 70% and 56% of untreated value, $P=0.04$ and $P=0.003$ by Dunnett's test, respectively) and lung-metastatic (LM) cells (to 78% and 32% of untreated value, $P=0.004$, $P=0.001$, respectively, assessed by Dunnett's test). In contrast, decreased TNFAIP8 expression was only observed with the 5 mM dose (34% of untreated value, $P=0.002$, Dunnett's test) in the bone-homed variants. Generally, the level of TNFAIP8 expression by the untreated parental and bone-homed cells lines was relatively similar and slightly higher in the lung-homed cells.

Treatment with metformin markedly increased GRB2 expression in the wild-type cells by 60% and 200% of untreated control value, in 0.3 mM and 5 mM treated samples respectively ($P=0.002$, by Dunnett's test). In contrast, metformin at its highest dose of 5 mM profoundly down-regulated the expression of GRB2 (by more than 99% compared to untreated controls) within both the bone- and lung-homed cells respectively ($P=0.0001$, Dunnett's test). The 0.3 mM concentration also down-regulated GRB2 expression in the BM cells by 50% compared to untreated controls, and in the LM cells by 99% compared to untreated cells ($P=0.001$ and $P=0.0001$, Dunnett's test, respectively) (Figure 5.6 and 5.7). The level of GRB2 expression was very low to undetectable in the parental MDA-MB-231 control cells, but much more expressed, and to a similar level in the metastatic bone and lung homing cells.

STAT3 expression was down-regulated to less than 50% of its expression in the untreated control cells ($P=0.0002$, Dunnett's test) in all cell lines at all tested concentrations ($P<0.0001$, One-way ANOVA test) and not expressed in the lung homed

cells treated with 5 mM of metformin ($P=0.0001$, Dunnett's test) (Figure 5.7). However, it was clearly noticeable that the untreated cells do not abundantly express STAT3, although the level of expression was relatively similar in the parental and bone-homed cells lines and markedly lower in the lung-homed cells (Figure 5.6).

Translocator protein expression (TSPO) was slightly increased in the wild type cells treated with 5 mM of metformin to 20% ($P=0.04$, Dunnett's test) and significantly reduced in the bone homed cells to 67%, and 71% of the untreated control cells, $P=0.001$, Dunnett's test, with 0.3 mM and 5 mM metformin treatment respectively. The expression of TSPO by lung homed cells was similarly significantly reduced at to 67%, and 70% of the untreated control cells, $P=0.001$, Dunnett's test, with 0.3 mM and 5 mM metformin treatment respectively. The levels of TSPO expression were relatively the same in the metastatic bone and lung-homed cells and slightly lower in the parental control cells (Figure 5.6 and 5.7).

Inconsistent with mass spectrometry result, no change in the expression of calmodulin was observed in both parental and lung-homing cells after metformin treatment ($P=0.7$, $P=0.9$, respectively, by One-way ANOVA test). However, calmodulin expression was significantly down-regulated to 34% of the untreated controls at 0.3 mM in the lung homed metastatic cells and not expressed at all when cells were treated with 5 mM metformin ($P=0.0001$, Dunnett's test) (Figure 5.6 and 5.7). Generally, the level of calmodulin expression was relatively similar in the untreated parental and bone-homed cells lines and markedly higher in the lung-homed cells.

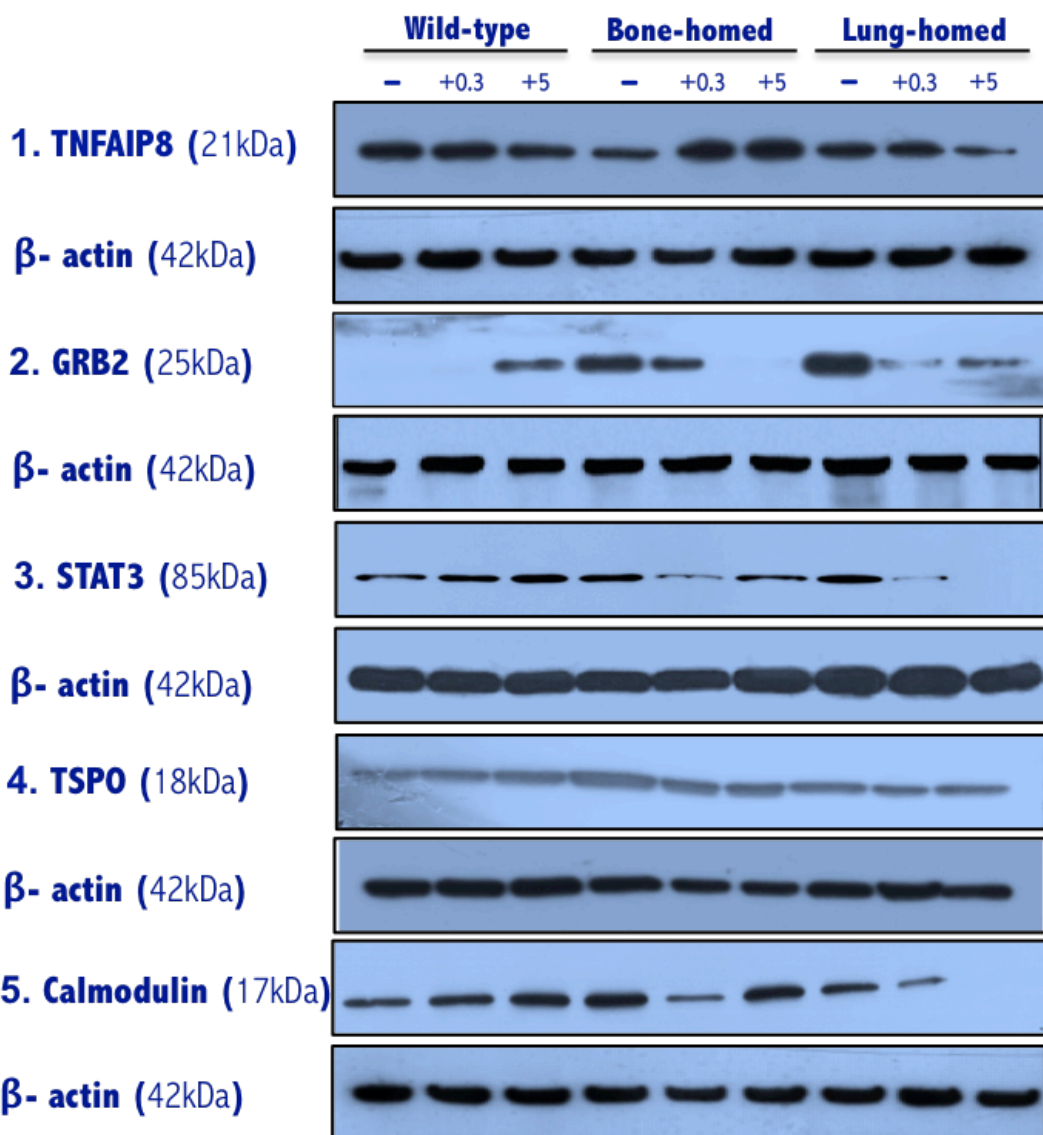


Figure 5.6: Representative cropped Western blots of target protein expression (TNFAIP8, GRB2, STAT3, TSPO and calmodulin).

The expression was tested within the wild type MDA-MB-231 (PCC) cells and its bone (BM) and lung homed (LM) variants treated with 0.3 mM and 5 mM of metformin. The images represent the expression of the candidate proteins (TNFAIP8, GRB2, STAT3, TSPO and Calmodulin), their corresponding molecular weights are indicated in brackets. β -actin (42kDa) served as a loading control of expression levels for all proteins tested. 20 μ g of protein total cell lysate of untreated and treated cells were loaded into each lane. (-) = Untreated cells, 0.3 and 5 are metformin doses in mM. For full images of the three independent experiments, see Supplementary materials CD (S3).

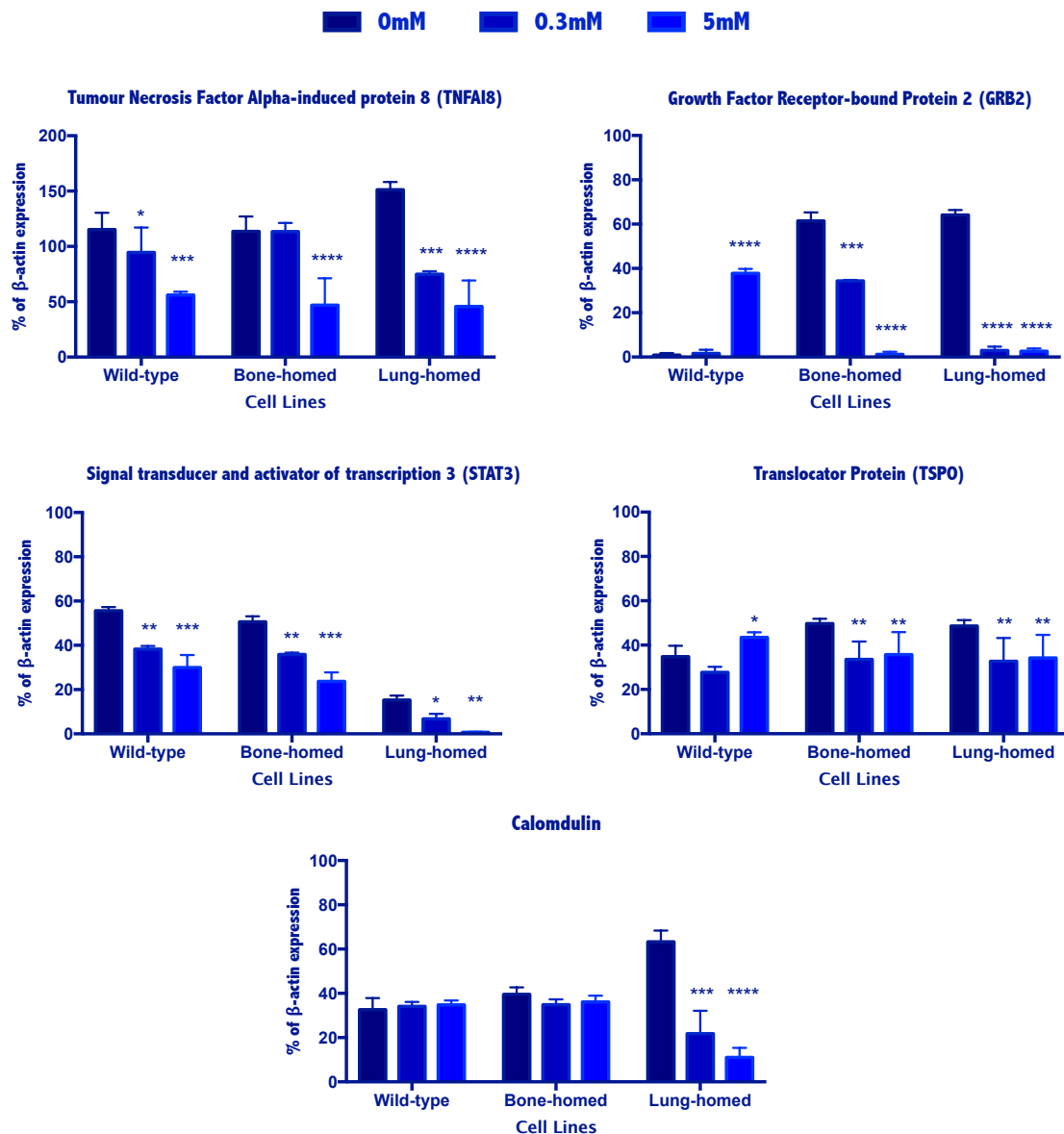


Figure 5.7: Representative Western blot analysis of target protein expression (TNFAIP8, GRB2, STAT3, TSPO and Calmodulin).

The expression was tested within the wild type MDA-MB-231 (PCC) and its bone (BM) and lung homed (LM) variants treated with 0.3 mM and 5 mM of metformin. The intensity of the relevant bands were determined by densitometry and normalized to β-actin, then plotted as the percentage of β-actin expression and expressed as mean±SD from each of the three independent experiments of three biological replicates. Treated cells from each group were compared to the untreated cells as a control. *P<0.05, **P<0.01, ***P<0.001 and ****P<0.0001.

5.3.2 Spike-In SILAC (SIS)-labelled proteomics quantification: first run

Having successfully identified some interesting proteins using a label-free mass spectrometry method, we decided to run a large-scale Spike-in SILAC comparison (experiment 2, Figure 5.2) in an attempt to identify a larger number of proteins for future analysis and to more fully understand the effect of metformin on these cells. Unfortunately, analysis of the data from the first 50 samples run on the mass-spectrometer out of a total of 75 samples revealed two issues, one of which was high levels of trypsin peptides relative to cellular-protein released peptides, and, the second, more worryingly, was a significant polymer contamination. Both of these issues were detrimental to the sensitivity of protein detection and very adversely impacted the overall quality of the eventual dataset. Therefore, we were unable to run the remaining 25 samples.

Evidence of the polymer contamination is shown in the screen shot of the data in figure 5.8. When these files were run through the MaxQuant software the total numbers of proteins quantified and identified in the samples before any filtering of the data were 1365 and 1367 in the first and last 5 gel slices respectively. This is considerably lower than the 4070 proteins quantified in the first preliminary analysis. The drop in the number of proteins can be clearly attributed to the building up of the polymer within the samples which suppresses the signals via peak-suppression. This prevents the detection of lower abundance proteins. Therefore, due to failure at this stage, preparation of the whole dataset after ordering all the fresh reagents and plasticware to eliminate any possible source of polyethylene glycol (PEG) contamination was repeated. The 44 Da PEG-like polymer trace was subsequently identified as originating from a commercial detergent used by the bottle-washing facility at the University of Sheffield.

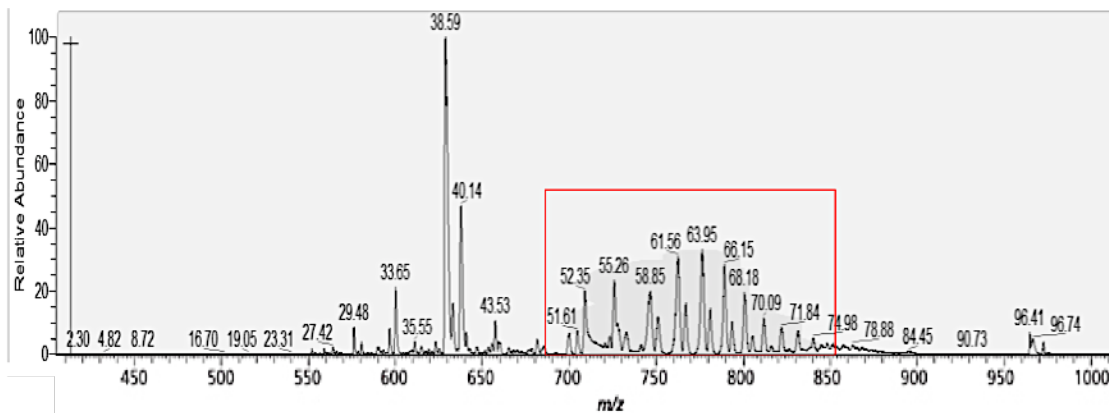


Figure 5.8: Example of an LC-MS/MS-spectrum showing the separation pattern of polyethylene glycol (PEG)-like detergent.

The spectrum is dominated by a series of m/z values with equidistant peaks; 44Da apart; which is typical for PEG and PEG-like molecules. Each peak in the grey highlighted area (within the red box) section represents the ethoxy structure, which indicates PEG contamination.

5.3.3 SILAC-based proteomics analysis of the repeat dataset

5.3.3.1 Method

For a full description of the SILAC-based experiment used in here, please refer to section 5.2.2.

5.3.3.2 Quality-check and sample correlation

Comparison of the repeat samples set was performed to ensure consistency across the experiment and eliminate any possible outliers (Following the steps mentioned in section 5.3.1.1).

Cluster analysis of the PCA (principle component analysis) of cell lines with and without treatment showed that only the 3 samples of bone-seeking cells treated with metformin had fully clustered together. In the other cells with and without treatments, two of the three samples were closely related but one sample of each group was separate (Figure 5.9A). When an unsupervised hierarchical clustering was constructed, the data showed a very similar pattern of distribution to the PCA clustering (Figure 5.9B) with most groups having one sample that was not as closely associated. All distributions of proteins were normal and not bimodal and therefore a parametric statistical test was used to analyse the data (Figure 5.9C). For representative scatter plots of all aligned intensities from paired samples please refer

to Supplementary materials CD (S4). The correlation r-measures are mostly between 0.5 and 0.8, which indicates a moderate to strong, positive, linear relationship between the variables. However, a few r-values are 0.3 or less suggesting a weak relationship. Overall, the quality check assessment suggested that the reproducibility of our data is reasonable enough for some further analysis.

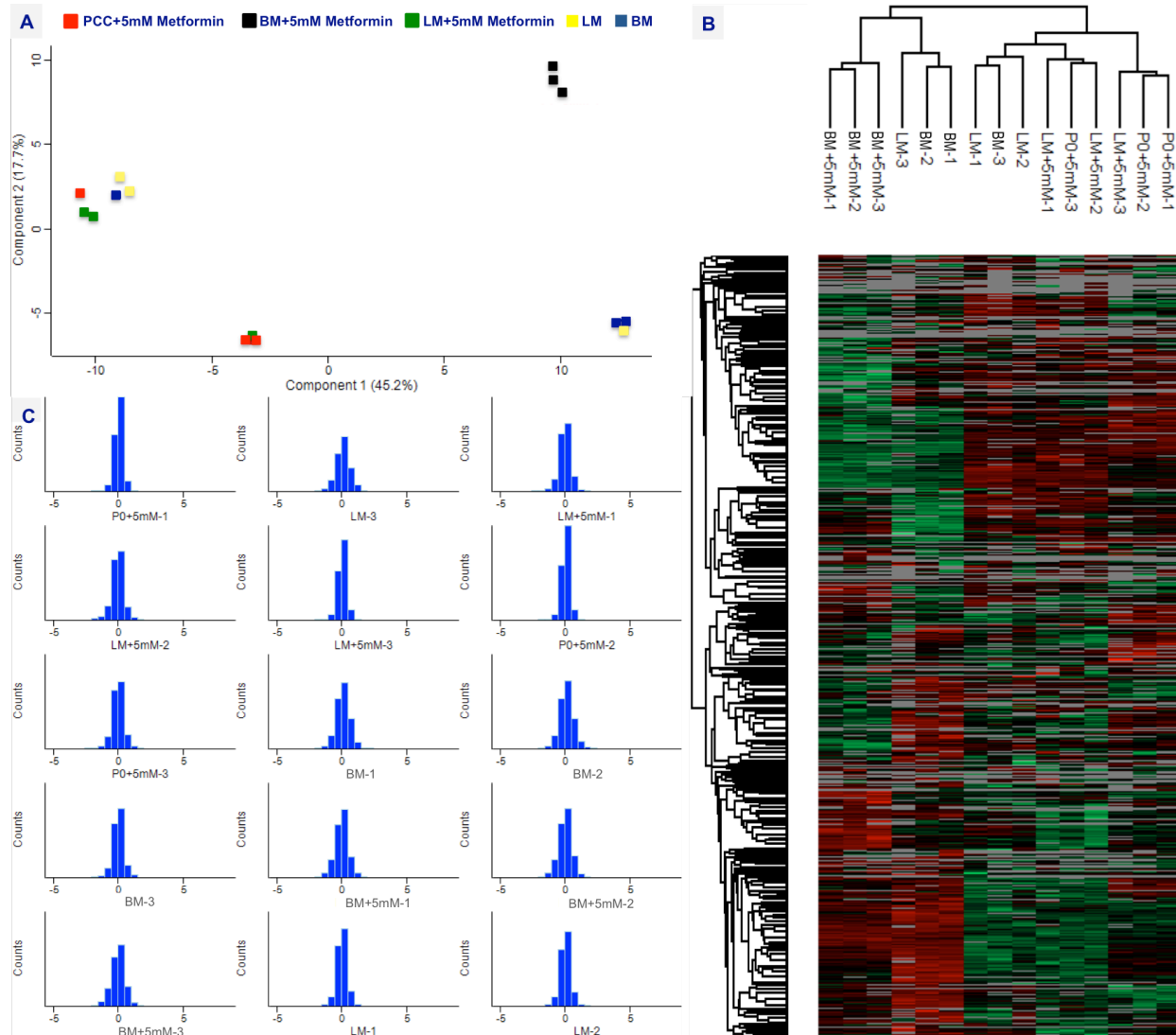


Figure 5.9: Reproducibility assessment of the SILAC-based quantification data.

(A) A dendrogram shows clustering of the replicates of the three cell lines/treatment combinations. (B) Unsupervised hierarchical clustering based on Spike-in SILAC quantification of triplicate samples with all identified proteins; Protein abundance values are indicated colorimetrically for each protein in each sample; indicating the correlations of protein expression red=high, black=mean value, green=low. (C) LFQ-intensities are normally distributed within all samples. P0 in the B and C graphs refers to the parental cells (PCC), BM: bone-homing cells, LM: lung-homing cells.

5.3.3.3 Inter-group comparison and candidate selection; proteins detected exclusively in either parental, bone or lung homed cells

Data were analysed using the aforementioned workflow in figure 5.1, with all data taken through RawMeat, MaxQuant and Perseus. Initially 4731 proteins were identified within the complete data set which was reduced to 2827 proteins identified following the removal of all proteins with < 1 unique + razor peptide across all samples. Next, this was further reduced to 2728 proteins following the removal of all reverse database hits. Finally, the identified proteins were assessed for the presence of at least 1 unique peptide/ID suggesting high quality protein identifications, resulting in a final protein number of 2651 (an excel spread sheet of the raw data is included, see Supplementary materials S5). Two complimentary approaches were taken towards the identification of the targets of interest:

1. Using the light / heavy (L/H) ratios: if there's a significant L:H ratio across all three replicates, that protein will be taken forward as interesting in our comparison of interest as having been increased or decreased compared to the PCC-untreated control cells in three biological replicates.
2. The reciprocal of the H/L ratios was determined, and then the log2 transformation of the L:H ratio was obtained, followed by the use of a parametric t-test to work out significant differences in the Log2-LFQ-intensity values between chosen cell-line/treatment pairs. Next, a check for the appropriate number of unique and unique + razor peptides across all replicates within both the heavy (H) and light-labelled (L) form of each protein of interest was performed.

When applying these tests and filters, an initial list of 44 proteins of potential interest was generated. However, closer examination revealed that 34 of them had at least one sample with zero LFQ-intensity value or they did not pass the 1.5-fold change cut off point within one of the triplicate samples. This resulted in only 10 proteins being identified as being consistently up-regulated with metformin treatment in one of the cell types (Table 5.3). However, unlike the pilot study, no down-regulated proteins were identified in this experiment.

Table 5.2: Proteins identified as significantly differentially expressed within the parental MDA-MB-231 (PCC) and its bone (BM) and lung (LM) homed variant cell lines.

Proteins here are progressively upregulated in protein expression and have at least a 1.5-fold increase between the heavy-labeled untreated cells (PCC) and cells treated with 5 mM of metformin (PCC, BM and LM). Fold change (FC) was calculated by comparing mean normalized LFQ intensity between samples. Status indicates the direction of the differential expression and in which cell type it occurs: PCC= Parental MDA-MB-231, BM = bone homing BC cells and LM= lung homing BC cells. Entry refers to UniProt entry <http://www.uniprot.org/>.

| Entry | Protein names | Biological functions | Status | FC |
|------------|---|---|-----------|-------|
| 1. P02794 | Ferritin heavy chain | Cellular iron homeostasis, immune response and negative regulation of cell proliferation | Up in BM | 4.13 |
| 2. P08133 | Annexin A6 | Apoptotic signalling pathway, ion transmembrane transport, mitochondrial calcium ion homeostasis and regulation of muscle contraction | Up in BM | 4.09 |
| 3. H0YM23 | Ankyrin repeat domain-containing protein 17 (Fragment) | RNA binding | Up in PCC | 7.37 |
| 4. O75208 | Ubiquinone biosynthesis protein COQ9, mitochondrial | Mitochondrial electron transport | Up in PCC | 4.30 |
| 5. O75607 | NADH dehydrogenase iron-sulfur protein 2, mitochondrial | rRNA processing and rRNA transcription | Up in PCC | 2.20 |
| 6. O75323 | Protein NipSnap homolog 2 | ATP biosynthetic process, negative regulation of ATP citrate synthase activity, oxidative phosphorylation, positive regulation of high voltage-gated calcium channel activity | Up in PCC | 1.98 |
| 7. O75438 | NADH dehydrogenase 1 beta subcomplex subunit 1 | Mitochondrial electron transport and mitochondrial respiratory chain complex I assembly | Up in PCC | 1.64 |
| 8. P50579 | Methionine aminopeptidase 2 | N-terminal protein amino acid modification, peptidyl-methionine modification, protein processing, aminopeptidase and metalloexopeptidase activity | Up in LM | 31.39 |
| 9. P29034 | Protein S100-A2 | Endothelial cell migration | Up in LM | 16.58 |
| 10. P13645 | Keratin, type I cytoskeletal 10 | (Contaminant protein) Skin cornification and keratinization | Up in LM | 1.62 |

| <p style="text-align: center;">The following proteins are of tentative interest but they have one replicate with zero LFQ-intensity Or they have not passed the 1.5 cut-off point in one of the triplicate samples</p> | | | | | |
|---|--------|--|--|----------|------|
| 11. | B7Z574 | Calpastatin | Endogenous calpain (calcium-dependent cysteine protease) inhibitor; involved in the proteolysis of amyloid precursor | Up in BM | 2.64 |
| 12. | O14933 | Ubiquitin/ISG15-conjugating enzyme E2 L6 | Cellular protein metabolic process, SG15-protein conjugation and modification-dependent protein catabolic process | Up in BM | 2.43 |
| 13. | Q92522 | Histone H1x | Nucleosome assembly | Up in BM | 2.27 |
| 14. | O43237 | Cytoplasmic dynein 1 light intermediate chain 2 | ER to Golgi vesicle-mediated transport, microtubule cytoskeleton organization and sister chromatid cohesion | Up in BM | 2.16 |
| 15. | P21912 | Succinate dehydrogenase iron-sulfur subunit, mitochondrial | Aerobic respiration, respiratory electron transport chain, succinate metabolic process and tricarboxylic acid cycle | Up in BM | 2.08 |
| 16. | P51970 | NADH dehydrogenase 1 alpha subcomplex subunit 8 | Mitochondrial electron transport and mitochondrial respiratory chain complex I assembly | Up in BM | 1.97 |
| 17. | Q9BRP8 | Partner of Y14 and mago | Exon-exon junction complex disassembly, nuclear-transcribed mRNA catabolic process and positive regulation of translation | Up in BM | 1.89 |
| 18. | P31040 | Succinate dehydrogenase flavoprotein subunit, mitochondrial | Anaerobic respiration, mitochondrial electron transport, oxidation-reduction process, succinate metabolic process and tricarboxylic acid cycle | Up in BM | 1.66 |
| 19. | B4DJ81 | NADH-ubiquinone oxidoreductase 75 kDa subunit, mitochondrial | ATP synthesis coupled electron transport | Up in BM | 1.65 |
| 20. | P17252 | Protein kinase C alpha type | Positive regulation of angiogenesis and blood vessel endothelial cell migration, apoptotic signalling pathway, cell adhesion, ERB2 signalling pathway, intracellular signal transduction, positive regulation of cell migration, adhesion, mitotic cell cycle and regulation of insulin secretion | Up in BM | 1.50 |
| 21. | Q9P0J0 | NADH dehydrogenase 1 alpha subcomplex subunit 13 | Negative regulation of intrinsic apoptotic signalling pathway, cellular response to interferon-beta, mitochondrial electron transport, respiratory chain complex I assembly, negative regulation of cell growth, positive regulation of cysteine-type endopeptidase activity, positive regulation of protein catabolic process | Up in BM | 1.48 |
| 22. | Q9Y3B7 | 39S ribosomal protein L11, mitochondrial | Mitochondrial translational elongation and termination, ribosomal large subunit assembly | Up in BM | 1.47 |

Table 5.3: Continued (Legend on the previous page)

| | | | | | |
|-----|--------|--|--|-----------|-------|
| 23. | P10515 | Dihydrolipoyllysine-residue acetyltransferase component of pyruvate dehydrogenase complex, | Regulation of acetyl-CoA biosynthetic process from pyruvate, glucose metabolic process, pyruvate metabolic process, tricarboxylic acid cycle | Up in BM | 1.34 |
| 24. | P49588 | Alanine-tRNA ligase, cytoplasmic | Alanyl-tRNA aminoacylation for protein translation, negative regulation of neuron apoptotic process and tRNA modification | Up in BM | 1.33 |
| 25. | Q8N183 | Mimitin, mitochondrial | Cellular respiration, mitochondrial respiratory chain complex I assembly, negative regulation of insulin secretion involved in cellular response to glucose stimulus and respiratory electron transport chain | Up in BM | 1.32 |
| 26. | P35221 | Catenin alpha-1 | Actin filament organization, apical junction assembly, epithelial cell-cell adhesion, establishment or maintenance of cell polarity, negative regulation of cell motility, negative regulation of extrinsic apoptotic signalling pathway, positive regulation of extrinsic apoptotic signalling pathway in absence of ligand and response to oestrogen | Up in BM | 1.27 |
| 27. | H0YEB6 | Sjogren syndrome/scleroderma autoantigen 1 (Fragment) | Cell cycle, cell division, mitosis | Up in PCC | 13.75 |
| 28. | O75170 | Serine/threonine-protein phosphatase 6 regulatory subunit 2 | Regulatory subunit of protein phosphatase 6 (PP6); involved in the regulation of phosphoprotein phosphatase activity | Up in PCC | 4.86 |
| 29. | O75251 | NADH dehydrogenase iron-sulfur protein 7, mitochondrial | Mitochondrial electron transport and mitochondrial respiratory chain complex I assembly | Up in PCC | 2.05 |
| 30. | O75381 | Peroxisomal membrane protein PEX14 | Microtubule anchoring, negative regulation of protein binding, negative regulation of sequence-specific DNA binding transcription factor activity and peroxisome organization | Up in PCC | 1.69 |
| 31. | O75394 | 39S ribosomal protein L33, mitochondrial | Mitochondrial translational elongation and termination | Up in PCC | 1.65 |
| 32. | O75436 | Vacuolar protein sorting-associated protein 26A | Intracellular protein transport, regulation of macroautophagy, retrograde transport (endosome to Golgi) and Wnt signalling pathway | Up in PCC | 1.67 |
| 33. | O75475 | PC4 and SFRS1-interacting protein | Nuclear transport, positive regulation of transcription from RNA polymerase II promoter and response to oxidative stress | Up in PCC | |
| 34. | O75477 | Erlin-1 | Negative regulation of cholesterol and fatty acids biosynthetic processes | Up in PCC | 1.58 |

Table 5.3: Continued (Legend on the previous page)

| | | | | | |
|-----|--------|---|--|-----------|------|
| 35. | O75569 | Interferon-inducible double-stranded RNA-dependent protein kinase activator A | Cellular response to oxidative stress, immune response, negative regulation of cell proliferation, positive regulation of intrinsic apoptotic signalling pathway, protein phosphorylation and protein stabilization | Up in PCC | 1.53 |
| 36. | P04350 | Tubulin beta-4A chain | Ciliary basal body-plasma membrane docking and regulation of G2/M transition of mitotic cell cycle | Up in PCC | 1.53 |
| 37. | P05976 | Myosin light chain 1/3, skeletal muscle isoform | Cardiac muscle contraction | Up in PCC | 1.52 |
| 38. | Q13867 | Bleomycin hydrolase | Homocysteine catabolic process, protein polyubiquitination, proteolysis, response to drug and toxic substance | Up in LM | 1.52 |
| 39. | O43396 | Thioredoxin-like protein 1 | Cell redox homeostasis and cellular response to oxidative stress | Up in LM | 1.51 |
| 40. | Q9H1E3 | Nuclear ubiquitous casein and cyclin-dependent kinase substrate 1 | Cellular glucose homeostasis, double-strand break repair, positive regulation of insulin receptor signalling pathway and regulation of DNA replication | Up in LM | 1.51 |
| 41. | P16989 | Y-box-binding protein 3 | 3'-UTR-mediated mRNA stabilization, cellular hyperosmotic response, cellular response to tumour necrosis factor, negative regulation of intrinsic apoptotic signalling pathway in response to osmotic stress, negative regulation of necroptotic process, negative regulation of skeletal muscle tissue, negative regulation of transcription from RNA polymerase II promoter | Up in LM | 1.51 |
| 42. | P33316 | Deoxyuridine 5-triphosphate nucleotidohydrolase, mitochondrial | DNA replication, dUMP biosynthetic process, dUTP catabolic process and nucleobase-containing small molecule interconversion | Up in LM | 1.50 |
| 43. | K7EIG1 | Clustered mitochondria protein homolog (Fragment) | Intracellular distribution of mitochondria | Up in LM | 1.50 |
| 44. | Q7Z434 | Mitochondrial antiviral-signalling protein | Activation of innate immune response to bacterium and virus, negative regulation of type I interferon production, positive regulation of chemokine (C-C motif) ligand 5 production, positive regulation of I-kappaB kinase/NF-kappaB signalling, positive regulation of protein import into nucleus, translocation and positive regulation of tumour necrosis factor secretion | Up in LM | 1.50 |

5.3.3.4 Inter-group comparison of metformin-untreated mammary cancer cells

Concerningly, the present study reveals low number of proteins, only 22, including proteins that involved in the regulation of cellular respiration, metabolic processes, mitochondrial respiratory chain assembly and cancer cell growth and proliferation (Listed in table 5.4) are differentially expressed between the most commonly used triple negative human breast cancer cell lines, MDA-MB-231 and its bone homed variant. No difference in protein expression was detected between the parental and lung-homing cell variants except some potential contaminants from the cell-culture media (identified within database searching as Bos-taurus proteins). This is in contrast to previous studies and suggests that there may be issues with the data set³³⁰.

The list of differentially expressed proteins generated in the present study was used to provide useful information about whether the differential protein expression seen with metformin treatment is solely attributed to the drug action or it is simply due to the changes that cells acquired during their progression to more aggressive phenotype in the absence of metformin influence. This comparison was extremely important to avoid false positive results and the choice of poor-quality candidates for further validation.

Table 5.5, lists some target proteins of potential interest in BC metastasis which have been identified within the metformin-treated cells, as well as the reasons why they have not been taken forward to be validated by Western blotting. The main reason is that some of these proteins stimulate cell proliferation, inhibit cell death and potentiate metastasis, therefore, if they were further up-regulated by metformin treatment, none of these proteins would satisfy the criteria to be chosen as potential targets for anti-metastasis therapy within BC.

Table 5.4: Proteins identified as significantly differentially expressed within the untreated bone and lung homing cells compared to the parental MDA-MB-231 cell-line.

Proteins here are up-regulated and have at least a 1.5-fold increase between the untreated BM and LM cells when compared to the untreated PCC cells. Fold change (FC) was calculated by comparing mean normalized LFQ intensity-values between samples. Status indicates the direction of the differential expression and in which cell type: BM = bone homing BC cells and LM= lung homing BC cells. Entry refers to UniProt entry <http://www.uniprot.org/>.

| Entry | Protein names | Biological Functions | Status | FC |
|------------|--|---|----------|------|
| 1. P08133 | Annexin A6 | Apoptotic signalling pathway, mitochondrial calcium ion homeostasis and ion transmembrane transport | UP in BM | 3.90 |
| 2. P17252 | Protein kinase C alpha type | Positive regulation of angiogenesis, apoptotic signalling pathway, positive regulation of cell migration and adhesion, ERBB2 signalling pathway, histone H3-T6 phosphorylation, intracellular signal transduction, positive regulation of lipopolysaccharide-mediated signalling pathway, positive regulation of mitotic cell cycle and regulation of insulin secretion | UP in BM | 2.68 |
| 3. B7Z574 | Calpastatin | Endogenous calpain (calcium-dependent cysteine protease) inhibitor; involved in the proteolysis of amyloid precursor protein | UP in BM | 2.52 |
| 4. P10515 | Dihydrolipoyllysine-residue acetyltransferase component of pyruvate dehydrogenase complex, mitochondrial | Regulation of acetyl-CoA biosynthetic process from pyruvate, glucose metabolic process, pyruvate metabolic process, cellular nitrogen compound metabolic process and tricarboxylic acid cycle | UP in BM | 2.25 |
| 5. P02794 | Ferritin heavy chain | Cellular iron ion homeostasis, negative regulation of cell proliferation, iron ion transport and negative regulation of fibroblast proliferation | UP in BM | 2.21 |
| 6. B8ZZA8 | Glutaminase kidney isoform, mitochondrial | Glutamine metabolic process | UP in BM | 2.08 |
| 7. O14933 | Ubiquitin/ISG15-conjugating enzyme E2 L6 | Cellular protein metabolic process, ISG15-protein conjugation and modification-dependent protein catabolic process | UP in BM | 2.06 |
| 8. B4DJ81 | NADH-ubiquinone oxidoreductase 75 kDa subunit, mitochondrial | ATP synthesis coupled electron transport | UP in BM | 2.04 |
| 9. Q2TAM5 | RELA protein | Positive regulation of NF-kappaB transcription factor activity | UP in BM | 2.02 |
| 10. Q9NQ50 | 39S ribosomal protein L40, mitochondrial | Mitochondrial translational elongation and termination | UP in BM | 1.92 |
| 11. Q9Y3B7 | 39S ribosomal protein L11, mitochondrial | Mitochondrial translational elongation and termination | UP in BM | 1.88 |
| 12. Q9P0J0 | NADH dehydrogenase 1 alpha subcomplex subunit 13 | Negative regulation of cell growth, mitochondrial electron transport, mitochondrial respiratory chain complex I assembly, negative regulation of apoptotic signalling pathway, positive regulation of protein catabolic process. | UP in BM | 1.83 |

Table 5.4: Continued (legend on previous page)

| | | | | | | |
|-----|--------|---|--|--------------|----------|-------------|
| 13. | O43237 | Cytoplasmic dynein 1 light intermediate chain 2 | ER to Golgi vesicle-mediated transport, microtubule organization and sister chromatid cohesion | cytoskeleton | UP in BM | 1.80 |
| 14. | P31040 | Succinate dehydrogenase flavoprotein subunit, mitochondrial | Anaerobic respiration, mitochondrial electron transport, respiratory electron transport chain, succinate metabolic process and tricarboxylic acid cycle | | UP in BM | 1.70 |
| 15. | Q8N183 | Mimitin, mitochondrial | Cellular respiration, mitochondrial respiratory chain complex I assembly, negative regulation of insulin secretion involved in cellular response to glucose stimulus and respiratory electron transport chain | | UP in BM | 1.68 |
| 16. | Q92522 | Histone H1x | Nucleosome assembly | | UP in BM | 1.67 |
| 17. | Q99798 | Aconitate hydratase, mitochondrial | Citrate metabolic process, generation of precursor metabolites and energy and tricarboxylic acid cycle | | UP in BM | 1.63 |
| 18. | P51970 | NADH dehydrogenase 1 alpha subcomplex subunit 8 | Mitochondrial electron transport and mitochondrial respiratory chain complex I assembly | | UP in BM | 1.63 |
| 19. | Q6WCQ1 | Myosin phosphatase Rho-interacting protein | Actin binding | | UP in BM | 1.60 |
| 20. | Q9H9H4 | Vacuolar protein sorting-associated protein 37B | Macroautophagy and protein transport | | UP in BM | 1.60 |
| 21. | P35221 | Catenin alpha-1 | Epithelial cell-cell adhesion, establishment or maintenance of cell polarity, gap junction assembly, negative regulation of cell motility, negative regulation of extrinsic apoptotic signalling pathway and response to oestrogen | | UP in BM | 1.53 |
| 22. | P49588 | Alanine-tRNA ligase, cytoplasmic | Alanyl-tRNA aminoacylation, tRNA aminoacylation for protein translation, tRNA processing and modification | | UP in BM | 1.50 |
| 23. | P13645 | Keratin, type I cytoskeletal (Human) | Contaminant, human skin | | UP in LM | 18 |
| 24. | P12763 | Alpha-2-HS-glycoprotein precursor (Bos taurus) | Contaminant, bovine serum | | UP in LM | 4.09 |
| 25. | Q3SZ57 | Alpha-fetoprotein precursor (Bos taurus) | Contaminant, bovine serum | | UP in LM | 4.01 |
| 26. | P02769 | Bovine serum albumin precursor (Bos taurus) | Contaminant, bovine serum | | UP in LM | 3.90 |

Table 5.5: Proteins identified as potential targets and reasons why not further validated by Western blot

| Potential candidate | Status | Fold change | Reasons why not taken for future validation |
|-----------------------------|---------------------------|-------------|--|
| Annexin A6 | Up in BM+ 5 mM metformin | 4.99 | Up in BM without treatment by 3.9-fold, it is a negative regulator of apoptotic process |
| Ferritin heavy chain | Up in BM+5 mM metformin | 4.13 | Up in BM without treatment by 2.21-fold, also it has a positive regulation of cell proliferation and was up-regulated by treatment |
| Calpastatin | Up in BM+5 mM metformin | 2.64 | Up-regulated by 2.5-fold in untreated BM cells and has zero LFQ-intensity in one of the triplicate samples |
| Histon H1x | Up in BM+5 mM metformin | 2.27 | Up-regulated by 1.6-fold in untreated BM cells and has zero LFQ-intensity in one of the triplicate samples |
| Protein kinase C alpha type | Up in BM+ 5 mM metformin | 1.5 | Has not passed the 1.5 cut-off point in one of the triplicate samples |
| Catenin alpha-1 | Up in BM+5 mM metformin | 1.27 | Has one zero LFQ-intensity and has not passed the 1.5 cut-off point in one of the triplicate samples |
| Methionine aminopeptidase-2 | Up in LM+ 5 mM metformin | 31.39 | Involved in up-regulation of angiogenesis, and considered as a potential target for anti-angiogenic drugs |
| Protein S100-A2 | Up in LM+ 5 mM metformin | 16.58 | Has zero LFQ-intensity in one of the triplicate samples |
| Tubulin beta-4A chain | Up in PCC+ 5 mM metformin | 1.53 | Has zero LFQ-intensity and has not passed the 1.5 cut-off point in one of the triplicate samples |

5.3.3.5 Global pathway regulation in response to metformin treatment within the Spike-In SILAC (SIS) proteomics experiment

Functional network-based analyses of the 44 proteins altered between metformin-treated (PCC, BM, LM cells) and the metformin-untreated control cells revealed marked activation of molecular processes involved in protein synthesis, cellular respiration, oxidative phosphorylation, ATP synthesis, cellular metabolism, and assembly of mitochondrial respiratory chain complex-1 (RCC-1), as well as signalling pathways associated with cell death and apoptosis and NF-kappa B signalling pathway (Figure 5.10). These altered pathways are all proposed among the direct mechanisms through which metformin can inhibit tumour development³³¹.

The Uniprot identifiers of the 44 proteins were then uploaded to the STITCH website where the output revealed a few interactions between the proteins that were in the majority mitochondrial dehydrogenases, as well as enzyme complexes located within the inner mitochondrial membrane, which are involved in the mitochondrial electron transport chain, oxidative phosphorylation and ATP synthesis (Figure 5.11). However, when the non-connected nodes were removed the interactions were neither significant nor interesting between the other proteins, with the exception of the mitochondrial dehydrogenases, with few unverified and predicted interactions, which indicate that these proteins are not functionally and/or biologically connected.

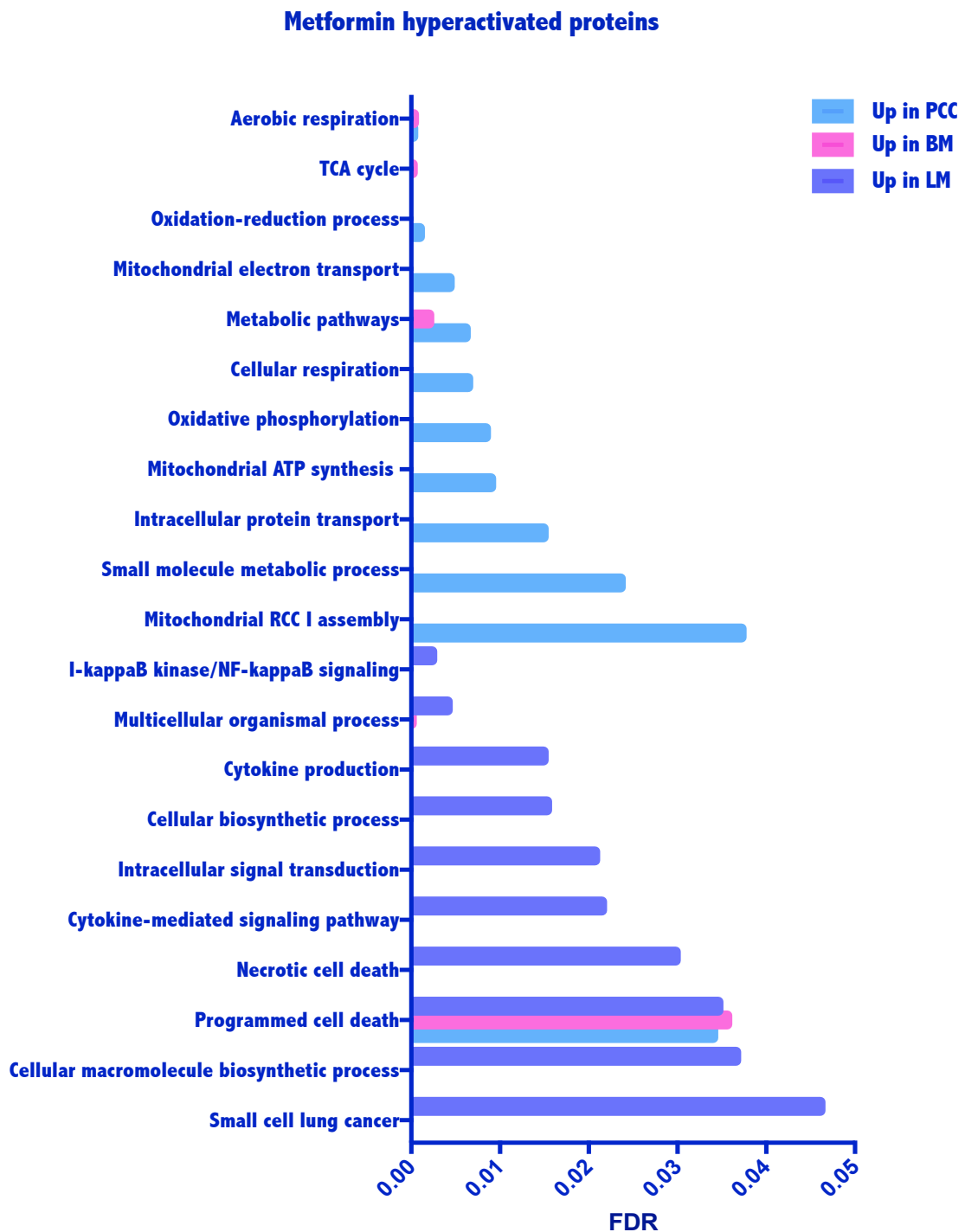


Figure 5.10: Key biological processes and pathways modified by metformin treatment in the parental, bone and lung metastatic breast cancer cells.

Bar graph shows the biological (BP) and KEGG pathways significantly overrepresented in upregulated proteins (Benjamini-Hochberg FDR < 0.05) following exposure to 5 mM metformin in the MDA-MB-231(BM) and MAD-MB-231(LM) cells. In the x-axis, the false discovery rate (enrichment factor) of each category is plotted. TCA: Tricarboxylic acid cycle, Mitochondrial RCC1: Mitochondrial respiratory chain complex.

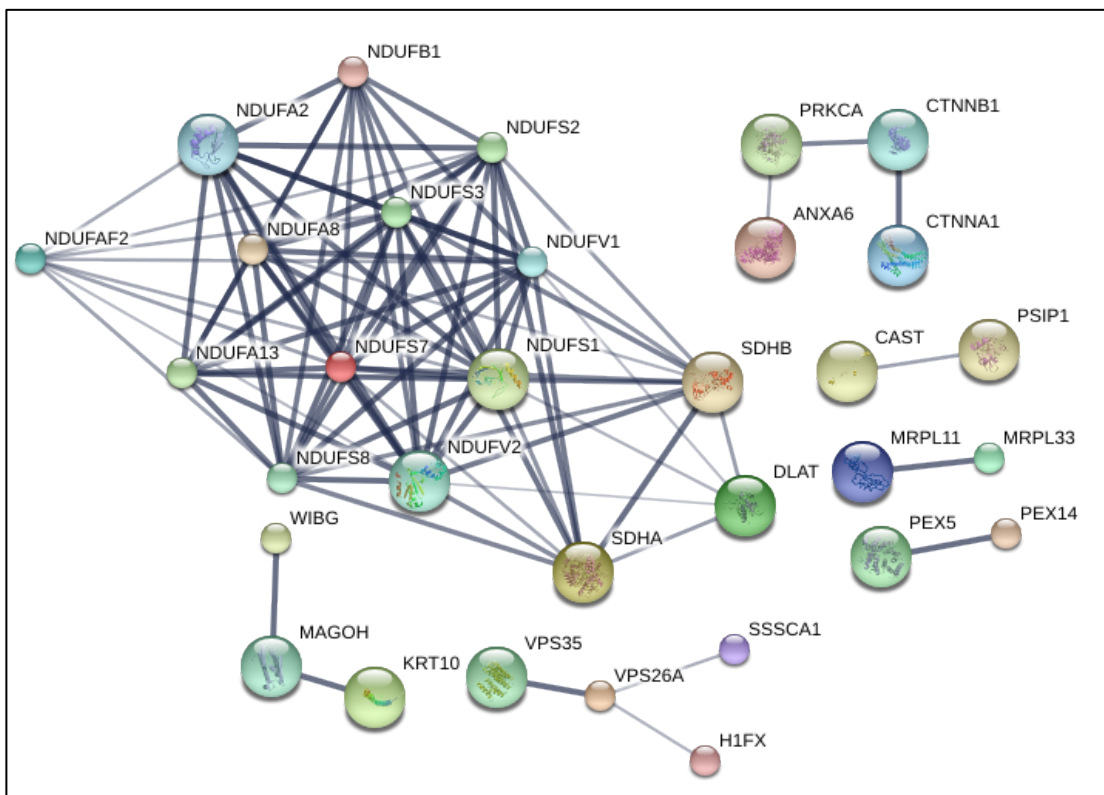


Figure 5.10: Networks identified by STITCH analysis showing the pattern of interactions between the proteins up-regulated by metformin treatment in the three cell lines, with non-connected nodes removed.

Protein-protein interactions are displayed in confidence view. In the network image, the red circle represents the first shell of interaction; NDUFS7: NADH:ubiquinone oxidoreductase core subunit S7. The edges between the nodes that represent protein-protein associations reflect the reliability and confidence of the interaction evidence; thicker lines represent stronger associations. Standard nomenclature gene name abbreviations were used to annotate individual proteins (This can be searched on www.Uniprot.org for more details).

5.3.3.6 Re-testing for candidate proteins identified in the pilot study

In order to examine the reproducibility of our pilot study, the 5 candidate proteins identified in the pilot study were re-examined in the SILAC-based experiment. Generally, there are two forms of data analyses, the first form is based on the analysis of statistically significant differences in the mean intensities between the samples, which have we employed earlier in our LFQ and SILAC-based studies. The second form is based on the detection of unique peptides and statistical significance, which we employed to re-test the targets.

We found that all of them were identified within the 2728 proteins obtained after the data filtration and removal of all proteins with < 1 unique + razor peptide across all samples. However, none of them survived the t-test suggesting that they were not significantly changed. However, these proteins can still be presented as differentially expressed based on the number of unique razor peptides across the three samples (At least 1 unique razor peptide) and importantly the direction of change (increase versus decrease of protein expression or fold-change) fits with the observations in the pilot study analysis, suggesting that these proteins may have relevance, albeit with the caveat that they did not reach the P<0.05 level or pass the cut-off point of 1.5-fold or more for up-regulation and <0.7-fold or less for down-regulation (Table 5.6) in the SILAC -based experiment.

Table 5.6: Re-test of candidate proteins within the Spike-In SILAC (SIS)-analysis data identified as potential targets for metformin

| Target protein ID | Wild-type cell+5 mM of metformin | | | | | Bone-homing cell+ 5mM of metformin | | | | | Lung-homing cell+ 5mM of metformin | | | | |
|-------------------|----------------------------------|----------|----------|---------|-------------|------------------------------------|----------|----------|---------|-------------|------------------------------------|----------|----------|---------|-------------|
| | Number of unique razor peptides | | | P-value | Fold change | Number of unique razor peptides | | | P-value | Fold change | Number of unique razor peptides | | | P-value | Fold change |
| | Sample 1 | Sample 2 | Sample 3 | | | Sample 1 | Sample 2 | Sample 3 | | | Sample 1 | Sample 2 | Sample 3 | | |
| TNFAIP8 | 2 | 2 | 2 | 0.12 | 0.91 | 1 | 2 | 2 | 0.74 | 0.8 | 2 | 1 | 2 | 0.65 | 0.65 |
| GRB2 | 10 | 10 | 11 | 0.72 | 1.27 | 9 | 11 | 11 | 0.81 | 0.79 | 9 | 11 | 10 | 0.21 | 0.72 |
| STAT3 | 16 | 14 | 11 | 0.45 | 0.85 | 15 | 17 | 17 | 0.14 | 1.23 | 14 | 9 | 16 | 0.15 | 0.97 |
| Calmodulin | 10 | 11 | 11 | 0.20 | 1.24 | 10 | 11 | 10 | 0.22 | 1.28 | 11 | 8 | 9 | 0.25 | 1.32 |
| TSPO | 3 | 2 | 2 | 0.65 | 1.34 | 2 | 3 | 3 | 0.45 | 0.87 | 4 | 3 | 2 | 0.52 | 0.91 |

Blue numbers; represent up-regulation, Red numbers; represent down-regulation.

5.4 Discussion

Understanding the molecular mechanisms associated with the anti-proliferative effects of metformin on triple negative metastatic breast cancer cells, and whether they are direct or indirect, primary or secondary (compensatory) effects, or ubiquitous or cell-type specific phenomenon, is fundamental to assess whether metformin can prevent, treat or ameliorate complications caused by cancer metastasis. In an effort to further characterize the complex molecular mechanisms/pathways of metformin action, our proteomic study of breast cancer cell lines, which have the propensity to undergo bone and lung metastasis, revealed several target proteins for metformin action, having functions in, for example, cellular metabolism, cell growth/proliferation, necrotic cell death and apoptosis, cell adhesion/motility /metastasis, signal transduction and transport. Mass spectrometry-based proteomics methods have been very useful in the analysis of complex biological samples across a great many disease types. These studies can both identify and quantify individual protein levels in a global and unbiased manner, and therefore can further improve our understanding of the molecular biology of cancer cells and highlight the cellular processes that are altered within such systems.

5.4.1 Quantitative proteomic analysis of metformin-action within breast cancer: current knowledge and literature gaps

To date, very few proteomic studies have attempted to determine the distinct features of invasive and metastatic breast cancer cell lines in response to metformin^{332, 333}. Only one previous *in vitro* proteomic study has been carried out which compared the effect of metformin on triple negative human breast cancer cell lines in which the investigators have attempted to examine the effects of metformin and phenformin in the context of breast cancer lung metastasis but, so far, no study has looked at BC bone metastasis³³³. The study demonstrated that metformin was able to inhibit local BC growth in immune-deficient mice injected with MDA-MB-436 breast cancer cells and reduced the number of metastatic lesions in the lungs. Metformin has also been shown to target the endothelial compartment in the blood vessels within the tumour resulting in a significant reduction of the endothelial cell component and the generation of dysplastic blood vessels. In the same study, a proteomic assay demonstrated that 5 mM metformin decreased the concentration of several crucial

angiogenesis-related proteins in a co-culture of triple negative BC cells and white adipose tissue (WAT) progenitor cells (targeting both neoplastic and microenvironment cells). However, lower doses of phenformin; a potent biguanide drug, were significantly more efficacious than metformin both *in vitro* and *in vivo*³³³.

Another study using both proteomic and phosphoproteomic label-free quantification methods reported that treating MCF7 cells with 10 mM metformin makes them less sensitive to the pro-growth stimuli and more sensitive to the apoptotic stimuli³³². Additionally, another study was conducted where the researchers attempted to identify whether metformin treatment would affect breast cancer lung metastasis, and reported that the administration of 825 mg/kg/day of metformin over 27 days, to female balb/c mice injected with 66cl4 cells, had a little or no effect on the number or size of metastatic lung lesions³³⁴. However, it was also noted that the metastatic lung lesions displayed increased signals for phosphorylated AMPK, when compared to surrounding normal lung tissue, suggesting that metformin treatment exerted an effect on the metastatic lung lesion. Moreover, a small epidemiological study involving 1,448 diabetic women with TNBC, reported that women who were taking metformin had a lower risk of distant metastases compared to those not taking metformin³³⁵.

Overall, there seems to be enough evidence to indicate a potential anti-metastasis role for metformin within breast cancer. Here, we present a large-scale quantitative global proteomic approach aimed at identifying metformin-induced changes at the proteome level. Observations from this study would provide an integrated picture of the complex alterations within metformin-regulated pathways in metastatic BC cell lines and highlight the modulation of expression of key signalling proteins.

5.4.2 Comparison of cell lines by global proteomics

We examined the similarity and differences of protein expression between the cell lines using two different proteomic techniques.

Initially label-free quantification was used, in a small-scale pilot experiment, to quantify and compare the levels of proteins between the wild-type MDA-MB-231 (PCC) cell-line and its bone-homed (BM) variant. For this study, the analysis was

performed where the MS signal intensities of the same peptides identified within both cell lines are quantified relative to each other without the use of an isotopic standard peptide. This is a frequently used method for determining the abundance of proteins within a proteome.

Next, the spike-In-SILAC labelling system was used which allowed reliable comparisons of proteomic differences between the two heavy and light-labelled samples within a single gel for each replicate, thus avoiding the difficulties associated with gel-to-gel variation and technical variation introduced when samples are prepared separately³³⁶. Furthermore, the labelling within the SILAC-based approach occurs at the protein level allowing samples to be mixed directly (in a 1:1 ratio) after cell lysis thus avoiding the variability associated with sample preparation. Next, the quantitative differences in protein abundance between the samples can be determined by analysing the MS signals of the labelled and unlabelled peptides in the spectrum. As a consequence, one potential limitation is the requirement for matching peptide pairs to be present in both samples; this can lead to a fraction of peptides that cannot be quantified (due to absence of a peptide in one isotopic channel) and consequently a failure to analyse proteins which are significantly expressed in one sample only. Other limitations include the requirements for a high signal-to-noise ratio and high mass accuracy within mass-spectrometry.

In our study, the depth of both proteomic analyses was limited to about 4070 proteins; this limitation might be partially attributed to the high degree of similarity of the three cell lines being compared at the protein level, as well as the limited front-end fractionation (with the use of only 5 SDS-PAGE gel bands). Indeed, more comprehensive mass spectrometric analysis of different BC cell lines can be performed to address this issue in order to further examine the generality of the enormous overlap of proteomes within an increasing number of molecular subtypes.

Both the label-free and SILAC-based quantifications showed an overlap in output data that was much higher than that frequently reported in any other metformin-based proteomics studies. However, in the previous studies^{332, 333}, the proteome was not sampled with the same degree of rigour as there was a selection of specific pathway-related peptides used for sequencing which can subsequently lead to substantial differences in the identified proteins. Additionally, this overlap is also

potentially expected as we have looked at changes in global protein expression and not the phosphoproteomics which is expected to change a lot more. This illustrates the importance of comprehensive proteomic coverage for accurate comparison between cell lines.

The data in this chapter demonstrated that treatment with the potential tissue accumulated doses of metformin results in a significant change in a number of proteomic markers in the non-metastatic TN breast cancer cell line (PCC) as well as the metastatic bone- and lung-derived cells. Of the 4070 proteins identified by label-free quantification, 33 proteins were significantly differentially expressed when compared to untreated cells, after adjusting for multiple comparisons. These proteins reflect a wide range of cellular activities that can be related to cancer, including PI3K/AKT signalling, proliferation, invasion/motility, apoptosis/cell cycle regulation and metastasis.

We observed an increase in the level of GRB2, and TSPO proteins and reduction in the expression of STAT3 and TNFAIP8, by both mass spectrometry and Western blotting after metformin treatment in the primary TN cell line (PCC). These associations have not been previously reported. However, most of the molecular, cellular, KEGG and signalling pathways reported in our mass spectrometry study are consistent with prior pre-clinical observations reported by another study, which was performed primarily in the MCF7 cells exposed to 10 mM of metformin³³². Therefore, metformin treatment at a dose as low as 0.3 mM can alter these identified pathways. This is a novel and promising finding for the role of therapeutically relevant concentrations of metformin within BC prevention and treatment in the clinical setting.

Interestingly, most, but not all, candidate proteins that were identified as changed by mass spectrometry analysis were consistently altered following metformin treatment in all three triple negative BC cancer cell lines, when assessed by Western blot, calmodulin is a good example of this, and this appears to be the case with other proteins detected in this study.

Inconsistent with the list of molecular and signalling pathways identified in the pilot study, most of the pathways identified to be up-regulated in the large-scale

Spike-In-SILAC experiment, were apparently related to molecular mitochondrial processes. In some ways this is not surprising as in diabetes, metformin has been reported to be a weak mitochondrial poison, working as a respiratory chain inhibitor and thereby reducing mitochondrial activity. This shifts cellular respiration toward aerobic glycolysis, a process called the conventional “Warburg effect”. In cancer, metformin is thought to prevent malignant cells from using their mitochondria for energy production. However, it has been suggested by several studies that aggressive cancer cells have functional mitochondria that can rescue the aerobic glycolysis process³³⁷⁻³³⁹. Additionally, a proteomic analysis of breast cancer cells with a tendency for brain homing has directly demonstrated up-regulation of mitochondrial enzymes involved in the tricarboxylic acid cycle (TCA) and oxidative phosphorylation³⁴⁰.

In our study, the current analysis (Figure 5.10) also supports an association between the up-regulation of mitochondrial oxidative phosphorylation and the TCA cycle in the three untreated cancer cells as well as an association with the tendency for BC metastasis, due to these proteins being up-regulated more in the BM and LM cells compared to PCC. However, we could not draw a firm conclusion as to whether the up-regulation of mitochondrial enzymes seen after metformin exposure was as a result of the direct effects of the drug or as a result of the aggressive phenotype of the cells used, as there is always one zero LFQ-value in each of the treatment groups. That said, mostly the same enzymes were also identified to be up-regulated by roughly a similar magnitude of fold changes in the untreated cells (1.5-2 fold), and these folds were not significantly higher after metformin treatment suggesting that it is not a metformin effect.

Our results are also consistent with the notion that mitochondrial toxins should be used for cancer chemoprevention as well as chemotherapy and provide further circumstantial evidence that at relatively high concentrations (5 mM), metformin targets the mitochondria. Although metformin is considered to be a weak mitochondrial toxin, this could be one of the mechanisms through which metformin can prevent cancer development.

It is important to note that it was beyond the framework of this project to identify global changes in the proteome of the untreated cells, except as controls for the purpose of comparison with treated cells. However, our findings were inconsistent

with previous work by Westbrook and colleagues who identified at least 75 proteins with statistically significant fold changes between BM and PCC cells³³⁰. In fact, they identified 8 proteins that were up-regulated in BM cells only and none of these 8 proteins appeared on our list. However, unlike our global proteomic approach, they used the 2D-DIGE gel-based method for proteomic analysis and not the Spike-in SILAC method which may account for some of the differences seen. Issues with the proteomic studies may also have accounted for these differences as discussed previously and below.

5.4.3 Issues in performing proteomics studies using cell lines

5.4.3.1 Candidate selection

Interesting candidate proteins were drawn from the pilot study (TNFAIP8, GRB2, STAT3, TSPO and calmodulin), but not from the large-scale Spike-In SILAC experiment (reasons are explained in section 5.3.3.3 and table 5.4). None of these proteins have been previously identified as potential targets for metformin treatment within breast cancer metastasis. However, it should be noted that the fold differences were not profound (1.5-1.7-fold), albeit not atypical for proteomic studies, and only borderline in most cases, and there was no strong on and off effect in the mass spectrometry results (although this was not the case in Western blot analysis where clear differences were seen).

The fold difference in these proteins within the three cell lines tested and within the treated and untreated groups is strongly influenced by the mean LFQ intensity, which is itself skewed if there is a zero value in one of the biological replicates (or even by a higher value in one sample). Although biological replicates are preferable to technical replicates for improving the efficiency of statistical testing, typically the biological variability is substantially greater than the technical variability. Therefore, our use of three biologically distinct repeats per cell line tested may account for the variability in mass spectrometry results within each triplicates of a biological population.

When candidates from the pilot study were re-tested in the main experiment the results imply that they could still be potential candidates (based on the presence of at least 1 unique peptide), or excluded as candidates (based on a lack of statistical

significance, potentially for over-interpretation of a zero value in one sample and failure to meet the cut-off point overall). This demonstrates both the value and the limitations of mass spectrometry analyses where different approaches could be used to analyse the data. Another possible limitation is the use of STITCH pathway analysis as an important criterion for candidate selection, as this can be limited by the fact that some of the relationships between the identified target proteins might be based on low quality publications and/or indirectly inferred interactions.

5.4.3.2 Technical issues and methodological constraints

Generally, the accuracy of proteomics analysis relies on the methodological approach being used. In this study, we performed proteomic profiling of three biological replicates per cell line by 1D gel electrophoresis with consecutive mass spectrometric protein analysis and then confirmed the validity of protein expression data by Western blotting using specific antibodies.

Major limitations of 1D gel electrophoresis include limiting the analysis to more abundant proteomic alterations because of the difficulties in detecting differentially expressed proteins of low abundance following peptide-extraction from the gel-slices, as well as the necessity for high-purity reagents to reduce interference by contaminants during heavy and light isotopic labelling. Therefore, in order to increase the sensitivity of the overall workflow and to overcome these limitations, several strategies can be employed such as optimization of the protein extraction protocol and downstream protein fractionation procedures.

Moreover, discordance between the candidate proteins observed within small-scale versus large-scale studies has been encountered in this work, which could be affected by both the biological system studied, variation between technical repeats and in addition the half-life and stability of the proteins being studied. These variables are critical to consider when interpreting proteomic findings based on pilot studies and show that interpretation of those results should be done with caution.

However, despite these limitations, our study has some strengths including the fact that we performed a thorough exploration of the metformin treatment altered proteomic markers identified in the pilot study using the same whole cell lysates from the three biological replicates used for the large-scale experiment; as validated by

Western blot analysis of the five selected candidate proteins. In addition, we had a sufficient number of treated samples to compare to a control/untreated group. Even though the majority of our candidates have not survived the statistical significance test in the large-scale SILAC experiment, they have passed the number of unique peptides test (Table 5.6).

Weaknesses of the SIS-analysis include a relatively small number of proteins identified as being differentially expressed. In addition, the cell lines used were primarily hormone receptor negative invasive and metastatic breast cancers, and it is unclear whether these results can be generalized to other BC subtypes. Ideally, we would have compared between the hormone receptor negative, hormone receptor positive (MCF7 or T47D) and early non-invasive (DCIS or ADH) cells to create a heterogeneous population of assessed tumour cell lines.

The five candidate proteins identified (**TNFAIP8**, **GRB2**, **STAT3**, **TSPO** and **calmodulin**) are now discussed in more detail.

5.4.4 Candidate proteins

5.4.4.1 Tumour necrosis factor alpha-induced protein 8 (TNFAIP8, 21kDa)

Tumour necrosis factor- α -induced protein 8 (TNFAIP8), an oncogenic anti-apoptotic factor and NF-kappa-B-inducible protein, is the first discovered member of the conserved TIPE family (tumour necrosis factor- α -induced protein 8-like) of proteins. TIPE members are newly described regulators of cell proliferation, oncogenesis, tumour progression and inflammation³⁴¹. However, the mechanisms behind these actions are as yet unknown.

Overexpression of TNFAIP8 frequently occurs in several types of cancer including breast and is associated with poor prognosis³⁴². Exogenous expression of TNFAIP8 in human breast cancer cells resulted in enhanced cell proliferation, migration and invasion³⁴³. At the same time, knocking down TNFAIP8 expression in breast tumour cells reduced their tumorigenicity³⁴³. In a recent study by Zhang and colleagues³⁴⁴, down-regulation of TNFAIP8 expression in human prostate cancer cells reduced pulmonary colonization of malignant cells and improved sensitivity of the tumour xenograft to radiation and docetaxel. Moreover, TNFAIP8 knockdown in prostate and breast cancer cells was found to be associated with decreased expression

levels of several oncogenes including S100P, MALAT1, MET, KRAS and FOXA1 as well as increased expression of several apoptotic and anti-proliferative genes such as FAT3 and IL-24. Similarly, TNFAIP8 knockdown cells also manifested reduced expression of several oncoproteins such as EGFR, SRC, ABL1, IL5 and GAP43³⁴⁵. Additionally, TNFAIP8 has been also found to be predominately involved in the hypoxia-inducible factor-1α (HIF-1α) signalling pathway and cancer development signalling networks³⁴⁵. Collectively, these studies outline a critical role for TNFAIP8 in the regulation of cancer cell survival and tumour progression in a multifaceted manner.

Here we have investigated, for the first time, the effects of metformin on the protein expression profile of TNFAIP8 in breast cancer cells that have the ability to metastasize to bone and lung. Our results indicate a unique cell-type based response to metformin treatment, while all cells significantly respond to the 5 mM dose; the metastatic lung cells were particularly sensitive to the clinically relevant dose of 0.3 mM. In conclusion, the present data demonstrated that metformin can significantly down-regulate the expression level of oncogenic TNFAIP8, and therefore may abolish its role in tumour progression. Moreover, in the era of targeted therapy, metformin may have the potential as an anti-metastatic agent to treat the lung spread of breast cancer.

5.4.4.2 Growth factor receptor-bound protein 2 (25 kDa)

The growth factor receptor-bound protein 2 (GRB2) has long been known as a key downstream protein in signal transduction initiated by various receptor tyrosine kinases (RTKs). Evidence suggests that GRB2 is used by RTKs to activate the mitogenic and transforming Ras/Raf/Mek/MAP kinase pathway³⁴⁶. Therefore, GRB2 inhibition will lead to MAPK inactivation. GRB2 was also found to be critical for the proliferation of BC cells that express EGFR or ErbB2 tyrosine kinases³⁴⁷. In a study that set out to determine the effect of disrupting the downstream tyrosine kinase signalling of EGFR in breast cancer cells that express high levels of ErbB2, down-regulation of GRB2 resulted in selective growth inhibition in breast cancer cells³⁴⁷. Other studies showed that following EGFR activation, increased association with GRB2 occurs, which intensifies EGFR oncogenic signalling and promotes cell growth³⁴⁶. Conversely, when GRB2 protein was down-regulated, EGFR signalling was disrupted and growth suppression occurred³⁴⁸ (Figure 5.12).

Furthermore, almost every paper that has been written on metformin in oncology proposes the impact of metformin on the role of insulin as a mechanism through which metformin might prevent cancer development. In this context, GRB2 has been found to mediate cross talk (and to propagate the signals) between the insulin receptor and the Ras/Raf/ERK pathway, a known driver of cell growth and proliferation. Insulin/IGF-1 is involved in carcinogenesis through up-regulation of the insulin/IGF receptor signalling pathway (see introduction chapter) whereby IGF-1 produced by the liver and binds to the IGF-1 and insulin receptors and transmits the signals to phosphoinositide 3-kinases (PI3K) and the Akt/protein kinase through insulin receptor substrate (IRS) proteins, and thus indirectly activating mTORC1 (Figure 5.12). The findings that GRB2 plays a critical role in breast carcinogenesis and therefore may have strong implications for novel molecular targeting strategies, has provide a rational for us to choose this protein as a candidate to explore the impact of metformin treatment on our aggressive metastatic BC cell lines. To our knowledge this is the first study exploring the inhibition of this protein in response to metformin treatment in breast cancer.

Consistent with the observations from our pilot study, Western blot validation analysis also demonstrated a significant up-regulation of GRB2 protein in the parental triple negative breast cancer cells and down-regulation in the fully bone-homed and lung homed cells. The most surprising aspect of the data is the strong on and off effect that metformin has on this protein in the parental and lung-homed cells respectively. The profound down-regulation of GRB2 in some cells may partially explain why it was undetectable in metformin-treated bone- and lung-homed cells in the large-scale experiment. However, the GRB2 was profoundly up-regulated following exposure to 5 mM of metformin in the parental MDA-MB-231 cell line, which may therefore, suggest that metformin might have a harmful effect in the early metastatic stage of triple negative BC. However, it is important to note, that this is only a single protein in a very complex set of pathways and its effects may be counteracted by the effects of metformin on another protein.

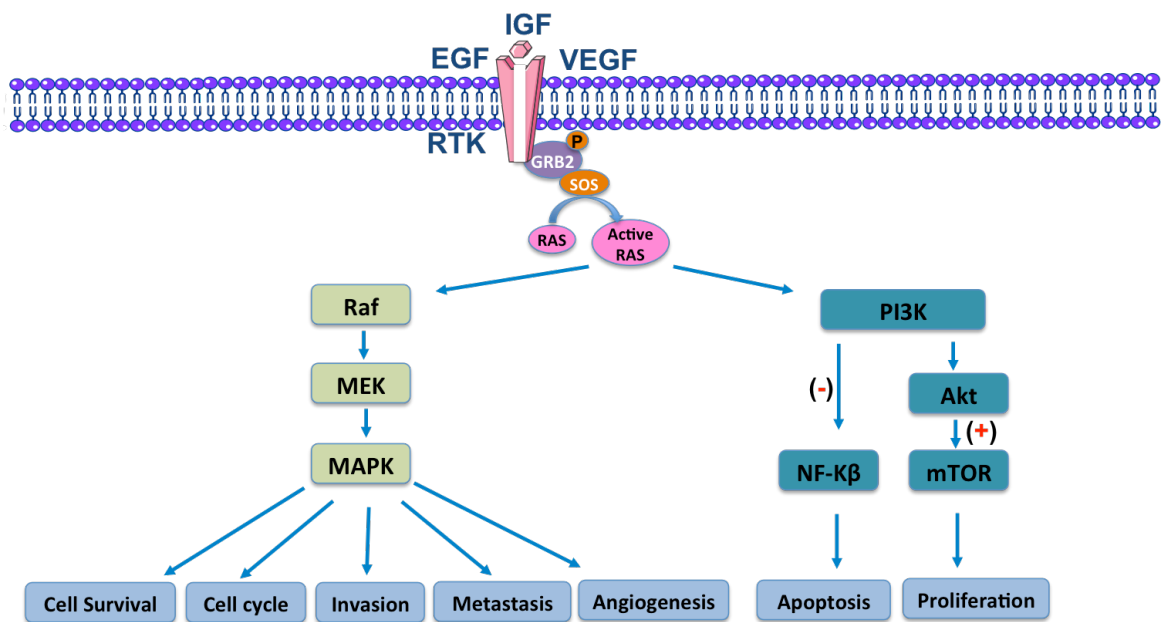


Figure 5.12: GRB2 mediates signalling between various receptor tyrosine kinases (RTKs) and the Raf/MEK/AMPK and PI3K/ERK pathways.

Upon ligand binding, activation of IGFR, EGFR or VEGFR occurs, which leads to increased receptor association with GRB2, followed by phosphorylation of SOS and subsequent activation of Ras. Ras, in turn, fosters several oncogenic signalling pathways, thereby increasing cell survival and proliferation through Raf/MEK/AMPK and PI3K/Akt/mTOR pathways. Conversely, when phosphorylation of GRB2 is inhibited or down-regulated, EGFR/IGFR/VEGFR signalling is disrupted and growth inhibition occurs (some elements of this figure were produced using Servier Medical Art: <http://www.servier.com/Powerpoint-image-bank>).

Together these findings provide an important insight into another unrecognized molecular action through which metformin may curtail the growth of TN metastatic breast cancer cells. Nonetheless, it remains to be elucidated if this action was exerted through the EGFR or the RAS/RAF/MAPK pathways via MAPK-dependent and/or independent mechanisms.

5.4.4.3 Signal transducer and activator of transcription-3 (85 kDa)

Signal transducer and activator of transcription-3 (STAT3), belongs to a family of transcription factors, which transcriptionally regulate a divergent array of cellular processes via integrating cytokine and growth factor signalling³⁴⁹. STAT3 is aberrantly constitutively activated in numerous epithelial and haematological malignancies, including more than 40% of breast cancer subtypes. Indeed, in breast cancer it is most frequently associated with triple-negative tumours and is thought to play a critical role in the pathogenesis of this highly aggressive cancer subtype³⁴⁹. In

contrast to tight regulation of STAT3 as a latent transcription factor in normal breast cells, its signalling in breast carcinogenesis is multifaceted. In various breast cancer types, STAT3 activation can be induced both directly or indirectly by receptors with intrinsic kinase activity such as epidermal growth factor receptors (EGFR) and vascular endothelial growth factor receptors (VEGFR). Furthermore, abnormal STAT3 signalling enhances BC progression through dysregulation of expression of the downstream target genes which regulate cell proliferation (e.g Bcl-2, and cyclin D), angiogenesis (e.g VEGF and Hif1 α) and epithelial to mesenchymal transition (e.g MMP-7, MMP-9 and Vimentin) (Figure 5.13).

Indeed, several studies have provided compelling evidence for the critical role of aberrant STAT3 activity in controlling a large number of phenotypic responses such as cell proliferation, survival, anti-apoptosis, angiogenesis, epithelial to mesenchymal transition, invasion and metastasis, therefore validating STAT3 as a promising therapeutic target for breast cancer^{337, 350} (reviewed in detail in references^{349, 351, 352}). These multiple modes of interactions make STAT3 a master linking point for a great number of signalling processes. However, this highly interconnected nature might render it difficult to target STAT3 signalling pathway as a treatment strategy due to lack of selectivity and risk of possible side effects.

Previous research has indicated that STAT3 is a critical regulator of metformin action in a panel of triple negative breast cancer cells (MDA-MB-231, MDA-MB-468, BT20, HCC70, HCC1806 and HCC1937) using a dose range of 10-20 mM. While ectopic expression of STAT3 partially attenuated the effect of metformin on these cells, STAT3 knockdown enhanced metformin-dependent growth inhibition and induced apoptosis³⁵³. In the same vein, metformin has been shown to act synergistically with a selective STAT3 inhibitor to inhibit cell growth and induce apoptosis in TNBC³⁵³. Additionally, recent studies suggest that metformin treatment reduces the expression of several key drivers of the epithelial-mesenchymal transition machinery in several types of cancer^{224, 354-356}. However, the potential activity of clinically relevant doses of metformin against STAT3 in the aggressive metastatic bone and lung homed cells has not been previously tested.

Due to its critical role in human oncogenesis, STAT3 activation may be paramount in the BC metastasis to bone and lung. Given the aforementioned

associations between activation of the STAT3 pathway in TNBC cells and stem cell maintenance, as well as the unique biological effect that metformin has exerted on both cells, the effect of the clinical and potential tissue accumulated doses of metformin on STAT3 levels in the three metastatic cell lines was investigated.

In our proteomic pilot study, we found that metformin significantly down-regulated STAT3 protein levels in both the parental and bone metastatic cell lines. We also performed Western blot analysis and demonstrated for the first time that the total STAT3 expression was significantly down-regulated in the three metastatic cell lines at both tested concentrations including a dose as low as 0.3 mM, with the lung-homed cells being the most responsive. However, the molecular mechanism by which metformin suppresses STAT3 in these cells remains unclear. Most noteworthy, however, STAT3 was not highly expressed by the three control cells when untreated, as demonstrated by their weak signal strength in Western blot.

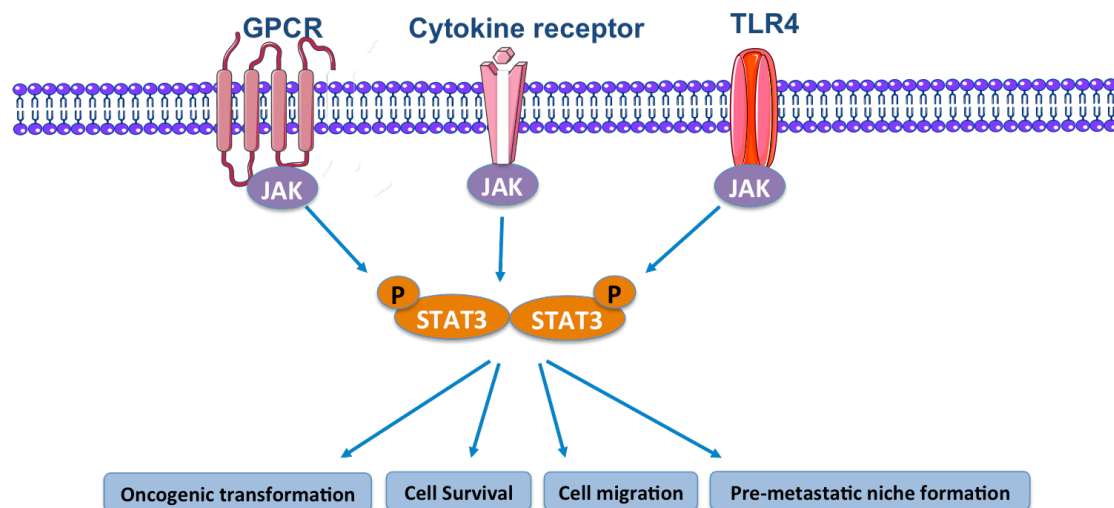


Figure 5.13: Activation and regulation of the STAT3 signalling pathway.

The recruitment and phosphorylation of the STAT3 pathway is triggered by activation of cell surface receptors (G-protein coupled receptor, growth factor Toll-like receptor 4, IL-6 or cytokine receptors) leading to activation of the JAK-family of proteins. Phosphorylation of STAT3 results in translocation of activated STAT3 dimers to the nucleus. In the nucleus, STAT3 binds to the promoters of genes and activates a sequence of downstream cellular processes that are required for cancer progression. STAT3, signal transducers and activators of transcription 3; JAK, Janus kinase; GPCR: G-protein coupled receptor, TLR-4: Toll-like receptor 4 and IL-6: interleukin-6 (some elements of this figure were produced using Servier Medical Art: <http://www.servier.com/Powerpoint-image-bank>).

5.4.4.4 Translocator protein (TSPO, 18kDa)

The translocator protein (TSPO), previously known as the peripheral benzodiazepine receptor (PBR), is an 18kDa outer mitochondrial membrane protein. TSPO is expressed in almost all tissues, although its expression is particularly high in organs involved in steroidogenesis, the process by which cholesterol is converted to active steroid hormones, such as adrenal glands, testes, prostate and ovaries, owing to the major role TSPO plays in steroid biosynthesis³⁵⁷. A large body of literature supports the notion that TSPO is excessively over-expressed in highly aggressive tumour phenotypes, including those of the breast, and this expression is strongly involved in mammary gland morphogenesis and advancing BC stage^{358, 359}. When compared with oestrogen receptor positive breast tumours, TSPO levels are found to be higher in ER-negative breast tumours. Furthermore, stable overexpression of TSPO in the non-transformed MCF10A cell line, in a 3D matrigel culture system, drives acinar cell proliferation and contributes to resistance to luminal apoptosis; changes that resemble phenotypes found in early stages of BC such as ADH and DCIS³⁶⁰. On the other hand, TSPO overexpression promotes the proliferation of MCF7 cells (luminal ER⁺), whereas silencing this protein diminishes the proliferation of MDA-MB- 231 cells (ER⁻, claudin-low)³⁶¹. Moreover, treating multiple cancer cells with synthetic TSPO ligands resulted in increased apoptosis and reduced the viability of both ER-positive and ER-negative cells³⁶². Taken together, these data suggest that targeting TSPO may prove useful for the treatment of receptor-negative BC subtypes, particularly in combination with other mitochondria-targeting agents providing a rational for testing the effect of metformin on TSPO protein expression at the most advance stages of breast cancer progression, namely bone and lung metastasis.

Consistent with our proteomic analysis data, this study reports for the first time that TSPO was up-regulated in the parental MDA-MB-231 cells treated with 5 mM of metformin and significantly down-regulated at both testing doses in both bone- and lung-homed cells, although it did not pass the statistical significance test in the large scale-experiment. These findings suggest that metformin could be effective against TSPO expression in the most aggressive phenotypes of BC that will home to the lung or the bone.

5.4.4.5 Calmodulin (17 kDa)

It has been recently demonstrated that the ubiquitous calcium-receptor protein, calmodulin, mediated EGF-initiated activation of the oncogenic Akt pathway in the majority of BC cell lines³⁶³. This effect was particularly evident in the ER-negative but not ER-positive phenotypes³⁶⁴. Calmodulin antagonists were shown to abolish the Akt pathway activation in mouse mammary epithelial cells and human ER-negative BC cells, thereby inactivating a number of apoptosis related proteins and interfering with programmed cell death, therefore, confirming the involvement of Akt signalling transduction pathways³⁶⁵.

Based on the broad spectrum functions of calmodulin; which are required by the malignant cells to achieve certain physiological processes such as growth, angiogenesis, metastasis and tumour stemness³⁶³, one can conclude that targeting of calmodulin-dependent signalling processes might offer great potential for the treatment of breast cancer.

Although calmodulin was reported to be significantly down-regulated by both drug doses in our pilot study, contrary to expectations, our Western blot study did not find a significant difference in calmodulin expression between metformin-treated and untreated parental and bone metastatic breast cancer cells and furthermore it did not pass the statistical significance test in the large-scale experiment. Surprisingly, the metastatic lung-homed cell line showed a unique response to both clinical and tissue accumulation doses of metformin demonstrating a clear reduction in calmodulin expression. The findings from our proteomics study and Western blot analysis in the presence of metformin treatment in the context of breast cancer represents a novel area that has not been tested before and the data suggest that although the action of metformin might not be calmodulin-dependent and not significantly important for bone metastasis, this pathway is potentially important for BC cells metastasizing to the lung.

In summary, to our knowledge this is the first study that evaluates the effect of the clinical relevant dose of 0.3 mM of metformin in the three metastatic breast cancer cell lines using global proteomics. In this chapter we have demonstrated that clinical- and potential tissue-relevant doses of metformin are associated with a number of

significant proteomic changes, including previously unreported changes in TNFAIP8, GRB2, STAT3, TSPO and calmodulin proteins in TNBC cells as well as their aggressive lung and bone homing metastatic variants, observed under our *in vitro* conditions. Our observation of these interactions suggest that treatment with metformin may provide significant benefits to triple negative cancer patients and combination targeting may have the potential for enhancing metformin's efficacy in the clinical setting. We have yet to determine if the GRB2, STAT3, TNFAIP8 and TSPO proteins are critical for metformin action in other molecular subtypes of breast cancer.

Although the label-free quantification pilot study used earlier in this project was promising, it was hampered with its limited capacity to achieve great depth and unfortunately most of the identified markers have not been further validated due to the time constraint. The complexity and overlap of the cellular proteome and the lack of reproducibility of some samples also hampered the in-depth quantitative proteomic profiling using Spike-in SILAC. This leads to a limitation in the interpretation of the data as only two of each triplicate clustered together as duplicates rendering it difficult to detect a statistical significant difference within small sample sizes; any test used will be much less powerful.

Another caveat is that, we have expected to see the same candidates identified in the pilot study with the same magnitude of significance in the large-scale experiment but we have not and we still do not know why. Ideally, the SILAC-based experiment could have been repeated but time and cost prevented that. Therefore, further work is needed to confirm these findings and to establish whether these are the only mechanisms by which metformin is working.

Furthermore, it would be interesting to compare the proteomic profiles of the metastatic cell lines with the pre-invasive models of disease in a future experiment.

6. Chapter 6: General discussion

The chemopreventive and chemotherapeutic effects of metformin are currently being evaluated for the treatment of different types of malignancies including breast cancer. Although its mechanism of action remains only partially understood, metformin is thought to curtail cell proliferation via activation of the AMPK signalling pathway, thus directly inhibiting the main anabolic processes that sustain cancer cell growth and proliferation. Although these mechanistic facts have long been appreciated, only recently significant uncertainties with respect to the right drug dosage to be used in the preclinical research have become a major concern. For example, a frequently cited criticism of almost all preclinical studies involving metformin is the use of *in vitro* concentrations that are considered to be 10-100 times higher than the maximally achievable therapeutic serum concentrations found in diabetic patients³⁶⁶. In contrast to the therapeutic serum concentrations of metformin in diabetic patients that is achieved in the micromolar range (approximately 20 μ mol/ml, in patients treated with 500-2000 mg/day orally), metformin toxicity across various breast cancer cell lines was achieved in the millimolar range (1-10 mM)³⁶⁷.

Although this appears to be quite a difference, there may be a few possible explanations. To begin with, the media used in tissue culture often contains supraphysiologic glucose concentrations (17 mM which is typically incompatible with human life) that may limit the response to metformin. Furthermore, it has been shown that metformin accumulates in the tissues of diabetic mice²⁵⁰ and humans³⁶⁸ at concentrations significantly higher than those in blood, which potentially justifies the use of the 1 mM and 5 mM concentrations applied in this study, to be considered potential tissue accumulation doses. Using a formula for dose translation from human to the *in vitro* setting based on the molecular weight of metformin and human plasma equivalency dosing range of 4 mg/l to 40 mg/l^{244, 245, 248, 249}, it is considered that a range of 0.03 mM to 0.3 mM would be similar, and certainly not higher, to that expected in human plasma. It should be taken into consideration that there is huge variation in the therapeutic concentrations reported to date due to inter-individual variations in the plasma concentration of metformin. Another critical issue is data on metformin concentrations in the major deep compartments and tumour tissues are evidently not available in clinical practice, therefore, the plasma values obtained

should be interpreted with caution as they are less informative and do not necessarily reflect metformin tissue concentrations. Indeed, this thesis set out to evaluate the *in vitro* effects of the clinically relevant doses of metformin, as well as the potential tissue accumulated doses on breast cancer growth and proliferation.

A growing body of evidence suggests that the anti-neoplastic activity of metformin in breast cancer tissues requires the expression of the right cell surface transport molecules as well as adequate tissue concentrations of the drug. Consequently, tumour cells that do not express the required transporters are immune to the direct effects of metformin as it is unlikely that metformin would accumulate to a concentration that would allow for direct action following conventional doses used in diabetic patients.

As a result, this thesis first aimed to investigate the expression of metformin transporters and their potential contribution to the antiproliferative effects of metformin more fully. The work performed in this thesis demonstrated that normal, pre-malignant, pre-invasive and invasive human breast cell lines and tissues as well as the metastatic bone-homed cell line express sufficient amount of metformin uptake (OCT1-2, PMAT) and efflux (MATE1) transporters to facilitate metformin disposition into various breast cells, which suggests that metformin has the potential to be efficacious in these cell lines.

To our knowledge this is the first time a comprehensive investigation of metformin uptake and efflux transporters in cultured cell lines/tissues representing the entire spectrum of breast disease progression has been demonstrated, although OCTs and MATEs expression has been previously reported in some of the invasive breast cancer cells²⁷⁹. Data from the *in vitro* cell-based assays, RT-qPCR and Western blot, suggest that gene and protein expression of metformin transporters differ at various stages of breast cancer development and probably reflect the role of these proteins in the delivery of essential nutrients and drugs into normal as well as cancer cells. Furthermore, data also suggest that multiple transporters are likely to be involved in metformin transport in breast cell lines and tissues and there might be an overlap between them. Both MCF7, T47D and MDA-MB-231(BM) cells expressed high level of OCT2, PMAT and MATE1 proteins and low level of OCT1 protein while the MDA-MB-231 cells expressed high level of OCT2, OCT3, PMAT and MATE1 proteins and low level of OCT1. Expression data demonstrate that unlike liver tissue

in which OCT1 has been demonstrated to be essential for metformin entry into the hepatocytes, OCT2-3 and PMAT may play a major role in metformin intracellular uptake in breast cancer cells.

In order to assess whether metformin activity requires expression of specific transporters, assessment of the relative contribution of each individual transporter to metformin uptake and excretion is required as future work. This can be achieved by using a combination of transporter-specific inhibitors and a cocktail of inhibitors to estimate their contribution to metformin transport. Alternatively, both transporter-competent, transporter-deficient and transporter-overexpressing cell lines can be used to confirm the involvement of a specific transporter in metformin uptake. Additionally, stable transporter-knockdown clones can be generated to elucidate the contributions of several transporters in metformin transport across biologic barriers. These models can be applied in future studies to explore intracellular accumulation and optimal dosing of metformin. However, the only caveat would be the presence of unidentified transporters that might also contribute to metformin uptake and excretion.

Data in this thesis also suggest that metformin might be actively transported across the mammary epithelium and accumulate in breast cancer cells due to inefficient egress as a result of lack of MATE2 efflux transporter but the relevance of this observation remains unclear until further uptake studies are performed. Uptake studies such as flow cytometry with fluorescently labelled metformin would enable the measurement of intracellular metformin concentrations and consequently determine the optimal dosing required for promotion of the anti-cancer activity. This emphasizes the need to screen cancer cell lines for transporter expression prior to selecting relevant cell lines for investigating the anticancer effects of metformin and also suggest the use of MATE2 as a potential clinical biomarker of metformin resistance. However, cellular uptake and excretion are not the only limiting factors for the anti-neoplastic activity of metformin as the presence of competent signalling pathways is also of prime importance.

In parallel with the cell-based assays results, an *ex vivo* experiment in the form of immunohistochemical staining of human surgical specimens also suggests that metformin might be of clinical significance in patients with pre-invasive disease as well as early stages of invasive breast cancer (stage I-II). However, it is quite

interesting to look at the hormonal receptor status in relation to transporter expression in breast tissues in future experiments.

Our *in vitro* and *ex vivo* data demonstrating variability in the influx transporter expression profiles in human breast cell lines and tissues, thus reflect the degree of variability among cells comprising human breast tumours, and hence suggest that the outcomes to metformin therapy in breast cancer could be highly variable. Hence it is vitally important that the relationship between transporter expression and metformin response in patient tumours should also be established in future studies.

It is also worth considering, the finding that invasive BC cell lines express low levels of some cationic transporters, compared to the normal, pre-malignant and pre-invasive cells, may justify the use of supra-pharmacological drug concentrations to target these immortalised cells *in vitro*. Interestingly, previous literature demonstrated that the uptake of metformin into BC cell lines could be greatly enhanced by ectopic expression of organic cation transporters such as OCT3²⁷⁹. This therefore, underscores the importance of the balance between the dosage and time of exposure as a key determinant for metformin's action to overcome the low abundance of tissue/cell-specific organic transporters.

While most of the previous investigators examined the effects of supra-pharmacological doses of metformin in breast cancer cell lines, in this study the anti-proliferative activity of the clinically relevant doses has been profiled across a panel of increasingly transformed human breast cell lines using 3 different cell proliferation assays (Chapter 4). In the cell counting and BrdU assays, metformin was found to inhibit the proliferation in a dose dependent manner in most cell lines. Data demonstrated that the clinical and potential tissue accumulation doses of metformin are potent inhibitors of the highly aggressive triple negative breast cancer cell line and its metastatic bone-homed variant compared to invasive breast cancer cells with positive oestrogen receptor status, although the pre-invasive cells were the most sensitive. Indeed, the ability of metformin to inhibit the proliferation of the pre-malignant cells might underlie the epidemiological observation that diabetics treated with metformin have a lower incidence of breast cancer. However, there is a caveat to the data as these pre-malignant cells have been transformed to grow in culture and have a much higher proliferation rate than the invasive cells, and than they would *in*

situ, so the results may simply relate to proliferation rate and not to their pre-invasive/pre-malignant nature.

Interestingly, there was a more uniform response to the anti-proliferative effect of the lowest clinical relevant dose of metformin (0.03 mM) in the colony survival assays across all the tested pre-invasive, invasive and metastatic bone-homed cell lines. Similarly, the clinically relevant doses have been also shown to arrest cell cycle progression in all breast cells regardless of their stage and hormonal receptor status. Additionally, these doses were effective in suppressing the migration ability of the three invasive cancer cells investigated.

Therefore, the data in this thesis demonstrate that clinical doses of metformin can produce anti-proliferative, anti-invasive and anti-metastatic effects *in vitro* indicating that metformin can act directly on target cells and is not solely reliant on reducing serum insulin levels. This does not minimize the proposed indirect, insulin-dependent, mechanism of action of metformin, but, rather, indicates that the anti-neoplastic effects of metformin on breast cancer likely represent a combination of both direct and indirect effects.

Importantly, in this thesis the cytotoxic effect of clinical doses of metformin has been assessed in assay media containing supraphysiological but sub-lethal glucose concentrations, namely 15.4 mmol/l (compared to 17 mmol/L in most of the previous studies). However, this dose is still 3 times higher than the mean fasting blood glucose values of healthy individuals (usually maintained between 4-6 mM)^{251, 369}. Although, high glucose concentrations have been reported to reduce metformin efficacy and promote the growth, motility, aggression and clonogenicity of breast cancer cells, *in vitro*^{251, 369, 370}, in this thesis, when the assay time was prolonged (72 hours) and the media were not renewed throughout the assay time, metformin was effective against all the cell lines.

Recently, there has been a rapid expansion in the number of *in vitro* studies evaluating the anti-tumour effects of metformin in both normal- and low-concentration glucose culture conditions. The results of these studies are promising and suggest that low glucose concentrations can enhance the cytotoxicity of metformin to cancer cells both *in vitro* and *in vivo*^{184, 356, 369-373}, particularly those with impaired glucose utilization¹³⁶. Interestingly, metformin sensitivity of some

breast cancer cells, such as T47D, has been shown to be independent of glucose concentrations³⁷¹. Moreover, it should be noted that culturing the cells in low glucose medium could potentially cause a genetic drift effect that would alter the results obtained as the cells become adjusted to the low glucose environment. Although it was not the primary focus of this study to use different glucose concentrations media to test the efficacy of metformin dosage, this would be an interesting future experiment.

Furthermore, the presence of high glutamine concentration in the culture medium is known to be protective toward electron transport chain dysfunction and might interfere with cellular response to metformin¹³⁶, however, to eliminate the variability in cellular response similar concentrations of glutamine were used to grow the pre-invasive and invasive cell lines in this project.

Furthermore, while our data provided some insight to the direct antineoplastic effects of metformin in the cultured cell model of breast cancer disease progression, however, due to the time constraint it was not possible to further examine the mechanisms that make some cells more sensitive to the clinical doses of metformin than others. In this context, previous studies suggesting that the LKB1-AMPK pathway activation within breast cancer cells is involved in the direct inhibitory effect of metformin are documented *in vitro* and indeed *in vivo*^{176, 177, 296, 374, 375}. It is now well established that the pre-neoplastic breast cells have functional LKB1/AMPK pathway, suggesting therefore, that metformin can restrain their growth and delay the onset of tumorigenesis, with its ability to induce a cytostatic effect³⁷⁶ (schematically represented in Figure 6.1). Similarly, MCF7 and T47D cells have been shown to have a competent LKB1/AMPK pathway while MDA-MB-231 has been demonstrated to be LKB1 deficient^{279, 376}. LKB1 is an upstream regulator that is required for the phosphorylation and activation of AMPK.

Our results demonstrating that clinical doses of metformin appeared to have an inhibitory effect against both the pre-neoplastic and neoplastic cells; regardless of their LKB1 status, with the greatest inhibitory effect seen in the breast cancer cell line lacking or having a dysfunctional liver kinase B1 compared to their cancer cells counterparts with competent LKB1/AMPK intracellular cascade.

Recently, the dependence of the antineoplastic activity of metformin on AMPK activation was confirmed by a study showing that metformin does not exert anti-proliferative effects in a cell line that expresses metformin transporters but lacks LKB1, namely MDA-MB-231 cells, despite achieving high intracellular concentrations, while low transporter expression cell line with a functional LKB1; such as MCF-7 and BT-20 cells, were more responsive²⁷⁹. This contradicts our finding that the MDA-MB-231 cells are more responsive to the cytostatic effect of metformin despite the lack of LKB1. A possible explanation for these contradictory findings is recent data that suggests that metformin can inhibit the growth of LKB1-deficient tumours by a separate mechanism involving induction of cellular-energy deficiency, by decreasing the mitochondrial ATP production and therefore failure to trigger a fully compensatory decrease in energy expenditure, leading to energy crisis causing cell death and necrosis, an observation that has been seen both *in vitro* and *in vivo*^{377, 378}.

By the same token, it should be noted that ascribing the antitumor properties of metformin to AMPK activation has been criticized both *in vitro* and *in vivo* as several other AMPK-independent mechanisms have been described in different cancer types including breast cancer^{124, 179, 209, 217, 376, 379-384}. Moreover, in light of the recent discovery of the so-called “biguanide paradox”, which suggests that metformin-mediated suppression of cancer growth does not depend on AMPK activation but rather, on its downregulation, in specific contexts, it has been suggested that biguanides may be more effective in combination with AMPK inhibitors, rather than AMPK activators³⁸⁵. Thus metformin dependence on AMPK activation remains a controversial issue.

As a result, it would be very interesting to thoroughly examine whether AMPK activation is required in both tumour and non-tumour breast cell lines to elicit the anti-proliferative effect of metformin. In this context AMPK-activators and AMPK-inhibitors compounds, such as AICAR and compound C respectively, could be employed in a series of experiments to assess whether they would abrogate or potentiate the effects of metformin. Indeed, it remains to be elucidated if screening the patients for genetic variability of the cation-selective transporters (OCT1-3 and PMAT) and LKB1 in neoplastic tissues may be necessary to establish their potential responsiveness to metformin treatment.

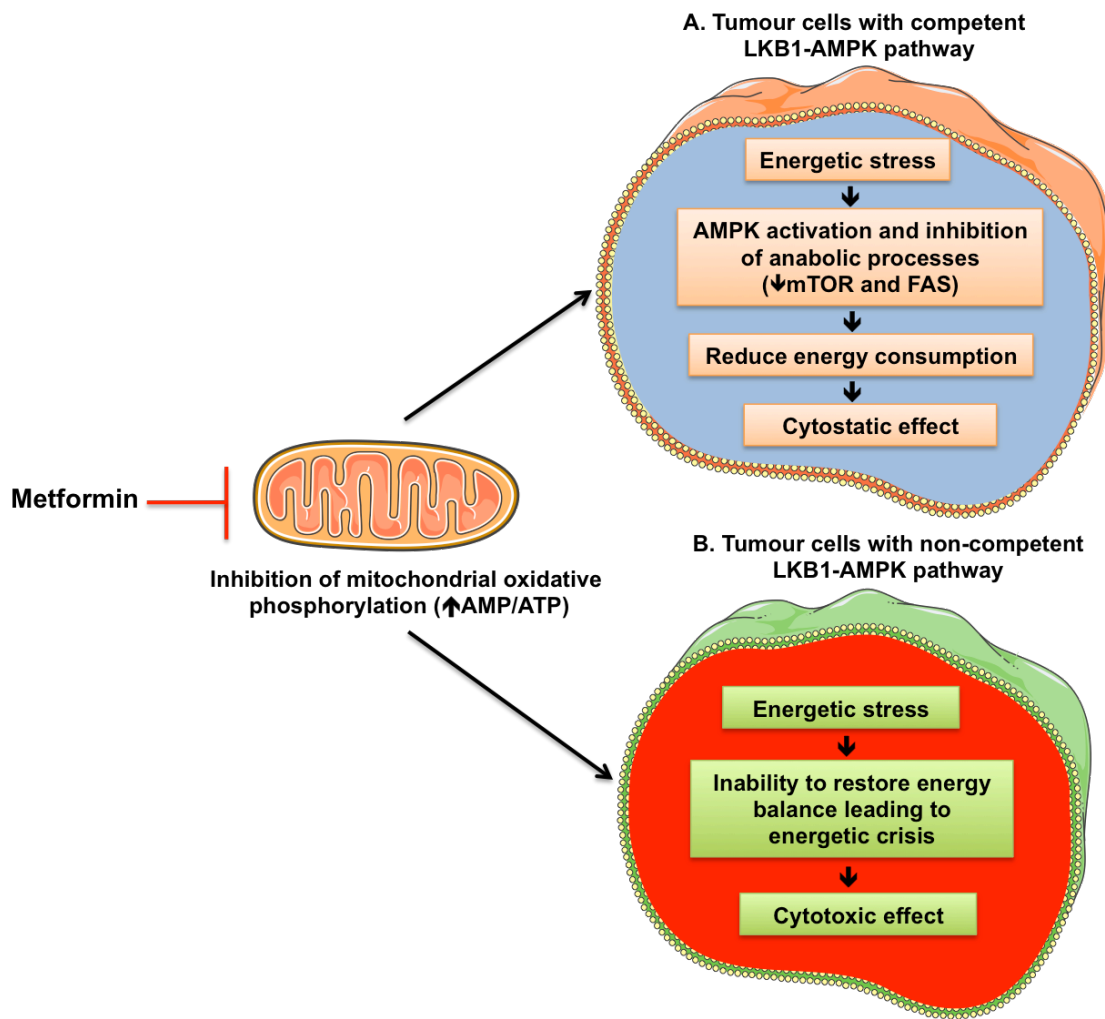


Figure 6.1: Mechanisms by which metformin is therapeutically beneficial in LKB1-positive and LKB1-negative cancer cells.

Metformin may act directly on target cells, provided that the cellular pharmacokinetic conditions are satisfied. (A) Metformin activates AMPK in normal cells, as well as some transformed cells where the LKB1-AMPK pathway is intact. In this case cells are able to cope with a modest degree of metformin-induced energy stress, in part by reducing the AMPK-dependent energy-consuming processes such as protein and lipid synthesis, thereby forcing the cell to adopt to the restrictions of a “low-energy” lifestyle to relieve the energetic stress, which ultimately leads to a cytostatic effect. (B) Metformin inhibits mitochondrial ATP synthesis and promotes cell death in LKB1-AMPK deficient neoplastic cells, as these cells are incapable of compensating for metformin-induced energy stress that renders them more sensitive, leading to a cytotoxic effect on the tumour cells. (Some elements of this figure were produced using Servier Medical Art: <http://www.servier.com/Powerpoint-image-bank>).

Moreover, based on the fact that cells growing in three-dimensional (3D) environments (e.g spheroids) express a number of physiological characteristics that

are more representative to the native tissue from which they originate than the same cells grown in classical two-dimensional (2D) culture flasks. Therefore, growing the breast cells in spheroids and treat them with the clinical and potential tissue accumulation doses of metformin will provide an *in vitro* model that sufficiently mimic *in vivo* condition, this is to evaluate if higher doses of metformin are required to target the tumour cells and this would be an interesting future experiment.

In light of the promising results from the proliferation studies, in chapter five the effects of metformin on the global proteomics in the highly aggressive triple negative cell (MDA-MB-231) and its bone- and lung-homed variants were investigated. Unfortunately, the Spike-In SILAC proteomics experiment, despite numerous repeats and protocol amendments, was not perfected due to several issues that were encountered during the processing of samples. The main issue was the difficulty in the reproducibility and the clustering of the three biological samples (all other limitations are previously discussed in section 5.4.3). This meant that important differences between the three metastatic subtypes might have been masked. Due to this, there is therefore no corroborative finding to compare the proteomic pilot study to, which was one of the aims of the SILAC study. Further work would therefore be to repeat the SILAC-based proteomics experiment (time and money constraints prevented this). As the majority of metformin effects are likely to be due to changes in phosphorylation rather than in the global proteome, further more informative phosphoproteomic studies using the same cell lines is also warranted

However, the preliminary findings of the proteomic pilot study of this thesis contribute new insights into the role of metformin in metastatic breast cancer. Additionally, the investigation into the importance of the identified candidate proteins; using Western blotting, validates and strengthens current data and demonstrates that metformin might work as a novel inhibitor for some attractive therapeutic target such as TNFAIP8 and STAT3; but the mechanisms mediating this inhibitory effect remain to be fully identified. Nevertheless, it is an important and interesting finding suggesting that metformin can hit important cellular targets and therefore may lead to new anti-cancer treatment strategies. Although this is a promising result, the proteomic analysis should be cautiously interpreted due to the issues encountered during the process, with the consideration of further assessment by

other protein expression methods, such as immunohistochemistry using tissue sections of patients treated with metformin before surgery. Ideally the results of this study would be further validated both *in vivo* and in a prospective clinical trial. If confirmed, the associations between these changes and the impact of metformin on breast cancer outcome should be evaluated.

6.1 General limitations of this thesis

This thesis, generally attempted to build a breast cancer disease case model that could test the effects of metformin in relevant cell lines such as MCF10AT, DCIS cell type, MCF7, T47D, MDA-MB-231 and one of the end-stage bone-homed breast cancer cells. However, with the benefit of hindsight there are several areas of this thesis that could be improved. Generally, there are obvious disadvantages when conducting work with cultured cell lines as previously noted³⁸⁶. Cell lines are prone to genotypic and phenotypic changes during their continual culture, resulting in variations in their growth rate, changes in hormone receptor content and clonogenicity²⁹², in order to attempt to control for this, low passage numbers have been consistently used throughout this thesis work^{292, 386}. Moreover, it is imperative to identify and characterize the cell lines to avoid the use of a false or contaminated cell line. As the cells were bought fresh from the ATCC at the beginning of the project we are confident that these are not contaminated or false, but if time and money permitting we could have double checked at the end of the thesis using HLA typing, karyotyping or DNA fingerprinting, or short tandem repeat (STR) profiling³⁸⁷. This was not done due to money constraints.

The other issue with most of these long established breast cancer cell lines is that they are derived from distant metastatic sites, especially aspirates or pleural effusions and not derived from primary breast tumours. This implies that most of these cell lines are derived from more aggressive and often metastatic tumours, which may therefore not reflect the specific types, grades or stages observed in primary breast cancer. Consequently, studies that rely on these lines will be biased toward more rapidly progressive and late-stage disease types of breast carcinoma, rather than earlier stages of breast cancer. Therefore, it would be of more clinical relevance to use cells that are derived directly from a primary tumour, as most drug therapies are directed against these. Furthermore, *ex vivo* models such as human tissue specimens

used in this study can maintain the architecture of the tissues closer to the *in vivo* setting, overtaking some of the limitations of the *in vitro* studies. However, using fixed tissue does not allow assessment of metformin activity and this would require ethics to collect fresh human samples, which are difficult to maintain in culture.

Further work encompassing a variety of breast cancer cell lines with different receptor status (ER, PR and HER2) would be beneficial to investigate the anti-neoplastic effect of metformin and explore the expression profile of metformin transporters, to resemble the variety of breast tumours with differing patterns of hormone receptor expression encountered in the clinical settings.

In the *in vitro* cell-based work, only one experimental technique was used to quantify the expression of metformin transporter proteins, namely Western blotting. Alternative techniques, such as immunocytochemistry and fluorescent cell surface protein expression using flow cytometry (FACS) could have been used to further corroborate and compliment the results obtained by Western blotting. Additionally, after confirmation of the transporter proteins expression, few other techniques can be used to block the expression/accumulation of the transporter proteins, leading to a decrease in their levels and eventual knockdown/silencing such as small interfering RNAs (siRNAs) or short hairpin RNAs (shRNAs), or the suppression of translation of specific mRNAs, as induced by microRNA (miRNA) to evaluate the contribution of each individual transporter in metformin response. The use of siRNAs and shRNAs techniques are future experiments that should be considered to take the results of this thesis forward and allow a detailed comparison of the transporter protein involvement in metformin response across all cell lines.

Furthermore, with regard to the *ex vivo* study, although the total sample size of 133 breast tissue specimens represents an adequate number and to date there is no equivalent published study to compare this number with, a larger number of tissue samples would have increased the statistical power of the study enabled improved conclusions to be drawn. Moreover, although the overall sample size was large, the number of specimens in each group was relatively small and this is a limitation of this study. Plausibly a total of 40 specimens per breast tissue subtype would provide an enhanced design to the body of the work performed. Particularly, the number of grade three specimens stained was 4, which is low when compared to other tissue subtypes.

However, time and resources prevented increasing the sample sizes in each group. Further work could potentially include investigating the expression of these transporters in full tissue sections rather than microarrays and increasing the sample sizes.

One of the general limitations of the *in vitro* cell based assays is that they are not 100% predictive. Therefore, inhibition of one step in the metastatic cascade by metformin treatment, such as migration, or inhibition of metastatic cell proliferation does not necessarily translate to complete inhibition of metastasis *in vivo*.

Although this thesis has demonstrated the expression of the transporters and an effect of metformin on breast epithelial cells, it is not known whether metformin treatment will inhibit the development of breast cancer prior to diagnosis. The promising results with metformin treatment in the pre-neoplastic and pre-invasive cells raise the questions of whether metformin alone can prevent the development of hyperplasia or revert early stages of breast cancer to normal breast epithelium. Thus future *in vivo* work using an animal model of spontaneous mammary tumour growth such as the PYMT model is warranted to establish whether metformin would have a preventative effect against breast cancer development.

Finally, it must be stressed that as metformin can accumulate in tissues over time and the cancer cells could be more sensitive in their tumour microenvironment, where they are deprived of the nutrients and growth factors found in culture conditions, *in vivo* studies are also warranted as future work to test the effect of the clinically relevant doses on tumour growth. Removal of the tissue after treatment will enable effects on the tumour microenvironment, such as angiogenesis, to also be assessed.

6.2 Final conclusion

In conclusion, the data in this thesis have shown that metformin transporters are present on breast epithelial cells, pre-neoplastic, pre-invasive and invasive breast cancer cells and that metformin has a cytostatic effect on the proliferation of these cells, causing cell cycle arrest, but not apoptosis at clinically relevant doses. The proteomic data suggest that metformin inhibits the expression of proteins within key cellular pathways in both triple negative breast cancer and the bone- and lung-homed

variants, with the lung-homed cells showing a greater response to metformin treatment. Taken together these data suggest that metformin has the potential to be a useful treatment for breast cancer, but further research is certainly required to identify biomarkers of response and mechanisms of action in breast cancer before metformin can be recommended in clinical practice.

7. References

1. Tavassoli, F. A., Devilee, Peter, Pathology and genetics of tumours of the breast and female genital organs. *International Agency for Research on Cancer: 2003*.
2. Fitzgibbons, P. L.; Henson, D. E.; Hutter, R. V. P.; Canc Comm Coll Am, P., Benign breast changes and the risk for subsequent breast cancer - An update of the 1985 consensus statement. *Archives of Pathology & Laboratory Medicine* **1998**, 122 (12), 1053-1055.
3. Guray, M.; Sahin, A. A., Benign breast diseases: Classification, diagnosis, and management. *Oncologist* **2006**, 11 (5), 435-449.
4. Wang, J. P.; Costantino, J. P.; Tan-Chiu, E.; et al.; Lower-category benign breast disease and the risk of invasive breast cancer. *Journal of the National Cancer Institute* **2004**, 96 (8), 616-620.
5. Hartmann, L. C.; Radisky, D. C.; Frost, M. H.; et al.; Understanding the Premalignant Potential of Atypical Hyperplasia through Its Natural History: A Longitudinal Cohort Study. *Cancer Prevention Research* **2014**, 7 (2), 211-217.
6. Wellings, S. R.; Jensen, H. M., Origin and progression of ductal carcinoma in human breast. *Journal of the National Cancer Institute* **1973**, 50 (5), 1111-1118.
7. Dupont, W. D.; Page, D. L., Risk-factors for breast-cancer in women with proliferative breast disease. *New England Journal of Medicine* **1985**, 312 (3), 146-151.
8. Page, D. L.; Dupont, W. D., Anatomic Markers Of Human Premalignancy And Risk Of Breast-Cancer. *Cancer* **1990**, 66 (6), 1326-1335.
9. Page, D. L.; Dupont, W. D., Anatomic indicators (histologic and cytologic) of increased breast-cancer risk. *Breast Cancer Research and Treatment* **1993**, 28 (2), 157-166.
10. Dion, L.; Racine, A.; Brousseau, S.; et al.; Atypical epithelial hyperplasia of the breast: state of the art. *Expert Review of Anticancer Therapy* **2016**, 16 (9), 943-953.
11. Chuaqui, R. F.; Zhuang, Z. P.; EmmertBuck, M. R.; et al.; Analysis of loss of heterozygosity on chromosome 11q13 in atypical ductal hyperplasia and in situ carcinoma of the breast. *American Journal of Pathology* **1997**, 150 (1), 297-303.
12. Lakhani, S. R.; Collins, N.; Stratton, M. R.; Sloane, J. P., Atypical ductal hyperplasia of the breast - clonal proliferation with loss of heterozygosity on chromosomes 16q and 17p. *Journal of Clinical Pathology* **1995**, 48 (7), 611-615.
13. O'Connell, P.; Pekkel, V.; Fuqua, S. A. W.; Osborne, C. K.; Clark, G. M.; Allred, D. C., Analysis of loss of heterozygosity in 399 premalignant breast lesions at 15 genetic loci. *Journal of the National Cancer Institute* **1998**, 90 (9), 697-703.
14. Allred, D. C.; O'Connell, P.; Fuqua, S. A. W.; Osborne, C. K., Immunohistochemical studies of early breast-cancer evolution. *Breast Cancer Research and Treatment* **1994**, 32 (1), 13-18.

15. Cancer Registration Statistics, England. In *Cancer diagnoses and age-standardised incidence rates for all cancer sites by age, sex and region*, Office for national statistics: 27 May 2015.
16. Allred, D. C., Ductal carcinoma in situ: terminology, classification, and natural history. *Journal of the National Cancer Institute. Monographs* **2010**, *2010* (41), 134-8.
17. Cowell, C. F.; Weigelt, B.; Sakr, R. A.; et al.; Progression from ductal carcinoma in situ to invasive breast cancer: Revisited. *Molecular Oncology* **2013**, *7* (5), 859-869.
18. Cancer Research institute report; UK; **2017**.
19. Myers, E. R.; Moorman, P.; Gierisch, J. M.; et al.; Benefits and harms of breast cancer screening a systematic review. *Journal of the American Medical Association* **2015**, *314* (15), 1615-1634.
20. Siziopikou, K. P., Ductal carcinoma in situ of the Breast. *Archives of Pathology & Laboratory Medicine* **2013**, *137* (4), 462-466.
21. Bane, A., Ductal carcinoma in situ: what the pathologist needs to know and why. *International journal of breast cancer* **2013**, *2013*, 914053-914053.
22. Allen, M. D.; Thomas, G. J.; Clark, S.; et al.; Altered microenvironment promotes progression of preinvasive breast cancer: Myoepithelial expression of alpha v beta 6 Integrin in DCIS Identifies high-risk patients and predicts recurrence. *Clinical Cancer Research* **2014**, *20* (2), 344-357.
23. Muggerud, A. A.; Hallett, M.; Johnsen, H.; et al.; Molecular diversity in ductal carcinoma in situ (DCIS) and early invasive breast cancer. *Molecular Oncology* **2010**, *4* (4), 357-368.
24. Bryan, B. B.; Schnitt, S. J.; Collins, L. C., Ductal carcinoma in situ with basal-like phenotype: a possible precursor to invasive basal-like breast cancer. *Modern Pathology* **2006**, *19* (5), 617-621.
25. Livasy, C. A.; Perou, C. M.; Karaca, G.; et al.; Identification of a basal-like subtype of breast ductal carcinoma in situ. *Human Pathology* **2007**, *38* (2), 197-204.
26. Leonard, G. D.; Swain, S. M., Ductal carcinoma in situ, complexities and challenges. *Journal of the National Cancer Institute* **2004**, *96* (12), 906-920.
27. Beckmann, M. W.; Niederacher, D.; Schnurch, H. G.; et al.; Multistep carcinogenesis of breast cancer and tumour heterogeneity. *Journal of Molecular Medicine-Jmm* **1997**, *75* (6), 429-439.
28. Wellings, S. R.; Jensen, H. M.; Marcum, R. G., Atlas of subgross pathology of human breast with special reference to possible precancerous lesions. *Journal of the National Cancer Institute* **1975**, *55* (2), 231-273.
29. Nguyen, D. X.; Bos, P. D.; Massague, J., Metastasis: from dissemination to organ-specific colonization. *Nature Reviews Cancer* **2009**, *9* (4), 274-U65.
30. Cancer Registration Statistics, England - Office for National Statistics. <https://www.ons.gov.uk/peoplepopulationandcommunity/healthandsocialcare/conditionsanddiseases/bulletins/cancerregistrationstatisticsengland/2015 - background-notes>.
31. IARC release GLOBOCAN 2012: Global cancer burden rises to 14.1 million new cases in 2012 and marked increase in breast cancers must be addressed | National Cancer Registry Ireland.

<https://www.ncri.ie/news/article/iarc-release-globocan-2012-global-cancer-burden-rises-141-million-new-cases-2012-and>.

32. Ferlay, J.; Soerjomataram, I.; Dikshit, R.; et al.; Cancer incidence and mortality worldwide: sources, methods and major patterns in GLOBOCAN 2012. *International Journal of Cancer* **2015**, *136* (5), E359-86.
33. Coleman, M. P.; Quaresma, M.; Berrino, F.; et al.; Cancer survival in five continents: a worldwide population-based study (CONCORD). *Lancet Oncology* **2008**, *9* (8), 730-756.
34. Ferlay, J.; Shin, H.-R.; Bray, F.; Forman, D.; Mathers, C.; Parkin, D. M., Estimates of worldwide burden of cancer in 2008: GLOBOCAN 2008. *International Journal of Cancer* **2010**, *127* (12), 2893-2917.
35. American Cancer Society. Cancer Facts & Figures. *American Cancer Society* **2014**.
36. Ford, D.; Peto, D. F.; Stratton, M.; et al.; Genetic heterogeneity and penetrance analysis of the BRCA1 and BRCA2 genes in breast cancer families. *American Journal of Human Genetics* **1998**, *62* (3), 676-689.
37. Key, T. J.; Verkasalo, P. K.; Banks, E., Epidemiology of breast cancer. *Lancet Oncology* **2001**, *2* (3), 133-140.
38. Santen, R. J.; Yue, W.; Wang, J.-P., Estrogen metabolites and breast cancer. *Steroids* **2014**.
39. Fredslund, S. O.; Bonefeld-Jørgensen, E. C., Breast cancer in the arctic - Changes over the past decades. *International Journal of Circumpolar Health* **2012**, *71* (1).
40. Wolff, M. S.; Weston, A., Breast cancer risk and environmental exposures. *Environmental Health Perspectives* **1997**, *105*, 891-896.
41. McPherson, K.; Steel, C. M.; Dixon, J. M., ABC of breast disease: Breast cancer-epidemiology, risk factors, and genetics. *British Medical Journal* **2000**, *321* (7261), 624-628.
42. Lee, S.; Mohsin, S. K.; Mao, S. F.; et al.; Hormones, receptors, and growth in hyperplastic enlarged lobular units: early potential precursors of breast cancer. *Breast Cancer Research* **2006**, *8* (1).
43. Allison, K. H., Molecular pathology of breast cancer what a pathologist needs to know. *American Journal of Clinical Pathology* **2012**, *138* (6), 770-780.
44. Weigelt, B.; Reis-Filho, J. S., Histological and molecular types of breast cancer: is there a unifying taxonomy? *Nature Reviews Clinical Oncology* **2009**, *6* (12), 718-730.
45. Perou, C. M.; Sorlie, T.; Eisen, M. B.; et al.; Molecular portraits of human breast tumours. *Nature* **2000**, *406* (6797), 747-752.
46. Rivenbark, A. G.; O'Connor, S. M.; Coleman, W. B., Molecular and cellular heterogeneity in breast cancer challenges for personalized medicine. *American Journal of Pathology* **2013**, *183* (4), 1113-1124.
47. Sorlie, T.; Perou, C. M.; Tibshirani, R.; et al.; Gene expression patterns of breast carcinomas distinguish tumor subclasses with clinical implications. *Proceedings of the National Academy of Sciences of the United States of America* **2001**, *98* (19), 10869-10874.
48. Massachusetts Institute of, T., Comprehensive molecular portraits of human breast tumors (BRCA). *European Nucleotide Archive* **2013**.

49. Sioshansi, S.; Huber, K. E.; Wazer, D. E., The implications of breast cancer molecular phenotype for radiation oncology. *Frontiers in oncology* **2011**, *1*, 12-12.
50. Eroles, P.; Bosch, A.; Alejandro Perez-Fidalgo, J.; Lluch, A., Molecular biology in breast cancer: Intrinsic subtypes and signaling pathways. *Cancer Treatment Reviews* **2012**, *38* (6), 698-707.
51. Herschkowitz, J. I.; Simin, K.; Weigman, V. J.; et al.; Identification of conserved gene expression features between murine mammary carcinoma models and human breast tumors. *Genome Biology* **2007**, *8* (5).
52. Kreike, B.; van Kouwenhove, M.; Horlings, H.; et al.; Gene expression profiling and histopathological characterization of triple-negative/basal-like breast carcinomas. *Breast Cancer Research* **2007**, *9* (5).
53. Cheang, M. C. U.; Chia, S. K.; Voduc, D.; et al.; Ki67 Index, HER2 status, and prognosis of patients with luminal B breast cancer. *Journal of the National Cancer Institute* **2009**, *101* (10), 736-750.
54. Feeley, L. P.; Mulligan, A. M.; Pinnaduwage, D.; et al.; Distinguishing luminal breast cancer subtypes by Ki67, progesterone receptor or TP53 status provides prognostic information. *Modern Pathology* **2014**, *27* (4), 554-561.
55. Azambuja, E.; Cardoso, F.; Castro, G.; et al.; Ki-67/MIB-1 as prognostic marker in women with early breast cancer: a meta-analysis of published studies involving 10.958 patients. *Breast Cancer Research and Treatment* **2005**, *94*, S127-S127.
56. Di Leo, A.; Cardoso, F.; Durbecq, V.; Giuliani, R.; Mano, M.; Atalay, G.; Larsimont, D.; Sotiriou, C.; Biganzoli, L.; Piccart, M. J., Predictive molecular markers in the adjuvant therapy of breast cancer: state of the art in the year 2002. *International Journal of Clinical Oncology* **2002**, *7* (4), 245-53.
57. Sotiriou, C.; Powles, T. J.; Dowsett, M.; et al.; Gene expression profiles derived from fine needle aspiration correlate with response to systemic chemotherapy in breast cancer. *Breast Cancer Research* **2002**, *4* (3).
58. Yersal, O.; Barutca, S., Biological subtypes of breast cancer: Prognostic and therapeutic implications. *World J Clin Oncol* **2014**, *5* (3), 412-24.
59. Willmann, L.; Erbes, T.; Halbach, S.; et al.; Exometabolom analysis of breast cancer cell lines: Metabolic signature. *Scientific Reports* **2015**, *5*, 13374.
60. Holliday, D. L.; Speirs, V., Choosing the right cell line for breast cancer research. *Breast Cancer Research* **2011**, *13* (4).
61. Prat, A.; Parker, J. S.; Karginova, O.; et al.; Phenotypic and molecular characterization of the claudin-low intrinsic subtype of breast cancer. *Breast Cancer Res* **2010**, *12* (5), R68.
62. Dias, K.; Dvorkin-Gheva, A.; Hallett, R. M.; Wu, Y.; Hassell, J.; et al.; Claudin-low breast cancer; clinical & pathological characteristics. In *PLoS One*, 2017; Vol. 12.
63. Goldhirsch, A.; Wood, W. C.; Coates, A. S.; et al.; Strategies for subtypes-dealing with the diversity of breast cancer: highlights of the St Gallen International Expert Consensus on the Primary Therapy of Early Breast Cancer 2011. *Annals of Oncology* **2011**, *22* (8), 1736-1747.
64. Cianfrocca, M.; Gradishar, W. J., Controversies in the therapy of early stage breast cancer. *Oncologist* **2005**, *10* (10), 766-779.

65. Burstein, H. J.; Temin, S.; Anderson, H.; et al.; Adjuvant Endocrine Therapy for Women With Hormone Receptor-Positive Breast Cancer: American Society of Clinical Oncology Clinical Practice Guideline Focused Update. *Journal of Clinical Oncology* **2014**, 32 (21), 2255-+.
66. Khatcheressian, J. L.; Wolff, A. C.; Smith, T. J.; et al.; American Society of Clinical Oncology 2006 update of the breast cancer follow-up and management guidelines in the adjuvant setting. *Journal of Clinical Oncology* **2006**, 24 (31), 5091-5097.
67. Nadji, M.; Gomez-Fernandez, C.; Ganjei-Azar, P.; Morales, A. R., Immunohistochemistry of estrogen and progesterone receptors reconsidered: experience with 5,993 breast cancers. *American Journal Of Clinical Pathology*.
68. Beatson, G. T., On the treatment of inoperable cases of carcinoma of the mamma - suggestions for a new method of treatment, with illustrative cases. *Cancer Journal for Clinicians* **1983**, 33 (2), 108-121.
69. Renoir, J.-M.; Marsaud, V.; Lazennec, G., Estrogen receptor signaling as a target for novel breast cancer therapeutics. *Biochemical Pharmacology* **2013**, 85 (4), 449-465.
70. SimpsonDavis, E. R. R. E.; Simpson, E. R.; Davis, S. R., Minireview: aromatase and the regulation of estrogen biosynthesis--some new perspectives. *Endocrinology*.
71. Karaer, Ö.; Oruç, S.; Koyuncu, F. M., Aromatase inhibitors: Possible future applications. *Acta Obstetricia et Gynecologica Scandinavica* **2004**, 83 (8), 699-706.
72. Ingle, J. N., Pharmacogenetics and pharmacogenomics of endocrine agents for breast cancer. *Breast Cancer Research* **2008**, 10.
73. Hughes, S. W. M.; Burley, D. M., Aminoglutethimide - a side-effect turned to therapeutic advantage. *Postgraduate Medical Journal* **1970**, 46 (537), 409-&.
74. Brodie, A. M. H.; Njar, V. C. O., Aromatase inhibitors and their application in breast cancer treatment. *Steroids* **2000**, 65 (4), 171-179.
75. Harris, A. L.; Dowsett, M.; Smith, I. E.; Jeffcoate, S., Aminoglutethimide induced hormone suppression and response to therapy in advanced post-menopausal breast-cancer. *British Journal of Cancer* **1983**, 48 (4), 585-594.
76. Barnadas, A.; Estevez, L. G.; Lluch-Hernandez, A.; et al.; An Overview of Letrozole in Postmenopausal Women with Hormone-Responsive Breast Cancer. *Advances in Therapy* **2011**, 28 (12), 1045-1058.
77. Miller, W. R., Aromatase inhibitors and breast cancer. **1997**; 23:171-187.
78. Mann, B. S.; Johnson, J. R.; Kelly, R.; Sridhara, R.; Williams, G.; Pazdur, R., Letrozole in the extended adjuvant treatment of postmenopausal women with history of early-stage breast cancer who have completed 5 years of adjuvant tamoxifen. *Clinical Cancer Research* **2005**, 11 (16), 5671-5677.
79. Altundag, K.; Ibrahim, N. K., Aromatase inhibitors in breast cancer: An overview. *Oncologist* **2006**, 11 (6), 553-562.
80. Chlebowski, R.; Cuzick, J.; Amakye, D.; Bauerfeind, I.; Buzdar, A.; Chia, S.; Cutuli, B.; Linforth, R.; Maass, N.; Noguchi, S.; Robidoux, A.; Verma, S.; Hadji, P., Clinical perspectives on the utility of aromatase inhibitors for the adjuvant treatment of breast cancer. *Breast* **2009**, 18, S1-S11.

81. Abe, O.; Abe, R.; Enomoto, K.; et al.; Effects of chemotherapy and hormonal therapy for early breast cancer on recurrence and 15-year survival: an overview of the randomised trials. *Lancet* **2005**, *365* (9472), 1687-1717.
82. Eifel, P.; Axelson, J. A.; Costa, J.; et al.; National Institutes of Health Consensus Development Conference statement: Adjuvant therapy for breast cancer, November 1-3, 2000. *Journal of the National Cancer Institute* **2001**, *93* (13), 979-989.
83. Weigelt, B.; Peterse, J. L.; van't Veer, L. J., Breast cancer metastasis: Markers and models. *Nature Reviews Cancer* **2005**, *5* (8), 591-602.
84. Koscielny, S.; Tubiana, M.; Le, M. G.; Valleron, A. J.; Mouriesse, H.; Contesso, G.; Sarrazin, D., Breast-cancer-relationship between the size of the primary tumor and the probability of metastatic dissemination. *British Journal of Cancer* **1984**, *49* (6), 709-715.
85. Carter, C. L.; Allen, C.; Henson, D. E., Relation of tumor size, lymph-node status, and survival in 24,740 breast-cancer cases. *Cancer* **1989**, *63* (1), 181-187.
86. de Mascarel, I.; Bonichon, F.; Durand, M.; et al.; Obvious peritumoral emboli: an elusive prognostic factor reappraised. Multivariate analysis of 1320 node-negative breast cancers. *European Journal of Cancer* **1998**, *34* (1), 58-65.
87. Page, D. L., Prognosis and breast-cancer - recognition of lethal and favorable prognostic types. *American Journal of Surgical Pathology* **1991**, *15* (4), 334-349.
88. Egeblad, M.; Werb, Z., New functions for the matrix metalloproteinases in cancer progression. *Nature Reviews Cancer* **2002**, *2* (3), 161-174.
89. Steeg, P. S., Tumor metastasis: mechanistic insights and clinical challenges. *Nature Medicine* **2006**, *12* (8), 895-904.
90. Lee, Y., Breast-carcinoma - pattern of metastasis at autopsy. *Journal of Surgical Oncology* **1983**, *23* (3), 175-180.
91. James, J. J.; Evans, A. J.; Pinder, S. E.; Gutteridge, E.; Cheung, K. L.; Chan, S.; Robertson, J. F. R., Bone metastases from breast carcinoma: histopathological-radiological correlations and prognostic features. *British Journal of Cancer* **2003**, *89* (4), 660-665.
92. Arpino, G.; Bardou, V. J.; Clark, G. M.; Elledge, R. M., Infiltrating lobular carcinoma of the breast: tumor characteristics and clinical outcome. *Breast Cancer Research* **2004**, *6* (3), R149-R156.
93. Molnar, I. A.; Molnar, B. A.; Vizkeleti, L.; Fekete, K.; Tamas, J.; Deak, P.; Szundi, C.; Szekely, B.; Moldvay, J.; Vari-Kakas, S.; Szasz, M. A.; Acs, B.; Kulka, J.; Tokes, A. M., Breast carcinoma subtypes show different patterns of metastatic behavior. *Virchows Archive* **2017**, *470* (3), 275-283.
94. Paget, S., Paget,stephen paper reproduced from the LANCET, 1889. *Cancer and Metastasis Reviews* **1989**, *8* (2), 98-101.
95. Nguyen, D. X.; Massague, J., Genetic determinants of cancer metastasis. *Nature Reviews Genetics* **2007**, *8* (5), 341-352.
96. Tazzyman, S.; Niaz, H.; Murdoch, C., Neutrophil-mediated tumour angiogenesis: Subversion of immune responses to promote tumour growth. *Seminars in Cancer Biology* **2013**, *23* (3), 149-158.

97. Wang, X.; Lu, H.; Urvalek, A. M.; Li, T.; et al.; KLF8 promotes human breast cancer cell invasion and metastasis by transcriptional activation of MMP9. *Oncogene* **2011**, *30* (16), 1901-1911.
98. Thiery, J. P., Epithelial-mesenchymal transitions in tumour progression. *Nature Reviews Cancer* **2002**, *2* (6), 442-454.
99. Huber, M. A.; Kraut, N.; Beug, H., Molecular requirements for epithelial-mesenchymal transition during tumor progression. *Current Opinion in Cell Biology* **2005**, *17* (5), 548-558.
100. Nguyen-Ngoc, K. V.; Cheung, K. J.; Brenot, A.; et al.; ECM microenvironment regulates collective migration and local dissemination in normal and malignant mammary epithelium. In *Proceedings of the National Academy of Sciences of the United States of America*, 2012; Vol. 109, pp E2595-604.
101. Condeelis, J.; Segall, J. E., Intravital imaging of cell movement in tumours. *Nat Rev Cancer* **2003**, *3* (12), 921-30.
102. Wyckoff, J. B.; Wang, Y.; Lin, E. Y.; Li, J. F.; Goswami, S.; Stanley, E. R.; Segall, J. E.; Pollard, J. W.; Condeelis, J., Direct visualization of macrophage-assisted tumor cell intravasation in mammary tumors. *Cancer Res* **2007**, *67* (6), 2649-56.
103. Kalluri, R.; Zeisberg, M., Fibroblasts in cancer. *Nature Reviews Cancer* **2006**, *6* (5), 392-401.
104. Qian, B.; Deng, Y.; Im, J. H.; Muschel, R. J.; Zou, Y.; Li, J.; Lang, R. A.; Pollard, J. W., A distinct macrophage population mediates metastatic breast cancer cell extravasation, establishment and growth. *Plos One* **2009**, *4* (8).
105. Siegel, R. L.; Miller, K. D.; Jemal, A., Cancer Statistics, 2017. *Cancer Journal for Clinicians* **2017**, *67* (1), 7-30.
106. Hanahan, D.; Weinberg, R. A., Hallmarks of cancer: the next generation. *Cell* **2011**, *144* (5), 646-674.
107. Hanahan, D.; Weinberg, R. A., The hallmarks of cancer. *Cell* **2000**, *100* (1), 57-70.
108. Warburg, O., Origin of cancer cells. *Science* **1956**, *123* (3191), 309-314.
109. Heiden, M. G. V.; Cantley, L. C.; Thompson, C. B., Understanding the warburg effect: the metabolic requirements of cell proliferation. *Science* **2009**, *324* (5930), 1029-1033.
110. Giovannucci, E.; Harlan, D. M.; Archer, M. C.; et al.; Regensteiner, J. G.; Yee, D., Diabetes and cancer: A consensus report. *Cancer Journal for Clinicians* **2010**, *60* (4), 207-221.
111. Yang, X.; Ko, G. T. C.; So, W. Y.; et al.; Associations of Hyperglycemia and Insulin Usage With the Risk of Cancer in Type 2 Diabetes: The Hong Kong Diabetes Registry. *Diabetes* **2010**, *59* (5), 1254-1260.
112. Orgel, E.; Mittelman, S. D., The links between insulin resistance, diabetes, and cancer. *Current Diabetes Reports* **2013**, *13* (2), 213-22.
113. Boyle, P.; Boniol, M.; Koechlin, A.; et al.; Diabetes and breast cancer risk: a meta-analysis. *Br J Cancer* **2012**, *107* (9), 1608-17.
114. Larsson, S. C.; Mantzoros, C. S.; Wolk, A., Diabetes mellitus and risk of breast cancer: A meta-analysis. *International Journal of Cancer* **2007**, *121* (4), 856-862.

115. Wang, C.; Wang, X.; Gong, G.; Ben, Q.; Qiu, W.; Chen, Y.; Li, G.; Wang, L., Increased risk of hepatocellular carcinoma in patients with diabetes mellitus: a systematic review and meta-analysis of cohort studies. *International Journal of Cancer* **2012**, *130* (7), 1639-48.
116. Ben, Q.; Xu, M.; Ning, X.; Liu, J.; Hong, S.; Huang, W.; Zhang, H.; Li, Z., Diabetes mellitus and risk of pancreatic cancer: A meta-analysis of cohort studies. *European journal of cancer* **2011**, *47* (13), 1928-37.
117. Larsson, S. C.; Wolk, A., Diabetes mellitus and incidence of kidney cancer: a meta-analysis of cohort studies. *Diabetologia* **2011**, *54* (5), 1013-8.
118. Deng, L.; Gui, Z.; Zhao, L.; Wang, J.; Shen, L., Diabetes mellitus and the incidence of colorectal cancer: an updated systematic review and meta-analysis. *Digestive Diseases and Sciences* **2012**, *57* (6), 1576-85.
119. Lambe, M.; Wigertz, A.; Garmo, H.; Walldius, G.; Jungner, I.; Hammar, N., Impaired glucose metabolism and diabetes and the risk of breast, endometrial, and ovarian cancer. *Cancer Causes Control* **2011**, *22* (8), 1163-71.
120. Hernandez-Diaz, S.; Adami, H. O., Diabetes therapy and cancer risk: causal effects and other plausible explanations. *Diabetologia* **2010**, *53* (5), 802-808.
121. Del Barco, S.; Vazquez-Martin, A.; Cufi, S.; Oliveras-Ferraros, C.; Bosch-Barrera, J.; Joven, J.; Martin-Castillo, B.; Menendez, J. A., Metformin: Multi-faceted protection against cancer. *Oncotarget* **2011**, *2* (12), 896-917.
122. Scarpello, J. H. B.; Howlett, H. C. S., Metformin therapy and clinical uses. *Diabetes & Vascular Disease Research* **2008**, *5* (3), 157-167.
123. Chong, C. R.; Chabner, B. A., Mysterious metformin. *Oncologist* **2009**, *14* (12), 1178-1181.
124. Viollet, B.; Guigas, B.; Sanz Garcia, N.; Leclerc, J.; Foretz, M.; Andreelli, F., Cellular and molecular mechanisms of metformin: an overview. *Clinical Science* **2012**, *122* (5-6), 253-270.
125. Pierotti, M. A.; Berrino, F.; Gariboldi, M.; Melani, C.; Mogavero, A.; Negri, T.; Pasanisi, P.; Pilotti, S., Targeting metabolism for cancer treatment and prevention: metformin, an old drug with multi-faceted effects. *Oncogene* **2013**, *32* (12), 1475-1487.
126. DeFronzo, R. A. a. G., A. M., Efficacy of metformin in patients with non-insulin-dependent diabetes mellitus. *National England Journal of Medicine* **1995**, *333*:541-549.
127. Bharatam, P. V.; Patel, D. S.; Iqbal, P., Pharmacophoric features of biguanide derivatives: An electronic and structural analysis. *Journal of Medicinal Chemistry* **2005**, *48* (24), 7615-7622.
128. Gong, L.; Goswami, S.; Giacomini, K. M.; et al.; Metformin pathways: pharmacokinetics and pharmacodynamics. *Pharmacogenetics and Genomics* **2012**, *22* (11), 820-827.
129. Graham, G. G.; Punt, J.; Arora, M.; et al.; Clinical pharmacokinetics of metformin. *Clinical Pharmacokinetics* **2011**, *50* (2), 81-98.
130. Ho, R. H.; Kim, R. B., Transporters and drug therapy: Implications for drug disposition and disease. *Clinical Pharmacology & Therapeutics* **2005**, *78* (3), 260-277.
131. Zhou, M.; Xia, L.; Wang, J., Metformin transport by a newly cloned proton-stimulated organic cation transporter (plasma membrane monoamine

- transporter) expressed in human intestine. *Drug Metabolism and Disposition* **2007**, *35* (10), 1956-1962.
132. Terada, T.; Inui, K.-i., Physiological and pharmacokinetic roles of H⁺/organic cation antiporters (MATE/SLC47A). *Biochemical Pharmacology* **2008**, *75* (9), 1689-1696.
133. Kimura, N.; Masuda, S.; Tanihara, Y.; et al.; Metformin is a superior substrate for renal organic cation transporter OCT2 rather than hepatic OCT1. *Drug metabolism and pharmacokinetics* **2005**, *20* (5), 379-86.
134. Wang, D. S.; Jonker, J. W.; Kato, Y.; Kusuvara, H.; Schinkel, A. H.; Sugiyama, Y., Involvement of organic cation transporter 1 in hepatic and intestinal distribution of metformin. *Journal of Pharmacology and Experimental Therapeutics* **2002**, *302* (2), 510-515.
135. Nakamichi, N.; Shima, H.; Asano, S.; et al.; Involvement of Carnitine/Organic Cation Transporter OCTN1/SLC22A4 in Gastrointestinal Absorption of Metformin. *Journal of Pharmaceutical Sciences* **2013**, *102* (9), 3407-3417.
136. Birsoy, K.; Possemato, R.; Lorbeer, F. K.; Bayraktar, E. C.; Thiru, P.; Yucel, B.; Wang, T.; Chen, W. W.; Clish, C. B.; Sabatini, D. M., Metabolic determinants of cancer cell sensitivity to glucose limitation and biguanides. *Nature* **2014**, *508* (7494), 108-+.
137. Mullen, A. R.; Wheaton, W. W.; Jin, E. S.; Chen, P.-H.; Sullivan, L. B.; Cheng, T.; Yang, Y.; Linehan, W. M.; Chandel, N. S.; DeBerardinis, R. J., Reductive carboxylation supports growth in tumour cells with defective mitochondria. *Nature* **2012**, *481* (7381), 385-U171.
138. Shu, Y.; Sheardown, S. A.; Brown, C.; Owen, R. P.; Zhang, S.; Castro, R. A.; Ianculescu, A. G.; Yue, L.; Lo, J. C.; Burchard, E. G.; Brett, C. M.; Giacomini, K. M., Effect of genetic variation in the organic cation transporter 1 (OCT1) on metformin action. *Journal of Clinical Investigation* **2007**, *117* (5), 1422-1431.
139. Zhou, G. C.; Myers, R.; Li, Y.; Chen, Y. L.; Shen, X. L.; Fenyk-Melody, J.; Wu, M.; Ventre, J.; Doepper, T.; Fujii, N.; Musi, N.; Hirshman, M. F.; Goodyear, L. J.; Moller, D. E., Role of AMP-activated protein kinase in mechanism of metformin action. *Journal of Clinical Investigation* **2001**, *108* (8), 1167-1174.
140. Caton, P. W.; Nayuni, N. K.; Kieswich, J.; Khan, N. Q.; Yaqoob, M. M.; Corder, R., Metformin suppresses hepatic gluconeogenesis through induction of SIRT1 and GCN5. *Journal of Endocrinology* **2010**, *205* (1), 97-106.
141. Algire, C.; Amrein, L.; Zakikhani, M.; Panasci, L.; Pollak, M., Metformin blocks the stimulative effect of a high-energy diet on colon carcinoma growth in vivo and is associated with reduced expression of fatty acid synthase. *Endocrine-Related Cancer* **2010**, *17* (2), 351-360.
142. Goodwin, P. J.; Pritchard, K. I.; Ennis, M.; Clemons, M.; Graham, M.; Fantus, I. G., Insulin-lowering effects of metformin in women with early breast cancer. *Clinical Breast Cancer* **2008**, *8* (6), 501-505.
143. Davidson, M. B.; Peters, A. L., An overview of metformin in the treatment of type 2 diabetes mellitus. *American Journal of Medicine* **1997**, *102* (1), 99-110.
144. Bodmer, M.; Meier, C.; Krahenbuehl, S.; Jick, S. S.; Meier, C. R., Metformin, sulfonylureas, or other antidiabetes drugs and the risk of lactic

- acidosis or hypoglycemia A nested case-control analysis. *Diabetes Care* **2008**, *31* (11), 2086-2091.
145. Wheaton, W. W.; Weinberg, S. E.; Hamanaka, R. B.; Soberanes, S.; Sullivan, L. B.; Anso, E.; Glasauer, A.; Dufour, E.; Mutlu, G. M.; Budigner, G. R. S.; Chandel, N. S., Metformin inhibits mitochondrial complex I of cancer cells to reduce tumorigenesis. *Elife* **2014**, *3*.
146. Liu, X.; Romero, I. L.; Litchfield, L. M.; Lengyel, E.; Locasale, J. W., Metformin Targets Central Carbon Metabolism and Reveals Mitochondrial Requirements in Human Cancers. *Cell Metabolism* **2016**, *24* (5), 728-739.
147. Sporn, M. B., Approaches to prevention of epithelial cancer during preneoplastic period. *Cancer Research* **1976**, *36* (7), 2699-2702.
148. Evans, J. M. M.; Donnelly, L. A.; Emslie-Smith, A. M.; Alessi, D. R.; Morris, A. D., Metformin and reduced risk of cancer in diabetic patients. *British Medical Journal* **2005**, *330* (7503), 1304-1305.
149. Bowker, S. L.; Majumdar, S. R.; Veugelers, P.; Johnson, J. A., Increased cancer-related mortality for patients with type 2 diabetes who use sulfonylureas or insulin - Response to Farooki and Schneider. *Diabetes Care* **2006**, *29* (8), 1990-1991.
150. Libby, G.; Donnelly, L. A.; Donnan, P. T.; Alessi, D. R.; Morris, A. D.; Evans, J. M. M., New users of metformin are at low risk of incident cancer a cohort study among people with type 2 diabetes. *Diabetes Care* **2009**, *32* (9), 1620-1625.
151. Wright, J. L.; Stanford, J. L., Metformin use and prostate cancer in Caucasian men: results from a population-based case-control study. *Cancer Causes & Control* **2009**, *20* (9), 1617-1622.
152. Liu, B.; Fan, Z.; Edgerton, S. M.; Deng, X.-S.; Alimova, I. N.; Lind, S. E.; Thor, A. D., Metformin induces unique biological and molecular responses in triple negative breast cancer cells. *Cell Cycle* **2009**, *8* (13), 2031-2040.
153. Bodmer, M.; Meier, C.; Krahenbuehl, S.; Jick, S. S.; Meier, C. R., Long-term metformin use is associated with decreased risk of breast cancer. *Diabetes Care* **2010**, *33* (6), 1304-1308.
154. Landman, G. W. D.; Kleefstra, N.; van Hateren, K. J. J.; Groenier, K. H.; Gans, R. O. B.; Bilo, H. J. G., Metformin Associated With Lower Cancer Mortality in Type 2 Diabetes - ZODIAC-16. *Diabetes Care* **2010**, *33* (2), 322-326.
155. Geraldine, N.; Marc, A.; Carla, T.; Chantal, M.; Stefaan, B.; Welcome, W.; Frank, B., Relation between diabetes, metformin treatment and the occurrence of malignancies in a Belgian primary care setting. *Diabetes Research and Clinical Practice* **2012**, *97* (2), 331-336.
156. Dowling, R. J. O.; Niraula, S.; Stambolic, V.; Goodwin, P. J., Metformin in cancer: translational challenges. *Journal of Molecular Endocrinology* **2012**, *48* (3), R31-R43.
157. Vigneri, P.; Frasca, F.; Sciacca, L.; Pandini, G.; Vigneri, R., Diabetes and cancer. *Endocrine-Related Cancer* **2009**, *16* (4), 1103-1123.
158. Baur, D. M.; Klotsche, J.; Hamnvik, O.-P. R.; et al.; Type 2 diabetes mellitus and medications for type 2 diabetes mellitus are associated with risk for and mortality from cancer in a German primary care cohort. *Metabolism-Clinical and Experimental* **2011**, *60* (10), 1363-1371.

159. Lai, S. W.; Chen, P. C.; Liao, K. F.; Muo, C. H.; Lin, C. C.; Sung, F. C., Risk of hepatocellular carcinoma in diabetic patients and risk reduction associated with anti-diabetic therapy: a population-based cohort study. *American journal of gastroenterology* **2012**, *107* (1), 46-52.
160. Li, D.; Yeung, S. C.; Hassan, M. M.; Konopleva, M.; Abbruzzese, J. L., Antidiabetic therapies affect risk of pancreatic cancer. *Gastroenterology* **2009**, *137* (2), 482-8.
161. Yang, T.; Yang, Y.; Liu, S., Association between Metformin Therapy and Breast Cancer Incidence and Mortality: Evidence from a Meta-Analysis. *Journal of Breast Cancer* **2015**, *18* (3), 264-270.
162. Franciosi, M.; Lucisano, G.; Lapice, E.; et al.; Metformin Therapy and Risk of Cancer in Patients with Type 2 Diabetes: Systematic Review. In *PLoS One*, **2013**; Vol. 8.
163. Hense, H.-W.; Kajueter, H.; Wellmann, J.; Batzler, W. U., Cancer incidence in type 2 diabetes patients - first results from a feasibility study of the D2C cohort. *Diabetology & Metabolic Syndrome* **2011**, *3*.
164. Col, N. F.; Ochs, L.; Springmann, V.; Aragaki, A. K.; Chlebowski, R. T., Metformin and breast cancer risk: a meta-analysis and critical literature review. *Breast Cancer Res Treat* **2012**, *135* (3), 639-46.
165. Currie, C. J.; Poole, C. D.; Gale, E. A. M., The influence of glucose-lowering therapies on cancer risk in type 2 diabetes. *Diabetologia* **2009**, *52* (9), 1766-1777.
166. Bosco, J. L. F.; Antonsen, S.; Sorensen, H. T.; Pedersen, L.; Lash, T. L., Metformin and incident breast cancer among diabetic women: A population-based case-control study in Denmark. *Cancer Epidemiology Biomarkers & Prevention* **2011**, *20* (1), 101-111.
167. Ferrara, A.; Lewis, J. D.; Quesenberry, C. P., Jr.; Peng, T.; Strom, B. L.; Van Den Eeden, S. K.; Ehrlich, S. F.; Habel, L. A., Cohort study of pioglitazone and cancer incidence in patients with diabetes. *Diabetes Care* **2011**, *34* (4), 923-9.
168. Morden, N. E.; Liu, S. K.; Smith, J.; Mackenzie, T. A.; Skinner, J.; Korc, M., Further exploration of the relationship between insulin glargine and incident cancer: a retrospective cohort study of older Medicare patients. *Diabetes Care* **2011**, *34* (9), 1965-71.
169. Chlebowski, R. T.; McTiernan, A.; Wactawski-Wende, J.; et al.; Diabetes, metformin, and breast cancer in postmenopausal women. *Journal of Clinical Oncology* **2012**, *30* (23), 2844-2852.
170. Ruiter, R.; Visser, L. E.; van Herk-Sukel, M. P.; et al.; Lower risk of cancer in patients on metformin in comparison with those on sulfonylurea derivatives: results from a large population-based follow-up study. *Diabetes Care* **2012**, *35* (1), 119-24.
171. Van Staa, T. P.; Patel, D.; Gallagher, A. M.; de Bruin, M. L., Glucose-lowering agents and the patterns of risk for cancer: a study with the General Practice Research Database and secondary care data. *Diabetologia* **2012**, *55* (3), 654-65.
172. Alimova, I. N.; Liu, B.; Fan, Z.; Edgerton, S. M.; Dillon, T.; Lind, S. E.; Thor, A. D., Metformin inhibits breast cancer cell growth, colony formation and induces cell cycle arrest in vitro. *Cell Cycle* **2009**, *8* (6), 909-915.
173. Zhuang, Y.; Miskimins, W. K., Cell cycle arrest in Metformin treated breast cancer cells involves activation of AMPK, downregulation of cyclin D1,

- and requires p27Kip1 or p21Cip1. *Journal of molecular signaling* **2008**, 3, 18-18.
174. Brown, K. A.; Hunger, N. I.; Docanto, M.; Simpson, E. R., Metformin inhibits aromatase expression in human breast adipose stromal cells via stimulation of AMP-activated protein kinase. *Breast Cancer Research and Treatment* **2010**, 123 (2), 591-596.
175. Ma, J.; Guo, Y.; Chen, S.; et al.; Metformin enhances tamoxifen-mediated tumor growth inhibition in ER-positive breast carcinoma. *Bmc Cancer* **2014**, 14.
176. Zakikhani, M.; Dowling, R.; Fantus, I. G.; Sonenberg, N.; Pollak, M., Metformin is an AMP kinase-dependent growth inhibitor for breast cancer cells. *Cancer Research* **2006**, 66 (21), 10269-10273.
177. Dowling, R. J. O.; Zakikhani, M.; Fantus, I. G.; Pollak, M.; Sonenberg, N., Metformin inhibits mammalian target of rapamycin-dependent translation initiation in breast cancer cells. *Cancer Research* **2007**, 67 (22), 10804-10812.
178. Zhuang, Y.; Miskimins, W. K., Metformin Induces Both Caspase-Dependent and Poly(ADP-ribose) Polymerase-Dependent Cell Death in Breast Cancer Cells. *Molecular Cancer Research* **2011**, 9 (5), 603-615.
179. Hadad, S. M.; Hardie, D. G.; Appleyard, V.; Thompson, A. M., Effects of metformin on breast cancer cell proliferation, the AMPK pathway and the cell cycle. *Clinical & translational oncology* **2013**.
180. Queiroz, E. A. I. F.; Puukila, S.; Eichler, R.; et al.; Metformin induces apoptosis and cell cycle arrest mediated by oxidative stress, AMPK and FOXO3a in MCF-7 breast cancer cells. *Plos One* **2014**, 9 (5).
181. Anisimov, V. N.; Berstein, L. M.; Egormin, P. A.; et al.; Effect of metformin on life span and on the development of spontaneous mammary tumors in HER-2/neu transgenic mice. *Experimental Gerontology* **2005**, 40 (8-9), 685-693.
182. Vazquez-Martin, A.; Oliveras-Ferraros, C.; Menendez, J. A., The antidiabetic drug metformin suppresses HER2 (erbB-2) oncoprotein overexpression via inhibition of the mTOR effector p70S6K1 in human breast carcinoma cells. *Cell Cycle* **2009**, 8 (1), 88-96.
183. Vazquez-Martin, A.; Oliveras-Ferraros, C.; Cufi, S.; Del Barco, S.; Martin-Castillo, B.; Lopez-Bonet, E.; Menendez, J. A., The anti-diabetic drug metformin suppresses the metastasis-associated protein CD24 in MDA-MB-468 triple-negative breast cancer cells. *Oncology Reports* **2011**, 25 (1), 135-140.
184. Zordoky, B. N. M.; Bark, D.; Soltys, C. L.; Sung, M. M.; Dyck, J. R. B., The anti-proliferative effect of metformin in triple-negative MDA-MB-231 breast cancer cells is highly dependent on glucose concentration: Implications for cancer therapy and prevention. *Biochimica Et Biophysica Acta-General Subjects* **2014**, 1840 (6), 1943-1957.
185. Boulay, A.; Rudloff, J.; Ye, J. J.; Zumstein-Mecker, S.; O'Reilly, T.; Evans, D. B.; Chen, S. U.; Lane, H. A., Inhibition of mTOR and estrogen receptor signaling in vitro induces cell death in models of breast cancer. *Clinical Cancer Research* **2005**, 11 (14), 5319-5328.
186. Feng, Z.; Hu, W.; de Stanchina, E.; Teresky, A. K.; Jin, S.; Lowe, S.; Levine, A. J., The regulation of AMPK beta 1, TSC2, and PTEN expression by p53: Stress, cell and tissue specificity, and the role of these gene products in

- modulating the IGF-1-AKT-mTOR pathways. *Cancer Research* **2007**, *67* (7), 3043-3053.
187. Klumper, H.-J.; Beijnen, J. H.; Gurney, H.; Schellens, J. H. M., Inhibitors of mTOR. *Oncologist* **2010**, *15* (12), 1262-1269.
188. Liu, H.; Scholz, C.; Zang, C.; Scheife, J. H.; et al.; Metformin and the mTOR inhibitor Everolimus (RAD001) sensitize breast cancer cells to the cytotoxic effect of chemotherapeutic drugs in vitro. *Anticancer Research* **2012**, *32* (5), 1627-1637.
189. Nahta, R.; O'Regan, R. M., Evolving strategies for overcoming resistance to HER2-directed therapy: Targeting the PI3K/Akt/mTOR pathway. *Clinical Breast Cancer* **2010**, *10*, S72-S78.
190. Vazquez-Martin, A.; Oliveras-Ferraro, C.; del Barco, S.; et al.; mTOR inhibitors and the anti-diabetic biguanide metformin: new insights into the molecular management of breast cancer resistance to the HER2 tyrosine kinase inhibitor lapatinib (TykerbA (R)). *Clinical & Translational Oncology* **2009**, *11* (7), 455-459.
191. Marsin, A. S.; Bertrand, L.; Rider, M. H.; et al.; Phosphorylation and activation of heart PFK-2 by AMPK has a role in the stimulation of glycolysis during ischaemia. *Curr Biol* **2000**, *10* (20), 1247-55.
192. Kudo, N.; Barr, A. J.; Barr, R. L.; Desai, S.; Lopaschuk, G. D., High rates of fatty acid oxidation during reperfusion of ischemic hearts are associated with a decrease in malonyl-CoA levels due to an increase in 5'-AMP-activated protein kinase inhibition of acetyl-CoA carboxylase. *Journal of biological chemistry* **1995**, *270* (29), 17513-20.
193. Salt, I. P.; Johnson, G.; Ashcroft, S. J.; Hardie, D. G., AMP-activated protein kinase is activated by low glucose in cell lines derived from pancreatic beta cells, and may regulate insulin release. *Biochem Journal* **1998**, *335* (Pt 3), 533-9.
194. Hardie, D. G., AMP-activated protein kinase: an energy sensor that regulates all aspects of cell function. *Genes Dev* **2011**, *25* (18), 1895-908.
195. Hardie, D. G.; Hawley, S. A.; Scott, J., AMP-activated protein kinase - development of the energy sensor concept. *Journal of Physiology-London* **2006**, *574* (1), 7-15.
196. Hadad, S. M.; Baker, L.; Quinlan, P. R.; et al.; Histological evaluation of AMPK signalling in primary breast cancer. *BMC Cancer* **2009**, *9*, 307.
197. Kisfalvi, K.; Sinnett-Smith, J.; Eibl, G.; Rozengurt, E., Metformin inhibits growth of human pancreatic cancer cells in vitro and in vivo. *Pancreas* **2009**, *38* (8), 1016-1017.
198. Buzzai, M.; Jones, R. G.; Amaravadi, R. K.; Lum, J. J.; DeBerardinis, R. J.; Zhao, F.; Viollet, B.; Thompson, C. B., Systemic treatment with the antidiabetic drug metformin selectively impairs p53-deficient tumor cell growth. *Cancer Research* **2007**, *67* (14), 6745-6752.
199. Vazquez-Martin, A.; Oliveras-Ferraro, C.; Cufi, S.; Martin-Castillo, B.; Menendez, J. A., Metformin and Energy Metabolism in Breast Cancer: From Insulin Physiology to Tumour-initiating Stem Cells. *Current Molecular Medicine* **2010**, *10* (7), 674-691.
200. Woods, A.; Johnstone, S. R.; Dickerson, K.; et al.; LKB1 is the upstream kinase in the AMP-activated protein kinase cascade. *Current Biology* **2003**, *13* (22), 2004-2008.

201. Woods, A.; Dickerson, K.; Heath, R.; et al.; Ca²⁺/calmodulin-dependent protein kinase kinase-beta acts upstream of AMP-activated protein kinase in mammalian cells. *Cell Metabolism* **2005**, *2* (1), 21-33.
202. Hemminki, A.; Markie, D.; Tomlinson, I.; et al.; A., A serine/threonine kinase gene defective in Peutz-Jegheus syndrome. *Nature* **1998**, *391* (6663), 184-187.
203. Hawley, S. A.; Gadalla, A. E.; Olsen, G. S.; Hardie, D. G., The antidiabetic drug metformin activates the AMP-activated protein kinase cascade via an adenine nucleotide-independent mechanism. *Diabetes* **2002**, *51* (8), 2420-2425.
204. Hardie, D. G.; Carling, D.; Carlson, M., The AMP-activated/SNF1 protein kinase subfamily: Metabolic sensors of the eukaryotic cells? *Annual Review of Biochemistry* **1998**, *67*, 821-855.
205. Carling, D., The AMP-activated protein kinase cascade - a unifying system for energy control. *Trends in Biochemical Sciences* **2004**, *29* (1), 18-24.
206. Shaw, R. J.; Lamia, K. A.; Vasquez, D.; et al.; The kinase LKB1 mediates glucose homeostasis in liver and therapeutic effects of metformin. *Science* **2005**, *310* (5754), 1642-1646.
207. Marignani, P. A., LKB1, the multitasking tumour suppressor kinase. *Journal of Clinical Pathology* **2005**, *58* (1), 15-19.
208. Shen, Z.; Shen, Z. Z.; Shao, Z. M.; Liu, G.; Wu, J., The tumor suppressor gene LKB1 is associated with prognosis in human breast carcinoma. *Breast Cancer Research and Treatment* **2002**, *76*, S124-S124.
209. Ben Sahra, I.; Laurent, K.; Loubat, A.; Giorgetti-Peraldi, S.; Colosetti, P.; Auberger, P.; Tanti, J. F.; Le Marchand-Brustel, Y.; Bost, F., The antidiabetic drug metformin exerts an antitumoral effect in vitro and in vivo through a decrease of cyclin D1 level. *Oncogene* **2008**, *27* (25), 3576-3586.
210. Isakovic, A.; Harhaji, L.; Stevanovic, D.; et al.; Dual antiglioma action of metformin: cell cycle arrest and mitochondria-dependent apoptosis. *Cellular and Molecular Life Sciences* **2007**, *64* (10), 1290-1302.
211. Janjetovic, K.; Harhaji-Trajkovic, L.; Misirkic-Marjanovic, et al.; In vitro and in vivo anti-melanoma action of metformin. *European Journal of Pharmacology* **2011**, *668* (3), 373-382.
212. Cantrell, L. A.; Zhou, C.; Mendivil, A.; et al.; Metformin is a potent inhibitor of endometrial cancer cell proliferation-implications for a novel treatment strategy. *Gynecologic Oncology* **2010**, *116* (1), 92-98.
213. Rattan, R.; Giri, S.; Hartmann, L. C.; Shridhar, V., Metformin attenuates ovarian cancer cell growth in an AMP-kinase dispensable manner. *Journal of Cellular and Molecular Medicine* **2011**, *15* (1), 166-178.
214. Holland, W.; Morrison, T.; Chang, Y.; Wiernsperger, B.; Stith, B. J., Metformin (glucophage) inhibits tyrosine phosphatase activity to stimulate the insulin receptor tyrosine kinase. *Biochemical Pharmacology* **2004**, *67* (11), 2081-2091.
215. Pollak, M., Metformin and other biguanides in oncology: Advancing the research agenda. *Cancer Prevention Research* **2010**, *3* (9), 1060-1065.
216. Pugeat, M.; Nader, N.; Hogeveen, K.; Raverot, G.; Dechaud, H.; Grenot, C., Sex hormone-binding globulin gene expression in the liver: Drugs and the metabolic syndrome. *Molecular and Cellular Endocrinology* **2010**, *316* (1), 53-59.

217. Kalender, A.; Selvaraj, A.; Kim, S. Y.; et al.; Metformin, independent of AMPK, inhibits mTORC1 in a rap GTPase-dependent manner. *Cell Metabolism* **2010**, *11* (5), 390-401.
218. Bhalla, K.; Hwang, B. J.; Dewi, R. E.; Twaddel, W.; Goloubeva, O. G.; Wong, K.-K.; Saxena, N. K.; Biswal, S.; Girnun, G. D., Metformin prevents liver tumorigenesis by inhibiting pathways driving hepatic lipogenesis. *Cancer Prevention Research* **2012**, *5* (4), 544-552.
219. Kakarala, M.; Wicha, M. S., Implications of the cancer stem-cell hypothesis for breast cancer prevention and therapy. *Journal of Clinical Oncology* **2008**, *26* (17), 2813-2820.
220. Li, X.; Lewis, M. T.; Huang, J.; Gutierrez, C.; et al.; Intrinsic resistance of tumorigenic breast cancer cells to chemotherapy. *Journal of the National Cancer Institute* **2008**, *100* (9), 672-679.
221. Hirsch, H. A.; Iliopoulos, D.; Tsichlis, P. N.; Struhl, K., Metformin Selectively Targets Cancer Stem Cells, and Acts Together with Chemotherapy to Block Tumor Growth and Prolong Remission (vol 69, pg 7507, 2009). *Cancer Research* **2009**, *69* (22), 8832-8833.
222. Iliopoulos, D.; Hirsch, H. A.; Struhl, K., Metformin decreases the dose of chemotherapy for prolonging tumor remission in mouse xenografts involving multiple cancer cell types. *Cancer Research* **2011**, *71* (9), 3196-3201.
223. Vazquez-Martin, A.; Oliveras-Ferraro, C.; Del Barco, S.; et al.; The anti-diabetic drug metformin suppresses self-renewal and proliferation of trastuzumab-resistant tumor-initiating breast cancer stem cells. *Breast Cancer Research and Treatment* **2011**, *126* (2), 355-364.
224. Vazquez-Martin, A.; Oliveras-Ferraro, C.; Cuff, S.; et al.; Metformin regulates breast cancer stem cell ontogeny by transcriptional regulation of the epithelial-mesenchymal transition (EMT) status. *Cell Cycle* **2010**, *9* (18), 3807-3814.
225. Rocha, G. Z.; Dias, M. M.; Ropelle, E. R.; et al.; Metformin amplifies chemotherapy-induced AMPK activation and antitumoral growth. *Clinical Cancer Research* **2011**, *17* (12), 3993-4005.
226. Jones, R. G.; Plas, D. R.; Kubek, S.; Buzzai, M.; Mu, J.; Xu, Y.; Birnbaum, M. J.; Thompson, C. B., AMP-activated protein kinase induces a p53-dependent metabolic checkpoint. *Molecular Cell* **2005**, *18* (3), 283-293.
227. Okoshi, R.; Ozaki, T.; Yamamoto, H.; et al.; Activation of AMP-activated protein kinase induces p53-dependent apoptotic cell death in response to energetic stress. *Journal of Biological Chemistry* **2008**, *283* (7), 3979-3987.
228. Campagnoli, C.; Berrino, F.; Venturelli, E.; et al.; Metformin decreases circulating androgen and estrogen levels in nondiabetic women with breast cancer. *Clinical Breast Cancer* **2013**, *13* (6), 433-438.
229. Samarajeewa, N. U.; Ham, S.; Yang, F.; Simpson, E. R.; Brown, K. A., Promoter-specific effects of metformin on aromatase transcript expression. *Steroids* **2011**, *76* (8), 768-771.
230. Thompson, A. M., Molecular pathways: Preclinical models and clinical trials with metformin in breast cancer. *Clinical Cancer Research* **2014**, *20* (10), 2508-2515.
231. Jiralerpong, S.; Palla, S. L.; Giordano, S. H.; et al.; Metformin and pathologic complete responses to neoadjuvant chemotherapy in diabetic

- patients with breast cancer. *Journal of Clinical Oncology* **2009**, *27* (20), 3297-3302.
232. Gandini, S.; Guerrieri-Gonzaga, A.; Pruneri, G.; et al.; Association of molecular subtypes with Ki-67 changes in untreated breast cancer patients undergoing pre-surgical trials. *Annals of Oncology* **2014**, *25* (3), 618-623.
233. Hadad, S.; Iwamoto, T.; Jordan, L.; et al.; Evidence for biological effects of metformin in operable breast cancer: a pre-operative, window-of-opportunity, randomized trial. *Breast Cancer Research and Treatment* **2011**, *128* (3), 783-794.
234. Niraula, S.; Dowling, R. J. O.; Ennis, M.; et al.; Metformin in early breast cancer: a prospective window of opportunity neoadjuvant study. *Breast Cancer Research and Treatment* **2012**, *135* (3), 821-830.
235. Campagnoli, C.; Pasanisi, P.; Abba, C.; et al.; Effect of different doses of metformin on serum testosterone and insulin in non-diabetic women with breast cancer: A randomized Study. *Clinical Breast Cancer* **2012**, *12* (3), 175-182.
236. Lord, S. R.; Patel, N.; Liu, D.; et al.; Neoadjuvant Window Studies of Metformin and Biomarker Development for Drugs Targeting Cancer Metabolism. *Journal of the National Cancer Institute Monographs* **2015**, (51), 81-86.
237. Lord, S.; Liu, D.; Cheng, W.-C.; et al.; Metformin increases 18F-FDG flux and inhibits fatty acid oxidation at clinical doses in breast cancer: Results of a phase 0 clinical trial. *European Journal of Surgical Oncology* **2016**, *42* (11).
238. Goodwin, P. J.; Parulekar, W. R.; Gelmon, K. A.; et al.; Effect of Metformin vs Placebo on Weight and Metabolic Factors in NCIC CTG MA.32. *Jnci-Journal of the National Cancer Institute* **2015**, *107* (3).
239. Hadad, S. M.; Coates, P.; Jordan, L. B.; et al.; Evidence for biological effects of metformin in operable breast cancer: biomarker analysis in a pre-operative window of opportunity randomized trial. *Breast Cancer Research and Treatment* **2015**, *150* (1), 149-155.
240. Bonanni, B.; Puntoni, M.; Cazzaniga, M.; et al.; Dual effect of metformin on breast cancer proliferation in a randomized presurgical trial. *Journal of Clinical Oncology* **2012**, *30* (21), 2593-2600.
241. Cazzaniga, M.; DeCensi, A.; Pruneri, G.; et al.; Effect of metformin on apoptosis in a presurgical trial in non-diabetic patients with breast cancer. *Cancer Research* **2012**, *72*.
242. Kalinsky, K.; Crew, K. D.; Refice, S.; et al.; Pre-surgical trial of metformin in overweight and obese, multiethnic patients with newly diagnosed breast cancer. *Cancer Research* **2012**, *72*.
243. Kajbaf, F.; De Broe, M. E.; Lalau, J.-D., Therapeutic Concentrations of Metformin: A Systematic Review. *Clinical Pharmacokinetics* **2016**, *55* (4), 439-459.
244. Lalau, J.-D.; Lemaire-Hurtel, A.-S.; Lacroix, C., Establishment of a database of metformin plasma concentrations and erythrocyte levels in normal and emergency situations. *Clinical Drug Investigation* **2011**, *31* (6), 435-438.
245. Lalau, J. D.; Lacroix, C., Measurement of metformin concentration in erythrocytes: clinical implications. *Diabetes Obesity & Metabolism* **2003**, *5* (2), 93-98.

246. Frid, A.; Sterner, G. N.; Londahl, M.; et al.; Novel assay of metformin levels in patients with type 2 diabetes and varying levels of renal function clinical recommendations. *Diabetes Care* **2010**, *33* (6), 1291-1293.
247. Dart, R. C., Medical toxicology. 3rd edition ed.; lippincott williams and wilkins: philadelphia, Pa 19106 USA, 2004.
248. Schulz, M.; Schmoldt, A., Therapeutic and toxic blood concentrations of more than 800 drugs and other xenobiotics. *Pharmazie* **2003**, *58* (7), 447-474.
249. Schulz, M.; Iwersen-Bergmann, S.; Andresen, H.; Schmoldt, A., Therapeutic and toxic blood concentrations of nearly 1,000 drugs and other xenobiotics. *Critical Care* **2012**, *16* (4).
250. Wilcock, C.; Bailey, C. J., Accumulation of metformin by tissues of the normal and diabetic mouse. *Xenobiotica* **1994**, *24* (1), 49-57.
251. Sadighi, S.; Amanpour, S.; Behrouzi, B.; et al.; Lack of Metformin Effects on Different Molecular Subtypes of Breast Cancer under Normoglycemic Conditions: An in vitro Study. *Asian Pacific Journal of Cancer Prevention* **2014**, *15* (5), 2287-2290.
252. Owen, M. R.; Doran, E.; Halestrap, A. P., Evidence that metformin exerts its anti-diabetic effects through inhibition of complex 1 of the mitochondrial respiratory chain. *Biochemical Journal* **2000**, *348*, 607-614.
253. Qu, Y.; Han, B. C.; Yu, Y.; et al.; Evaluation of MCF10A as a Reliable Model for Normal Human Mammary Epithelial Cells. *Plos One* **2015**, *10* (7).
254. Dawson, P. J.; Wolman, S. R.; Tait, L.; Heppner, G. H.; Miller, F. R., MCF10AT: A model for the evolution of cancer from proliferative breast disease. *American Journal of Pathology* **1996**, *148* (1), 313-319.
255. Miller, F. R.; Santner, S. J.; Tait, L.; Dawson, P. J., MCF10DCIS.com xenograft model of human comedo ductal carcinoma in situ. *Journal of the National Cancer Institute* **2000**, *92* (14), 1185-1186.
256. Nutter, F.; Holen, I.; Brown, H. K.; et al.; Different molecular profiles are associated with breast cancer cell homing compared with colonisation of bone: evidence using a novel bone-seeking cell line. *Endocrine-Related Cancer* **2014**, *21* (2), 327-341.
257. Kang, Y. B.; Siegel, P. M.; Shu, W. P.; Drobniak, M.; et al.; A multigenic program mediating breast cancer metastasis to bone. *Cancer Cell* **2003**, *3* (6), 537-549.
258. Schmittgen, T. D.; Lee, E. J.; Jiang, J.; Sarkar, A.; Yang, L.; Elton, T. S.; Chen, C., Real-time PCR quantification of precursor and mature microRNA. *Methods* **2008**, *44* (1), 31-8.
259. Bustin, S. A.; Vandesompele, J.; Pfaffl, M. W., Standardization of qPCR and RT-qPCR. *Genetic Engineering & Biotechnology News* **2009**, *29* (14), 40-43.
260. Hanukoglu, I.; Tanese, N.; Fuchs, E., Complementary-DNA sequence of a human cytoplasmic actin - interspecies divergence of 3' non-coding regions. *Journal of Molecular Biology* **1983**, *163* (4), 673-678.
261. Detre, S.; Jotti, G. S.; Dowsett, M., A quickscore method for immunohistochemical semiquantitation - validation for estrogen-receptor in breast carcinomas. *Journal of Clinical Pathology* **1995**, *48* (9), 876-878.
262. Andrzejewski, S.; Gravel, S.-P.; Pollak, M.; St-Pierre, J., Metformin directly acts on mitochondria to alter cellular bioenergetics. *Cancer & metabolism* **2014**, *2*, 12-12.

263. Munshi, A.; Hobbs, M.; Meyn, R. E., Clonogenic cell survival assay. *Chemosensitivity: in Vitro Assays* **2005**, *110*, 21-28.
264. Rafehi, H.; Orlowski, C.; Georgiadis, G. T.; Ververis, K.; El-Osta, A.; Karagiannis, T. C., Clonogenic Assay: Adherent Cells. *Journal of Visualized Experiments* **2011**, (49).
265. Verweij, J.; Pinedo, H. M., Mitomycin C: mechanism of action, usefulness and limitations. *Anticancer Drugs* **1990**, *1* (1), 5-13.
266. Nies, A. T.; Koepsell, H.; Damme, K.; Schwab, M., Organic cation transporters (OCTs, MATEs), in vitro and in vivo evidence for the importance in drug therapy. *Drug Transporters* **2011**, *201*, 105-167.
267. Christensen, M. M.; Pedersen, R. S.; Stage, T. B.; et al.; A gene-gene interaction between polymorphisms in the OCT2 and MATE1 genes influences the renal clearance of metformin. *Pharmacogenet Genomics* **2013**, *23* (10), 526-34.
268. Choi, J.; Yee, S.; Ramirez, A.; et al.; A Common 5' -UTR variant in MATE2-K is associated with poor response to metformin. *Clin Pharmacol Ther* **2011**, *90* (5), 674-84.
269. Dujic, T.; Zhou, K.; Donnelly, L. A.; et al.; Association of organic cation transporter 1 with intolerance to metformin in type 2 diabetes: A GoDARTS Study. *Diabetes* **2015**, *64* (5), 1786-93.
270. Tzvetkov, M. V.; Vormfelde, S. V.; Balen, D.; et al.; The effects of genetic polymorphisms in the organic cation transporters OCT1, OCT2, and OCT3 on the renal clearance of metformin. *Clinical pharmacology and therapeutics* **2009**, *86* (3), 299-306.
271. Shu, Y.; Brown, C.; Castro, R. A.; et al.; Effect of genetic variation in the organic cation transporter 1, OCT1, on metformin pharmacokinetics. *Clinical pharmacology and therapeutics* **2008**, *83* (2), 273-80.
272. Becker, M. L.; Visser, L. E.; van Schaik, R. H.; Hofman, A.; Uitterlinden, A. G.; Stricker, B. H., Genetic variation in the multidrug and toxin extrusion 1 transporter protein influences the glucose-lowering effect of metformin in patients with diabetes: A preliminary study. In *Diabetes*, 2009; Vol. 58, pp 745-9.
273. Song, I. S.; Shin, H. J.; Shim, E. J.; Jung, I. S.; Kim, W. Y.; Shon, J. H.; Shin, J. G., Genetic variants of the organic cation transporter 2 influence the disposition of metformin. *Clinical pharmacology and therapeutics* **2008**, *84* (5), 559-62.
274. Chen, Y.; Li, S.; Brown, C.; Cheatham, S.; et al.; Effect of genetic variation in the organic cation transporter 2 on the renal elimination of metformin. *Pharmacogenet Genomics* **2009**, *19* (7), 497-504.
275. Jablonski, K. A.; McAteer, J. B.; de Bakker, P. I.; Franks, P. W.; Pollin, T. I.; Hanson, R. L.; Saxena, R.; Fowler, S.; et al.; Common variants in 40 genes assessed for diabetes incidence and response to metformin and lifestyle intervention in the diabetes prevention program. *Diabetes* **2010**, *59* (10), 2672-81.
276. Tkac, I.; Klimcakova, L.; Javorsky, M.; et al.; Pharmacogenomic association between a variant in SLC47A1 gene and therapeutic response to metformin in type 2 diabetes. *Diabetes, obesity & metabolism* **2013**, *15* (2), 189-91.
277. Stocker, S. L.; Morrissey, K. M.; Yee, S. W.; et al.; The effect of novel promoter variants in MATE1 and MATE2 on the pharmacokinetics and

- pharmacodynamics of metformin. *Clinical pharmacology and therapeutics* **2013**, 93 (2), 186-94.
278. Yoon, H.; Cho, H. Y.; Yoo, H. D.; Kim, S. M.; Lee, Y. B., Influences of organic cation transporter polymorphisms on the population pharmacokinetics of metformin in healthy subjects. *Aaps j* **2013**, 15 (2), 571-80.
279. Cai, H.; Zhang, Y.; Han, T.; Everett, R. S.; Thakker, D. R., Cation-selective transporters are critical to the AMPK-mediated antiproliferative effects of metformin in human breast cancer cells. *International Journal of Cancer* **2016**, 138 (9), 2281-2292.
280. Gray, J.; Neve, R., A collection of breast cancer cell lines for the study of functionally distinct cancer subtypes. *caArray* **2012**.
281. Gordon, L. A.; Mulligan, K. T.; Maxwell-Jones, H.; Adams, M.; Walker, R. A.; Jones, J. L., Breast cell invasive potential relates to the myoepithelial phenotype. *Int J Cancer* **2003**, 106 (1), 8-16.
282. Rizwan, A.; Cheng, M.; Bhujwalla, Z. M.; Krishnamachary, B.; Jiang, L.; Glunde, K., Breast cancer cell adhesome and degradome interact to drive metastasis. *Breast Cancer* **2015**, 1, 15017.
283. Su, Y.; Pogash, T. J.; Nguyen, T. D.; et al.; Development and characterization of two human triple - negative breast cancer cell lines with highly tumorigenic and metastatic capabilities. *Cancer Medicine* **2016**, 5 (3), 558-573.
284. Hilgendorf, C.; Ahlin, G.; Seithel, A.; Artursson, P.; Ungell, A.-L.; Karlsson, J., Expression of thirty-six drug transporter genes in human intestine, liver, kidney, and organotypic cell lines. *Drug Metabolism and Disposition* **2007**, 35 (8), 1333-1340.
285. Reid, Y. A., Characterization and authentication of cancer cell lines: an overview. *Methods in molecular biology (Clifton, N.J.)* **2011**, 731, 35-43.
286. Chowdhury, S.; Yung, E.; Pintilie, M.; et al., MATE2 expression is associated with cancer cell response to metformin. *Plos One* **2016**, 11 (12).
287. Barretina, J.; Caponigro, G.; Stransky, N.; et al.; The Cancer Cell Line Encyclopedia enables predictive modelling of anticancer drug sensitivity (vol 483, pg 603, 2012). *Nature* **2012**, 492 (7428), 290-290.
288. Liu, L. L.; Zhao, H.; Ma, T. F.; Ge, F.; Chen, C. S.; Zhang, Y. P., Identification of valid reference genes for the normalization of RT-qPCR expression studies in human breast cancer cell lines treated with and without transient transfection. *Plos One* **2015**, 10 (1).
289. Fang, X.; Cai, Y.; Liu, J.; Wang, Z.; Wu, Q.; Zhang, Z.; Yang, C. J.; Yuan, L.; Ouyang, G., Twist2 contributes to breast cancer progression by promoting an epithelial-mesenchymal transition and cancer stem-like cell self-renewal. *Oncogene* **2011**, 30 (47), 4707-4720.
290. Barber, R. D.; Harmer, D. W.; Coleman, R. A.; Clark, B. J., GAPDH as a housekeeping gene: analysis of GAPDH mRNA expression in a panel of 72 human tissues. *Physiological Genomics* **2005**, 21 (3), 389-395.
291. Greenbaum, D.; Colangelo, C.; Williams, K.; Gerstein, M., Comparing protein abundance and mRNA expression levels on a genomic scale. *Genome Biology* **2003**, 4 (9).
292. Osborne CK, H. K., Trent JM, Biological differences among MCF-7 human breast cancer cell lines from different laboratories | SpringerLink. **1987**.

293. Lee, A. V.; Oesterreich, S.; Davidson, N. E., MCF-7 Cells-changing the course of breast cancer research and care for 45 Years. *Journal of the National Cancer Institute* **2015**, *107* (7).
294. Wang, Y.; Zhang, M.-X.; Duan, X.-y.; Zhou, S.-n.; Ermek, T.; Wang, Y.-n.; Cai, H.; Wang, J.-s., Effects of antidiabetic drug metformin on human breast carcinoma cells with different estrogen receptor expressing in vitro. *Chinese journal of cellular and molecular immunology* **2011**, *27* (3), 253-6.
295. Madiraju, A. K.; Erion, D. M.; Rahimi, Y.; et al.; Metformin suppresses gluconeogenesis by inhibiting mitochondrial glycerophosphate dehydrogenase. *Nature* **2014**, *510* (7506), 542-+.
296. Dowling, R. J. O.; Zakikhani, M.; Sonenberg, N.; Pollak, M., Metformin mediated AMPK activation inhibits translation initiation in breast cancer cells. *Proceedings of the American Association for Cancer Research Annual Meeting* **2007**, *48*, 1059-1059.
297. Barnabas, N.; Cohen, D., Phenotypic and molecular characterization of MCF10DCIS and SUM breast cancer cell lines. *International journal of breast cancer* **2013**, *2013*, 872743-872743.
298. Yang, J.; Elias, J. J.; Petrakis, N. L.; Wellings, S. R.; Nandi, S., Effects of hormones and growth factors on human mammary epithelial cells in collagen gel culture. **1981**.
299. Salle, V.; Soutou, B.; Magnien, V.; Israel, L.; Crepin, M., Growth factors of cultured epithelial cells of breast diseases and breast carcinoma. *Bull Cancer* **1992**, *79* (2), 133-40.
300. Sheffield, L. G.; Welsch, C. W., Cholera-toxin-enhanced growth of human-breast cancer cell-lines invitro and invivo - interaction with estrogen. *International Journal of Cancer* **1985**, *36* (4), 479-483.
301. Snider, R. M.; McKenzie, J. R.; Kraft, L.; Kozlov, E.; Wikswo, J. P.; Cliffel, D. E., The effects of cholera toxin on cellular energy metabolism. In *Toxins (Basel)*, 2010; Vol. 2, pp 632-48.
302. Stampfer, M. R., Cholera-toxin stimulation of human mammary epithelial-cells in culture. In *Vitro-Journal of the Tissue Culture Association* **1982**, *18* (6), 531-537.
303. Bhute, V. J.; Ma, Y.; Bao, X.; Palecek, S. P., The Poly (ADP-Ribose) polymerase inhibitor veliparib and radiation cause significant cell line dependent metabolic changes in breast cancer cells. *Scientific Reports* **2016**, *6*.
304. Risinger, A. L.; Dybdal-Hargreaves, N. F.; Mooberry, S. L., Breast cancer cell lines exhibit differential sensitivities to microtubule-targeting drugs independent of doubling time. *Anticancer Research* **2015**, *35* (11), 5845-5850.
305. Shen, G. X., Mitochondrial dysfunction, oxidative stress and diabetic cardiovascular disorders. *Cardiovascular & Hematological Disorders - Drug Targets* **2012**, *12* (2), 106-112.
306. Mosmann, T., Rapid colorimetric assay for cellular growth and survival - application to proliferation and cyto-toxicity assays. *Journal of Immunological Methods* **1983**, *65* (1-2), 55-63.
307. Strober, W., Trypan blue exclusion test of cell viability. *Current protocols in immunology* **2015**, *111*, 3:1-3.
308. Marinello, P. C.; da Silva, T. N. X.; Panis, C.; et al.; Mechanism of metformin action in MCF-7 and MDA-MB-231 human breast cancer cells

- involves oxidative stress generation, DNA damage, and transforming growth factor beta 1 induction. *Tumor Biology* **2016**, *37* (4), 5337-5346.
309. Rajh, M.; Dolinar, K.; Mis, K.; Pavlin, M.; Pirkmajer, S., Medium renewal blocks anti-proliferative effects of metformin in cultured MDA-MB-231 breast cancer cells. *Plos One* **2016**, *11* (5).
310. Davies, G.; Lobanova, L.; Dawicki, W.; Groot, G.; Gordon, J. R.; Bowen, M.; Harkness, T.; Arnason, T., Metformin inhibits the development, and promotes the resensitization, of treatment-resistant breast cancer. *Plos One* **2017**, *12* (12).
311. Thurber, A. E.; Nelson, M.; Frost, C. L.; Levin, M.; Brackenbury, W. J.; Kaplan, D. L., IK channel activation increases tumor growth and induces differential behavioral responses in two breast epithelial cell lines. *Oncotarget* **2017**, *8* (26), 42382-42397.
312. Li, B.; Takeda, T.; Tsuji, K.; Kondo, A.; Kitamura, M.; Wong, T. F.; Yaegashi, N., The antidiabetic drug metformin inhibits uterine leiomyoma cell proliferation via an AMP-activated protein kinase signaling pathway. *Gynecological Endocrinology* **2013**, *29* (1), 87-90.
313. Storozhuk, Y.; Hopmans, S. N.; Sanli, T.; et al.; Metformin inhibits growth and enhances radiation response of non-small cell lung cancer (NSCLC) through ATM and AMPK. *British Journal of Cancer* **2013**, *108* (10), 2021-2032.
314. Zhang, J.; Li, G.; Chen, Y.; Fang, L.; Guan, C.; Bai, F.; Ma, M.; Lyu, J.; Meng, Q. H., Metformin Inhibits Tumorigenesis and Tumor Growth of Breast Cancer Cells by Upregulating miR-200c but Downregulating AKT2 Expression. *Journal of Cancer* **2017**, *8* (10), 1849-1864.
315. Reshkin, S. J.; Bellizzi, A.; Albarani, V.; Guerra, L.; Tommasino, M.; Paradiso, A.; Casavola, V., Phosphoinositide 3-kinase is involved in the tumor-specific activation of human breast cancer cell Na⁺/H⁺ exchange, motility, and invasion induced by serum deprivation. *Journal of Biological Chemistry* **2000**, *275* (8), 5361-5369.
316. Hopkins, D. M.; Morris, J. A.; Oates, K.; Huddart, H.; Staff, W. G., X-RAY- microanalysis of bulk hydrated specimens of neoplastic and nonneoplastic human urothelium. *Journal of Pathology* **1992**, *166* (3), 317-322.
317. Nelson, M. T.; Short, A.; Cole, S. L.; et al.; Preferential, enhanced breast cancer cell migration on biomimetic electrospun nanofiber 'cell highways'. *Bmc Cancer* **2014**, *14*.
318. Sung, Y. M.; Xu, X.; Sun, J.; Mueller, D.; Sentissi, K.; Johnson, P.; Urbach, E.; Seillier-Moiseiwitsch, F.; Johnson, M. D.; Mueller, S. C., Tumor suppressor function of Syk in human MCF10A in vitro and normal mouse mammary epithelium in vivo. *Plos One* **2009**, *4* (10).
319. Foulkes, W. D.; Smith, I. E.; Reis-Filho, J. S., Triple-Negative Breast Cancer. *New England Journal of Medicine* **2010**, *363* (20), 1938-1948.
320. Lehmann, B. D.; Bauer, J. A.; Chen, X.; Sanders, M. E.; Chakravarthy, A. B.; Shyr, Y.; Pietenpol, J. A., Identification of human triple-negative breast cancer subtypes and preclinical models for selection of targeted therapies. *Journal of Clinical Investigation* **2011**, *121* (7), 2750-2767.
321. Perou, C. M., Molecular stratification of triple-negative breast cancers. *Oncologist* **2011**, *16*, 61-70.

322. Ginestier, C.; Hur, M. H.; Charafe-Jauffret, E.; et al.; ALDH1 is a marker of normal and malignant human mammary stem cells and a predictor of poor clinical outcome. *Cell Stem Cell* **2007**, *1* (5), 555-567.
323. Ricardo, S.; Vieira, A. F.; Gerhard, R.; et al., Breast cancer stem cell markers CD44, CD24 and ALDH1: expression distribution within intrinsic molecular subtype. *Journal of Clinical Pathology* **2011**, *64* (11), 937-946.
324. Marotta, L. L. C.; Almendro, V.; Marusyk, A.; et al., The JAK2/STAT3 signaling pathway is required for growth of CD44(+)CD24(-) stem cell-like breast cancer cells in human tumors. *Journal of Clinical Investigation* **2011**, *121* (7), 2723-2735.
325. Wong, M. H.; Stockler, M. R.; Pavlakis, N., Bisphosphonates and other bone agents for breast cancer. *The Cochrane database of systematic reviews* **2012**, (2), Cd003474.
326. Coleman, R. E.; McCloskey, E. V., Bisphosphonates in oncology. *Bone* **2011**, *49* (1), 71-6.
327. Lacey, D. L.; Boyle, W. J.; Simonet, W. S.; Kostenuik, P. J.; Dougall, W. C.; Sullivan, J. K.; San Martin, J.; Dansey, R., Bench to bedside: elucidation of the OPG-RANK-RANKL pathway and the development of denosumab. *Nature reviews Drug discovery* **2012**, *11* (5), 401-19.
328. Geiger, T.; Wisniewski, J. R.; Cox, J.; Zanivan, S.; Kruger, M.; Ishihama, Y.; Mann, M., Use of stable isotope labeling by amino acids in cell culture as a spike-in standard in quantitative proteomics. *Nature Protocols* **2011**, *6* (2), 147-157.
329. Geiger, T.; et al., Comparative proteomic analysis of eleven common cell lines. *PeptideAtlas* **2012**.
330. Westbrook, J. A., CAPG and GIPC1: Breast Cancer Biomarkers for Bone Metastasis Development and Treatment (vol 108, djv336, 2016). *Jnci-Journal of the National Cancer Institute* **2016**, *108* (4).
331. Pryor, R.; Cabreiro, F., Repurposing metformin: an old drug with new tricks in its binding pockets. In *Biochem J*, 2015; Vol. 471, pp 307-22.
332. Sacco, F.; Silvestri, A.; Posca, D.; Pirro, S.; Gherardini, P. F.; Castagnoli, L.; Mann, M.; Cesareni, G., Deep proteomics of breast cancer cells reveals that metformin rewires signaling networks away from a pro-growth State. *Cell Systems* **2016**, *2* (3), 159-171.
333. Orecchioni, S.; Reggiani, F.; Talarico, G.; Mancuso, P.; Calleri, A.; Gregato, G.; Labanca, V.; Noonan, D. M.; Dallaglio, K.; Albini, A.; Bertolini, F., The biguanides metformin and phenformin inhibit angiogenesis, local and metastatic growth of breast cancer by targeting both neoplastic and microenvironment cells. *International Journal of Cancer* **2015**, *136* (6), E534-E544.
334. Phoenix, K. N.; Vumbaca, F.; Fox, M. M.; Evans, R.; Claffey, K. P., Dietary energy availability affects primary and metastatic breast cancer and metformin efficacy. *Breast Cancer Research and Treatment* **2010**, *123* (2), 333-344.
335. Bayraktar, S.; Hernandez-Aya, L. F.; Lei, X.; Meric-Bernstam, F.; Litton, J. K.; Hsu, L.; Hortobagyi, G. N.; Gonzalez-Angulo, A. M., Effect of metformin on survival outcomes in diabetic patients with triple receptor-negative breast cancer. *Cancer* **2012**, *118* (5), 1202-1211.

336. Hannigan, A.; Burchmore, R.; Wilson, J. B., The optimization of protocols for proteome difference gel electrophoresis (DiGE) analysis of preneoplastic skin. *Journal of Proteome Research* **2007**, *6* (9), 3422-3432.
337. Yue, P.; Turkson, J., Targeting STAT3 in cancer: how successful are we? *Expert Opinion on Investigational Drugs* **2009**, *18* (1), 45-56.
338. Jia, L.; Uddin, N.; Gribben, J. G., Activation of mitochondrial STAT3 increases mitochondrial respiration and inhibits oxidative stress in chronic lymphocytic leukemic cells. *Blood* **2011**, *118* (21), 133-133.
339. Meier, J. A.; Larner, A. C., Toward a new STATe: The role of STATs in mitochondrial function. *Seminars in Immunology* **2014**, *26* (1), 20-28.
340. Chen, E. I.; Hewel, J.; Krueger, J. S.; Tiraby, C.; Weber, M. R.; Kralli, A.; Becker, K.; Yates, J. R., III; Felding-Habermann, B., Adaptation of energy metabolism in breast cancer brain metastases. *Cancer Research* **2007**, *67* (4), 1472-1486.
341. Goldsmith, J. R.; Chen, Y. H., Regulation of inflammation and tumorigenesis by the TIPE family of phospholipid transfer proteins. *Cellular & Molecular Immunology* **2017**, *14* (6), 482-487.
342. Kumar, D.; Gokhale, P.; Broustas, C.; Chakravarty, D.; Ahmad, I.; Kasid, U., Expression of SCC-S2, an antiapoptotic molecule, correlates with enhanced proliferation and tumorigenicity of MDA-MB 435 cells. *Oncogene* **2004**, *23* (2), 612-616.
343. Zhang, C. B.; Chakravarty, D.; Sakabe, I.; Mewani, R. R.; Boudreau, H. E.; Kumar, D.; Ahmad, I.; Kasid, U. N., Role of SCC-S2 in experimental metastasis and modulation of VEGFR-2, MMP-1, and MMP-9 expression. *Molecular Therapy* **2006**, *13* (5), 947-955.
344. Zhang, C. B.; Kallakury, B. V.; Ross, J. S.; Mewani, R. R.; Sheehan, C. E.; Sakabe, I.; Luta, G.; Kumar, D.; Yadavalli, S.; Starr, J.; Sreenath, T. L.; Srivastava, S.; Pollard, H. B.; Eidelman, O.; Srivastava, M.; Kasid, U. N., The significance of TNFAIP8 in prostate cancer response to radiation and docetaxel and disease recurrence. *International Journal of Cancer* **2013**, *133* (1), 31-42.
345. Day, T. F.; Mewani, R. R.; Starr, J.; Li, X.; Chakravarty, D.; Ressom, H.; Zou, X. J.; Eidelman, O.; Pollard, H. B.; Srivastava, M.; Kasid, U. N., Transcriptome and proteome analyses of TNFAIP8 knockdown cancer cells reveal new insights into molecular determinants of cell survival and tumor progression. *Cancer Gene Networks* **2017**, *1513*, 83-100.
346. Lowenstein, E. J.; Daly, R. J.; Batzer, A. G.; Li, W.; Margolis, B.; Lammers, R.; Ullrich, A.; Skolnik, E. Y.; Barsagi, D.; Schlessinger, J., The SH2 And SH3 domain containing protein grb2 links receptor tyrosine kinases to Ras signaling. *Cell* **1992**, *70* (3), 431-442.
347. Tari, A. M.; Hung, M. C.; Li, K. Y.; Lopez-Berestein, G., Growth inhibition of breast cancer cells by Grb2 downregulation is correlated with inactivation of mitogen-activated protein kinase in EGFR, but not in ErbB2, cells. *Oncogene* **1999**, *18* (6), 1325-1332.
348. Baselga, J., Targeting tyrosine kinases in cancer: The second wave. *Science* **2006**, *312* (5777), 1175-1178.
349. Yu, H.; Lee, H.; Herrmann, A.; Buettner, R.; Jove, R., Revisiting STAT3 signalling in cancer: new and unexpected biological functions. *Nature Reviews Cancer* **2014**, *14* (11), 736-746.

350. Wei, W.; Twardy, D. J.; Zhang, M.; Zhang, X.; Landua, J.; Petrovic, I.; Bu, W.; Roarty, K.; Hilsenbeck, S. G.; Rosen, J. M.; Lewis, M. T., STAT3 Signaling Is Activated Preferentially in Tumor-Initiating Cells in Claudin-Low Models of Human Breast Cancer. *Stem Cells* **2014**, *32* (10), 2571-2582.
351. Banerjee, K.; Resat, H., Constitutive activation of STAT3 in breast cancer cells: A review. *International Journal of Cancer* **2016**, *138* (11), 2570-2578.
352. Kim, B. H.; Yi, E. H.; Ye, S. K., Signal transducer and activator of transcription 3 as a therapeutic target for cancer and the tumor microenvironment. *Archives of Pharmacal Research* **2016**, *39* (8), 1085-1099.
353. Deng, X.-S.; Wang, S.; Deng, A.; Liu, B.; Edgerton, S. M.; Lind, S. E.; Wahdan-Alaswad, R.; Thor, A. D., Metformin targets STAT3 to inhibit cell growth and induce apoptosis in triple-negative breast cancers. *Cell Cycle* **2012**, *11* (2), 367-376.
354. Zhao, Z. Q.; Cheng, X. M.; Wang, Y. B.; Han, R.; Li, L.; Xiang, T.; He, L. H.; Long, H. X.; Zhu, B.; He, Y., Metformin Inhibits the IL-6-Induced Epithelial-Mesenchymal Transition and Lung Adenocarcinoma Growth and Metastasis. *Plos One* **2014**, *9* (4).
355. Wang, Y. D.; Wu, Z. Y.; Hu, L. K., Epithelial-Mesenchymal Transition Phenotype, Metformin, and Survival for Colorectal Cancer Patients with Diabetes Mellitus II. *Gastroenterology Research and Practice* **2017**.
356. Valaee, S.; Yaghoobi, M. M.; Shamsara, M., Metformin inhibits gastric cancer cells metastatic traits through suppression of epithelial-mesenchymal transition in a glucose-independent manner. *Plos One* **2017**, *12* (3).
357. Papadopoulos, V.; Baraldi, M.; Guilarte, T. R.; Knudsen, T. B.; Lacapere, J. J.; Lindemann, P.; Norenberg, M. D.; Nutt, D.; Weizman, A.; Zhang, M. R.; Gavish, M., Translocator protein (18 kDa): new nomenclature for the peripheral-type benzodiazepine receptor based on its structure and molecular function. *Trends in Pharmacological Sciences* **2006**, *27* (8), 402-409.
358. Choi, J.; Ifuku, M.; Noda, M.; Guilarte, T. R., Translocator protein (18 kDa)/peripheral benzodiazepine receptor specific ligands induce microglia functions consistent with an activated state. *Glia* **2011**, *59* (2), 219-230.
359. Veenman, L.; Gavish, M., The role of 18 kDa mitochondrial translocator protein (TSPO) in programmed cell death, and effects of steroids on TSPO expression. *Current Molecular Medicine* **2012**, *12* (4), 398-412.
360. Wu, X.; Gallo, K. A., The 18-kDa Translocator Protein (TSPO) Disrupts Mammary Epithelial Morphogenesis and Promotes Breast Cancer Cell Migration. *Plos One* **2013**, *8* (8).
361. Li, W.; Hardwick, M. J.; Rosenthal, D.; Culty, M.; Papadopoulos, V., Peripheral-type benzodiazepine receptor overexpression and knockdown in human breast cancer cells indicate its prominent role in tumor cell proliferation. *Biochemical Pharmacology* **2007**, *73* (4), 491-503.
362. Carmel, I.; Fares, F. A.; Leschner, S.; Scherubl, H.; Weisinger, G.; Gavish, M., Peripheral-type benzodiazepine receptors in the regulation of proliferation of MCF-7 human breast carcinoma cell line. *Biochemical Pharmacology* **1999**, *58* (2), 273-278.
363. Berchtold, M. W.; Villalobo, A., The many faces of calmodulin in cell proliferation, programmed cell death, autophagy, and cancer. *Biochimica Et Biophysica Acta-Molecular Cell Research* **2014**, *1843* (2), 398-435.

364. Coticchia, C. M.; Revankar, C. M.; Deb, T. B.; Dickson, R. B.; Johnson, M. D., Calmodulin modulates Akt activity in human breast cancer cell lines. *Breast Cancer Research and Treatment* **2009**, *115* (3), 545-560.
365. Ichikawa, J.; Kiyohara, T., Suppression of EGF-induced cell proliferation by the blockade of Ca²⁺ mobilization and capacitative Ca²⁺ entry in mouse mammary epithelial cells. *Cell Biochemistry and Function* **2001**, *19* (3), 213-219.
366. He, L.; Wondisford, F. E., Metformin action: concentrations matter. *Cell Metabolism* **2015**, *21* (2), 159-162.
367. Thor, A., and S. M. Anderson., Preclinical studies of metformin action in breast cancer. *ASCO Educational Book:46-49.* **2011**.
368. Bailey, C. J.; Mynett, K. J.; Page, T., Importance of the intestine as a site of metformin-stimulated glucose-utilization. *British Journal of Pharmacology* **1994**, *112* (2), 671-675.
369. Zhuang, Y.; Chan, D. K.; Haugrud, A. B.; Miskimins, W. K., Mechanisms by Which Low Glucose Enhances the Cytotoxicity of Metformin to Cancer Cells Both In Vitro and In Vivo. *Plos One* **2014**, *9* (9).
370. Wahdan-Alaswad, R.; Fan, Z.; Edgerton, S. M.; Liu, B.; Deng, X.-S.; Arnadottir, S. S.; Richer, J. K.; Anderson, S. M.; Thor, A. D., Glucose promotes breast cancer aggression and reduces metformin efficacy. *Cell Cycle* **2013**, *12* (24), 3759-3769.
371. G, A.; M, J.; EG, V.; S, J.; Department of Medical Oncology, C. R. C. G., University of Groningen, University Medical Center Groningen, Hanzeplein 1, 9713 GZ, Groningen, The Netherlands.; Ariaans, G.; Jalving, M.; Vries, E. G. E. d.; Jong, S. d., Anti-tumor effects of everolimus and metformin are complementary and glucose-dependent in breast cancer cells. **2017**.
372. Sinnett-Smith, J.; Kisfalvi, K.; Kui, R.; Rozengurt, E., Metformin inhibition of mTORC1 activation, DNA synthesis and proliferation in pancreatic cancer cells: dependence on glucose concentration and role of AMPK. *Biochemical and biophysical research communications* **2013**, *430* (1), 352-7.
373. Bikas, A.; Jensen, K.; Patel, A.; Costello, J., Jr.; McDaniel, D.; Klubo-Gwiezdzinska, J.; Larin, O.; Hoperia, V.; Burman, K. D.; Boyle, L.; Wartofsky, L.; Vasko, V., Glucose-deprivation increases thyroid cancer cells sensitivity to metformin. *Endocrine-Related Cancer* **2015**, *22* (6), 919-32.
374. Shaw, R. J.; Bardeesy, N.; Manning, B. D.; Lopez, L.; Kosmatka, M.; DePinho, R. A.; Cantley, L. C., The LKB1 tumor suppressor negatively regulates mTOR signaling. *Cancer Cell* **2004**, *6* (1), 91-99.
375. Shaw, R. J.; Kosmatka, M.; Bardeesy, N.; Hurley, R. L.; Witters, L. A.; DePinho, R. A.; Cantley, L. C., The tumor suppressor LKB1 kinase directly activates AMP-activated kinase and regulates apoptosis in response to energy stress. *Proceedings of the National Academy of Sciences of the United States of America* **2004**, *101* (10), 3329-3335.
376. Hardie, D. G.; Alessi, D. R., LKB1 and AMPK and the cancer-metabolism link - ten years after. *BMC Biol* **2013**, *11*, 36.
377. Algire, C.; Amrein, L.; Bazile, M.; Zakikhani, M.; David, S.; Pollak, M., Metformin inhibits in vivo growth of MC38 colon carcinoma in the absence of LKB1 expression. *Proceedings of the American Association for Cancer Research Annual Meeting* **2010**, *51*, 17-17.

378. Algire, C.; Amrein, L.; Bazile, M.; David, S.; Zakikhani, M.; Pollak, M., Diet and tumor LKB1 expression interact to determine sensitivity to anti-neoplastic effects of metformin in vivo. *Oncogene* **2011**, *30* (10), 1174-1182.
379. Vincent, E. E.; Coelho, P. P.; Blagih, J.; Griss, T.; Viollet, B.; Jones, R. G., Differential effects of AMPK agonists on cell growth and metabolism. *Oncogene* **2014**, *34* (28), 3627.
380. Liu, X.; Chhipa, R. R.; Pooya, S.; Wortman, M.; Yachyshin, S.; Chow, L. M. L.; Kumar, A.; Zhou, X.; Sun, Y.; Quinn, B.; McPherson, C.; Warnick, R. E.; Kendler, A.; Giri, S.; Poels, J.; Norga, K.; Viollet, B.; Grabowski, G. A.; Dasgupta, B., Discrete mechanisms of mTOR and cell cycle regulation by AMPK agonists independent of AMPK. **2014**.
381. Huang, X.; Wullschleger, S.; Shpiro, N.; Sakamoto, K.; Mcburnie, W.; Fleming, S., Important role of the LKB1-AMPK pathway in suppressing tumorigenesis in PTEN-deficient mice. **2008**.
382. Lee, K.-H.; Hsu, E.-C.; Guh, J.-H.; Yang, H.-C.; Wang, D.; Kulp, S. K.; Shapiro, C. L.; Chen, C.-S., Targeting energy metabolic and oncogenic signaling pathways in triple-negative breast cancer by a novel adenosine monophosphate-activated protein kinase (AMPK) activator. **2011**.
383. Zadra, G.; Photopoulos, C.; Tyekucheva, S.; Heidari, P.; Weng, Q. P.; Fedele, G.; Liu, H.; Scaglia, N.; Priolo, C.; Sicinska, E.; Mahmood, U.; Signoretti, S.; Birnberg, N.; Loda, M., A novel direct activator of AMPK inhibits prostate cancer growth by blocking lipogenesis. **2014**.
384. Foretz, M.; Hébrard, S.; Leclerc, J.; Zarrinpashneh, E.; Soty, M.; Mithieux, G.; Sakamoto, K.; Andreelli, F.; Viollet, B., Metformin inhibits hepatic gluconeogenesis in mice independently of the LKB1/AMPK pathway via a decrease in hepatic energy state. In *The Journal of Clinical Investigation*, **2010**; *120*, 2355-69.
385. Zadra, G.; Batista, J. L.; Loda, M., Dissecting the dual role of AMPK in cancer: from experimental to human studies. **2015**.
386. Burdall, S. E.; Hanby, A. M.; Lansdown, M. R.; Speirs, V., Breast cancer cell lines: friend or foe? In *Breast Cancer Research*, **2003**; *5*, 89-95.
387. Cabrera CM, C. F., Nieto A, Cortés JL, Montes RM, Catalina P, Concha A, Identity tests: determination of cell line cross-contamination **2006**.